UNIVERSITY OF CALIFORNIA
RIVERSIDE

Toxicological Evaluation of Thirdhand Smoke Using *In-vitro* Models

A Dissertation submitted in partial satisfaction
of the requirements for the degree of

Doctor of Philosophy

in

Environmental Toxicology

by

Vasundhra Bahl

December 2015

Dissertation Committee:
Dr. Prue Talbot, Chairperson
Dr. Yinsheng Wang
Dr. Roya Bahreini

The Dissertation of Vasundhra Bahl is approved:

Committee Chairperson

University of California, Riverside

Acknowledgements

The text and figures in Chapter 2, in part or in full, are a reprint of the material as it appears in Current Protocols in Stem Cell Biology 2012, Chapter 1:Unit 1C.13. The co-author (Rachel Behar) listed in this publication performed experiments dealing with human embryonic stem cells and wrote the corresponding protocols. The co-authors (Sabrina Lin, Jo-Hao Weng and Yuhuan Wang) listed in this publication helped with cell culture. The co-author (Dr. Prue Talbot) listed in this publication directed and supervised the research which forms the basis for this chapter.

The text and figures in Chapter 3, in part or in full, are a reprint of the material as it appears in Plos One, 2014, 6;9(10):e108258. The co –author (Dr. Peyton Jacob) listed in this publication, supervised the chemical analysis of THS extracts and the co-author (Christopher Havel), listed in this publication performed the chemical analysis. The co-author (Dr. Suzaynn Schick) listed in this publication supplied fabric with THS residue. The co-author (Dr. Prue Talbot), listed in this publication directed and supervised the research which forms the basis for this chapter.

This dissertation is an account of research carried out over the past five years, and it would not have been possible without the support from my family, adviser and friends. First and foremost, I thank my parents and younger brother Kartikeya, for their unconditional love and unwavering support throughout course of my Ph.D. and in life in general.

I express my deepest gratitude to my adviser Dr. Prue Talbot for guiding my research and providing a warm and conducive lab environment to accomplish the work described here. She helped and supported me in every possible way. Besides my adviser, I thank my dissertation committee members; Dr. Yinsheng Wang and Dr. Roya Bahreini for providing feedback and suggestions. I am grateful to Dr. Evan Snyder for providing the mouse neural stem cell line, Dr. Suzaynn Schick for providing material for extraction of thirdhand smoke, Dr. Peyton Jaboc III for providing LC-MS/MS data, Dr. Mohamad Sleiman for providing the GCMS data, and to Atena Zahedi for providing MitoTimer transfected mouse neural stem cells.

I would like to acknowledge the contributions of several other people who helped with various aspects of my research. I thank Pura Tech and Christopher Havel for help with handling and analyzing LC-MS/MS samples and to Laurie Graham for help with building the acrylic smoke exposure chambers for the indoor THS generation experiment. I am thankful to CIRM interns, Kimberly Johnson and Hyung Jun Shim, and to undergrads George Phandthong, Julian Hartzell and Allison Ibarra who helped collect and analyze data for parts of the project. I also thank Nikki Weng for help with data collection for Chapter 4, Jacklyn Whitehead for making recipes for cell area quantification in CL quant and Kristen Diaz for help with data analysis for Chapter 5.

I thank Tobacco-Related Disease Research Program of California for providing funding that led to development of this research project.

I express heartfelt gratitude towards Dr. Kamlesh Asotra and Yuhuan Wang for being a source of motivation. I would like to thank my lab mates Dr. Sabrina Lin, Rachel Behar, Monique Williams, Barbra Davis, Nikki Weng, Atena Zahedi, Careen Khachatoorian and Giovanna Pozuelos for helping with research work, being amazing friends and for making my stay at the Talbot lab very memorable.

Dedication

This dissertation is dedicated to my parents, Kalpna Bahl and Harish Bahl. Their love and support have made me who I am and helped me to accomplish what I have.

ABSTRACT OF THE DISSERTATION

Toxicological Evaluation of Thirdhand Smoke Using In-Vitro Models

by

Vasundhra Bahl

Doctor of Philosophy, Graduate Program in Environmental Toxicology
University of California, Riverside, December, 2015
Dr. Prue Talbot, Chairperson

Thirdhand smoke (THS), which recently emerged as a potential health hazard, is the residue left on surfaces when secondhand smoke clears. It contains volatile organic compounds (VOCs), nicotine and related alkaloids, and chemicals formed during aging such as tobacco specific nitrosamines. The purpose of this dissertation was to evaluate the cytotoxicity of THS using *in vitro* models. A protocol was optimized to extract THS from fabrics into cell culture medium at room temperature for 1 hour. This protocol was effective for evaluating cytotoxicity of the extracts using mouse neural stem cells (mNSC) in the MTT assay. Fresh THS extracts from terrycloth exposed to 133 cigarettes over 11 months killed mNSC, disrupted motility and the cytoskeleton, and caused fragmentation and vacuolization of cells. THS aged at room temperature for 5 months no longer killed mNSC, indicating that the above effects were caused by VOCs that were lost from THS during aging. Twenty-five VOCs in THS were screened for cytotoxicity to mNSC and adult lung cells, and acrolein was identified as the most toxic VOC. Acrolein killed mNSC and adult lung cells at 10^{-5} M and decreased proliferation at 10^{-6} M by

affecting the expression of *TFDP 1*, *CASP 3, ANAPC 2,* and *WEE1,* genes involved in cell cycle regulation. A smoker's car was then simulated, and car seat cover and carpet were exposed to low levels cigarette smoke for 1 month. THS from these fabrics induced single strand DNA breaks in mNSC and adult skin cells. Terrycloth exposed to THS in an indoor chamber became more cytotoxic with longer exposure and lost toxicity after aging in the absence of fresh smoke. Because proteins enhanced extraction of cytotoxic chemicals, infants mouthing THS contaminated objects may have elevated intake of THS toxicants due to proteins in their saliva. Batches of THS that did not affect cell survival/proliferation caused stress-induced mitochondrial hyperfusion, increased mitochondrial membrane potential, increased ATP production; increased oxidative stress; and decreased expression of genes involved in mitochondrial function. These data show that relatively low levels of THS can disrupt cellular functions and have the potential to adversely impact health.

Table of Contents

List of Figures

List of Tables

Chapter 1: Introduction

Tobacco Smoke: A well-recognized health hazard:

Cigarette smoking is prevalent worldwide and is recognized as a human health hazard (WHO; CDC). Nearly 20% of the world's adult population smokes cigarettes (Tobacco Atlas, global health observatory, WHO), and in some countries this percentage is much higher. Smoking causes about 6 million deaths/year world-wide (WHO), with an additional 600,000 being caused by indirect exposure to secondhand tobacco smoke (WHO). In the US alone, 18% of the adults above 18 years of age smoke cigarettes and 480,000 people die every year due to adverse health effects caused by cigarette smoke (CDC), although this number has recently been challenged and may be an underestimate (Freedman et al., 2015). About 20,830,000 premature deaths were caused by direct and indirect exposure to cigarette smoke between1965-2014 (USDHHS, 2014).

Cigarette smoking has been directly linked to an increased risk of cardiovascular disease, lung diseases such as chronic obstructive pulmonary disease (COPD), emphysema, and worsening of pre-existing conditions such as asthma (USDHHS, 2014). According to the Surgeon General's report (2014), cigarette smoking complicates diabetes, impairs immune function, and causes adverse reproductive effects including decreased fertility, miscarriages, low birth weights, still births, student infant death syndrome, and ectopic implantation and (Martin et al. 2002). Smoking accounts for about 30% of all deaths due to cancers of multiple organs including lung, larynx, oral cavity, pharynx, stomach, pancreas, kidney and bladder with lung cancer being the most prevalent (CDC, 2015).

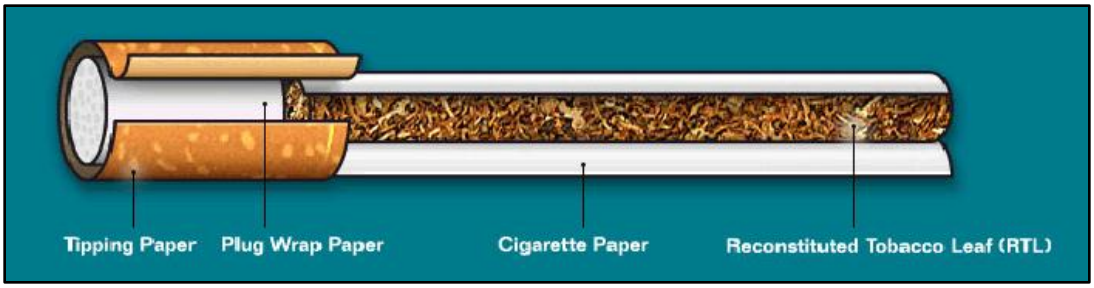

Fig 1.1. Schematic diagram depicting the parts of a tobacco cigarette. (From Smoker News World)

Components of a Cigarette:

.A cigarette is a drug delivery device specifically designed to deliver nicotine to the brain. Dried tobacco leaves serve as the source of nicotine which acts as a stimulant for the brain. Even though several tobacco products are available which include cigars, cigarillos, bidis, kreteks, pipe tobaccos, and smokeless products, cigarettes are the most widely used. Cigarettes consist of tobacco leaves rolled up in a porous paper, which is lit on one end, while the other end is used to inhale the smoke through the mouth. Cellulose fibers or wood pulp are often added along with dried tobacco leaves. Most cigarettes have a filter made of cellulose acetate at the mouth end that removes some of the harmful chemicals and also reduces the flow of smoke to reduce its harshness. The filter is wrapped in a silicone treated colored tipping paper. Cigarettes are usually 5-8 mm in diameter and 70 -100 mm in length, with the tipping paper being about 15-25 mm in length. Cigarettes are specifically engineered for nicotine delivery, and various parameters such as packing density, color and flavor are highly controlled through cigarette design (Wigand, 2006).

Tobacco leaves contains about 3000 compounds including organic acids, alcohols, aldehydes, ketones, quinones, alkaloids and bases, alkenes and alkynes, amino acids, carbohydrates, esters, inorganic elements, N-heterocyclic compounds,

phenols, sterols, oxygenated terpenes, isoprenes and related compounds in addition to nicotine. Several other compounds are formed during post-harvest curing of tobacco leaves. Curing, which enhances the flavors of tobacco leaves and reduces their moisture content, is done either through application of heat or letting the leaves age in ambient air. The curing method affects the composition of the tobacco leaves such as the sugar and volatile organic compound content and thus can influence the flavor of a tobacco cigarette (Wigand, 2006).

Types of Cigarette Smoke

Mainstream Smoke: The smoke that a person actively inhales is known as mainstream smoke. It consists of about 7,000 chemicals that are usually inhaled through a filter (Rodgman & Perfetti, 2012). These chemicals include nicotine, the main addictive compound in tobacco, particulate matter or "tar", and gas phase components.

The particulate phase of mainstream smoke contains chemicals like carboxylic acids, phenols, water, humectants, nicotine, terpenoids, paraffin waxes, tobacco-specific nitrosamines (TSNAs), polyaromatic hydrocarbons (PAHs), and catechols. The vapor phase consists of chemicals like nitrogen, oxygen, carbon dioxide, CO, acetaldehyde, methane, hydrogen cyanide, nitric acid, acetone, acrolein, ammonia, methanol, hydrogen sulfide, hydrocarbons, gas phase nitrosamines, and carbonyl compounds (CDC, 2010). In addition, smoke contains inorganic constituents which include heavy metals like arsenic, barium, cobalt, lead and mercury; and also some radioactive isotopes of strontium, cesium and rubidium (Stedman, 1968).

Smoking results in a variety of health problems, the predominant ones being cancer and cardiovascular disease (Munters & Nawrot, 2011). Smokers have an increased incidence of myocardial infraction, stroke, and cardiovascular disease when compared to non-smokers. Smokers inhale PAHs, TSNAs, and cadmium, which are classified by the IARC as class 1 carcinogens (IARC, 2012). It was seen in the 1920s

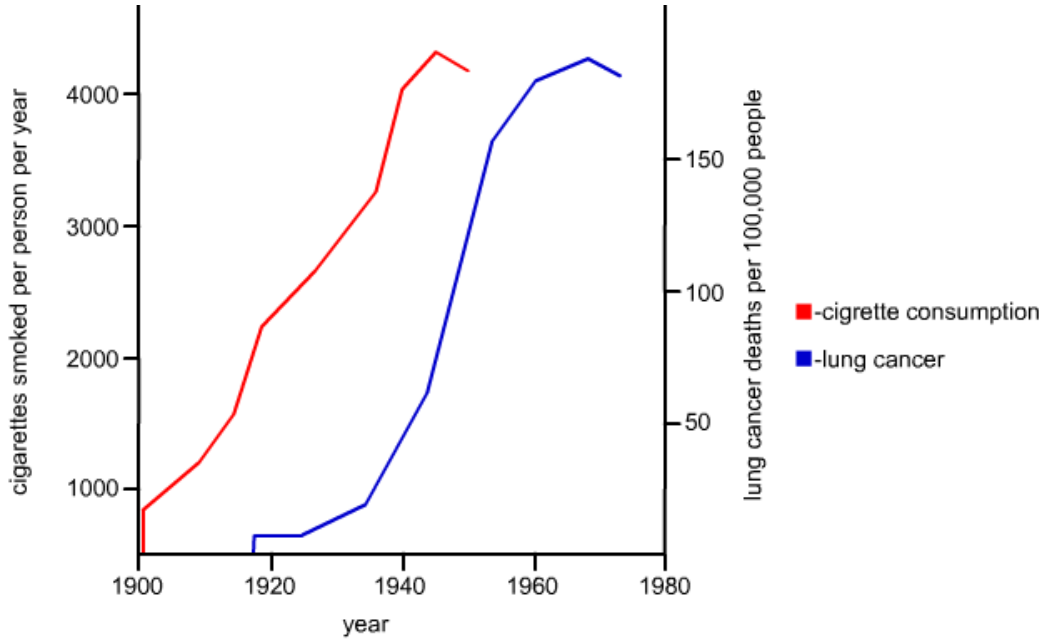

Fig 1.2 Graph showing the 20 year lag between start of prevalent cigarette consumption and lung cancer in men. (Association of British Pharmaceutical Industry, 2013)

that the prevalence of lung carcinomas had increased. This was attributed to the use of tobacco cigarettes that had become widespread during the beginning of the 20th century (Doll & Hill, 1950).

There is evidence establishing a connection between cigarette smoking and cancers of the nasal cavities and paranasal sinuses, nasopharynx, stomach, liver, kidney (renal cell carcinoma), uterine cervix, esophagus and myeloid leukemia in addition to lung, oral cavity, pharynx, larynx, esophagus, pancreas, urinary bladder and renal pelvis (Sasco, Secretan, & Straif, 2004). In addition, epigenetic changes, such as

methylation of genes, occur more frequently in smokers than in non-smokers (Launay et al., 2009). The epigenetic changes induced by tobacco smoke remain years after a smoker quits smoking (Launay et al., 2009). Smoking decreased methylation in the promoter region of the gene coding for platelet mitochondrial monoamine oxygenase (MAO-B), thus increasing its expression in smokers as well as people who have quit smoking. 5-hydroxytryptamine (5-HT), a product of MAO-B catabolism, is involved in cardiovascular damage, addiction, predisposition to cancer, and behavioral and mental health problems. Figure 1.3 shows the various adverse health effects caused by cigarette smoking and the number of death caused by those health effects in the US.

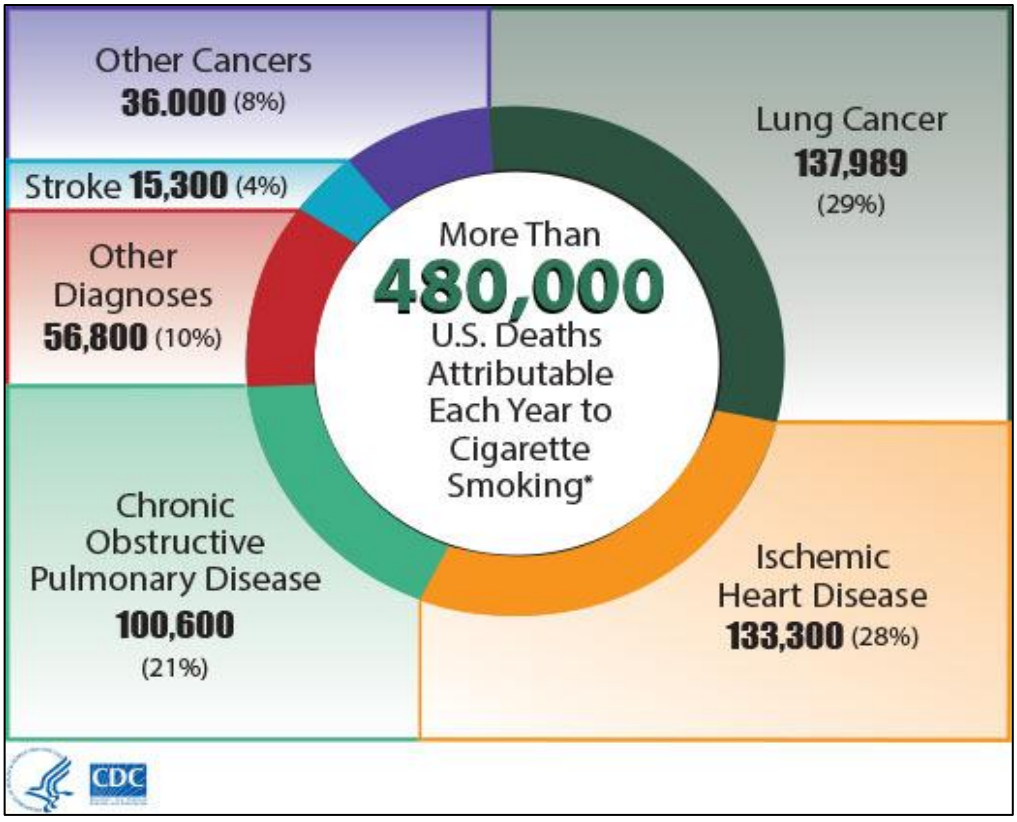

Fig 1.3. Adverse effects caused by cigarette smoke and number of deaths attributed to those adverse effects. (CDC).

Secondhand Smoke (SHS) or Environmental Tobacco Smoke (ETS):

Exposure to cigarette smoke occurs not only through active smoking but also through inhalation of secondhand smoke (SHS) or environmental tobacco smoke. SHS consists mainly of the sidestream smoke that comes off the end of a burning cigarette, smoke that leaks out of the cigarette paper and users mouth, and the smoke exhaled by a smoker (CDC, 2015). Its inhalation is referred to as passive smoking. The chemical composition of SHS is slightly different from that of mainstream smoke as it contains higher concentrations of carcinogens. Also, it contains smaller particles than mainstream smoke and these can be deposited much deeper in the lungs (American Cancer Society, 2015).

Sidestream smoke has higher levels of PAHs, nitrosamines, aza-arenes, aromatic amines, carbon monoxide, ammonia, pyridine, 1,3-butadiene, acrolein, isoprene, benzene, and toluene than mainstream smoke (CDC, 2010). Some examples of ratios of levels of compound in sidestream vs. mainstream smoke are shown in the table below. Although most of the compounds shown in this table are higher in sidestream smoke than in mainstream smoke, sidestream smoke is more likely to disperse and get diluted in the environment where smoking occurs. The concentrations available for exposure therefore depend upon factors like the location and ventilation.

Table 1.1. Ratios of levels of compounds found in side-stream and mainstream smoke. (IARC, 2012)

Compound	Ratio (sidestream : mainstream smoke)
Nicotine	7.1 : 1
Carbon monoxide	4.8 : 1
Ammonia	455 : 1
Formaldehyde	36.5 : 1
Acrolein	18.6 : 1
Benzo(a)pyrene	14 : 1
N-nitrosonornicotine (NNN)	0.43 : 1
4-(methylnitrosamino)-1-(3-pyridyl)-1-butanone (NNK)	0.40 : 1

The U.S Environmental Protection Agency (EPA) classifies SHS as a known human carcinogen, and it has been linked to lung cancer, leukemia, lymphoma, brain tumors in children, as well as cancers of the bladder, rectum, stomach and breast in adults (American Cancer Society, 2015). The levels of 4-(methylnitrosamino)-1-(3-Pyridyl)-1-Butanol (NNAL), which is a metabolite of NNK, a carcinogenic tobacco specific nitrosamine (TSNA) are consistently high in people exposed to secondhand smoke (Hecht et al., 2006). Exposure to secondhand smoke can also cause respiratory complications like asthma, coughing, compromised lung function, and cardiovascular disease (USDHHS, 2014).

Exposure of pregnant women to secondhand smoke can result in lower birth weights (Khader, Al-Akour, Alzubi, & Lataifeh, 2011), spontaneous abortion, sudden infant death syndrome, impaired neurological development, and asthma (USDHHS,

2004). Secondhand smoke exposure also causes mental retardation, learning and behavioral problems, growth retardation, and disorders such as attention deficit hyperactivity disorder (ADHD) (Neuman et al., 2007). It is also linked to obesity, hypertension, and gestational diabetes in women (Cupul-Uicab et al., 2012). *In utero* tobacco smoke exposure changes the pattern of gene-specific as well as global DNA methylation (Breton et al., 2009) (Prescott, 2008).

Although everyone residing with smokers is at risk for exposure and adverse health effects caused by secondhand smoke, the most vulnerable population includes infants, children, and unborn fetuses. SHS exposure can have adverse effects on development of the brain (Sekizawa, Joad, Pinkerton, & Bonham, 2010) and aggravate respiratory ailments such as asthma (Janson, 2004). The chemicals causing these effects are deposited on surfaces and constitute another kind of environmental tobacco smoke known as thirdhand smoke (THS) described below.

THS: THS refers to the chemicals in cigarette smoke that remain indoors on surfaces and linger after smoking ceases. THS contains the chemicals present in SHS and can thus potentially cause similar health effects to people who are exposed. There is a need to evaluate the potential adverse health effects caused by THS and a complete research agenda for attacking this problem has been proposed (Matt, Quintana, Destaillats, et al., 2011).

THS, a term introduced in 2006 (Szabo, White, & Hayman, 2006), consists of residual and volatile chemicals that remain in indoor environments after secondhand smoke has cleared (Matt, Quintana, Zakarian, et al., 2011). THS has gained attention as a potential health hazard in the recent past and the need for a toxicological

evaluation of THS is widely recognized (Matt, Quintana, Destaillats, et al., 2011) (Winickoff et al., 2009). THS consists of: (1) Particulate and chemical constituents of tobacco smoke adsorbed onto surfaces; (2) Compounds formed by the chemical reaction of these constituents with other environmental constituents and pollutants such as oxygen, ozone and nitrous acid (HONO).; and (3) Volatile and semi-volatile compounds as well as novel chemical species produced *de novo* from smoke deposits that become desorbed and released back into the ambient indoor air. Conventional ventilation technologies do not clear out smaller particles and gases which often settle on surfaces including carpets, curtains, upholstery, furniture and clothes of smokers and people exposed to secondhand smoke (Matt, Quintana, Zakarian, et al., 2011). The chemicals composition of THS changes with time due to volatilization, degradation, and reaction with the ambient environment, a process termed “aging” (Petrick, Sleiman, Dubowski, Gundel, & Destaillats, 2011). The chemical composition of THS also depends on the frequency of smoking and the length of time that smoking has occurred indoors..

Chemicals in Mainstream and Side stream Cigarette Smoke

Cigarette smoke contains about 7,000 – 10,000 different chemicals, many of which are known to cause adverse health effects (Rodgman & Perfetti, 2012). These include alkaloids, such as nicotine which is the main addictive compound in cigarette smoke, and in most commercial cigarettes, its concentration ranges from 6-18 mg/g (Rodgman & Perfetti, 2012). Cigarettes smoke contain other alkaloids as shown in Table 1.2

Table 1.2. Examples of Chemicals in Cigarette Smoke.

Alkaloids	Poly Aromatic Hydrocarbons	Volatile Organic Chemicals	Heavy metals ng/cigarette
nicotine	acenaphthylene,	formaldehyde	lead (6 – 149) and to 48.0)
myosmine	acenaphthene,	acrolein	cadmium (10 – 250)
cotinine	anthracene,	Oxides of carbon, nitrogen and sulfur	chromium (1.1 – 1.7)
anabasine	benz[a]anthracene,	1,3-butadiene,	antimony (0.10 – 0.13)
anatabine	benzo[a]pyrene (B[a]P),	acrylonitrile,	thallium (0.6 – 2.4)
nornicotine	benzo[b]fluoranthene (B[b]F),	benzene	mercury (0.46 – 6.5)
N'-nitrosonornicotine (NNN)	benzo[k]fluoranthene (B[k]F),	acetaldehyde	cobalt (0.012)
4-(methylnitrosoamino)-1-(3-pyridyl)-1-butanone (NNK)	benzo[g,h,i]perylene,,		arsenic (1.5 – 21)
N'-nitrosoanatabine (NATB)	dibenz[a,h]anthracene,		Ra^{228}
N'-nitrosoanabasine (NAB)	fluoranthene,		Pb^{210}
N-nitrosodimethylamine	fluorene,		Ra^{226}
N-nitrosoethylmethylamine	indeno[1,2,3-cd]pyrene,		
N-nitrosodiethylamine,	naphthalene,		
N-nitro-sopyrrolidine	phenanthrene		
N-nitrosomorpholine	pyrene		

Another class of nicotine derivatives found in cigarette smoke are the tobacco specific nitrosamines (TSNAs) with N'-nitrosonornicotine (NNN), 4-(methylnitroso amino)-1-(3-pyridyl)-1-butanone (NNK), N'-nitrosoanatabine (NATB) and N'-nitrosoanabasine (NAB) being the most abundant. TSNAs are formed during the curing and burning of tobacco (Roton, Wiernik, Wahlberg, Vidal, & Match, 2005). The levels of TSNAs in mainstream cigarette smoke, which a smoker inhales, range from 200 to 600 ng/cigarette (Adams, O'Mara-Adams, & Hoffmann, 1987). NNN and NNK are the strongest carcinogens of all the TSNAs. NNK induces tumors in lungs, the nasal cavity, trachea, and liver in rats, mice and Syrian golden hamsters. NNN caused tumors in esophagus, nasal cavity, trachea and lungs (Hecht & Hoffmann, 1988). These are also classified as human carcinogens by the International Agency for Research on Cancer (IARC, 20007).

Polycyclic aromatic hydrocarbons (PAH) constitute another important class of carcinogenic chemicals that are present in cigarette smoke (Rodgman & Perfetti, 2012). Examples of some PAHs found in tobacco smoke are shown in Table 1. Most of these are products of tobacco combustion, and their concentration in sidestream smoke is about 10 fold higher in than in mainstream smoke (Lodovici, Akpan, Evangelisti, & Dolara, 2004). PAHs are highly reactive compounds and get metabolized to epoxides which form adducts with DNA causing genotoxicity (Shimada & Fujii-Kuriyama, 2004) (Kondraganti et al., 2003). PAH exposure has been linked to lung, bladder and stomach cancers (IPCS, 1998). Embryotoxic effects have also been reported in animal models including mice and rats (IPCS, 1998).

Cigarette smoke contains volatile organic chemicals (VOCs), which constitute about 400-500 compounds primarily in the gas phase of cigarette smoke. They include oxides of carbon, nitrogen and sulfur and some low molecular aldehydes and ketones such as acetaldehyde (30 – 650 µg/cigarette), formaldehyde (2 – 50 µg/cigarette) and acrolein (2.5 – 60 µg/cigarette) (Rodgman & Perfetti, 2012). According to Fowles and Dybing (2003), VOCs such as 1,3-butadiene, acrylonitrile, arsenic, acetaldehyde and benzene have the highest cancer risk index of all the carcinogens present in cigarette smoke (Fowles & Dybing, 2003). *In vitro* studies using lung epithelial cells have shown that cigarette smoke containing VOCs is cytotoxic, whereas the gas phase of cigarette smoke with VOCs removed through binding to filters made of activated carbon, is no longer cytotoxic (Pouli et al., 2003). *In vitro* studies have also shown that functioning of the hamster oviduct is inhibited by VOCs in both mainstream and sidestream smoke (Knoll et al 1995; Knoll and Talbot 1998; Geiseke and Talbot 2005). VOCs in cigarette smoke contains reactive oxygen species (ROS) and reactive nitrogen species (RNS), which are responsible for promoting cell death in lungs (Sussan and Biswal 2011).

Apart from the above mentioned organic compounds, cigarette smoke also contains heavy metals such as lead (6 – 149 ng/cigarette) and cadmium (10 – 250 ng/ cigarette). These are usually absorbed by the tobacco plant from the soil. Since tobacco burns at a temperature of about 900°C, metals get volatilized and can be inhaled along with cigarette smoke. Other heavy metals found at lower concentrations are shown in Table 1.2. Some radioactive metals such as Pb^{210}, Ra^{226} and Ra^{228} have also been reported in tobacco smoke (Papastefanou, 2009). Heavy metals have a fairly long biological half-life and can therefore remain inside the body for a prolonged time. Metals such as lead can accumulate in various organs including the bones and cause adverse

effects on mineral metabolism (Chiba & Masironi, 1992). Cadmium and nickel are absorbed by the tobacco plant from the soil. Increased cadmium levels due to cigarette smoking have been linked to peripheral arterial disease (Navas-Acien et al., 2004), whereas nickel is a potential carcinogen (Kasprzak, Sunderman, & Salnikow, 2003). Cadmium from maternal smoking causes a decrease in glutathione peroxidase levels in cord blood cells. This happens due to formation of cadmium-selenium complexes thus decreasing the bioavailability of selenium for glutathione peroxidase activity (Lloyd, Lloyd, & Clayton, 1983). Heavy metal exposure from cigarette smoke has also been correlated to hypertension (Afridi et al., 2010).

Chemical Composition of THS

THS consists of semi-volatile, volatile, and non-volatile chemicals, including carcinogens such as TSNAs, arsenic, lead, and cyanide. It is therefore a potential hazard for those residing in THS environments such as homes, hotels, and offices where smoking occurs**.** The constituents of THS can react with chemical species present in the ambient environment such as nitrous acid (HONO) and ozone, and give rise to novel compounds in the course of time. This process is termed “aging” and can significantly alter the chemical composition of THS over time (Petrick et al., 2011). For example, 1-(N-methyl-N-nitrosamino)-1-(3-pyridinyl)-4-butanal) or NNA is formed by the oxidation of residual nicotine in THS due to interactions of nicotine with the ambient environment (Sleiman et al., 2010).

The volatile organic chemicals (VOCs) present in cigarette smoke are sorbed onto surfaces when smoking occurs and can later be emitted into the indoor atmosphere. These compounds can often be detected in a THS environment several

hours after smoking has occurred, increasing the risk of exposure to toxic VOCs. Sleiman et al (2014) conducted a study to identify and quantify the levels of VOCs in indoor air hours after smoking had occurred. The various types of VOCs detected were nitrogenated VOCs and semi VOCs such as 3-ethenylpyridine, acrylonitrile and acetonitrile; aromatic hydrocarbons like furan, 2',5'-dimethylfuran and benzene; carbonyls and chlorinated VOCs like 2-butanone, acetaldehyde, acetone and acrolein; and alkanes/alkenes such as butane, isobutene and isoprene. These chemicals were detected for up to 18 hours after smoking had stopped. This study also gives valuable indication as to which compounds can be used as biomarkers for THS, as the transition from secondhand to thirdhand smoke is not very clear and precise. Secondhand smoke biomarkers include nicotine and 3-ethenylpyridine and their concentration in the study reported by Sleiman et al (2014) in THS was similar to that reported in the secondhand smoke literature. Therefore these compounds are not useful as biomarkers of THS. On the other hand some chemicals detected in THS, such as acrolein, alkanes and acrylonitrile, are rarely reported in to be present in secondhand smoke. This makes these compounds strong candidates for THS biomarkers that can be used to estimate levels of THS in property and cars. It is noteworthy, that after 18 hours of smoking, the percentage of carbonyls and nitriles in the air was high and volatile amines were almost absent. The authors therefore propose that disappearance of amines and the persistence of acetonitrile can be used to identify a transition from secondhand smoke to THS. Even though the VOCs concentration reported in the above study fell to levels much below that of secondhand about 2 hours after smoking, this does not accurately reflect a real life scenario. Inside a smoker's home or vehicle, smoking is likely to occur

at least every few hours thus keeping the VOCs in indoor air at levels that could potentially be dangerous to people inhaling them.

In addition to VOCs, THS consists of non-volatile or semi-volatile chemicals that stick to surfaces and build up over time (Schick, 2011). These chemicals consist of nicotine, its derivatives such as myosmine and cotinine, and oxidation products, which are mainly TSNAs. These chemicals, apart from being present in secondhand smoke, are also formed de-novo on indoor surfaces as a result of reactions of residual THS with the ambient air, especially nitrous acid (HONO). HONO is present in indoor environments at much higher concentration than outdoors, and its main sources are combustion of fuels in kitchens, other unvented combustion appliances, and cigarette smoking. Typical indoor levels are 5-15 parts per billion by volume (ppbv). Levels as high at 100 ppbv and 30 ppbv have been reported in homes in cars, respectively (Lee et al., 2002). These high levels of HONO are favorable for the conversion of nicotine to TSNAs. The three main TSNAs reported in THS are 1-(N-methyl-N-nitrosamino)-1-(3-pyridinyl)-4-butanal) (NNA), 4-(methylnitrosamino)-1-(3-pyridinyl)-1-butanone (NNK), and N'-nitroso nornicotine (NNN). NNN and NNK are present in cigarette smoke, but NNA is specific to THS (Sleiman et al., 2010) and has recently been reported to cause DNA damage (Hang et al., 2013). Whole THS also caused DNA damage to cultured human liver cells and human lung epithelial cells (Hang et al., 2013).

Exposure to THS

Thirdhand smoke (THS) residue builds up on surfaces over time as smoking continues in indoor environments (Matt, Quintana, Zakarian, et al., 2011) (Fortmann et al., 2010). The level of non-volatile compounds on surfaces increases over time, and

VOC in indoor air increase to a level that is higher than non-THS environments due to off-gassing of VOCs from THS coated surfaces (Singer, Hodgson, & Nazaroff, 2002). People residing in homes and work places where smoking takes place are therefore regularly exposed to THS through dermal contact and inhalation. In addition, oral exposure may occur, especially in infants and toddlers who come in contact with exposed surfaces more than adults and who are also likely to ingest dust particles and mouth THS coated fabrics (Matt, Quintana, Destaillats, et al., 2011). In a study carried out by Quintana et al (2103), nicotine wipe sampling was done in three kinds of homes, cars and hotel environments: non-smoking environments, environments with smokers residing in them but having a ban on indoor smoking, and smoking environments. Nicotine levels were highest on surfaces in smoking environments, followed by smoking environments with smokers but having a ban on indoor smoking, and finally by non-smoking environments. Another study examined the persistence of THS in homes where smokers had previously resided (Matt, Quintana, Zakarian, et al., 2011). Nicotine levels on surfaces, dust, and in air decreased when smokers (who had been smoking for at least the past 5 or 6 months) moved out of these houses and non-smokers moved in. The decrease observed about 6 months after the new residents moved in was as follows: surface nicotine decreased from 75-85 µg /m^2 to 44-54 µg /m^2; dust nicotine levels decreased from 84-90 µg /g to 70-84 84-90 µg /g; and air nicotine levels fell from 78-90 µg /m^3 to 39-44 µg /m^3. However the levels were still higher than those found in homes where smokers had never resided. These studies indicated that THS is a potential hazard for people residing in THS environments even when no active smoking occurs. It is well documented that nicotine is very easily absorbed through the skin (Satora, Goszcz, Gomółka, & Biedroń, 2009). Recently, it

was also shown using an *in vitro* skin permeability assay that THS nicotine can permeate through the skin (Hammer, Fischer, Mueller, & Hoefer, 2011). These findings were confirmed by a field study that measured urine cotinine levels of children residing in THS homes where smokers had previously resided. The urine cotinine levels were about 40 ng/ml which is higher than found in children residing in homes where smoking never occurred (about 8 ng/ml) (Matt, Quintana, Zakarian, et al., 2011).

Other chemicals in tobacco smoke, such as 3-ethylpyridine, naphthalene, and cresol isomers, are adsorbed onto indoor surfaces and later desorbed into the air, raising the gas phase concentration hours after smoking has occurred (Singer et al., 2002) and making such volatilized chemicals available for inhalation. In addition to the above-mentioned compounds, tobacco specific nitrosamines (TSNAs) are formed as a result of chemical reactions between nicotine sorbed onto surfaces and gaseous nitrous acid (HONO) present in the atmosphere (Sleiman et al., 2010). These TSNAs include *N*-Nitrosonornicotine (NNN), 4-(methylnitrosamino)- 1-(3-pyridyl)-1-butanone (NNK), and 1-(N-methyl-N-nitrosamino)-1-(3-pyridinyl)-4-butanal) (NNA). While NNK is a constituent of tobacco smoke and is formed during curing and burning of tobacco (Hecht & Hoffmann, 1988), NNA has been reported only in THS (Sleiman et al., 2010).

Since TSNAs are known carcinogens, it is essential to determine if TSNAs in THS pose a significant cancer risk to the exposed population. The median cancer risk associated with non-dietary consumptions of the two known carcinogenic nitrosamines is higher for children aged 1-6 years in homes where smoking occurs (additional 9.6 cancer cases per 100,000 children exposed) as compared to homes where smoking does not occur (additional 3.3 cancer cases per 100,000 children exposed). This risk to

children is much higher than the risk to adults. In an entire life time (birth to 70 years of age), the median cancer risk is higher for people residing in THS environments (19 additional cases/100,000 people exposed) as compared to those in non-smoking environments (6.4 additional cases/100,000 people exposed) (Ramírez et al., 2014). Cancer risk through dermal exposure is also higher in people residing in THS environments. In an entire lifespan, the median cancer rate for people in THS environments is 21 additional cases/1,000,000 people exposed as compared to 7.3 cases/1,000,000 people not residing in THS environments (Ramírez et al., 2014). This study also revealed a correlation between nicotine and TSNA concentrations in smokers' homes, indicating that most of the TSNAs were formed due to conversion of nicotine from cigarette smoke and not from other sources, although other sources such as cooking and burning of fuel may contribute to the total TSNA levels inside a home.

It is widely accepted that there is no safe level of exposure to mainstream cigarette smoke and secondhand smoke (USDHHS, 2014). It is therefore extremely important to evaluate the effects that THS has on populations that are exposed, especially in light of documented effects of cigarette smoke on brain development in children (Dwyer, McQuown, & Leslie, 2009) and in the development of (Brown et al., 2003).

Health Impact of THS

While the effects of mainstream and secondhand smoke exposure on human health are well documented (USDHHS, 2014), the health effects of THS have not been extensively investigated. The existing evidence on tobacco smoke toxicity makes a strong argument for a rigorous experimental evaluation of THS toxicity (Matt,

Quintana, Destaillats, et al., 2011). It is now known that THS residue builds up in indoor environments where smoking occurs or has occurred and is available to people residing there. The impact of THS will depend on the route of exposure and is likely to be different for adults and children (Klaassen, 2013). Adults are likely to be exposed to THS VOCs through inhalation and to THS residue through dermal contact, but ingestion exposure is likely to be minimal. In contrast, for toddlers and young children, oral exposure will contribute significantly and might affect them in a manner that is different from inhalation and dermal exposure. Others factors that can contribute to differences in impact on adults and children are the lower body mass of children and higher sensitivity of developing organs, such as the brain, to environmental toxicants (Grandjean et al., 2008).

Recent studies have been carried out to evaluate THS toxicity, although few have given important insights in to the potential impact of THS on human health. One of the first studies conducted on THS toxicity used cigarette smoke residue collected on cotton fabric that was extracted in artificial human sweat.(Hammer, Fischer, Mueller, & Hoefer, 2011) THS extract from fabric exposed to 5 or 10 cigarettes impaired survival of murine fibroblasts in *in vitro* assays. Extracts from fabric exposed to 10 cigarettes also affected the size and cell density of human fibroblasts and caused vacuolization (Hammer et al., 2011). In another study, mice were exposed to THS by placing cotton upholstery material (cotton and fiber) and carpet exposed to cigarette smoke from two packs of cigarettes/day for 5 days inside their cages (Martins-Green et al., 2014). Adverse effects were observed on wound healing through up-regulation of keratin genes and genes involved in epithelial migration and down-regulation of inflammatory and immune response genes. The up-regulation of keratin genes is

responsible for causing wounds to become crusty and fragile thus preventing proper healing.

In addition to wound healing, the above mentioned study reported that THS affected the liver and lungs in mice. In THS exposed livers, lipid aggregates leading to steatosis or non-alcoholic fatty liver disease (NAFLD) were observed and total plasma lipids and triglycerides were elevated (Martins-Green et al., 2014). NAFLD adversely affects liver function, such as glucose, fatty acid and lipoprotein metabolism, and can also lead to drug induced toxicity at doses that would be considered therapeutic for a healthy individual (Tarantino et al., 2007). Martins-Green et al (2014) also reported adverse effects on lungs of mice exposed to THS. The walls of alveoli were disrupted in the alveolar sacs but were thicker in the alveoli in the terminal respiratory bronchioles, which can result in compromised lung function. The lungs also up-regulated pro-inflammatory cytokines and down-regulated anti-inflammatory cytokines. Mainstream cigarette smoke has also been shown to induce a pro-inflammatory response in the lungs (Kuschner, D'Alessandro, Wong, & Blanc, 1996). A pro-inflammatory response can potentially lead to fibrosis of the lungs (Bringardner, Baran, Eubank, & Marsh, 2009). Mice in the study by Martins-Green et al (2014) probably had exposure through dermal and oral routes as well as inhalation of VOCs present in THS. Therefore it is difficult to attribute the effects observed to a particular route of exposure.

Neurotoxicity and behavioral effects of THS have also been reported. Neurite length was reduced when bird neurons were treated with THS extracts from fabric exposed to 10 cigarettes *in-vitro* (Hammer et al., 2011). This is likely to have

implication for brain function and brain development during pre-natal to early childhood (Schwab, Kapfhammer, & Bandtlow, 1993). These findings are further supported by a behavioral study showing that mice exposed to THS were hyperactive compared to unexposed controls (Martins-Green et al., 2014). These data are consistent with numerous previous findings, which correlate tobacco smoke exposure to hyperactivity and other neurobehavioral disorders in children (Kabir, Connolly, & Alpert, 2011) (Law et al., 2003).

Reproductive toxicity of THS has also been addressed in several studies. Hammer et al (2011) described reproductive toxicity using artificial sweat extracts of THS from 5 or 10 cigarettes. Fertilized eggs zebrafish that were exposed to THS extract showed delayed onset of melanogenesis and pigmentation. Prior to hatching most of the treated embryos died, and those that survived had delayed hatching. Apart from delay in melanogenesis and hatching, metabolic effects, such as an increased heart rate in THS treated embryos, were also described in the above study (Hammer et al, 2011).

Another THS reproductive toxicity study focused on prenatal lung development in rat fetus lung explants exposed to NNK and NNA, two TSNAs present in THS (Rehan, Sakurai, & Torday, 2011). Lung explants from 19 day old rat embryos were cultured and treated with NNK and NNA at 10^{-5} M, 10^{-8} M and 10^{-11} M. Exposure of the developing lung to NNK and NNA caused disruption of homeostatic signaling by down-regulation of PPARγ and up-regulation of fibronectin and calponin. These alterations caused trans-differentiation of lipo-fibroblasts to myofibroblasts, thus preventing surfactant synthesis, which is needed for normal functioning of lung cells.

These alterations were accompanied by a decrease in the BCL-2/Bax ratio suggesting apoptosis (Rehan et al., 2011). These effects, which are highly detrimental to normal lung development, are especially significant since NNA is exclusively found in THS and is not present in secondhand smoke, making THS potentially more dangerous than secondhand smoke for fetal lung development. However, both SHS and THS are complex mixtures with thousands of chemicals and further studies are required to determine how their developmental toxicities compare. Moreover, exposure to THS and SHS is very different, with the uptake being much higher in case of SHS exposure; therefore a direct comparison cannot be made based on the above study.

TSNAs and polyaromatic hydrocarbons (PAHs) in cigarette smoke cause DNA damage that can lead to cancer (Hang, 2010;(DeMarini, 2004). NNN, NNK and NNA are known rodent carcinogens and mutagens (Hecht & Hoffmann, 1988) with NNK being a trans-placental carcinogen in Syrian golden hamsters (Correa, Joshi, Castonguay, & Schã, 1990). THS extract causes DNA strand breaks in liver cells when treated *in vitro* and tested by the alkaline single cell gel electrophoresis (SCGE) or comet assay (Hang et al., 2013). DNA damage to the liver can affect the overall metabolism of an organism as the liver is the most vital organ for metabolism and detoxification of drugs and environmental toxicants. THS increases oxidative DNA damage in hypoxanthine phosphoribosyl transferase 1 (HPRT 1) and polymerase β genes in cultured human lung epithelial cells (Hang et al., 2013) It can therefore be concluded that long term *in vivo* studies are needed to evaluate the genotoxic potential of THS. It is important to test THS genotoxicity in prenatal stages of development, which are generally more sensitive to lower doses of environmental pollutants than adults (Grandjean et al., 2008). Studies done to date demonstrate the need for further

research involving realistic THS levels and acute as well as chronic experiments focusing on multiple endpoints and cellular processes.

Remediation of THS: Why is it needed?

THS remediation refers to the removal of THS residue from indoor surfaces to reduce or eliminate exposure to the THS chemicals. It is important to identify the most efficient ways to eliminate THS residue such as washing or chemical treatment and then develop standardized protocols for remediation (Matt et al, 2011). A part of this dissertation deals with methods for removal of some THS chemicals, such as nicotine and its derivatives through washing with water and with organic solvents, such as methanol. An assessment of the toxicity of the extracts obtained after different methods of washing is also presented to gain an insight into the efficiency of these methods in the removal of toxicity.

Our methods can serve as a basis for developing further rigorous methods that can be applied to the remediation of property contaminated by THS, such as houses, office buildings, and cars before being rented or sold. Moreover, our methods can help parents to minimize exposure of their children to THS chemicals. This is extremely important as exposure of children and infants to THS are of prime concern and standardized protocols will help protect them from THS environments where smoking has occurred in the past.

Toxicological Evaluation using *In Vitro* Models

In vitro cellular models are valuable tools for investigating the adverse effects of environmental pollutants (Talbot 2008; Talbot and Lin 2012). The traditional use of

animal models for toxicity testing has several drawbacks, such as the need to sacrifice animals, costs associated with conducting animal studies, and the length of time required for obtaining meaningful results (Hartung, 2008). Animal models may not accurately predict the effects of chemicals on humans because of differences in animal and human physiology and metabolism (Shanks, Greek, & Greek, 2009) (Hartung, 2008) (Turpeinen et al., 2007). This limitation of animal testing can be eliminated by evaluating the effects of environmental toxicants on the survival and physiology of cells *in vitro* (Eisenbrand et al., 2002). *In vitro* toxicity testing has gained popularity and offers many advantages over animal models. Some advantages include the elimination of animal sacrifice, relatively low costs, shorter duration to get results, and the possibility of high-throughput screening of toxicants (Davila, Rodriguez, Melchert, & Acosta, 1998). The possibility of using human cells from different organs and stages of the life cycle can help gain insights into the difference in sensitivity of various organs and young vs. adult cells in a timely cost effective manner (Davila et al., 1998).

In vitro models are therefore effective alternatives to animal models based on the principle of the three Rs: refinement, reduction, and replacement (Russel and Burch, 2015). Refinement alternatives refer to those that will minimize pain and distress in animals, and replacement methods refer to the replacement of live animals with cellular models and human studies. Although *in vitro* models may not offer reduction, (which means knowing the statistically correct number of animals needed in a study to get relevant data), they are very effective as refinement and replacement models (Russel and Burch, 2015). Several in vitro methods have been developed and validated for use in toxicological evaluation and are known to be accurate and predictive. A classic example is the Embryonic Stem Cell Test for embryo toxicity validated by the

European Centre for the Validation of Alternative Methods (ECVAM) (Genschow et al., 2002). For the validation of this test, 20 chemicals classified as non-embryo toxic, weekly embryo toxic, and strongly embryo toxic based on data with animals/humans were tested on cultures of primary limb buds cells of rat embryos and mouse embryonic pluripotent stem cells across four different laboratories. The test was highly predictive of *in vivo* embryo toxicity. In 78% of the experiments the results were similar to those obtained from *in-vivo* studies (Genschow et al., 2002).

In vitro assays can be designed and developed to determine effects of toxicants on cell health in general, as well as to understand the effects on specialized cell function through the use of cells associated with a particular function (Ekwall, Silano, & Zucco, 1990). In addition to this, the mechanisms underlying the potency of a toxicant can be deciphered by using various cell based assays, such as microscopy, DNA, RNA, and protein analysis, biochemical analysis of enzyme levels, and metabolic profiling of cells, thereby eliminating or reducing the need for animal testing (Dix et al., 2007). Mechanistic studies involving particular cells of a target organ can also be effectively done through *in vitro* cell culture (Mossman, 1983). The ToxCast program initiated by the US Environmental Protection Agency (EPA) is an example of high-throughput screening of environmental toxicants using *in vitro* assays and has evaluated over 2000 compounds found in industrial and consumer products and food additives using *in vitro* cell based toxicity assays (USEPA, 2015).

Cell Types Used for Evaluation of THS Toxicity

Different cell types have been used in the present study including cells from the brain, lung and skin. These cells are valuable tools for *in vitro* toxicity assays and were chosen to represent the organs that are most likely to be affected by THS.

Mouse neural stem cells (mNSC): Isolated from the neonatal mouse cerebellum, these cells represent stem cells from the neonatal brain, which is still undergoing development and is sensitive to environmental toxicants. These cells were immortalized using retrovirus mediated transduction of the c-myc oncogene (Ryder, Snyder, & Cepko, 1990) and are well suited for *invitro* testing due to their rapid growth rate and ease of culturing. Since cigarette smoke affects brain development (Dwyer et al., 2009) (Yolton, Dietrich, Auinger, Lanphear, & Hornung, 2004), it is important to evaluate the effects of THS on the developing brain. Infants and young children are at risk of exposure to THS through dermal and oral contact and through inhalation of VOCs that are emitted from THS on indoor surfaces. We have used mNSC to evaluate the toxicity of THS and to identify the VOCs in THS that are cytotoxic. In addition to being suitable for *in vitro* cytotoxicity screens, this cell type is highly useful for studying mitochondrial toxicity due to the distinct punctate appearance of its mitochondria, which. makes it possible to quantitatively evaluate the effects of toxicants on mitochondrial morphology, detect stress responses in mitochondria, and evaluate disruption in the balance

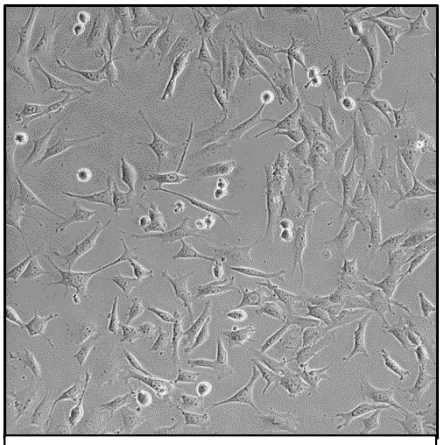

Fig 1.4. Mouse neural stem cells (mNSC) obtained from neonatal mouse cerebellum and immortalized using myc gene transduction.

between mitochondrial fission and fusion. mNSC have therefore has been used extensively for the studies reported in this dissertation.

Human pulmonary fibroblasts (hPF) and human aveolar epithelial cells (A549): hPF are primary cells, which have not been immortalized, that were isolated from the adult human lung (ScienCell). hPF have a variety of functions in the lung such as secretion

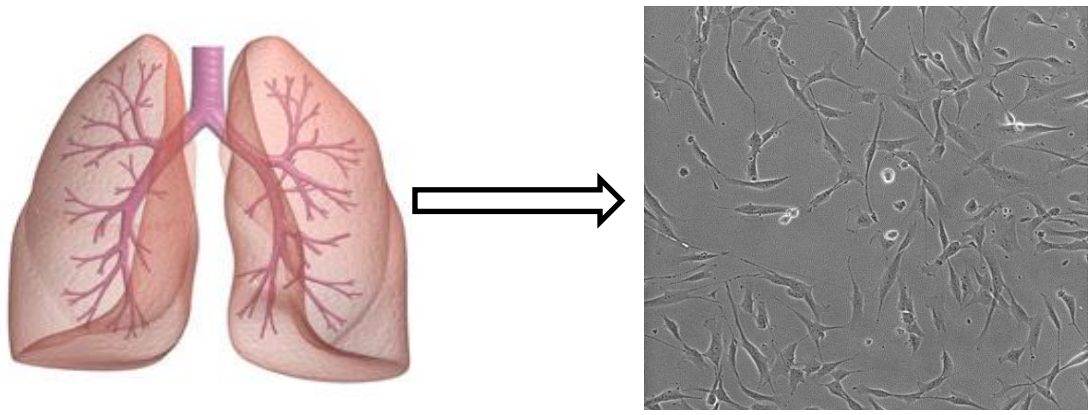

Fig 1.5. Human pulmonary fibroblasts (hPF) isolated from adult lung. Lung image obtained from http://www.hsmc.co.uk/

of type III collagen and elastin and formation of the extracellular matrix. A549 cells area lungadenocarcinoma derived cell line isolated from a 58 year old Caucasian male. They exhibit epithelial morphology in culture. Effects of toxicants on these cell types *in vitro*can give insights into their potential effect on lung function in response to toxicant exposure. We have used A549 cells to test the effects of VOCs that were identified in THS (Sleiman et al., 2014) because inhalation of these VOCs is a major route of THS exposure in children and adults alike. VOCs with the maximum number of Disability Adjusted Life Years (DALYs), as reported by Sleiman et al (2014), were tested on these

cell types. Their sensitivity to the VOCs was compared, and the most cytotoxic VOCs have been identified.

Human dermal fibroblasts (hDF): These are primary cells isolated from the forearm skin of a 56 year old Caucasian female (Promo Cell) and serve as a model for adult skin. These cells are used to assess THS toxicity because skin is the first organ that comes in contact with THS residue settled on surfaces. hDFs were used for testing

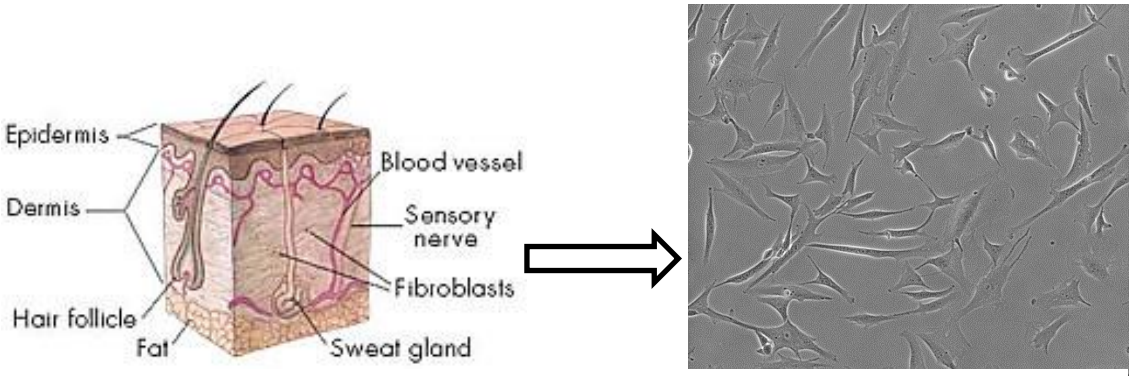

Fig 1.6. Human dermal fibroblasts (hDFs) obtained from the forearm of an adult female. Diagram of human skin layers obtained from the National Institute of General Medical Sciences Web site.

cytotoxicity and genotoxicity of the water soluble components of THS residue which was generated using realistic levels of cigarette smoke exposures to mimic cigarette smoking inside a car. Fibroblasts were chosen because: (1) they are easy to culture and have a faster growth rate than other cell types, such as keratinocytes and are therefore well suited for toxicity screening and (2) Adverse effects on fibroblasts affect the normal physiology of the skin since fibroblasts secrete growth factors that are required for wound healing (Werner, Krieg, & Smola, 2007).

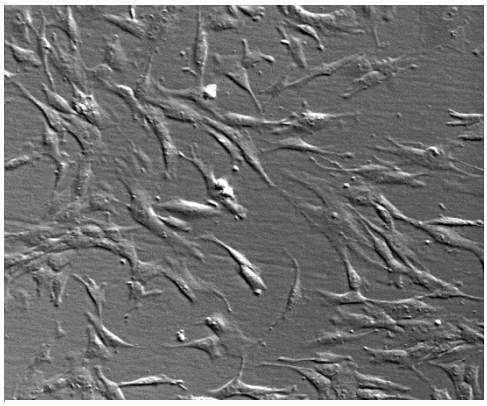

Fig 1.7. Human embryonic palatal mesenchymal cells (hEPM) obtained from a female fetus.

Human palatal mesenchyme cells (hPM): These cells were obtained from the palate of a female fetus and show a fibroblast-like morphology when cultured. These cells model the palate of a fetus/infant which is likely to be directly exposed to THS in case of oral exposure through mouthing of objects having THS residue. These cells were used to determine if the cells in the palate would be more sensitive than dermal fibroblasts.

Design of Thirdhand Smoke Generation Experiments:

Three different experimental designs were used for THS generation for conducting the studies described throughout this dissertation. We used controlled sidestream smoke exposures to generate THS deposits on various different fabrics used in homes and in cars. These include natural fabrics, such as cotton terrycloth, and synthetic fabrics such as polyester, car seat cover material, and car carpet. These fabrics were chosen because they are widely used in home and car upholstery and can accumulate smoke over many years inside a smoker's home or car. It is therefore important to investigate how these fabrics behave in terms of adsorption of cigarette smoke constituents and how readily they release these chemicals, therefore making them available for exposure through dermal, oral and inhalation routes (Matt et al, 2011).

In the first THS generation experiment, cotton terrycloth was exposed to cigarette smoke in a smoke generation chamber which is the size of a real life room and

is ventilated to allow for exchange of air and volatile organic compounds (VOCs) from cigarette smoke (S. F. Schick et al., 2014). Terrycloth was exposed to cigarette smoke from about 133 Marlboro Red cigarettes for over 11 months.

The second THS generation experiment was done using car seat cover and car carpet material placed inside acrylic chambers. This experiment models a car and the smoke exposures were scaled down to simulate exposure from 20 cigarettes over 8 hours inside a car for 60 days. These acrylic chambers were covered but ventilation ports allowed free exchange of air and VOCs. The chambers were placed outdoors to mimic a car, which would be exposed to sunlight and other outdoor conditions

In the third experiment, terrycloth was exposed to cigarette smoke in the same in-door chamber described above, but this experiment was conducted in a more controlled manner over 1 year with a batch of fabric being removed from the chamber approximately every month. This was done to understand the dynamics of THS accumulation and how cytotoxicity varies with time of accumulation the levels of toxicity of its aqueous extract.

The above experiments mimic different situations, but were designed to address two basic aspects of THS: toxicity and remediation, as have been described in the earlier sections of this introduction.

Assays used for In-Vitro Toxicological Evaluation

A wide range of *in vitro* assays have been used throughout this dissertation to evaluate toxicity of THS. These include assays for cell viability, assessment of cell morphology, genotoxicity, and mitochondrial toxicity.

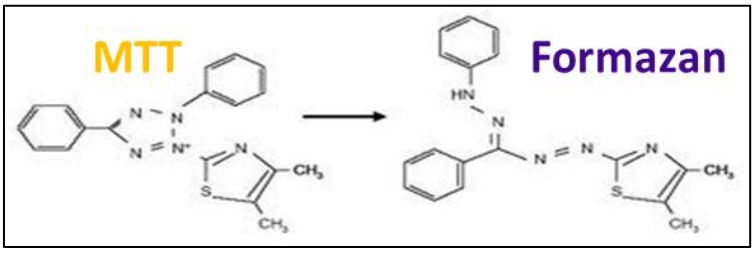

Fig 1.8. Conversion of MTT to insoluble formazan through the action of mitochondrial reductase of metabolically active cells is the basis of the MTT assay.

MTT assay: The MTT assay is spectrophotometric assay that is usually the first step towards determining the effects of a treatment on cell survival in response to a toxicant. It relies on the metabolism of a tetrazolium salt called 3-(4,5-dimethylthiazol-2-yl)-2,5-diphenyltetrazolium bromide by mitochondrial reductases of metabolically active cells. MTT is converted to a purple colored insoluble formazan that absorbs light at 560 nm.

Cell viability is determined by the intensity of purple color at the end of an experiment (Mossman, 1983). This assay has been widely used throughput this dissertation to obtain dose response curves and determine which doses to use for other more sophisticated assays. The MTT assay is also used as medium to high throughput assay to screen multiple chemicals on various cell types. A cell counting method based on transmittance through the cell suspension was developed. This method makes cell counting rapid and more accurate as compared to the traditional hemocytometer method.

Live cell imaging assay: Live cell imaging has been used extensively to look at the effects of THS treatment on morphology and the rate of proliferation. These

experiments were done using the Nikon BioStation CT, which is a high content incubator with 5% CO_2 and 95% relative humidity where cells are incubated at 37°C. The incubator has a camera which is used to capture images of cells at a desired frequency. These images are then analyzed visually for effects on morphology or quantified for rate of proliferation using CL quant software (Talbot et al., 2014).

Fluorescent staining and microscopy: Fluorescent labeling was used to visualize antigens or particular organelles in cells through use of antibodies or organelle specific probes. on The cytoskeletal proteins, actin and tubulin, were evaluated using fluorophore labeled phalloidin (a molecule that binds to actin filaments) and anti-tubulin antibody, respectively. Fluorescent microscopy was also used to evaluate mitochondrial toxicity using MitoTracker Red CMXRos, mitochondria specific probe and Mitosox, a probe for superoxide anions.

Polymerase chain reaction (PCR): PCR is widely used in toxicity studies to determine the effects of toxicants on expression of genes likely to be affected by toxicants (Walker, 2001). RT^2 profiler arrays were used to identify gene targets of THS and its component acrolein. These arrays are based on real time PCR and each consisted of 84 different genes related to specific cellular processes. RT- PCR was used as a follow-up to check the accuracy of RT^2 profiler array plates.

Single Cell Gel Electrophoresis (Comet) Assay: The comet assay is routinely used for genotoxicity testing. It is based on the fact that damaged DNA with strand breaks is easily broken and travels towards the anode more readily than intact DNA when subjected to an electric field (Tice et al., 2000). Single cells treated with the toxicant are encapsulated in agarose gel and subjected to electrophoresis. Damaged

DNA with strand breaks flows out of the cells and appears as comet tails when stained with a nucleic acid specific dye like SYBR green. The length and intensity of comet tails is then scored using software like CometScore to quantify extent of DNA damage. The alkaline comet assay that detects single strand breaks was used in this study to evaluate genotoxicity, since THS contains carcinogens such as TSNAs.

Scope of Dissertation

Chapter 2 describes a protocol that was developed to use 96 well plate assays for cytotoxicity testing and a cell counting method based on light transmittance for the adaptation of stem cells to 96 well plate assays. The counting method described in this chapter was used throughout this dissertation for performing experiments with cells.

Chapter 3 deals with the development of a protocol for extracting THS from natural (cotton) and synthetics (polyester) fabrics. Extraction was carried out using various methods and the chemical composition of extracts was determined. This chapter compares the amount of chemicals retained and released by the various fabrics. The efficiency ofxtraction protocols using different solvents is also described.. Finally, the chapter describes a theoretical model for the intake levels of nicotine and tobacco related nitrosamines from THS exposed fabrics by toddlers and adults.

Chapter 4 describes the cytotoxicity of THS to mNSC and compares fresh versus aged THS. It also deals with the cytotoxicity of volatile organic compounds present in THS to mNSC and adult lung cells. Acrolein emerged as the most cytotoxic VOC. Its mode of action and effect on genes regulating cell cycle progression is reported.

Chapter 5 describes two THS generation experiments, one performed outdoors (car simulation experiment) and one indoors (exposure chamber experiment). The chapter shows that THS produced from low levels of cigarette smoke was genotoxic to mNSC and adult skin cells. Also, cytotoxicity increases with increased cigarette smoke exposure and decreases with aging. The addition of protein to extraction medium enhanced the extraction of cytotoxic THS chemicals.

The focus of Chapter 6 is mitochondrial toxicity of sub-lethal concentrations of THS. These concentrations were tested for impact on mitochondrial morphology, membrane potential, ATP generation and oxidative stress. This chapter also describes the effect of THS on transcription of genes related to mitochondrial function and how these genes could be responsible for the other observed effects.

Chapter 7 summarizes the key findings of this project.

References:

American Cancer Society. Health Risks of Secondhand Smoke. (last updated 2015 November 13; accessed 2015 November 30).

Adams, J. D., O'Mara-Adams, K. J., & Hoffmann, D. (1987). Toxic and carcinogenic agents in undiluted mainstream smoke and sidestream smoke of different types of cigarettes. *Carcinogenesis*, *8*(5), 729–731.

Afridi, H. I., Kazi, T. G., Kazi, N. G., Jamali, M. K., Arain, M. B., Sirajuddin, … Shah, A Q. (2010). Evaluation of cadmium, lead, nickel and zinc status in biological samples of smokers and nonsmokers hypertensive patients. *Journal of Human Hypertension*, *24*(1), 34–43. http://doi.org/10.1038/jhh.2009.39

Breton, C. V, Byun, H.-M., Wenten, M., Pan, F., Yang, A., & Gilliland, F. D. (2009). Prenatal tobacco smoke exposure affects global and gene-specific DNA methylation. *American Journal of Respiratory and Critical Care Medicine*, *180*(5), 462–7. http://doi.org/10.1164/rccm.200901-0135OC

Bringardner, B. D., Baran, C. P., Eubank, T. D., & Marsh, B. (2009). NIH Public Access, *10*(2), 287–301. http://doi.org/10.1089/ars.2007.

Brown, B.G., Borschke, A.J., Dolittle, D.J. (2003). An analysis of the role of tobacco-specific nitrosamines in the carcinogenicity of tobacco smoke. Nonlinearity in Biology Toxicology Medicine, 1(2), 179–198

Centers for Disease Control and Prevention. Smoking and Cancer [last updated 2015 September 1; accessed 2015 November 22].

Chiba, M., & Masironi, R. (1992). Toxic and trace elements in tobacco and tobacco smoke. *Bulletin of the World Health Organization*, *70*(2), 269–275.

Correa, E., Joshi, P. A., Castonguay, A., & Schã, H. M. (1990). The Tobacco-specific Nitrosamine 4- (Methylnitrosamino) -1- (3-pyridyl) -1-butanone Is an Active Transplancental Carcinogen in Syrian Golden Hamsters Is an Active Transplacental Carcinogen in Syrian Golden Hamsters, 3435–3438.

Cupul-Uicab, L. a., Skjaerven, R., Haug, K., Melve, K. K., Engel, S. M., & Longnecker, M. P. (2012). In utero exposure to maternal tobacco smoke and subsequent obesity, hypertension, and gestational diabetes among women in the MoBa cohort. *Environmental Health Perspectives*, *120*(3), 355–360. http://doi.org/10.1289/ehp.1103789

Davila, J. C., Rodriguez, R. J., Melchert, R. B., & Acosta, D. (1998). Predictive value of in vitro model systems in toxicology. *Annu Rev Pharmacol Toxicol*, *38*, 63–96. http://doi.org/10.1146/annurev.pharmtox.38.1.63

DeMarini, D. M. (2004). Genotoxicity of tobacco smoke and tobacco smoke condensate:

a review. *Mutation Research*, *567*(2-3), 447–74. http://doi.org/10.1016/j.mrrev.2004.02.001

Dix, D. J., Houck, K. a., Martin, M. T., Richard, A. M., Setzer, R. W., & Kavlock, R. J. (2007). The toxcast program for prioritizing toxicity testing of environmental chemicals. *Toxicological Sciences*, *95*(1), 5–12. http://doi.org/10.1093/toxsci/kfl103

Doll, R., & Hill, A. B. (1950). Smoking and Carcinoma of the Lung. *British Medical Journal*, *2*(4682), 739–748. Retrieved from http://www.ncbi.nlm.nih.gov/pmc/articles/PMC2038856/

Dwyer, J. B., McQuown, S. C., & Leslie, F. M. (2009). The dynamic effects of nicotine on the developing brain. *Pharmacology & Therapeutics*, *122*(2), 125–39. http://doi.org/10.1016/j.pharmthera.2009.02.003

Eisenbrand, G., Pool-Zobel, B., Baker, V., Balls, M., Blaauboer, B. ., Boobis, a, … Kleiner, J. (2002). Methods of in vitro toxicology. *Food and Chemical Toxicology*, *40*(2-3), 193–236. http://doi.org/10.1016/S0278-6915(01)00118-1

Ekwall, B., Silano, V., & Zucco, F. (1990). Chapter 7 - Toxicity Tests with Mammalian Cell Cultures. *Short-Term Toxicity Tests for Non-Genotoxic Effects*, 75–98.

Fortmann, A. L., Romero, R. a, Sklar, M., Pham, V., Zakarian, J., Quintana, P. J. E., … Matt, G. E. (2010). Residual tobacco smoke in used cars: futile efforts and persistent pollutants. *Nicotine & Tobacco Research : Official Journal of the Society for Research on Nicotine and Tobacco*, *12*(10), 1029–36. http://doi.org/10.1093/ntr/ntq144

Fowles, J., & Dybing, E. (2003). Application of toxicological risk assessment principles to the chemical constituents of cigarette smoke. *Tobacco Control*, *12*(4), 424–430. http://doi.org/10.1136/tc.12.4.424

Freedman, N. D., Ph, D., Hartge, P., Sc, D., Lewis, C. E., Ockene, J. K., … Ph, D. (2015). Smoking and Mortality — Beyond Established Causes, 631–640. http://doi.org/10.1056/NEJMsa1407211

Genschow, E., Spielmann, H., Scholz, G., Seiler, A., Brown, N., Piersma, A., … Becker, K. (2002). The ECVAM international validation study on in vitro embryotoxicity tests: results of the definitive phase and evaluation of prediction models. European Centre for the Validation of Alternative Methods. *Alternatives to Laboratory Animals : ATLA*, *30*(2), 151–176.

Gieseke, C., & Talbot, P. (2005). Cigarette Smoke Inhibits Hamster Oocyte Pickup by Increasing Adhesion between the Oocyte Cumulus Complex and Oviductal Cilia. *Biology of Reproduction*, 73(3), 443-451.

Grandjean, P., Bellinger, D., Bergman, A., Cordier, S., Davey-Smith, G., Eskenazi, B., … Weihe, P. (2008). The faroes statement: human health effects of developmental exposure to chemicals in our environment. *Basic & Clinical Pharmacology & Toxicology*,

102(2), 73–5. http://doi.org/10.1111/j.1742-7843.2007.00114.x

Hammer, T. R., Fischer, K., Mueller, M., & Hoefer, D. (2011). Effects of cigarette smoke residues from textiles on fibroblasts, neurocytes and zebrafish embryos and nicotine permeation through human skin. *International Journal of Hygiene and Environmental Health*, *214*(5), 384–91. http://doi.org/10.1016/j.ijheh.2011.04.007

Hang, B. (2010). Formation and repair of tobacco carcinogen-derived bulky DNA adducts. *Journal of Nucleic Acids*, *2010*, 709521. http://doi.org/10.4061/2010/709521

Hang, B., Sarker, A. H., Havel, C., Saha, S., Hazra, T. K., Schick, S., … Gundel, L. a. (2013). Thirdhand smoke causes DNA damage in human cells. *Mutagenesis*, *28*(4), 381–91. http://doi.org/10.1093/mutage/get013

Hartung, T. (2008). Thoughts on limitations of animal models. *Parkinsonism and Related Disorders*, *14*(SUPPL.2), 83–85. http://doi.org/10.1016/j.parkreldis.2008.04.003

Hecht, S. S., Carmella, S. G., Le, K.-A., Murphy, S. E., Boettcher, A. J., Le, C., … Hennrikus, D. J. (2006). 4-(Methylnitrosamino)-1-(3-Pyridyl)-1-Butanol and Its Glucuronides in the Urine of Infants Exposed To Environmental Tobacco Smoke. *Cancer Epidemiology, Biomarkers & Prevention : A Publication of the American Association for Cancer Research, Cosponsored by the American Society of Preventive Oncology*, *15*(5), 988–92. http://doi.org/10.1158/1055-9965.EPI-05-0596

Hecht, S. S., & Hoffmann, D. (1988). Tobacco-specific nitrosamines, an important group of carcinogens in tobacco and tobacco smoke. *Carcinogenesis,* 9 (6), 875-884. doi: 10.1093/carcin/9.6.875.

IARC. (2012). Second-hand tobacco smoke. *IARC Monographs on the Evaluation of Carcinogenic Risks to Humans*, *100 E*, 215–265.

Janson, C. (2004). The effect of passive smoking on respiratory health in children and adults. *The International Journal of Tuberculosis and Lung Disease : The Official Journal of the International Union against Tuberculosis and Lung Disease*, *8*(5), 510–6.

Klaassen, K. (Ed.). (2013). *Casarett & Doull's Toxicology: The Basic Science of Poison* (8th ed.). New York, New York: McGraw-Hill.

Kabir, Z., Connolly, G. N., & Alpert, H. R. (2011). Secondhand smoke exposure and neurobehavioral disorders among children in the United States. *Pediatrics*, *128*(2), 263–270. http://doi.org/10.1542/peds.2011-0023

Kasprzak, K. S., Sunderman, F. W., & Salnikow, K. (2003). Nickel carcinogenesis. *Mutation Research - Fundamental and Molecular Mechanisms of Mutagenesis*, *533*(1-2), 67–97. http://doi.org/10.1016/j.mrfmmm.2003.08.021

Khader, Y. S., Al-Akour, N., AlZubi, I. M., & Lataifeh, I. (2011). The Association Between Second Hand Smoke and Low Birth Weight and Preterm Delivery. *Maternal and Child*

Health Journal, *15*(4), 453–459. http://doi.org/10.1007/s10995-010-0599-2

Knoll, M., Shaoulian, R., Magers, T., & Talbot, P. (1995) Ciliary beat frequency of hamster oviducts is decreased *in vitro* by exposure to solutions of mainstream and sidestream cigarette smoke. *Biology of Reproduction*, 53, 29-37.

Knoll, M., & Talbot, P. (1998). Cigarette smoke inhibits oocyte cumulus complex pick-up by the oviduct in vitro independent of ciliary beat frequency. *Reproductive Toxicology,* 12, 57-68.

Kondraganti, S. R., Fernandez-Saluguero, P., Gonzalez, F. J., Ramos, K. S., Jiang, W., & Moorthy, B. (2003). Polycyclic aromatic hydrocarbon-inducible DNA adducts: Evidence by 32P-postlabeling and use of knockout mice for AH receptor-independent mechanisms of metabolic activation in vivo. *International Journal of Cancer*, *103*(1), 5–11. http://doi.org/10.1002/ijc.10784

Kuschner, W. G., D'Alessandro, a., Wong, H., & Blanc, P. D. (1996). Dose-dependent cigarette smoking-related inflammatory responses in healthy adults. *European Respiratory Journal*, *9*(10), 1989–1994. http://doi.org/10.1183/09031936.96.09101989

Launay, J. M., Del Pino, M., Chironi, G., Callebert, J., Paoc'h, K., Mégnien, J. L., … Rendu, F. (2009). Smoking induces long-lasting effects through a monoamine-oxidase epigenetic regulation. *PLoS ONE*, *4*(11). http://doi.org/10.1371/journal.pone.0007959

Law, K. L., Stroud, L. R., LaGasse, L. L., Niaura, R., Liu, J., & Lester, B. M. (2003). Smoking during pregnancy and newborn neurobehavior. *Pediatrics*, *111*(6 Pt 1), 1318–1323. http://doi.org/10.1542/peds.111.6.1318

Lee, K., Xue, J., Geyh, A. S., Özkaynak, H., Leaderer, B. P., Weschler, C. J., & Spengler, J. D. (2002). Nitrous acid, nitrogen dioxide, and ozone concentrations in residential environments. *Environmental Health Perspectives*, *110*(2), 145–149. http://doi.org/10.1289/ehp.02110145

Lloyd, B., Lloyd, R. S., & Clayton, B. E. (1983). Effect of smoking, alcohol, and other factors on the selenium status of a healthy population. *Journal of Epidemiology and Community Health*, *37*(3), 213–217.

Lodovici, M., Akpan, V., Evangelisti, C., & Dolara, P. (2004). *Sidestream tobacco smoke as the main predictor of exposure to polycyclic aromatic hydrocarbons*. *Journal of Applied Toxicology*. http://doi.org/10.1002/jat.992

Martin, J. a, Hamilton, B. E., Ventura, S. J., Menacker, F., Park, M. M., & Sutton, P. D. (2002). Births: final data for 2001. *National Vital Statistics Reports : From the Centers for Disease Control and Prevention, National Center for Health Statistics, National Vital Statistics System*, *51*(2), 1–102.

Martins-Green, M., Adhami, N., Frankos, M., Valdez, M., Goodwin, B., Lyubovitsky, J., … Curras-Collazo, M. (2014). Cigarette smoke toxins deposited on surfaces:

implications for human health. *PloS One*, *9*(1), e86391. http://doi.org/10.1371/journal.pone.0086391

Matt, G. E., Quintana, P. J. E., Destaillats, H., Gundel, L. a, Sleiman, M., Singer, B. C., … Hovell, M. F. (2011). Thirdhand tobacco smoke: emerging evidence and arguments for a multidisciplinary research agenda. *Environmental Health Perspectives*, *119*(9), 1218–26. http://doi.org/10.1289/ehp.1103500

Matt, G. E., Quintana, P. J. E., Zakarian, J. M., Fortmann, A. L., Chatfield, D. a, Hoh, E., … Hovell, M. F. (2011). When smokers move out and non-smokers move in: residential thirdhand smoke pollution and exposure. *Tobacco Control*, *20*(1), e1. http://doi.org/10.1136/tc.2010.037382

Mossman, B. T. (1983). In vitro approaches for determining mechanisms of toxicity and carcinogenicity by asbestos in the gastrointestinal and respiratory tracts. *Environmental Health Perspectives*, *VOL. 53*, 155–161. http://doi.org/10.1289/ehp.8353155

Munters, E., & Nawrot, T. S. (2011). An Epidemiological Appraisal of Smoking - Related Outcomes, *42*.

Navas-Acien, A., Selvin, E., Sharrett, a R., Calderon-Aranda, E., Silbergeld, E., & Guallar, E. (2004). Lead, cadmium, smoking, and increased risk of peripheral arterial disease. *Circulation*, *109*(25), 3196–3201. http://doi.org/10.1161/01.CIR.0000130848.18636.B2

Neuman, R. J., Lobos, E., Reich, W., Henderson, C. a., Sun, L.-W., & Todd, R. D. (2007). Prenatal Smoking Exposure and Dopaminergic Genotypes Interact to Cause a Severe ADHD Subtype. *Biological Psychiatry*, *61*(12), 1320–1328. http://doi.org/10.1016/j.biopsych.2006.08.049

Papastefanou, C. (2009). Radioactivity of tobacco leaves and radiation dose induced from smoking. *International Journal of Environmental Research and Public Health*, *6*(2), 558–567. http://doi.org/10.3390/ijerph6020558

Petrick, L. M., Sleiman, M., Dubowski, Y., Gundel, L. a., & Destaillats, H. (2011). Tobacco smoke aging in the presence of ozone: A room-sized chamber study. *Atmospheric Environment*, *45*(28), 4959–4965. http://doi.org/10.1016/j.atmosenv.2011.05.076

Pouli, A. E., Hatzinikolaou, D. G., Piperi, C., Stavridou, A., Psallidopoulos, M. C., & Stavrides, J. C. (2003). The cytotoxic effect of volatile organic compounds of the gas phase of cigarette smoke on lung epithelial cells. *Free Radical Biology and Medicine*, *34*(3), 345–355. http://doi.org/10.1016/S0891-5849(02)01289-3

Prescott, S. L. (2008). Effects of early cigarette smoke exposure on early immune development and respiratory disease. *Paediatric Respiratory Reviews*, *9*(1), 3–9; quiz 10. http://doi.org/10.1016/j.prrv.2007.11.004

Russell, W., & Burch, R. (2015). *The Principles of Humane Experimental Technique*. Baltimore, Maryland: Johns Hopkins University.

Ramírez, N., Özel, M. Z., Lewis, A. C., Marcé, R. M., Borrull, F., & Hamilton, J. F. (2014). Exposure to nitrosamines in thirdhand tobacco smoke increases cancer risk in non-smokers. *Environment International*, *71*, 139–147. http://doi.org/10.1016/j.envint.2014.06.012

Rehan, V. K., Sakurai, R., & Torday, J. S. (2011). Thirdhand smoke: a new dimension to the effects of cigarette smoke on the developing lung. *American Journal of Physiology. Lung Cellular and Molecular Physiology*, *301*(1), L1–8. http://doi.org/10.1152/ajplung.00393.2010

Rodgman, A., & Perfetti, T. A. (2012). *The Chemical Components of Tobacco and Tobacco Smoke*. CRC Press. Retrieved from https://books.google.com/books?id=RiwSYFgZ2fEC

Roton, C. De, Wiernik, a, Wahlberg, I., Vidal, B., & Match, S. (2005). Factors Influencing the Formation of Tobacco-Specific Nitrosamines in French Air-Cured Tobaccos in Trials and at the Farm Level *, *21*(6).

Ryder, E. F., Snyder, E. Y., & Cepko, C. L. (1990). Establishment and characterization of multipotent neural cell lines using retrovirus vector-mediated oncogene transfer. *Journal of Neurobiology*, *21*(2), 356–375. http://doi.org/10.1002/neu.480210209

Sussan, T., & Biswal, S. (2011). Smoking and COPD and Other Respiratory Diseases. In D. Bernhard (Ed.), *Cigarette Smoke Toxicity: Linking Individual Chemicals to Human Diseases*. Hoboken, New Jersey: John Wiley & Sons.

Sasco, A. J., Secretan, M. B., & Straif, K. (2004). Tobacco smoking and cancer: a brief review of recent epidemiological evidence. *Lung Cancer*, *45, Supple*, S3–S9. http://doi.org/http://dx.doi.org/10.1016/j.lungcan.2004.07.998

Satora, L., Goszcz, H., Gomółka, E., & Biedroń, W. (2009). Green tobacco sickness in Poland. *Polskie Archiwum Medycyny Wewnetrznej*, *119*(3), 184–186. http://doi.org/10.1080/10599240802612661

Schick, S. (2011). Thirdhand smoke: here to stay. *Tobacco Control*, *20*(1), 1–3. http://doi.org/10.1136/tc.2010.040279

Schick, S. F., Farraro, K. F., Perrino, C., Sleiman, M., van de Vossenberg, G., Trinh, M. P., … Balmes, J. (2014). Thirdhand cigarette smoke in an experimental chamber: evidence of surface deposition of nicotine, nitrosamines and polycyclic aromatic hydrocarbons and de novo formation of NNK. *Tobacco Control*, *23*(2), 152–9. http://doi.org/10.1136/tobaccocontrol-2012-050915

Schwab, M. E., Kapfhammer, J. P., & Bandtlow, C. E. (1993). Inhibitors of neurite growth. *Annual Review of Neuroscience*, *16*, 565–595.

http://doi.org/10.1146/annurev.neuro.16.1.565

Sekizawa, S.-I., Joad, J. P., Pinkerton, K. E., & Bonham, A. C. (2010). Secondhand tobacco smoke exposure differentially alters nucleus tractus solitarius neurons at two different ages in developing non-human primates. *Toxicology and Applied Pharmacology*, *242*(2), 199–208. http://doi.org/10.1016/j.taap.2009.10.009

Shanks, N., Greek, R., & Greek, J. (2009). Are animal models predictive for humans? *Philosophy, Ethics, and Humanities in Medicine : PEHM*, *4*, 2. http://doi.org/10.1186/1747-5341-4-2

Shimada, T., & Fujii-Kuriyama, Y. (2004). Metabolic activation of polycyclic aromatic hydrocarbons to carcinogens by cytochromes P450 1A1 and 1B1. *Cancer Science*, *95*(1), 1–6. http://doi.org/10.1111/j.1349-7006.2004.tb03162.x

Singer, B. C., Hodgson, A. T., & Nazaroff, W. W. (2002). Effect of sorption on exposures to organic gases from environmental tobacco smoke (ets) (January).

Sleiman, M., Gundel, L. a, Pankow, J. F., Jacob, P., Singer, B. C., & Destaillats, H. (2010). Formation of carcinogens indoors by surface-mediated reactions of nicotine with nitrous acid, leading to potential thirdhand smoke hazards. *Proceedings of the National Academy of Sciences of the United States of America*, *107*(15), 6576–81. http://doi.org/10.1073/pnas.0912820107

Sleiman, M., Logue, J. M., Luo, W., Pankow, J. F., Gundel, L. a, & Destaillats, H. (2014). Inhalable constituents of thirdhand tobacco smoke: chemical characterization and health impact considerations. *Environmental Science & Technology*, *48*(22), 13093–101. http://doi.org/10.1021/es5036333

Stedman, R. L. (1968). The chemical composition of tobacco and tobacco smoke. *Chemical Reviews*, *68*(2), 153–207. http://doi.org/10.1021/cr60252a002

Szabo, E., White, V., & Hayman, J. (2006). Can home smoking restrictions influence adolescents' smoking behaviors if their parents and friends smoke? *Addictive Behaviors*, *31*(12), 2298–2303. http://doi.org/10.1016/j.addbeh.2006.02.025

Talbot, P. (2008). In vitro assessment of reproductive toxicity of tobacco smoke and its constituents. *Birth Defects Research. Part C, Embryo Today : Reviews*, *84*(1), 61–72. http://doi.org/10.1002/bdrc.20120

Talbot, P., Zur Nieden,, N., Lin, S., Martinez, I., Guan, B., & Bhanu, B. (2014). Use of video bioinformatics tools in stem cell biolog. In S. Sahu & D. Casciano (Eds.), *Handbook of Nanotoxicology, Nanomedicine and Stem Cell Use in Toxicology* (pp. 379-402). West Sussex: John Wiley.

Tarantino, G., Conca, P., Basile, V., Gentile, A., Capone, D., Polichetti, G., & Leo, E. (2007). A prospective study of acute drug-induced liver injury in patients suffering from non-alcoholic fatty liver disease. *Hepatology Research*, *37*(6), 410–415.

http://doi.org/10.1111/j.1872-034X.2007.00072.x

Tice, R. R., Agurell, E., Anderson, D., Burlinson, B., Hartmann, a, Kobayashi, H., … Sasaki, Y. F. (2000). Single Cell Gel / Comet Assay : Guidelines for In Vitro and In Vivo Genetic Toxicology Testing. *Environmental and Molecular Mutagenesis*, *35*(3), 206–21. Tobacco smoke and involuntary smoking (2012). Second-hand tobacco smoke. IARC Monographs on the Evaluation of Carcinogenic Risks to Humans, 100 E, 215–265.

Turpeinen, M., Ghiciuc, C., Opritoui, M., Tursas, L., Pelkonen, O., & Pasanen, M. (2007). Predictive value of animal models for human cytochrome P450 (CYP)-mediated metabolism: a comparative study in vitro. *Xenobiotica; the Fate of Foreign Compounds in Biological Systems*, *37*(12), 1367–1377. http://doi.org/10.1080/00498250701658312

USDHHS. (2004). Chapter 5 Reproductive and Developmental Effects from Exposure to Secondhand Smoke. *Surgeions General's Report: The Health Consequences of Involuntary Exposure of Tobacco Smoke*, 165–256.

USDHHS. (2014). The Health Consequences of Smoking—50 Years of Progress: A Report of the Surgeon General. Atlanta, GA: U.S. Department of Health and Human Services, Centers for Disease Control and Prevention, National Center for Chronic Disease Prevention and Health Promotion, Office on Smoking and Health.

USEPA. (2015). ToxCast & Tox21 Summary Files from invitrodb_v2. Retrieved from http://www2.epa.gov/chemical-research/toxicity-forecaster-toxcasttm-data on October 28, 2015. Data released October 2015.

Walker, N. J. (2001). Real-time and quantitative PCR: Applications to mechanism-based toxicology. *Journal of Biochemical and Molecular Toxicology*, *15*(3), 121–127. http://doi.org/10.1002/jbt.8

Wigand, J.S. (2006). Additives , cigarette design and tobacco product regulation. A report to: World Health Organization tobacco free initiative tobacco product regulation group, 1–45.

Werner, S., Krieg, T., & Smola, H. (2007). Keratinocyte-fibroblast interactions in wound healing. *The Journal of Investigative Dermatology*, *127*(5), 998–1008. http://doi.org/10.1038/sj.jid.5700786

Winickoff, J. P., Friebely, J., Tanski, S. E., Sherrod, C., Matt, G. E., Hovell, M. F., & McMillen, R. C. (2009). Beliefs about the health effects of "thirdhand" smoke and home smoking bans. *Pediatrics*, *123*(1), e74–e79. http://doi.org/10.1542/peds.2008-2184

Yolton, K., Dietrich, K., Auinger, P., Lanphear, B. P., & Hornung, R. (2004). Exposure to Environmental Tobacco Smoke and Cognitive Abilities among U.S. Children and Adolescents. *Environmental Health Perspectives*, *113*(1), 98–103.

Chapter 2: Adaptation of Stem Cells to 96-Well Plate Assays: Use of Human Embryonic and Mouse Neural Stem Cells in the MTT Assay

INTRODUCTION

Human embryonic stem cells (hESC) offer tremendous potential in toxicological studies and drug development (Talbot and Lin, 2011). Not only can hESC be adapted to rapid, inexpensive in vitro assays, but they also model prenatal stages of development and therefore can be used to evaluate risk during the most sensitive period of the life cycle (Grandjean et al., 2008) (Lin, Fonteno, Weng, & Talbot, 2010). However, hESC are difficult to adapt to 96-well plate assays because they survive best when plated as small colonies, which are difficult to count and plate accurately. To address this problem, two methods have been developed to carry out the MTT assay (Basic Protocol 2) using hESC. In the first (Basic Protocol 3), plating is done with Rho-associated kinase inhibitor (ROCKi); (Watanabe et al., 2007) (Ohgushi et al., 2010), which allows accurate counting and plating of single hESC and improves single-cell survival. The second method (Alternate Protocol) involves plating hESC as small colonies without the use of ROCKi, but with adaptations to enable accurate counting and plating of small colonies. In addition, the MTT assay was adapted for use with mouse neural stem cells (see Basic Protocol 1) to provide another stem cell model for toxicological evaluations. These protocols allow the MTT assay or other 96-well plate based assays to be carried out rapidly and accurately with high reproducibility between replicate experiments.

When performing these experiments, cells are incubated at 37°C with 5% CO_2 and 95% relative humidity. Cells are allowed to attach for 24 hr after plating, then

chemical treatment is given for 48 hr. MTT is added at the end of the treatment, and 2 hr later, absorbance readings are recorded. Human ESC are maintained in mTeSR medium with supplements, and mNSC are maintained in DMEM supplemented with 10% FBS, 5% horse serum, 1% penicillin/streptomycin, and 1% sodium pyruvate.

Three general procedures for using stem cells with the MTT assay (Basic Protocol 2) are presented. The protocol for mNSC (Basic Protocol 1), which is the easiest to perform, is presented first, followed by plating hESC with ROCKi (Basic Protocol 3), and concluding with hESC plated as small colonies (Alternate Protocol).

Basic Protocol 1: Preparing mNSC for the MTT Assay

This protocol begins with a description of the general procedure for growing mNSC in 25-cm^2 tissue culture flasks using sterile technique (Freshney, 2006). The cells are cultured at 37°C in an incubator with 5% CO_2 and 95% relative humidity. The protocol is adapted from a prior publication (Parker et al., 2005).

Prior to the MTT assay (Basic Protocol 2), it is necessary to determine cell concentration and generate a standard curve (Support Protocol 2). Single mNSC can be counted with a hemocytometer or spectrophotometer (Support Protocol 1). Hemocytometer counting is relatively time consuming, and the coefficient of variation (CV) is nearly 10%. In contrast, the spectrophotometric method using the standard curve generated in Support Protocol 2 is rapid and more accurate, with a CV of 1.5%. The use of a spectrophotometer requires setting up a standard curve (percentage transmittance versus cell concentration). Once the standard curve is established, the

spectrophotometric method provides a more accurate rapid means to determine cell concentration.

The method for generating a standard curve for percent transmittance versus cell concentration is described in Support Protocol 2. This will be used for adjusting cell concentration so that the desired number of cells can be plated in the MTT assay. A standard curve should be generated by individual labs following this protocol, as percent transmittance readings may vary with different spectrophotometers.

The MTT assay (see Basic Protocol 2) is based on plating 1250 mNSC/well in a 96-well plate over 72 hr of incubation. This cell number was chosen as the appropriate plating density for mNSC after plating different cell numbers from 1250/well through 20,000/well and adding MTT.

Materials

mNSC (*UNIT 2D.6*) growing in 25-cm^2 tissue culture flasks, Dulbecco's phosphate buffered saline pH 7.4 (DPBS; Invitrogen, cat. no.25200-056), 0.05% trypsin-EDTA (Invitrogen, cat. no. 25200-056) prepared in DPBS, mNSC culture medium (see recipe), 15-ml conical centrifuge tubes (BD Biosciences, cat. no. 352097), Centrifuge, 25-cm^2 (T-25) tissue culture flasks (Thermo Scientific, cat. no. 136196z).

1. Remove a 25-cm^2 culture flask of mNSC from the incubator and check its confluency with an inverted phase-contrast microscope. If the confluency is 70% to 80%, aspirate the mNSC culture medium from the flask. This protocol is based on having 70% to 80% confluency
2. Add 2 ml of DBPS along the side of the flask and swirl gently for 15 to 30 sec.
3. Remove the DPBS.

4. Add 2 ml of 0.05% trypsin-EDTA and place the flask in the incubator for 1 min.

5. Remove the flask from the incubator and gently tap it 3 to 4 times.

6. Add 3 ml of mNSC culture medium and mix gently so the cells come off the surface of the flask.

7. Transfer the cells to a 15-ml conical tube.

8. Centrifuge 2 min at 335.4 × *g*, room temperature.

9. Decant the supernatant gently, taking care that the pellet does not mix with the supernatant.

10. Add 2 ml of medium slowly along the side of the tube and mix to break up the pellet. This should be done very carefully and gently, so that the cells are not damaged. Cell concentration does not need to be determined at this point, assuming that the flask being passaged is 70% to 80% confluent.

11. Add 3 ml of mNSC culture medium to a new flask, and transfer 100 µl of the cell suspension to the flask.

12. Place the flask inside an incubator at 37°C with 5% CO_2 and 95% relative humidity.

13. Check every day to see if cells have reached 70% to 80% confluency

Support Protocol 1: Determining Cell Concentration with a Hemacytometer or a Spectrophotometer

Materials

75% ethanol, mNSC culture medium (see recipe), 0.4% trypan blue (optional; Invitrogen, cat. no. 15250), Hemocytometer, Microscope, Additional reagents and equipment for preparing cells for MTT assay with mNSC (Basic Protocol 1)

1. Clean a hemocytometer and its coverslip with 75% ethanol and allow them to dry.

2. Obtain a cell pellet as described in Basic Protocol 1.

3. Resuspend the pellet in 1 ml of mNSC culture medium.

4. Take 100 µl of this suspension and mix it with 900 µl of mNSC culture medium in a separate vial.

5. Take 10 µl of this suspension and pipet it onto both grids of a hemocytometer

6. Count the number of cells in the four sections of each grid, using a microscope, taking care to count only the live cells, which appear shiny and spherical, versus dead cells, which appear shriveled and dark.

0.4% trypan blue can be used to stain dead cells before placing cells on the hemocytometer to facilitate identification of live cells.

7. If cells are being counted for plating in the MTT assay, perform three counts for each cell suspension, because the cells will lose their viability if they remain in suspension for long.

It is best to complete counting within 5 min. In contrast, if cells are being counted to generate a standard curve, eight counts for each sample should be done, to minimize error in generating the curve.

8. Calculate the average of all the counts and obtain the cell concentration in the original suspension using the following formula: cells/ml = average count × 10,000.

Support Protocol 2: Standard Curve Generation for Counting Cells With a Spectrophotometer

Materials

mNSC culture (80% to 85% confluent; see Basic Protocol 1), Phosphate-buffered saline (PBS; e.g., Invitrogen) pH 7.4, mNSC culture medium (see recipe),

Spectrophotometer (e.g., Thermo Scientific BioMate), and cuvettes. Additional reagents and equipment for preparing and trypsinizing mNSC (Basic Protocol 1) and counting cells using a hemocytometer (Support Protocol 1)

1. Switch on the spectrophotometer before processing the cell sample and allow it to warm up.

2. Set it to 560 nm in the transmittance mode and use PBS as a blank.

3. Trypsinize a flask of mNSC that is 80% to 85% confluent according the procedures described in Basic Protocol 1 for culturing mNSC, and centrifuge to prepare a cell pellet.

4. Suspend the pellet in 1 ml of mNSC culture medium and mix gently.

5. Take the smallest volume that is sufficient for the cuvette being used and record the percent transmittance of this suspension at 560 nm.

6. Dilute a fraction of this cell suspension 1:2 using PBS, and record the percent transmittance at 560 nm.

7. Record percent transmittance readings in the same way for dilutions of 1:4. 1:8, 1:16, 1:32, 1:64, and 1:128.

All dilutions are made serially by adding PBS to the previous dilution.

8. Check the accuracy of percent transmittance readings by recording the value for the same dilution five times. *A CV of <5% is acceptable.*

9. Obtain cell counts for the dilutions 1:2, 1:4, 1:8, and 1:16 using a hemocytometer by the method described in Support Protocol 1, and calculate the cell concentration/ml for all dilutions.

10. Plot the cell concentration on the *x* axis of semi-log graph paper and percent transmittance values on the *y* axis.

11. Repeat the whole procedure three times on different days using different batches of cells.

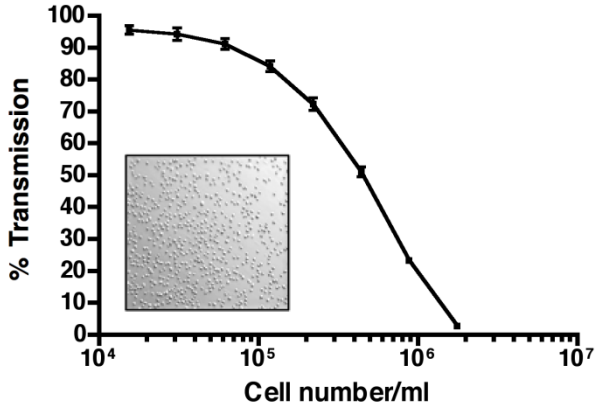

Figure 2.1 Standard curve for determining mNSC concentration. This curve was produced by averaging three experiments performed on different days using different batches of cells. Eight cell counts were obtained for dilutions 1:2, 1:4, 1:8, and 1:16 using a hemocytometer. Percent transmittance readings were obtained for the undiluted sample, as well as dilutions 1:2 through 1:128. The micrograph (insert) shows mNSC in suspension.

.

The curves generated on 3 days should be similar and can be averaged to produce a standard curve for future experiments with mNSC. Figure 2.1 shows an example of a standard curve generated for mNSC. Individual labs following this protocol should generate their own standard curve, as percent transmittance may vary with different spectrophotometers. This procedure can also be used with hESC and other cell types.

Support Protocol 3: Plating mNSC for The MTT Assay

Materials

mNSC culture medium (see recipe), mNSC culture (80% to 85% confluent; see Basic Protocol 1), Phosphate-buffered saline (PBS; e.g., Invitrogen) pH 7.4, 96-well plates (BD

Biosciences, cat. no. 353936). Additional reagents and equipment for preparing and trypsinizing mNSC (Basic Protocol 1).

1. Add 50 µl mNSC culture medium to all the wells being used in a 96-well plate.

2. Treat a flask of mNSC that is 80% to 85% confluent with trypsin as described in Basic Protocol 1.

3. Pellet cells as described in Basic Protocol 1, and resuspend in 1 ml of mNSC culture medium.

The pellet should be soft so that it can be easily resuspended in fresh medium.

4. Pipet 200 µl of this suspension into a separate vial and dilute1:4 or 1:8 with PBS.

These dilutions should fall on the linear part of the standard curve.

5. Measure percent transmittance using PBS as the blank

6. Determine the cell concentration of the dilution used from the standard curve, and multiply this value by the dilution factor to determine the concentration of cells in the stock suspension.

7. Calculate the dilution factor for plating cells at 1250 cells/well by the following formula:

Dilution factor = (cell concentration of undiluted sample)/25,000 cells/ml'

This dilution will give the concentration required to pipet 1250 cells in 50 µl from the diluted stock.

8. Dilute the cell suspension using culture medium.

9. Mix thoroughly and gently by swirling the vial containing the cells.

10. Take the plate containing medium from step 1 and add 50 µl of this cell suspension to each well of the 96-well plate. Flick the tube to resuspend cells before adding cells to each well. Do not resuspend by pipetting.

If more than one plate is being used, prepare cell dilutions separately for each plate.

11. Place the plate in an incubator at 37°C with 5% CO_2 and 95% relative humidity for 24 hr. Proceed to Basic Protocol 2.

Basic Protocol 2: MTT Assay

The MTT assay is a widely used cytotoxicity assay that relies on the conversion of yellow colored MTT to a purple insoluble formazan, which can be dissolved in DMSO. The absorbance of the formazan can be read at 570 nm (Mossman, 1983). The strength of the signal obtained can be used to measure cell viability, survival, or proliferation.

Materials

Test chemicals (e.g., phenol; Sigma, cat. no. W322318), mNSC culture medium (see recipe), mNSC (Support Protocol 3) or hESC (Basic Protocol 3 or Alternate Protocol) growing in 96-well plates, MTT (Sigma, cat. no. M5655-1G; stored in the dark; keep room lights off while working with MTT), Dimethylsulfoxide (DMSO; Fisher, cat. no. D128-500), 0.22-µm syringe filters (Pall Life Sciences, cat. no. pn4612), syringes (BD, cat. no. 309604), Microsoft Excel or equivalent spreadsheet software, GraphPad Prism or equivalent data analysis software.

Prepare plates

1. Prepare the highest dose of test chemical by dissolving it in culture medium.
2. Filter with a syringe under sterile conditions using a 0.22 µm filter.
3. Prepare all the lower doses by serially diluting the higher dose with culture medium.

4. Remove the 96-well plate containing the cells from the incubator after 24 hr of incubation.

5. Remove old medium from the wells carefully, without disturbing the cells.

6. Add 100 µl of fresh culture medium to the control wells.

7. Add 100 µl of the doses of test chemical to all the other wells.

8. Incubate the plate in an incubator at 37° C with 5% CO_2 and 95% relative humidity for 48 hr.

Perform MTT assay

9. Dissolve MTT at 5 mg/ml in PBS. Filter sterilize using a 0.22-µm filter

10. Add 20 µl of the 5 mg/ml MTT to each well, without removing medium.

11. Incubate for 2 hr in an incubator at 37° C with 5% CO_2 and 95% relative humidity.

12. Take out the plate and remove medium gently without touching the bottom of the wells, so as not to disturb the attached cell layer.

13. Place plate upside down on a paper towel for 1 min to completely drain the wells.

14. Add 100 µl DMSO to each well and let it sit at room temperature for 10 min.

15. Gently mix the DMSO in each well with a 10-µl pipet tip, taking care that no bubbles are introduced. Do not use a higher-volume pipet, as it may introduce bubbles.

16. Set the microplate reader to 570 nm and use DMSO as the blank, with absorbance set at 0.

17. Record absorbance for all the wells.

Perform data analysis

18. Enter the absorbance data into a Microsoft Excel spreadsheet and calculate percent- age of control for each dose

19. Enter these data into GraphPad or similar software and calculate the averages and standard deviations. Alternatively, Excel can be used for this.

20. Calculate the coefficient of variation (CV) for the control row labeled CN1 in the plate design shown in Figure 2.2. *A* CV higher than 10% indicates inconsistency in plating.

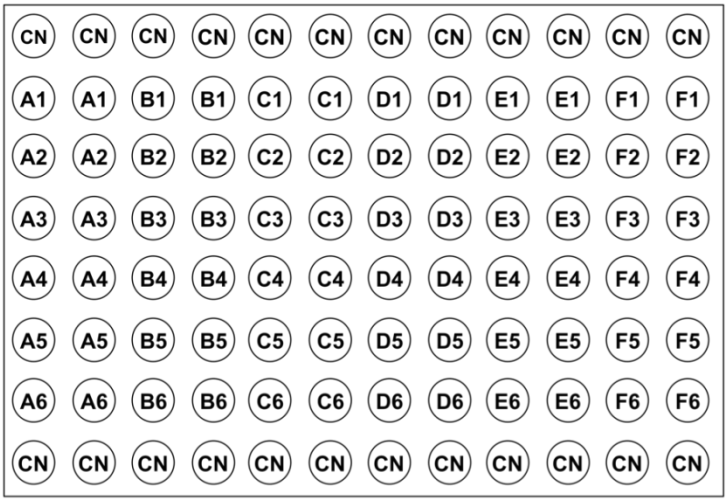

Figure 2.2 MTT plate design. Single, double, or triple replicates can be carried out. The top controls (CN) are used to generate the coefficient of variation for plating accuracy, and the bottom controls are used to assess the possibility of a vapor effect. The numbers 1 to 6 represent low to high doses plated. Letters A, B, etc. designate different test groups. In this design, six different chemicals can be tested in duplicate on one plate.

21. Check if the absorbance readings obtained for the control row CN2 are significantly different from CN1. A significant difference indicates vapor effect, as discussed in the Commentary.

22. Generate dose-response curves, with doses on the *x* axis and percentage of control on the *y* axis.

23. Calculate the IC_{50} values for each treatment, according to the instructions in the software.

24. Determine if any of the doses are significantly different than the control.

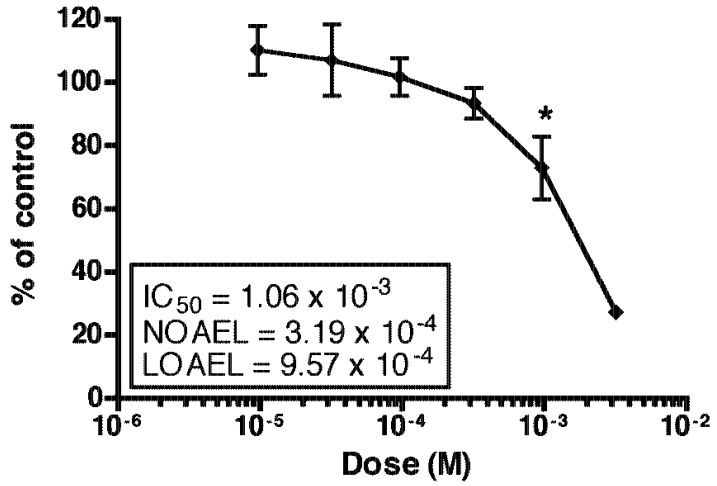

Figure 2.3 Dose-response curve showing the effect of phenol on mNSC. The x axis shows the doses tested, and the y axis shows the percent of the control (n = 3). IC_{50} = inhibitory concentration at 50%, LOAEL = lowest observed adverse effect level, NOAEL = no observable adverse effect level. * = $p<0.05$.

The highest dose that is not significantly different from the control is the NOAEL and the lowest dose that is significantly different from the control is the LOAEL. An example of a dose-response curve obtained with this protocol using mNSC treated with phenol is shown in Figure 2.3.

Support Protocol 4: Assay Validation for the MTT Assay with mNSC: Plate Uniformity and Signal Variability

The MTT assay needs to be validated for plate uniformity and signal variability arising due to drift or edge effects in the plate. This can be done using the Assay Guidance

Wiki software tool provided by NIH (*http://assay.nih.gov/assay/index.php/ Assay Validation 2011*). The assay is validated by choosing a high, mid, and low dose of a test chemical from the dose-response curve generated for that chemical. The tool checks if there is sufficient separation in signal obtained for the three doses, and if there is signal variability due to differential heating of plates in the incubator. Two sets of MTT experiments are done with these doses on two different days with two plates/ day. The plate design can be found at the NIH Chemical Genomics Center (NCGC) Web site. The MTT data obtained from both plates is entered into the NIH Assay Guidance Wiki software tool, which computes the CV for each dose and for signal separation. It also checks for edge effects and drift. This is a useful tool that gives an insight into factors that may affect readings in the assay.

Materials

mNSC, (mNSC culture medium (see recipe), test chemicals (e.g., phenol; Sigma, cat. no. W322318), MTT (Sigma, cat. no. M5655-1G) dissolved in PBS at 5 mg/ml. MTT should be stored in dark and room lights should be off, while working with MTT. DMSO (Fisher, cat. no. D128-500), 96-well plates (BD Biosciences, cat. no. 353936), NIH Assay Guidance Tool: download from *http://assay.nih.gov/assay/ index.php/Assay Validation 2011* (under Navigation menu), additional reagents and equipment for plating mNSC (Support Protocol 3) and, MTT assay (Basic Protocol 2)

1. Plate mNSC at 1250 cells/well, using a flask that is about 80% confluent, in two 96-well plates (as previously described in Support Protocol 3) and incubate for 24 hr in a 37°C incubator with 5% CO_2 and 95% relative humidity.

2. Prepare high, mid, and low doses of the test chemical (phenol is used in this example) in mNSC culture medium.

Table 2.1 Example of Results from the Plate Uniformity and Signal Variability Assay Validation for hESC and mNSC

Plate no. mNSC results	Required results	hESC results							
		1	2	3	4	1	2	3	4
Drift or edge effect	None	None	None	None	None	None	None	None	None
COV of low signal (high	All ≤20%	12.6	14.5	13.9	15.7	14.3	6.2	12.3	6.8
COV of mid	All ≤20%	4.6	8.8	3.9	4.5	5.25	5.8	6.1	9.9
COV of high signal (low	All ≤20%	4.4	6.9	4.3	4.5	4.8	5.9	5.1	4.0
Signal window	≥2	12.73	7.07	9.94	12.42	5.56	4.64	8.31	11.15
Z’	≥0.4	0.72	0.62	0.62	0.70	0.46	0.51	0.61	0.70
Inter-plate test	<2 fold shift	Yes	Yes	Yes	Yes	Yes	Yes	Yes	Yes
Inter-day test	<2 fold shift	Yes	Yes	Yes	Yes	Yes	Yes	Yes	Yes

3. Remove a plate from the incubator and add chemicals, such that both the plates have a different design with respect to the positioning of doses. The plates should be removed from the incubator one at a time.

4. Incubate for 48 hr.

5. Perform the MTT assay (Basic Protocol 2).

6. Enter data into the NIH Assay Guidance Tool software to check for plate uniformity and signal variability. An example of data obtained with the NIH Assay Guidance Tool is shown in Figure 2.4 and Table 2.1.

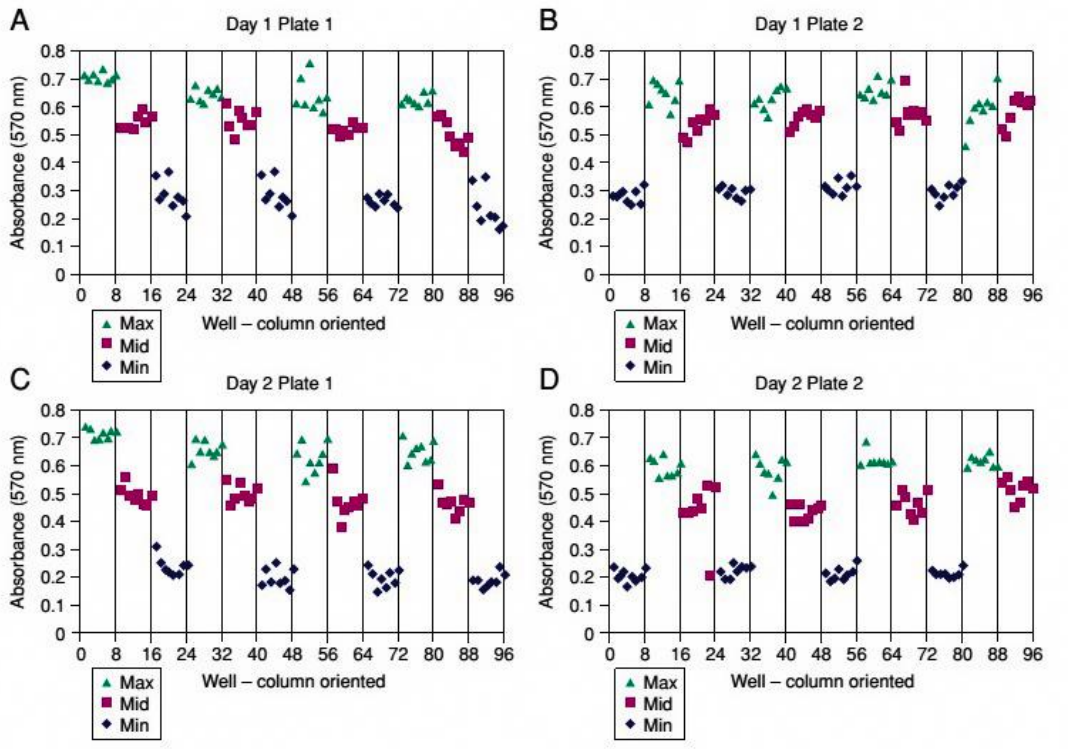

Figure 2.4 The NIH Assay Guidance Wiki generates graphical data to check for edge effects and drift in the MTT plates. The validation experiment was carried out according to Support Protocol 4 (Assay Validation: Plate Uniformity and Signal Variability), and no edge effects or drift were seen. (**A**) Day 1 Plate 1. (**B**) Day 1 Plate 2. (**C**) Day 2 Plate 1. (**D**) Day 2 Plate 2. These figures depict absorbance readings obtained for the three doses plotted as a function of column number. Different colors depict different doses: green, low dose/high signal; pink, mid dose/mid signal; blue, high dose/low signal. The readings from eight wells of one column of the plate are clustered together; for example, 1 to 8 on the x axis corresponds to eight wells in column 1. All the wells in each column had the same dose of chemicals.

Basic Protocol 3: Preparation of hESC for the MTT Assay Using the Single-Cell Method with ROCK Inhibitor

Rho associated kinase inhibitor (ROCKi) Y-27632 is an antagonist of the Rho pathway. By using this compound, hESC can be suspended and plated as single cells with high efficiency (Watanabe et al., 2007). This protocol describes how to use ROCKi when setting up and carrying out an MTT assay.

Materials

Matrigel (BD Biosciences, cat. no. 354234); (store frozen, Matrigel should be diluted 1:2 in DMEM/F12), aliquotted, and frozen; work quickly to ensure the Matrigel does not thicken, DMEM/F12 medium (e.g., Invitrogen), hESC (H9 line from WiCell; also see Lin and Talbot, 2011, , mTeSR culture medium kit (includes basal medium plus supplements; Stem Cell Technologies, cat. no. 05850), 10 mM ROCK inhibitor (ROCKi, Y-27632; Tocris Bioscience, cat. no. 1254) stock solution, phosphate-buffered saline (PBS; e.g., Invitrogen) pH 7.4, DMEM medium (serum-free; e.g., Invitrogen), 4% (w/v) trypan blue, Accutase (eBioscience, cat. no. 00-4555-56), Glass beads (3 mm diameter, e.g., Fisher Scientific, cat. no. 11-312), sterile Test chemical (e.g., phenol, Sigma Aldrich, cat. no. W322318), dimethyl sulfoxide (DMSO) (Fisher Scientific, cat. no. D128-500), Tissue culture treated 6-well and 96-well flat bottom plates (BD Falcon, cat. nos. 353046 and 353072), 15-ml conical centrifuge tubes (BD Biosciences, cat. no. 352097), Centrifuge, 3-ml syringes (BD Biosciences, cat. no. 309604), Acrodisc syringe filters (Pall, 0.2 µm, 25 mm, cat. no. PN 4612), additional reagents and equipment for culture of hESC (Lin and Talbot, 2011), counting cells using a hemacytometer (Support Protocol 1), and MTT assay (Basic Protocol 2).

Preparation before the experiment

1. The day Matrigel will be used, take an aliquot (frozen at a 1:2 dilution) from the freezer and thaw it in the refrigerator for at least 1 to 2 hr. Dilute the aliquot of Matrigel 1:15 with serum-free DMEM/F12 medium to give a working concentration of 1:30, and then add 50 µl of Matrigel to each well of a 96-well plate at least 1.5 hr before the plate is needed. Extra Matrigel can be used to coat another plate and stored for up to 2 weeks in the refrigerator.

Culturing of hESC

2. Culture hESC in 6-well plates as described in (Lin & Talbot, 2011).

Procedure for ROCKi treatment

3. Once two wells in a 6-well plate are 60% of 70% confluent, remove mTeSR medium from the wells with a pipettor and 1000-µl pipet tip.

4. Add ROCK inhibitor to mTeSR medium, making a 1:1000 dilution from the 10 mM ROCK inhibitor stock.

5. Add 1 ml mTeSR and ROCKi to one well in the 6-well plate and incubate for 2 hr.

6. Coat the wells in a 96-well plate with 50 µl of Matrigel (prepared as in step 1) for at least 1.5 hr (the number of wells may vary according to each experiment).

7. After 2 hr of ROCKi pretreatment, remove mTeSR medium from the 6-well plate.

8. Wash each well with 1 ml of PBS.

9. Add 1000 µl of Accutase to each well of the 6-well plate and incubate for 2.5 min, making sure to not exceed 3 min.

10. Add approximately 10 sterile glass beads and roll them gently across the whole surface to allow the beads to lift the colonies off of the bottom of the well.

11. Add 2 ml of mTeSR medium to neutralize the Accutase.

12. Gently aspirate and release the medium to rinse cells from the bottom of the dish into the suspension.

13. Collect the cell suspension in a 15-ml conical centrifuge tube, and then centrifuge 3 min at 23.6 × *g*, room temperature.

14. During these 3 min, remove Matrigel from the pre-coated 96-well plate (see step 1).

15. After centrifugation, carefully discard the supernatant (the pellet is very delicate) and break the pellet up gently with 3 ml mTeSR plus ROCKi.

16. Count cell number via a hemocytometer described in Support Protocol 1 (with 760 µl of mTeSR culture medium, 140 µl of 4% trypan blue, and 100 µl of cell suspension).

17. After determining cell number/ml with the hemocytometer, calculate to find the dilution factor necessary to plate 5000 cells/100 µl of suspension into each well of a 96-well flat-bottom plate. Note that there is approximately 2.9 ml of cell suspension left.

18. In addition to the wells plated for testing chemicals, plate 24 additional control wells with cells to calculate of the coefficient of variation.

These wells should not be treated with chemicals (refer to the plate design). Hint: If you will be using the entire 96-well plate for an experiment, you will need approximately 12 ml of cell suspension to plate all controls and treated wells.

19. Incubate the plate in a 37°C incubator with 95% relative humidity and 5% CO_2 for 24 hr to allow cells to attach.

Preparation of the test chemical

20. Prepare a stock solution or the highest dose being tested in the appropriate volume of mTeSR culture medium. Some chemicals may not dissolve in mTeSR, in which case another solvent will be needed.

21. In a sterile hood, filter the stock solution with a syringe and 0.22-µm filter.

22. Serially dilute the stock solution to obtain the required test doses.

23. After 24 hr of incubation, remove the plate from the CO_2 incubator and aspirate medium from the wells by pipetting, being careful not to disturb the cells at the bottom.

24. Add 100 µl of test solution to each well, such that each concentration of the chemical is tested in duplicate, and each set of duplicates has a control with no test chemical.

25. Incubate the plate in the CO_2 incubator for 48 hr. The length of treatment can be varied depending on the purpose of the experiment. However, if the time is altered, the number of cells plated may have to be adjusted.

Perform the MTT assay

26. Perform the MTT assay as described in Basic Protocol 2 and analyze data as described in that protocol. A dose-response curve showing the effect of phenol on hESC plated as single cells using ROCKi is shown in Figure 2.5.

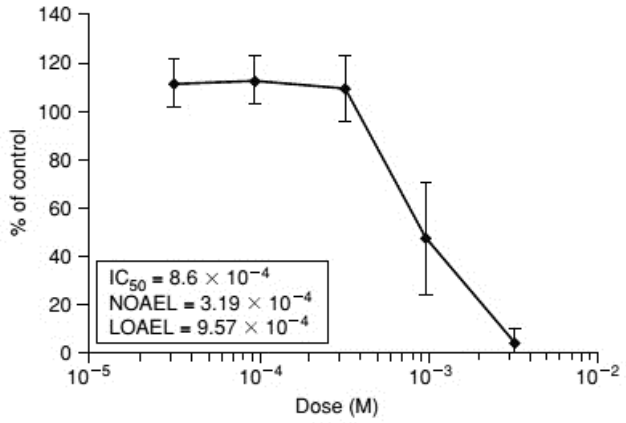

Figure 2.5 Phenol dose-response curve using ROCKi to generate single cells. The x axis shows the doses tested, and the y axis shows the percent of the control (n = 3). IC_{50} = inhibitory concentration at 50% and the NOAEL = no observable adverse effect level. ** = $p \leq 0.01$. The LOAEL is between 3.19×10^{-5} and 9.37×10^{-5} M.

Alternative Protocol: Preparation of Human Embryonic Stem Cells for the MTT Assay Using the Small-Colony Method

The hESC colony method involves plating small colonies of hESC that attach and grow without use of the ROCKi. This protocol will discuss how to generate 2 to 8 cells/colony, how to determine cell concentration in small colonies using a spectrophotometer, and how to set up a 96-well plate with a uniform number of colonies per well.

Materials

mTeSR culture medium kit (includes basal medium plus supplements, Stem Cell Technologies, cat. no. 05850), Accutase (eBioscience, cat. no. 00-4555-56), Glass beads (3 mm diameter, e.g., Fisher Scientific, cat. no. 11-312), sterile Phosphate-buffered saline (PBS; e.g., Invitrogen) pH 7.4, test chemicals, dimethyl sulfoxide (DMSO), tissue culture–treated 6-well and 96-well flat-bottom plates (BD Falcon, cat. nos. 353046 and 353072), 15-ml conical centrifuge tubes (BD Biosciences, cat. no. 352097), inverted phase-contrast microscope, 3-ml syringes (BD Biosciences, cat. no. 309604), acrodisc syringe filters (Pall, 0.2 μm, 25 mm, cat. no. PN 4612), additional reagents and equipment for preparing Matrigel (Basic Protocol 2), culturing hESC (Lin and Talbot, 2011; *UNIT 1A.5*), preparing standard curve (Support Protocol 2), counting cells using a hemocytometer (Support Protocol 1), and MTT assay (Basic Protocol 2).

Preparation before the experiment

1. Prepare Matrigel as described in Basic Protocol 3.
2. Culture hESC in 6-well plates as described in Lin and Talbot (2011)

Preparing a 96-well plate for the MTT assay

3. When two wells in the 6-well plates are 60% to 70% confluent, replate the cells into a 96-well plate according to the following protocol.

a. Coat the wells in a 96-well plate with Matrigel for 1.5 hr (the number of wells may vary according to each experiment).

b. Remove the Matrigel from each well without touching the pipet tip to the bottom of the plate.

c. Add 50 µl of mTeSR culture medium to each well that has been coated with Matrigel.

4. After the 96-well plate is fully prepared, remove the medium from the wells in the 6-well plate that are 60% to 70% confluent.

5. Add 1 ml of PBS to each well and rinse gently but thoroughly.

6. Remove the PBS and add 1 ml of Accutase.

7. Incubate for 1 min in a 37°C, 5% CO_2 humidified incubator.

8. Add approximately 10 glass beads and shake gently across the whole surface to allow the beads to lift the colonies off of the bottom of the well.

9. Neutralize the Accutase with 1 ml of mTeSR culture medium.

10. Collect the cells into a 15-ml conical centrifuge tube with a pipettor and 1000-µl pipet tip. Centrifuge 3 min at 23.6 × *g*, room temperature.

11. Carefully discard the supernatant and resuspend the pellet in mTeSR culture medium by pipetting up and down gently just enough to break the pellet and make

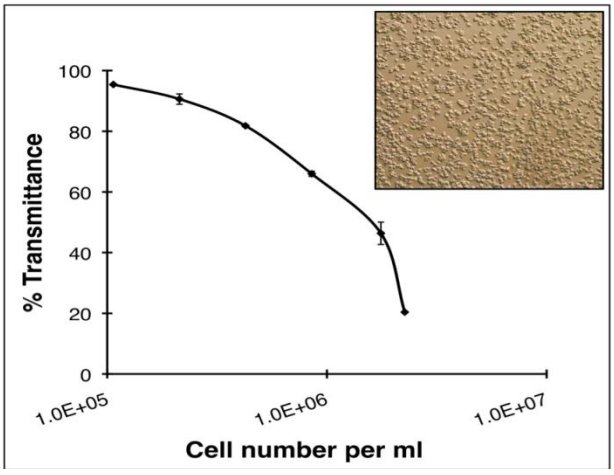

Figure 2.6 Standard curve for hESC. This curve was generated by obtaining eight cell counts for dilutions of 1:2, 1:4, 1:8, and 1:16 using a hemocytometer and obtaining percent trans mittance readings for an undiluted sample as well as dilutions 1:2 through 1:128. The micrograph (insert) shows hESC in a uniform small-colony suspension

small colonies of cells (the pellet should be easily breakable).

12. View the cell suspension using an inverted phase-contrast microscope to ensure that the pellet has been broken into small colonies of 2 to 8 cells. Figure 2.6 shows how the colonies should appear at this step.

hESC standard curve formation

13. Prepare a standard curve for counting cells as described in Support Protocol 2.

Cell counting using a spectrophotometer

14. From the cell suspension described above, take a 100-µl sample.

15. Generate a 1:6 dilution using this sample and 700 µl of PBS (be sure when diluting that you flick or swirl the suspension and do not pipet the sample, to maintain the small colonies).

The transmittance of this dilution should lie on the linear part of the standard curve you previously generated.

16. Measure percent transmittance using PBS as the blank

17. Determine the cell concentration of the dilution from the standard curve

18. Use this value to calculate the cell concentration in the undiluted sample by multiplying with the dilution factor (e.g., 1:6) that was used for measuring percent transmittance.

19. Calculate the dilution factor needed for plating the cells at 20,000 cells/well using the following formula:

Dilution factor = cell concentration of the undiluted sample/400,000 cells/ml.

This dilution will give the concentration required to pipet 20,000 cells in 50 µl from the diluted stock.

Dilute the cell suspension using the dilution factor.

For example, if the dilution factor is 4.0, then 4.0 multiplied by 900 µl (amount of stock I have left) = 3600.

3600 µl minus 900 µl (volume of remaining stock) = 2700 µl of mTeSR medium should be added to stock.

20. Add the amount of mTeSR medium needed to dilute the stock and mix thoroughly but gently by inverting or flicking the vial containing the cells.

Plating hESC in a 96-well plate for the MTT assay

21. From the diluted stock, add 50 µl of colony suspension to the wells of a 96-well plate, in which 50 µl mTeSR culture medium was previously added. Flick the tube before each pipetting to disperse the colonies. Do not resuspend by pipetting, as this will break up the colonies. If more than one plate is being used, prepare cell dilutions separately for each plate. Aspirate the cells from the middle of the colony suspension, not the top or bottom. The number of wells plated is calculated according to the number of chemicals and doses tested, taking care that each dose is tested in duplicates or triplicates.

22. In addition to the wells for testing the chemicals, plate up to 24 additional control wells to calculate of the coefficient of variation and check for vapor effects.

These wells should not be treated with chemicals (refer to the plate design in Fig. 2.2).

23. Incubate the plate in a 37°C, 5% CO_2 incubator with 95% relative humidity for 24 hr to allow attachment of the cells.

Preparation of the test chemical

24. Prepare a stock solution of the highest dose being tested by dissolving the required amount of test chemical in the appropriate amount of mTeSR medium or required solvent such as DMSO.

25. Filter the stock solution in a sterile hood using a syringe and a 0.22-μm filter.

26. Obtain the required doses of the test chemicals by serially diluting the stock solution.

27. After 24 hr of incubation, remove the plate from the CO_2 incubator and aspirate the medium from the wells by pipetting, being careful not to touch the attached cells at the bottom of the wells.

28. Add 100 μl of test compound solution to each well, so that each concentration of the test chemical is evaluated in duplicate, and each set of duplicates has a control with no test chemical (refer to plate design).

29. Incubate the plate in a 37°C, humidified CO_2 incubator for 48 hr. The length of treatment can be varied depending on the purpose of the experiment. If the length of treatment is changed, the number of cells plated may need to be changed. At the completion of treatment, the control wells should be about 80% confluent.

MTT assay

30. Perform the MTT assay as described in Basic Protocol 2 (and analyze data as described in that protocol. An example of a dose-response curve for hESC incubated in phenol is shown in Figure 2.7.

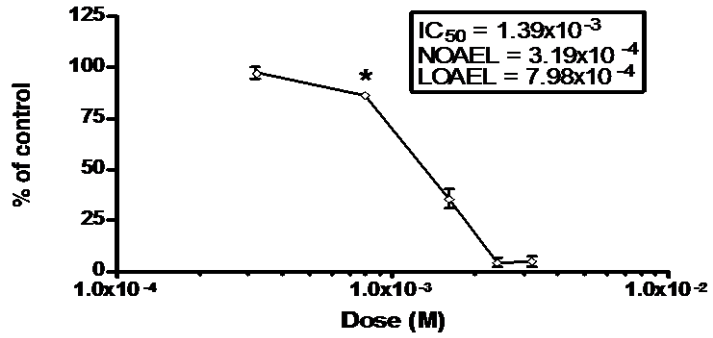

Figure 2.7 Phenol dose-response curve using the small-colony method. The x axis shows the doses tested, and the y axis shows the percent of the control (n = 3). IC_{50} = inhibitory concentration at 50%, LOAEL = lowest observed adverse effect level, NOAEL = no observable adverse effect level. * = $p < 0.05$.

Support protocol 5: Assay Validation for the Small-Colony Procedure with hESC: Plate Uniformity and Signal Variability

The details of this protocol are given in Support Protocol 4 (Assay Validation: Plate Uniformity and Signal Variability). This procedure can be used for both the small-colony procedure and the single cell using ROCK inhibitor procedure.

For materials, see Support Protocol 4 (substitute hESC for mNSC).

1. According to the instructions found on the Web site *http://assay.nih.gov/assay/index.php/Assay Validation 2011*, follow the 2 day, 2 experiment time course.

2. Perform the steps of Support Protocol 4, and carry out the MTT assay (at step 5 of Support Protocol 4), using small colonies of hESC as described in Basic Protocol 3.

3. Enter data into the NIH Assay Guidance Wiki software to check for plate uniformity and signal variability. An example of data obtained with this Wiki using hESC exposed to 5-fluorouracil is shown in Figure 2.8 and Table 2.1.

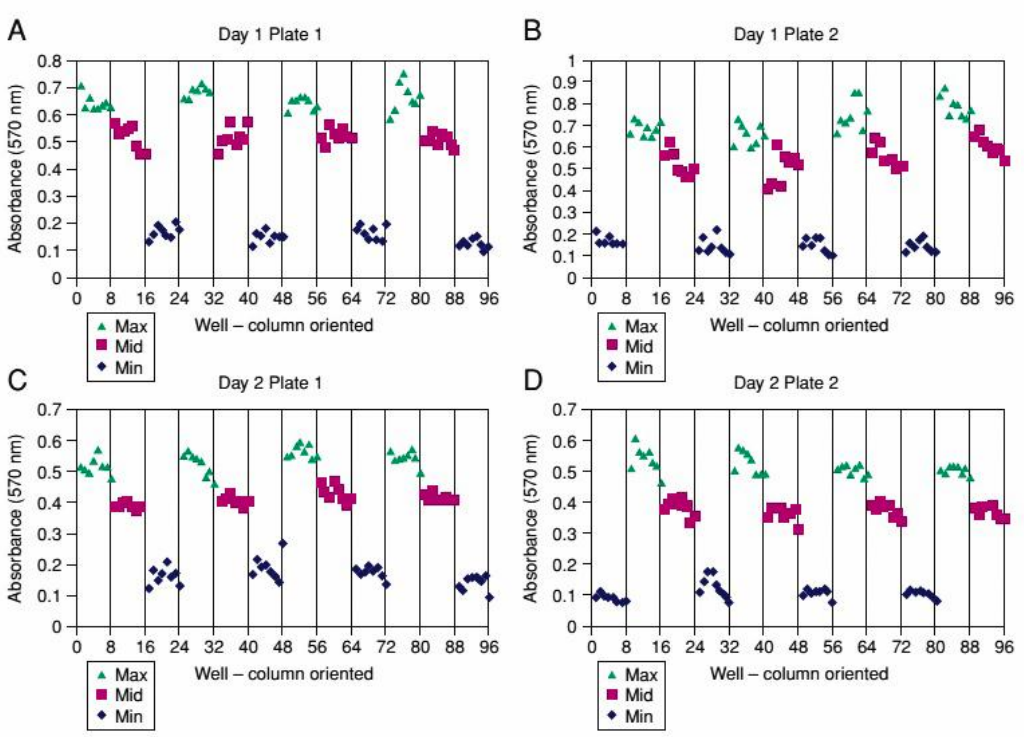

Figure 2.8 The NIH Assay Guidance Wiki generates graphical data to check for edge effects and drift in the MTT plates. The validation experiment was carried out according to Support Protocol 4 (Assay Validation: Plate Uniformity and Signal Variability), and no edge effects or drift were seen. (**A**) Day 1 Plate 1. (**B**) Day 1 Plate 2. (**C**) Day 2 Plate 1. (**D**) Day 2 Plate 2. These figures depict absorbance readings obtained for the three doses plotted as a function of column number. Different colors depict different doses: green, low dose/high signal; pink, mid dose/mid signal; blue, high dose/low signal. The readings from eight wells of one column of the plate are clustered together—for example, 1 to 8 on x axis corresponds to eight wells in column 1. All the wells in each column had the same dose of chemical.

Reagents and Solutions

For culture recipes and steps, use sterile tissue culture–grade water. For other purposes, use deionized, distilled water or equivalent in recipes and protocol steps.

mNSC culture medium, Dulbecco's minimal essential medium (Lonza, cat. no. 12-741F) supplemented with: 10% fetal bovine serum (Invitrogen, cat. no. 16000), 5% horse serum (Invitrogen, cat. no. 16050-130), sodium pyruvate (Lonza, cat. no. 13-115E), 1× penicillin/streptomycin (Invitrogen, cat. no. 15140-122).

Commentary

Background Information

The MTT cytotoxicity assay can be used to study cell proliferation, cell death, and cell survival. This assay is based on the conversion of MTT (3-(4,5-dimethylthiazol-2-yl)-2,5-diphenyltetrazolium bromide, a yellow tetrazole) to an insoluble purple formazan by the action of mitochondrial and endoplasmic reticulum enzymes in living cells (Mossman, 1983) (Berridge, Tan, McCoy, & Wang, 1996). At the end of the experiment, the insoluble formazan is dissolved in dimethyl sulfoxide (DMSO), and absorbance is read at 570 nm.

When performing the MTT assay, there are several critical factors that need to be considered to obtain reliable results. These include accurately plating the appropriate cell number in each well, selecting the appropriate dose range, and selecting the time of expo- sure. The cell number/well should be the same in all wells in all experiments for cross comparisons to be reliable. This introduces a need to count the cells accurately before plating for an experiment. Hemocytometer counting can be done effectively for cell types that grow as single cells, such as mouse neural stem cells (mNSC), but counting cells that plate best as small colonies, such as human ESC (hESC), is challenging and cannot be done rapidly and accurately with a hemocytometer. hESC can be plated accurately as single cells using the ROCK inhibitor Y27632, which blocks Rho-associated coiled coil kinase and reduces the rate of dissociation-induced apoptosis (Watanabe et al., 2007) (Ohgushi et al., 2010). Although this method, described in Basic Protocol 3, has been widely used, the inclusion of ROCK inhibitor can alter results of the MTT assay (Fujimura, Usuki, Kawamura, & Izumo, 2011). Therefore, we have devised an alternative method (the Alternate Protocol) to count and plate hESC cells in colonies, so

that the use of ROCK inhibitor can be circumvented. This method makes use of a spectrophotometrically generated standard curve for cell number versus percent transmittance and is described in Support Protocol 2 (Standard Curve Generation for Count- ing Cells with a Spectrophotometer). A similar curve was constructed, as described in Support Protocol 2, for use with mNSC, as turbidometric counting gives a more reliable and faster method to count cells than a hemocytometer. The coefficient of variation for both hESC and mNSC is 1.5% with the spectrophotometer and 10% or greater with the hemocytometer.

Once cell concentration can be determined accurately, it is necessary to determine how many cells to plate per well. This will be affected by the length of the incubation period in a test chemical as well as the growth rate of the cell type being used. For the experimental protocols to be described the optimal cell number to be plated was determined to be 1250 cells/well and 20,000 cells/well for mNSC and hESC colonies, respectively. This number could vary if the length of the treatment is longer or shorter than 48 to 72 hr or if growth is stimulated by the treatment.

The final concentrations of the chemical to be tested can be chosen after a preliminary screen, and the doses that induce or inhibit cell proliferation are then tested further using the plate design described in this unit. The data are then used for the generation of a dose-response curve from which the IC_{50}, LOAEL (lowest observed adverse effect level), and NOAEL (no observed adverse effect level) can be determined. Validation of the assay for plate uniformity and signal variability is done using to the NIH Assay Guidance Tool, as described in Support Protocol 4 (Assay Validation: Plate Uniformity and Signal Variability). It is important to validate the assay

for every cell line to make sure that there are no drift or edge effects in the plate due to differential heating of the plate at the edges or inconsistency in cell plating. Three doses of a chemical are used for validation. The parameters measured are the coefficient of variation for the three test doses and the signal window, and the Z, which measure the separation between the signals obtained for the different doses. If all the criteria of the NIH Assay Guidance Tool are fulfilled, the assay is validated for a particular cell line, and it can be then used to test the cytotoxicity of chemicals.

Critical Parameters and Troubleshooting

Passaging mNSC

It is important to wash cells with PBS before adding trypsin, so as to remove traces of FBS, which inhibits the activity of trypsin. Do not trypsinize cells for more than 1 min, as this can damage the cells. View the flask with a microscope, and, if the cells are still attached, tap the flask with the palm to help them detach. Suspend the pellet obtained after centrifugation very gently with a pipet, as vigorous pipetting can damage or kill cells. The shelf life of 0.05% trypsin made in DPBS is 1 week at 4° C.

Counting cells with a hemocytometer

It is important to count only living cells, which appear spherical and shiny, while using a hemocytometer. In case there is trouble recognizing living cells, use trypan blue, which stains dead cells blue, and thus these can be excluded from the count. Normally, very few cells will be dead.

Plating mNSC for MTT assay

Plating cells in a 96-well plate is time consuming, but it is important to do this step as quickly as possible to keep the cells from dying. Flick the tube containing the

cells before each pipetting, but avoid pipetting cells. Pre- pare 1 to 2 ml of extra cell suspension, which will help in plating uniform numbers of cells in each well. Do not stack plates in the incubator, as this can lead to edge effects, and always put plates on the same shelf in the incubator.

Hemocytometer versus spectrophotometric method for determining cell concentration

A hemocytometer is usually used to count single cells. However, preparing the hemocytometer, counting the cells with a microscope, and taking replicate counts is time consuming. Generating a standard curve based on turbidity of the cell suspension has proven to be quite reliable, accurate, and rapid.

ROCKi protocol versus small-colony protocol for hESC

Use of the ROCKi protocol adds some expense to the MTT test. However, the ROCKi protocol (Basic Protocol 3) is somewhat easier to perform than the small-colony protocol (Al ternate Protocol). When experimentally comparing the ROCKi protocol to the small-colony protocol using phenol as the test chemical, ROCKi treatment caused a leftward shift in the dose-response curve. For phenol, the ROCKi protocol generated an IC_{50} of 9.37×10^{-5} M, while the small-colony protocol generated an IC_{50} of 1.39×10^{-3} M. Toxicity tests with methylmercury were likewise affected by the use of ROCKi (Fujimura et al., 2011). Thus, the ROCKi protocol has applications and is convenient, but may not be suitable for all toxicological testing.

Volatile chemicals can produce a vapor effect in 96-well plate assays

Volatile chemicals, such as ethanol, can produce a vapor effect, which causes cell death in wells adjacent to the volatile chemical (Blein, Ronot, & Adolphe, 1991). In the recommended plate design (Fig. 2.2), vapor effects are observed when the control well(s) closest to the highest dose has an absorbance less than that of the control well next to the lowest dose. The means of the controls on the top and bot- tom of the plate can be compared using a *t* test. If a significant difference is found, a vapor effect may have occurred. Individual wells in the bottom controls can be inspected to identify which chemical(s) may have caused he effect. If a vapor effect is found, additional experiments should be run to determine the highest dose of a particular chemical that can be used without affecting adjacent wells.

Adaptability of other 96-well plate assays

The three protocols described for the MTT assay can be readily adapted to other 96-well plate assays, such as the XTT, LDH, or the BrdU assay. The hESC small-colony protocol (Alternate Protocol) should be especially useful as it does not require ROCKi and it can easily be introduced into any lab working with hESC.

Selection of dose range

For studies that will be screening many chemicals, it is best to do an initial screening where all chemicals are tested at a specified dose range in a single column of the 96-well plate. After the dose range to be studied has been determined from the screen, these doses can be tested as duplicates or triplicates in multiple experiments, using different batches of cells. The plate design in Figure 2.2 allows single, double, or triple replicates to be carried out in the 96-well plate.

Preparation of small colonies of hESC

This is one of the most important steps when plating for a 96-well plate MTT experiment. When breaking the pellet of hESC to create a suspension of homogenously sized colonies, pipetting must be done in a very gentle fashion. After pipetting a few times, take a small sample of cells and view them using a microscope to see the size of the colonies. This can be repeated until the colonies appear to have 2 to 8 cells/colony.

When measuring cell concentration, and during plating of the cells, it is important to keep the hESC colonies uniformly distributed in suspension. From our experience, flicking the microcentrifuge tube or 15-ml conical tube containing the colonies is the best method to keep them evenly distributed in suspension. Even distribution is important

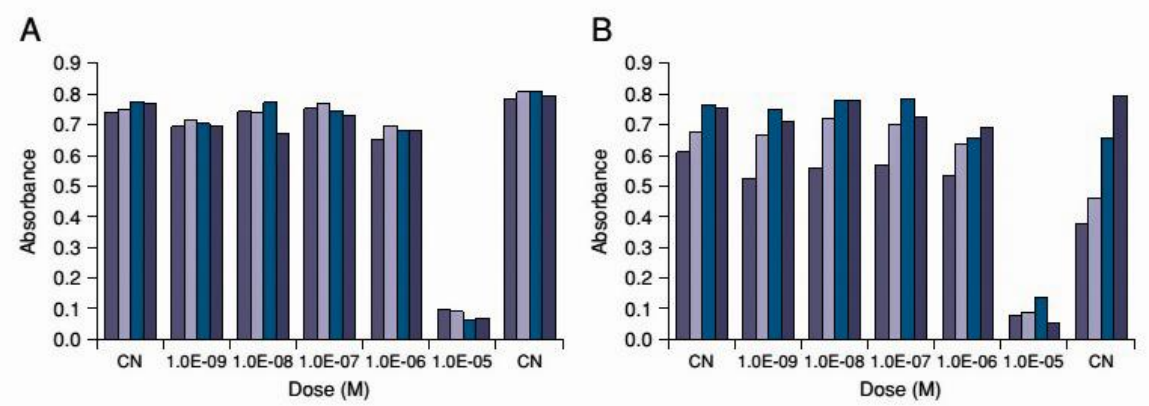

Figure 2.9. Variation in the MTT assay results when flicking versus swirling is used to keep cells in suspension. 5-fluorouracil treatment of hESC is shown here where (**A**) represents the flicking of cell suspension in a 15-ml conical tube before plating each well with cells and (**B**) represents swirling of the cell suspension in a 10-ml glass beaker before plating each well with cells. The colored bars show quadruplicates for each dose. CN = control.

and necessary to enable accurate pipetting of uniform numbers of cells/well in 96-well plates. In addition to flicking, we have also tried swirling in the 15-ml conical tube as well as swirling in a 10-ml glass beaker. Both swirling techniques leave variation between replicates. In Figure 2.9, replicate wells are shown for flicking in a 15-ml tube

and for swirling in a small 10-ml beaker. It is clear that the flicking method gives more consistent distribution of hESC colonies than the swirling method.

Anticipated Results

As shown in Figures 2.3, 2.5, and 2.7, a dose-response curve can be generated that can be used to determine the cytotoxicity of a compound being tested. Parameters including the IC_{50}, NOAEL, and LOAEL can be obtained from the dose-response curve.

Time Considerations

Once the standard curve has been generated and the assay has been validated using the NIH Assay Guidance Wiki, approximately 1 week will be needed to conduct an experiment using hESC or mNSC.

References

Berridge, M., Tan, A., McCoy, K., & Wang, R. (1996). The biochemical and cellular basis of cell proliferation assays that use tetrazolium salts. *Biochemica*, (4), 4–9. Retrieved from http://lifescience.roche.com/wcsstore/RASCatalogAssetStore/Articles/BIOCHEMICA_96_4_p14-19.pdf

Blein, O., Ronot, X., & Adolphe, M. (1991). Cross contamination associated with the use of multiwell culture plates for cytotoxicity assesment of volatile chemicals, 79–82.

Freshney, R. I. (2005) Basic Principles of Cell Culture, in Culture of Cells for Tissue Engineering (eds G. Vunjak-Novakovic and R. I. Freshney), John Wiley & Sons, Inc., Hoboken, NJ, USA. doi: 10.1002/0471741817.ch1

Fujimura, M., Usuki, F., Kawamura, M., & Izumo, S. (2011). Inhibition of the Rho/ROCK pathway prevents neuronal degeneration in vitro and in vivo following methylmercury exposure. *Toxicology and Applied Pharmacology*, *250*(1), 1–9. http://doi.org/10.1016/j.taap.2010.09.011

Grandjean, P., Bellinger, D., Bergman, A., Cordier, S., Davey-Smith, G., Eskenazi, B., … Weihe, P. (2008). The faroes statement: human health effects of developmental exposure to chemicals in our environment. *Basic & Clinical Pharmacology & Toxicology*, *102*(2), 73–5. http://doi.org/10.1111/j.1742-7843.2007.00114.x

Lin, S., Fonteno, S., Weng, J.-H., & Talbot, P. (2010). Comparison of the toxicity of smoke from conventional and harm reduction cigarettes using human embryonic stem cells. *Toxicological Sciences : An Official Journal of the Society of Toxicology*, *118*(1), 202–12. http://doi.org/10.1093/toxsci/kfq241

Lin, S., & Talbot, P. (2011). Embryonic Stem Cell Therapy for Osteo-Degenerative Diseases, *690*(2), 31–56. http://doi.org/10.1007/978-1-60761-962-8

Mossman, B. T. (1983). In vitro approaches for determining mechanisms of toxicity and carcinogenicity by asbestos in the gastrointestinal and respiratory tracts. *Environmental Health Perspectives*, *VOL. 53*, 155–161. http://doi.org/10.1289/ehp.8353155

Ohgushi, M., Matsumura, M., Eiraku, M., Murakami, K., Aramaki, T., Nishiyama, A., … Sasai, Y. (2010). Molecular pathway and cell state responsible for dissociation-induced apoptosis in human pluripotent stem cells. *Cell Stem Cell*, *7*(2), 225–39. http://doi.org/10.1016/j.stem.2010.06.018

Parker, M. a., Anderson, J. K., Corliss, D. a., Abraria, V. E., Sidman, R. L., Kook, I. P., … Snyder, E. Y. (2005). Expression profile of an operationally-defined neural stem cell clone. *Experimental Neurology*, *194*(2), 320–332. http://doi.org/10.1016/j.expneurol.2005.04.018

Talbot, P. and Lin, S. (2011). Mouse and human embryonic stem cells: Can they improve human health by preventing disease? *Current Topics and. Medicinal Chemistry* 11:1638-1652.

Watanabe, K., Ueno, M., Kamiya, D., Nishiyama, A., Matsumura, M., Wataya, T., … Sasai, Y. (2007). A ROCK inhibitor permits survival of dissociated human embryonic stem cells. *Nature Biotechnology*, *25*(6), 681–686. http://doi.org/10.1038/nbt1310

Chapter 3: Thirdhand Cigarette Smoke: Factors Affecting Exposure and Remediation

Introduction

Thirdhand smoke (THS) consists of residual tobacco smoke that sorbs to indoor surfaces and remains after the majority of the airborne components of the smoke have cleared. THS raises the concentration of nicotine and other smoke constituents in indoor environments occupied by smokers (Fortmann et al., 2010) (Matt et al., 2011). During aging, the chemicals in THS can desorb back into the air or react to form new chemicals. For example, nicotine reacts with ambient nitrous acid (HONO) to form tobacco specific nitrosamines (TSNAs) (L. M. Petrick, Sleiman, Dubowski, Gundel, & Destaillats, 2011) (Sleiman et al., 2010). Exposure to THS and remediation of buildings and vehicles contaminated with THS have received little attention in the past and are important, especially in light of recent health-related studies that indicate the potentially hazardous nature of THS (Hammer, Fischer, Mueller, & Hoefer, 2011) (Hang et al., 2013) (Martins-Green et al., 2014) (Rehan, Sakurai, & Torday, 2011).

The negative health effects of active smoking and secondhand smoke exposure have been analyzed *in vitro*, in animals, and studies of human volunteers and populations (CDC, 2014) (DiCarlantonio, 1999) (Gieseke, 2005) (Riveles et al., 2007) (Talbot & Lin, 2011). Active smoking and secondhand smoke exposure adversely affect health across all age groups (CDC, 2014) (Hofhuis, Jongste, & Merkus, 2003) (Öberg, Jaakkola, Woodward, Peruga, & Prüss-Ustün, 2011). In contrast, little is known about the level of human exposure to THS and the resulting health effects. THS exposure can occur through the skin, by ingestion, and by inhalation. Infants and small children could

be at greater risk than adults because their skin is thinner, their surface to volume ratio is higher, and because they spend more time in contact with THS-contaminated surfaces and where they can mouth THS-contaminated objects. If ingested, the fraction of THS that is soluble in saliva and digestive fluids will be available for intake (passage into the body but not across absorptive barriers) (Lehman-McKeeman, 2007). The extent of intake will depend on the concentration of THS chemicals, the fraction of THS that is in the air and on surfaces, and their solubility in saliva or sweat. The concentration of THS chemicals will vary with the number of cigarettes smoked in the room, the air exchange rate, and the time elapsed since smoking. Therefore, when evaluating exposure, it is important to consider that THS is dynamic and that aging can change the composition of THS over time.

Remediation, which is the removal of THS residue from surfaces in indoor environments or the safe containment of THS, is another important aspect of THS contamination that needs study (Matt et al., 2011). Methods of remediation will depend upon the level of contamination as well as the type of material. The materials commonly found indoors, such as natural and synthetic fibers, carpets, paper and wall board, each differ in their capacities to adsorb, absorb, bind, and release THS chemicals.

As a first step to understanding THS exposure and remediation, we measured the concentrations of nicotine, nicotine-related alkaloids and tobacco-specific nitrosamines in cotton and polyester fabrics repeatedly exposed to cigarette smoke in an experimental chamber. We tested organic and aqueous solvent extraction and evaluated the effect of aging on the extractable chemicals. The resulting data were then

used to model exposures that toddlers and adults could receive in environments containing THS.

Materials and Methods

Exposure of fabric to cigarette smoke: 100% cotton terrycloth, and 100% polyester fleece were purchased at retail and washed three times in a domestic washing machine using an unscented, enzyme-free laundry detergent (Country Save powdered laundry detergent, Arlington, WA) in hot water with two rinses/cycle, and washing again with no detergent. After line drying, fabrics were hung in a 6 m^3 stainless steel chamber at UCSF and exposed to cigarette smoke (Schick et al., 2012). Marlboro Red cigarettes were smoked according to ISO protocol 3308: 2012. The smoke was diluted with conditioned, filtered air and conducted through the smoke aging chamber in experiments lasting 1-8 hours. Particle concentration at the outlet of the chamber was measured using a laser photometer calibrated gravimetrically (Dusttrak II, model 8530, TSI Inc., Shoreview MI). Aerosol flow rates through the chamber were measured using an air velocity transmitter (model 641-b Dwyer Instruments, Michigan City IN). After smoking, air flow was turned off, and the chamber was closed while it still contained detectable levels of smoke. Smoke was generated 0-8 times/month and was not ventilated between experiments. The time that the cloth sample was in the chamber, the number of hours of smoke, the average particle concentration for each experiment and the air velocity through the chamber were logged. The total particle mass that the fabric was exposed to was calculated as $sm = a\ x\ b\ c\ x\ 60\frac{m}{h} x \frac{1liter}{1000\ cubic\ meters}$ where a = air velocity in liters/minute, b = hours of smoke and c = average smoke particle concentration.

A sheet of cotton terrycloth and a sheet of polyester fleece were exposed to smoke. The terrycloth was exposed to smoke containing 1329 mgs of particles for 114 hours over 1 year. The polyester fleece was exposed to 1846 mgs of smoke particles for 257 hours over 10 months. The cotton terrycloth and polyester fleece were folded and stored in separate polyethylene bags at room temperature in the dark. The terrycloth was stored 8 months and the polyester 1 month prior to shipment. Samples were wrapped in aluminum foil, placed in polyethylene bags and shipped at ambient temperature, overnight, to the Talbot Laboratory at UCR. Upon receipt, samples were transferred to amber glass bottles and stored at room temperature (RT) in the dark.

Organic solvent extractions: Samples of fabric were incubated at RT overnight in 50% MeOH /1% HCl and were vortexed for 3-5 minutes at RT. Solvent was removed by squeezing the fabric in the vial with a spatula, fibers and dust were removed by centrifugation, and the extract was analyzed as described below.

Aqueous Extractions: Aqueous extracts of THS were prepared in Dulbecco's Modified Eagle Medium (DMEM). Terrycloth and polyester fleece were weighed and cut into very small pieces using scissors. Either 0.05 or 0.125g of fabric/ml were extracted in DMEM in 15 ml conical tubes on a rotating shaker. The medium was recovered by placing the fabric in a syringe and centrifuging at 4,000 g for 5 minutes The recovered medium was passed through a 0.22µm filter, aliquoted into 1.5 ml vials, and stored at -80ºC.

To examine the effect of repeated aqueous extraction on chemical yield, three samples of terrycloth and two samples of polyester were extracted five times, serially at RT with media being replaced every hour for 5 hours. To determine the effect of time

and temperature, the terrycloth was extracted under four conditions: RT for 1 hour; RT for 2 hours; 4°C for 1 hour; and 4°C for 2 hours. For extraction at 4°C, tubes were placed in a beaker of ice on a rocker shaker. To examine the effect of aging, extraction was done after storing the terrycloth for 11, 16 and 19 months and the polyester for 11 and 19 months in amber glass jars at RT.

Chemical Analysis of THS extracts:

1 mL extracts of THS were shipped to UCSF on dry ice where they were analyzed using liquid chromatography-tandem mass spectrometry (LC-MS/MS) (Jacob, Goniewicz, Havel, Schick, & Benowitz, 2013) (Sarker et al., 2014). The method was modified to include NNA in the analysis, by treating the extract with pentafluorophenylhydrazine (PFPH) to convert NNA to the pentafluorophenylhydrazone derivative which enhances sensitivity of detection (Pang & Lewis, 2011).

LC-MS/MS: The samples were analyzed on a Thermo Scientific Vantage LC-MS/MS with an Accela UPLC system using a 3 x 150 mm 2.6 micron Phenomenex Kinetex PFP column as detailed in [20].

Limits of quantification: The limits of quantitation for each of the chemicals analyzed are as follows: nicotine: 1.02 ng/ml; myosmine: 0.305 ng/ml; 2,3'-bipyridine: 0.914 ng/ml; cotinine: 0.914 ng/ml; N-formylnornicotine: 0.305 ng/ml; nicotelline: 0.030 ng/ml; NNN: 0.030 ng/ml; NNK; 0.0130 ng/ml; NNA 0.010 ng/ml.

Statistical analyses: The concentrations of chemicals in aqueous extracts were converted to grams/gram of fabric. Averages of four samples in each group were then calculated using Microsoft Excel. ANOVA (one way analysis of variance) was performed using GraphPad Prism to determine if the chemical concentrations in extracts made

under different conditions varied significantly. ANOVA was also used to analyze extracts made from terrycloth after 11, 16 and 19 months of aging. Groups differing significantly ($p < 0.05$) from the 11 month samples were identified using Dunnett's posthoc test. Data were checked to determine if they satisfied the assumptions of ANOVA (normal distribution and homogeneity of variances). T-tests were used to determine if the chemical concentrations in aqueous extracts were different from those in methanol/HCL extracts.

Results

Fabrics used for extraction: THS was extracted from 100% cotton terrycloth, and 100% polyester fleece. Terrycloth is a loosely knit natural fabric with many thin fibers that provide a large surface area for absorption of chemicals. One surface of polyester has numerous short highly packed fibers while the other is comprised of a large tightly woven mesh of fibers (Fig. 3.1).

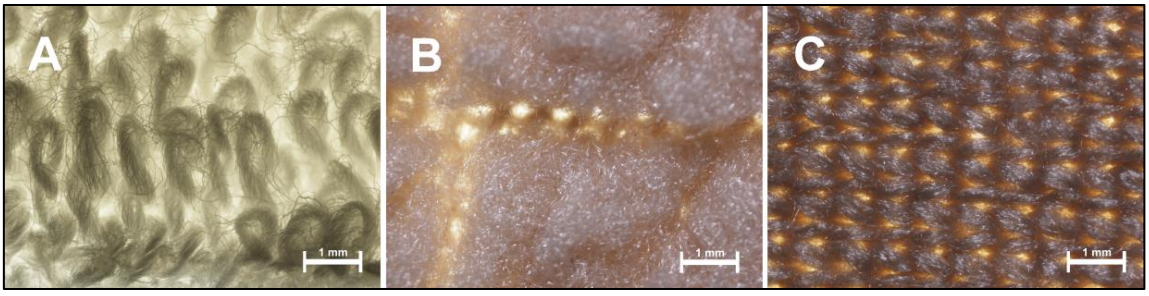

Figure 3.1. Micrographs of fabrics used for THS extraction. (A) Terrycloth is a loosely knit fabric made of loops of cotton which increase its surface area tremendously and contribute to the absorption of THS. **(B)** Polyester is a more tightly knit fabric with one fuzzy surface and **(C)** one compact tightly woven surface.

Aqueous and methanol:HCl solvents extracted THS chemicals from cotton fabric: The concentrations of nicotine and related chemicals in the aqueous extracts of THS from cotton terrycloth after 31 months of aging were similar to those in methanol:HCl extracts (Fig. 3.2 A and B). Negligible amounts of nicotine and related chemicals were recovered when aqueous extraction was followed by methanol:HCl extraction. Nicotine (50-60 µg/gram of fabric) was the most abundant of the chemicals analyzed. Myosmine, bipyridine, formylnornicotine and cotinine were present in 1-2 µg/gm of fabric quantities, while the TSNAs and nicotelline were the least abundant (nanogram/gram of fabric) of the chemicals analyzed in THS extracts from terrycloth.

Extraction of polyester fabric yielded lower concentrations of THS chemicals: The concentrations of all chemicals tested were lower in extracts of polyester fleece than in extracts of cotton terrycloth (Fig. 3.2 C and D). As an example, in aqueous extracts approximately 40 times less nicotine was extracted from polyester than from terrycloth.

For polyester fleece, methanol:HCl and aqueous extracts had similar concentrations of nicotine and other chemicals. However, when aqueous extraction was followed by methanol:HCl extraction, higher concentrations of myosmine and 2,3'-bipyridine were obtained than with aqueous extractions alone. All other chemicals were retrieved at lower concentrations in the methanol:HCl extract that followed the aqueous extraction. This suggests two possibilities: that polyester binds less of the nicotine, nicotine- related alkaloids and TSNAs than cotton or that these compounds are harder to extract from polyester than from cotton.

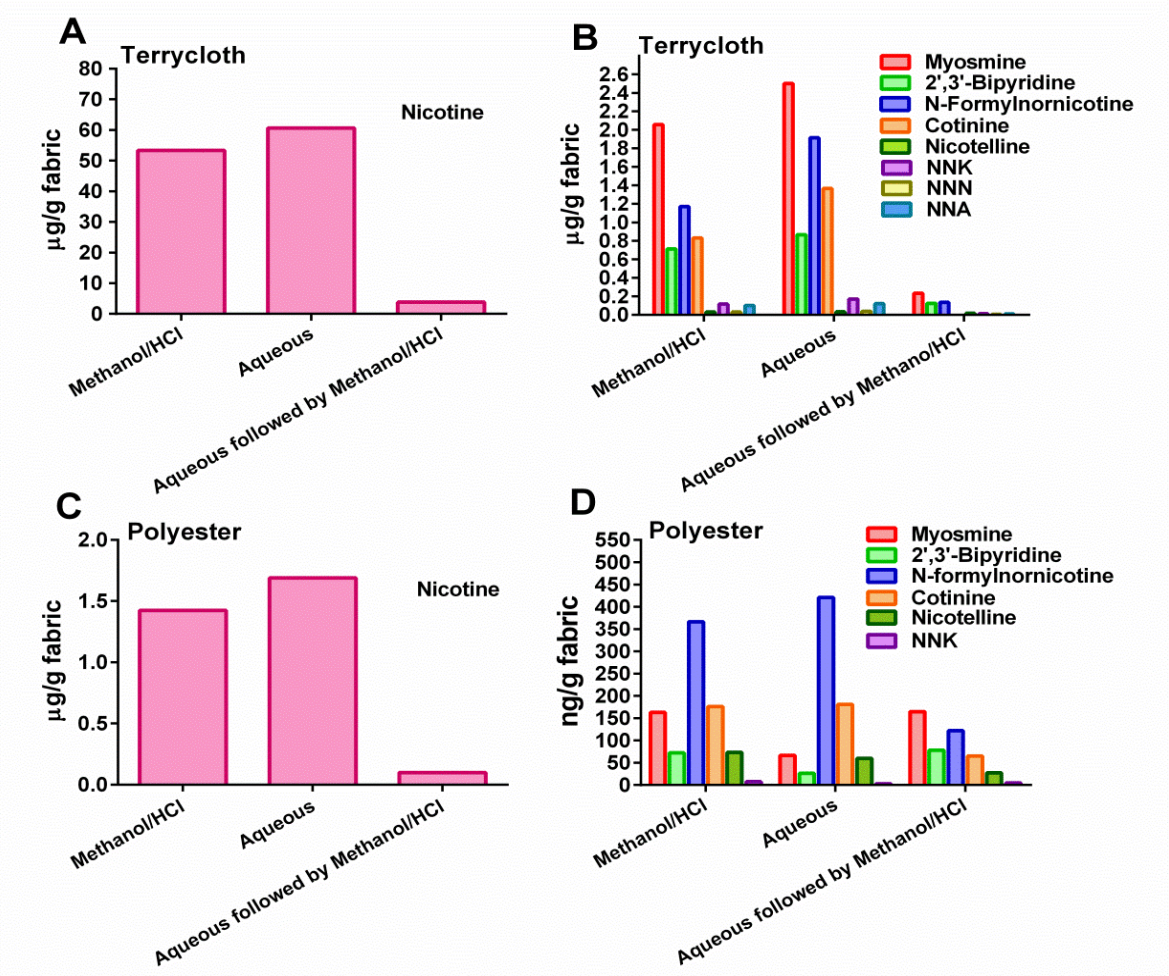

Figure 3.2. Comparison of chemical concentrations in aqueous and methanol:HCl extracts of terrycloth and polyester exposed to THS. Terrycloth was extracted after 31 months of aging and polyester was extracted after 19 months of aging. Results for aqueous extracts are an average of three experiments, and all other groups are averages of two experiments.

Serial aqueous extractions from terrycloth and polyester: To determine if all nine chemicals were removed from terrycloth and polyester during 1 hour of aqueous extraction, the same fabric samples were extracted five times. Each extraction lasted one hour (Fig. 3.3). All of the chemicals were extractable by water successfully removed from cotton terrycloth during the first hour of extraction. Concentrations of some chemicals (e.g., nicotine, myosmine and nicotelline) were very similar from batch to batch, while others, such as cotinine, NNA, and NNN, varied somewhat in concentration among batches. For polyester, cotinine was found only in the first hour extracts. Nicotine and N-formylnornicotine were found in the first and the second hour extracts.

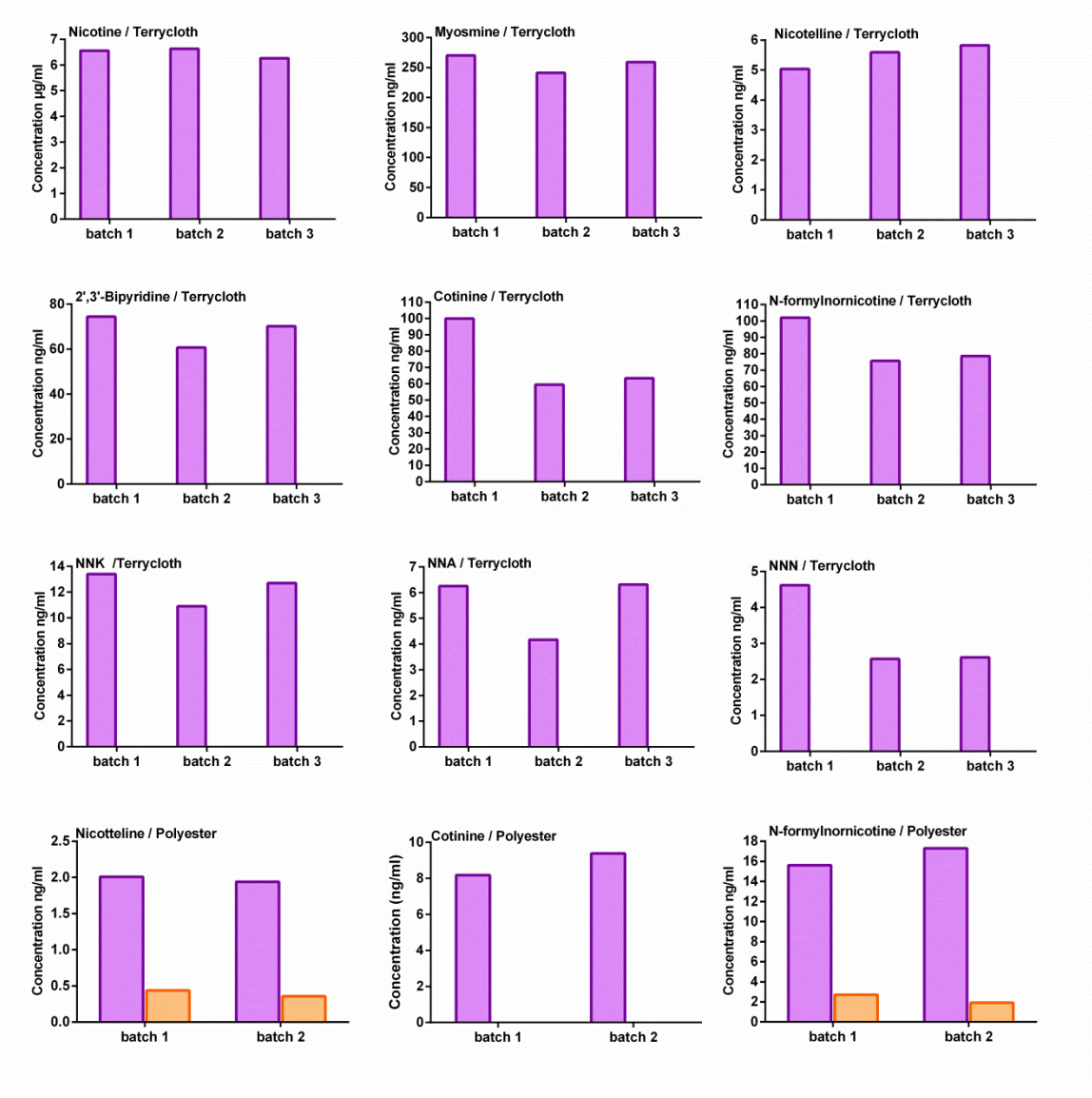

Figure 3.3 Iterative aqueous extractions from terrycloth and polyester. Extractions were done for a total 5 hours with extraction medium being replaced every hour. After every hour, extracts were analyzed for nicotine and its derivatives. Graphs represent chemical concentrations in three different batches of extracts. No chemicals were found in extracts after 1 hour for terrycloth and after 2 hours for polyester.

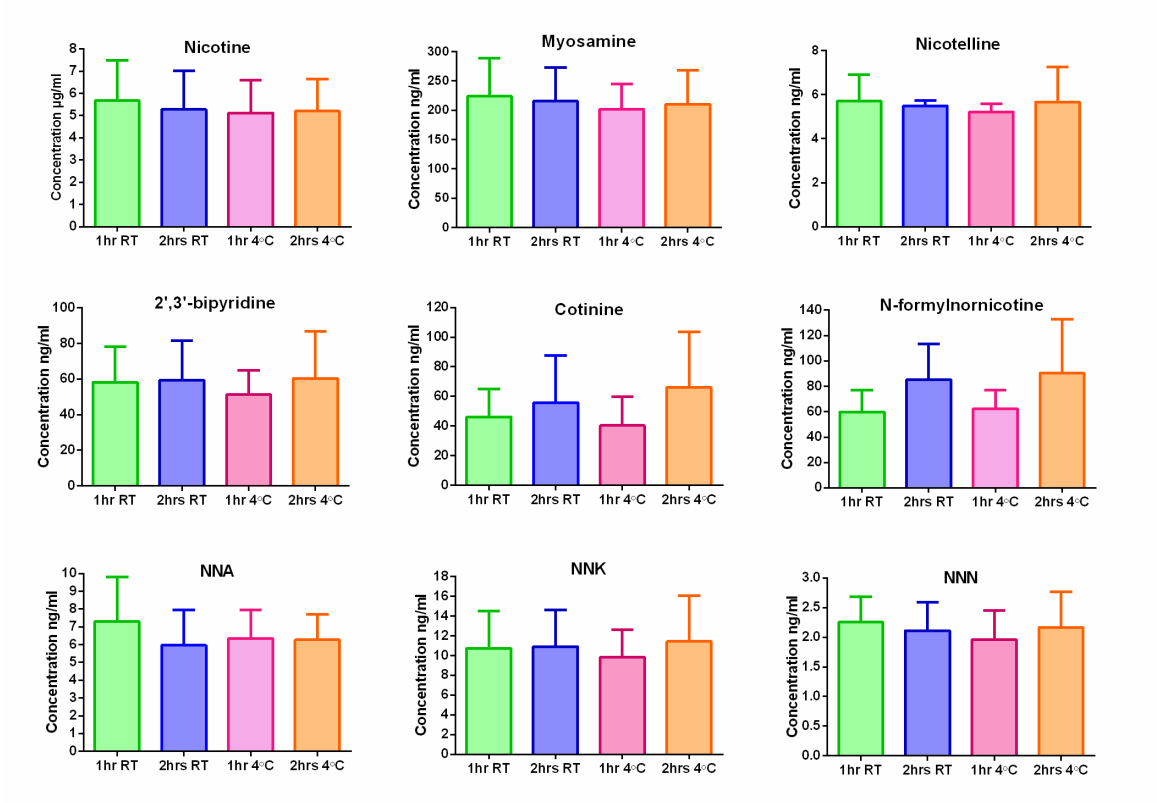

Figure 3.4. Concentration of chemicals in aqueous extracts of THS from terrycloth when temperature and time of extraction were varied. Extracts were made at RT and at 4ºC for 1 and 2 hours. Each bar is the mean ± standard deviation of three experiments. Chemical concentrations did not vary significantly with temperature or time of extraction when tested by ANOVA.

One hour of aqueous extraction at RT removes THS chemicals from cotton terrycloth: The effects of temperature and time on the concentration of chemicals recovered by aqueous extraction was tested (Fig. 3.4). Extracts were made at RT and at 4°C for 1 or 2 hours. Chemical concentrations appeared to be similar for each extract. When tested by ANOVA, no significant differences in chemical concentrations were found between extraction conditions. Data for each chemical were therefore combined in Table 3.1, which also includes the combined data for polyester. These data confirm that 1 hour at RT is sufficient time to achieve the maximum yield of each chemical from cotton terrycloth using aqueous medium and that changing the time or

temperature does not improve extraction efficiency. All chemicals were more abundant in extracts of terrycloth than in polyester, and NNN and NNA were not detected in the extracts of polyester.

Table.3.1. Chemicals identified in aqueous THS extracts

Chemical	Terrycloth THS aqueous extract			Polyester THS aqueous extract	
	May 2012	Oct 2012	Jan 2013	Jan 2013	Sept 2013
Nicotine µg/g	105.8±25.5	112.92±8.59	69.6±30.4	0.557±0.82	1.689
Cotinine µg/g	0.899±0.13	1.04±0.14	0.446±0.04	0.269±0.06	0.18
N-formylnor-nicotine µg/g	3.9±0.72	1.138±0.13	1.047±0.27	0.427±0.09	0.420
Myosmine	4.844±0.31	4.518±0.25	3.010±0.12	X	0.066
2,3'-	1.242±0.08	1.196±0.03	0.681±0.06	X	0.026
Nicotelline	105.8±25.5	113.22±20.61	104.95±10.	36.35±10.6	59.61
NNA ng/g	229.3±95.6	218.8±16.4	88.3±8.8	X	X
NNK ng/g	169.5±27.2	218.8±16.38	132.36±9.7	X	3.2
NNN ng/g	37.10±5.18	45.84±3.08	31.25±3.46	X	X

X = not detected

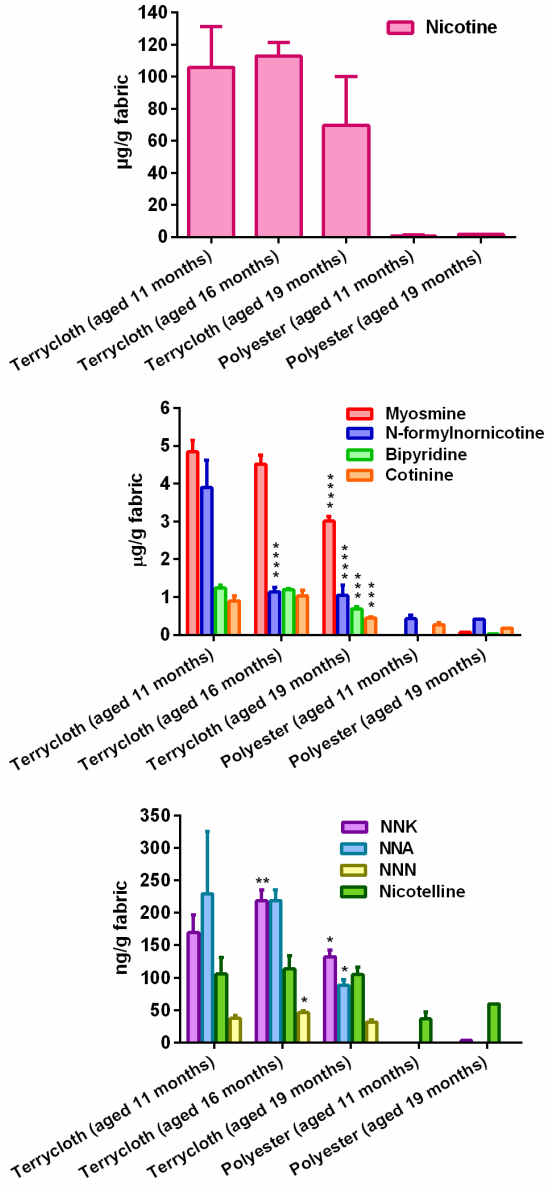

Figure 3.5. Effect of aging on the concentration of nicotine and its derivatives in aqueous extracts of terrycloth and polyester exposed to THS. Aqueous extracts of THS were made from terrycloth after 11, 16 and 19 months of aging and from polyester after 11 and 19 months of aging. **(A)** Nicotine and **(B)** Myosmine, N-formylnornicotine, bipyridine and cotinine were present in higher concentration than **(C)** nicotelline, NNK, NNA and NNN. Each bar is the average ± standard deviation of three extracts, except polyester (aged 19 months) which had only two experiments. ANOVA was used for testing significance followed by Dunnett's posthoc test in which comparisons were made to the samples aged for 11 months. **** $p < 0.0001$; *** $0.0001 < p < 0.001$; ** $0.001 < p < 0.01$; * $p < 0.05$.

Effect of aging on the concentrations of THS chemicals in extracts from terrycloth and polyester: In extracts of terrycloth, nicotine concentrations (105.8, 112.9, and 69.6 µg/gram of fabric) at 11, 16, and 19 months of aging (Fig. 3.5) were not significantly different when evaluated by ANOVA ($p = 0.0595$). Extracts of polyester made after 11 and 19 months of aging had very low amounts of nicotine (557 ng/g fabric and 168.8 ng/g fabric) in contrast to terrycloth that aged for similar times (Fig. 3.5 A).

Myosmine, N-formylnornicotine, 2,3'-bipyridine, and cotinine were present in extracts of terrycloth at µg/gram of fabric concentrations (Fig. 3.5B). The concentrations of extractable myosmine ($p < 0.0001$), 2,3'-bipyridine ($p < 0.0001$) and cotinine ($p = 0.0001$) decreased significantly after 19 months of aging (January 2013). The concentration of N-formylnornicotine decreased significantly ($p < 0.0001$) after 16 months of aging, but did not decrease further by 19 months. For this group of chemicals, the extract of polyester which aged 11 months contained only N-formylnornicotine and cotinine, and these were present in low concentrations compared to the corresponding terrycloth sample (11 months) (Fig. 3.5B). Extracts of polyester made after 19 months of aging had very low levels of myosmine, 2,3'-bypiridne, N-formylnornicotine and cotinine. All the chemicals in extracts of polyester were present at concentrations less than 1 µg/gram of fabric (Fig. 3.5 B).

In extracts of terrycloth, concentrations of nicotelline, NNA, NNK and NNN were in the ng/gram of fabric range (Fig. 3.5 C). Of these chemicals, only nicotelline did not decrease in concentration with aging, supporting its use as a tracer for tobacco smoke particulate matter (Jacob et al., 2013). The concentration of NNA decreased significantly by 19 months of aging ($p = 0.0108$). For both NNN and NNK, there was a slight but

significant increase in concentration at 16 months of aging ($p = 0.0020$ and 0.0004 respectively), followed by a significant decrease in NNK ($p = 0.0421$) at 19 months.

In extracts of polyester made after 11 months of aging, nicotelline was detected in very small amounts, but the three TSNAs were absent. After 19 months of aging, very small amounts of NNK were also detected (Fig. 3.5C). Statistical analysis was not performed for extracts of polyester since the extract prepared after 19 months of aging had only two experiments.

Discussion:

While the concentrations of some extractable THS chemicals in cotton terrycloth and polyester fleece changed during aging, in general THS chemicals remained on these fabrics for over 1.5 years after the last exposure to smoke. Nicotine and its derivatives, including NNK, a known carcinogen, were rapidly extracted from cotton fabric in an aqueous medium that is similar in composition to saliva and sweat. This implies that an infant that mouths cloth that has been exposed to cigarette smoke will be exposed to significant amounts of cigarette smoke toxins. There was a large difference in the quantity of chemicals extracted from cotton cloth and polyester cloth, showing that natural and synthetic fibers have different abilities to bind and release THS chemicals. These observations are important in understanding human exposure to THS and devising strategies for remediation

. Changes in the concentration of an individual chemical constituent of THS on a surface depend on multiple processes including sorbtion, desorbtion and chemical reactions. Whether a chemical remains on a surface or rapidly desorbs and is removed by ventilation depends on its volatility and chemical properties. Whether a chemical

reacts or remains intact depends on its chemical properties and the availability of other chemicals in the environment. With the exception of nicotelline, the chemicals we analyzed are semivolatile organic compounds, which means they will be present in both the gas phase and solid phase at normal indoor temperatures. For terrycloth, myosmine, 2',3';-bipyridine, N-formylnornicotine and cotinine decreased significantly during aging, possibly due to breakdown into other chemicals, volatilization, or conversion reactions with the ambient environment

The increased concentrations of both NNN and NNK at 16 months of aging followed by a decrease at 19 months could be due to formation of fresh TSNAs from settled nicotine before reaching a threshold and starting to decrease due to further conversions. Although NNA concentrations did not change in our extracts, the formation of NNA may have occurred prior to our first extraction, after 11 months of aging. Also, NNA, being an aldehyde, is more reactive than NNN and NNK and could have combined with other chemicals during aging. For polyester, the concentrations of all chemicals in aqueous extracts were very low. The increase in the number of chemicals that were present in the polyester sample that aged 19 months vs. 11 months may be an artifact caused by analyzing chemicals close to their lower limit of quantification (0.01ng/ml to 1ng/ml for different chemicals). The difference in the concentrations of chemicals extracted from cotton terrycloth and polyester fleece may be due to their surface chemistry. Our data are in agreement with prior studies showing that polar substances like nicotine and dyes do not bind well to polyester (L. Petrick, Destaillats, Zouev, Sabach, & Dubowski, 2010), (Koh, 2001).

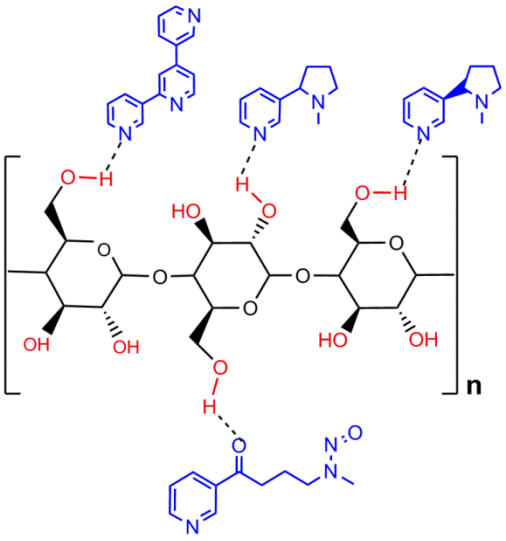

Figure 3.6. Chemical interactions of nicotine and its derivatives with terrycloth through hydrogen bonds. Terrycloth absorbs nicotine and related chemicals as these are polar in nature and can form hydrogen bonds with the free hydroxyl groups in terrycloth.

Cotton, which is made of cellulose, has three free hydroxyl groups/glucose monomer that can form hydrogen bonds with the polar groups on nicotine and its derivatives (Fig. 3.6) (L. Petrick et al., 2010), (Nishiyama, Sugiyama, Chanzy, & Langan, 2003) (Senthilkumar, Ghanty, Kolandaivel, & Ghosh, 2012). In contrast, polyester which is a polymer of terepthalic acid and ethylene glycol, is highly oleophilic (Bendak & El-Marsafi, 1991), and its hydrophobicity tends to repel polar compounds. However, it is possible that these THS compounds adsorb more strongly to polyester than to cotton and the DMEM or methanol:HCl extractions we used are not rigorous enough to fully extract them from polyester. THS contains thousands more chemicals than we analyzed, including many non-polar, non-water soluble chemicals. The interactions of other classes of chemicals with indoor surface materials will need to be characterized in future studies.

Our data clearly show that fabrics in indoor environments act as reservoirs for THS smoke chemicals. Although the samples used in this study received relatively light exposure to cigarette smoke, significant amounts of nicotine and related chemicals were extractable from cotton cloth 19 months after smoke exposure had stopped. In studies where smoke is released into a large chamber and allowed to mix with the air, age and interact with surfaces before particle concentrations are measured, the mass of particles

emitted by a single cigarette ranges from 7-22 mg, with averages between 8 and 14 mg (Daisey, 1998) (Klepeis, Apte, Gundel, Sextro, & Nazaroff, 2003) (Leaderer & Hammond, 1991) (Replace, 2007). Using an average emission factor of 10 mg per cigarette, the cotton cloth was exposed to the equivalent of 133 cigarettes and the polyester was exposed to the equivalent of 185 cigarettes. These exposures translate to 7-9 days of exposure in a room where 20 cigarettes are smoked per day or 27-37 days of exposure in a room where 5 cigarettes are smoked per day. While the health effects of these chemicals in THS residue are not yet known, it may become desirable or even necessary in the future to remediate property with THS residue before it is rented or sold (Matt et al., 2011). Our data demonstrate that nicotine and related compounds, including two carcinogens, can easily be removed from cotton fabrics by standard washing methods.

Since indoor surfaces act as reservoirs of THS, toddlers and infants could be exposed to THS chemicals by sucking on household fabrics, and all age groups could be exposed dermally by touching contaminated surfaces. To evaluate the exposure that could be received from cotton fabric containing THS residue, we examined a hypothetical scenario for dermal exposure to an adult. An adult wearing a 500g cotton outfit containing THS residue from 20 cigarettes will be exposed to about 7,894µg of nicotine/day and 32.7 µg of TSNAs/day, with a small fraction of this contributing to intake, assuming that the outfit would be washed frequently and could reasonably contain THS from 20 cigarettes before being washed.

A more accurate scenario can be developed for ingestion exposure to a toddler, where the intake will be roughly equal to the exposure. The main source of THS

exposure to a toddler would be through mouthing fabrics used in toys, drapes and upholstery that are not frequently washed and have long-term accumulation of THS. For terrycloth containing THS from about 133 cigarettes (as used in this study), a 12 kg toddler mouthing and sucking 5 grams of cloth for 1 hour would be exposed to 529 µg of nicotine/day and 2.2 µg of TSNAs/day. Since the exposure and intake are equal, the toddler would receive 44µg/kg body weight of nicotine and 0.183µg/kg body weight of TSNAs per day. These intake values for the toddler would be less than those received by an active smoker but higher than respiratory exposure in passive smokers (6.8 x higher for nicotine and 16 x higher for TSNAs) (Table 3.2).

Table 3.2. Estimated nicotine and TSNAs exposure to a toddler

Chemical	Inhalation Exposure Active Smoker	Inhalation Exposure Passive Smoker	Estimated Oral Exposure to THS
	Adult[a]	Toddler[b]	Toddler[c]
Nicotine	22,000 µg/day (Foulds, 2008)	77.76 µg/day (Okoli, Kelly, & Hahn, 2007)	**529 µg/day**
TSNA	7.2 µg /day (Ashley et al., 2010)	0.137 µg /day (Hecht, 2004)	**2.2 µg/day**

[a] Based on smoking 1 pack/day.

[b] Based on respiration rate of 30 breaths/minute and tidal volume of 60 ml in a room with 30µg/m^3 nicotine and 53ng/m^3 of TSNA.

[c] Based on 1 hour of mouthing 5 grams of terrycloth exposed to 133 cigarettes and aged 19 months.

Nicotine exposure causes cognitive impairment in children, affects brain development, and has been linked to obesity, hypertension, type-2 diabetes, respiratory dysfunction and impaired fertility in people exposed early in their lives (Yolton, Dietrich,

Auinger, Lanphear, & Hornung, 2004) (Dwyer, McQuown, & Leslie, 2009) (Bruin, Gerstein, & Holloway, 2010). Although the intake value for TSNAs is much less than doses known to cause tumors in rodent models (Brown et al., 2003), the above scenarios may underestimate exposure if significant levels of chemicals were lost during the first 11 months of aging or if THS accumulates from more than 133 cigarettes. TSNAs are known to contribute to pancreatic cancer (Edderkaoui & Thrower, 2013). It will be interesting to determine in future studies if there is a correlation between TSNA exposure during infancy and the recent increase in pancreatic or other types of cancer in adults. Exposure of toddlers to nicotine and TSNAs in THS is therefore a matter of concern and may need regulation.

Conclusion:

Our data show that fabrics exposed to cigarette smoke act as reservoirs of THS chemicals that are available for exposure long after smoking had ceased. Our extraction protocol could be scaled-up and applied to indoor environments requiring remediation and nicotine, nicotine-related alkaloids and TSNAs could be removed from cotton fabrics by simple washing. Our calculations enable an estimate of the oral and dermal exposure that toddlers and adults would receive from cotton fabrics exposed to THS from a relatively small number of cigarettes under controlled laboratory conditions. Estimated exposure concentrations to nicotine from THS are above those toddlers and adults would receive from inhalation of environmental tobacco smoke. It will be important in future studies to determine actual intake and uptake levels of THS chemicals in humans and establish if these concentrations are high enough to produce harm.

References:

Ashley, D. L., O'Connor, R. J., Bernert, J. T., Watson, C. H., Polzin, G. M., Jain, R. B., … McCraw, J. M. (2010). Effect of differing levels of tobacco-specific nitrosamines in cigarette smoke on the levels of biomarkers in smokers. *Cancer Epidemiology, Biomarkers & Prevention : A Publication of the American Association for Cancer Research, Cosponsored by the American Society of Preventive Oncology*, *19*(6), 1389–98. http://doi.org/10.1158/1055-9965.EPI-10-0084

Bendak, A, & El-Marsafi, S. (1991). Effects of Chemical Modifications on Polyester Fibres. *Journal of Islamic Academy of Sciences*, *4*(4), 275–284.

Brown, B.G., Borschke, A.J., Dolittle, D.J. (2003). An analysis of the role of tobacco-specific nitrosamines in the carcinogenicity of tobacco smoke. Nonlinearity in Biology Toxicology Medicine, 1(2), 179–198.

Bruin, J. E., Gerstein, H. C., & Holloway, A. C. (2010). Long-term consequences of fetal and neonatal nicotine exposure: a critical review. *Toxicological Sciences : An Official Journal of the Society of Toxicology*, *116*(2), 364–74. http://doi.org/10.1093/toxsci/kfq103

CDC (Centers for Disease Control and Prevention). 2014. Surgeon General's Report: The Health Consequences of Smoking—50 Years of Progress. Available: http://www.cdc.gov/tobacco/data_statistics/sgr/50th-anniversary/index.htm. Accessed 28th January 2014.

Daisey, J.M., Mahanama, K.R., Hodgson, A.T. (1998). Toxic volatile organic compounds in simulated environmental tobacco smoke: emission factors for exposure assessment. *Journal of Exposure Analysis and Environmental Epidemiology,* 8(3), 313-34.

DiCarlantonio, G. (1999). Inhalation of Mainstream and Sidestream Cigarette Smoke Retards Embryo Transport and Slows Muscle Contraction in Oviducts of Hamsters (Mesocricetus auratus). *Biology of Reproduction*, *61*(3), 651–656. http://doi.org/10.1095/biolreprod61.3.651

Dwyer, J. B., McQuown, S. C., & Leslie, F. M. (2009). The dynamic effects of nicotine on the developing brain. *Pharmacology & Therapeutics*, *122*(2), 125–39. http://doi.org/10.1016/j.pharmthera.2009.02.003

Edderkaoui, M., & Thrower, E. (2013). Smoking and Pancreatic Disease. *Journal of Cancer Therapy*, *4*(10A), 34–40. http://doi.org/10.4236/jct.2013.410A005

Fortmann, A. L., Romero, R. a, Sklar, M., Pham, V., Zakarian, J., Quintana, P. J. E., … Matt, G. E. (2010). Residual tobacco smoke in used cars: futile efforts and persistent pollutants. *Nicotine & Tobacco Research : Official Journal of the Society for Research on Nicotine and Tobacco*, *12*(10), 1029–36. http://doi.org/10.1093/ntr/ntq144

Foulds J, Delnevo C, Ziedonis DM, Steinberg MB (2008) Health Effects of Tobacco, Nicotine, and Exposure to Tobacco Smoke Pollution. In: Brick J editor. Handbook of the Medical Consequences of Alcohol and Drug Abuse. New York: Haworth Press. pp. 423-459.

Gieseke, C. (2005). Cigarette Smoke Inhibits Hamster Oocyte Pickup by Increasing Adhesion Between the Oocyte Cumulus Complex and Oviductal Cilia. *Biology of Reproduction*, *73*(3), 443–451. http://doi.org/10.1095/biolreprod.105.041152

Hammer, T. R., Fischer, K., Mueller, M., & Hoefer, D. (2011). Effects of cigarette smoke residues from textiles on fibroblasts, neurocytes and zebrafish embryos and nicotine permeation through human skin. *International Journal of Hygiene and Environmental Health*, *214*(5), 384–91. http://doi.org/10.1016/j.ijheh.2011.04.007

Hang, B., Sarker, A. H., Havel, C., Saha, S., Hazra, T. K., Schick, S., … Gundel, L. a. (2013). Thirdhand smoke causes DNA damage in human cells. *Mutagenesis*, *28*(4), 381–91. http://doi.org/10.1093/mutage/get013

Hecht, S. S. (2004). Carcinogen derived biomarkers: applications in studies of human exposure to secondhand tobacco smoke. *Tobacco Control*, *13 Suppl 1*, i48–56. http://doi.org/10.1136/tc.2002.002816

Hofhuis, W., Jongste, J. C. De, & Merkus, P. J. F. M. (2003). Adverse health effects of prenatal and postnatal tobacco smoke exposure on children. Archives of Disease in Childhood, 88,1086–1090. doi: 10.1136/adc.88.12.1086

Jacob, P., Goniewicz, M. L., Havel, C. M., Schick, S. F., & Benowitz, N. L. (2013). Nicotelline: A proposed biomarker and environmental tracer for particulate matter derived from tobacco smoke. *Chemical Research in Toxicology*, *26*(11), 1615–1631. http://doi.org/10.1021/tx400094y

Klepeis, N. E., Apte, M. G., Gundel, L. a., Sextro, R. G., & Nazaroff, W. W. (2003). Determining Size-Specific Emission Factors for Environmental Tobacco Smoke Particles. *Aerosol Science and Technology*, *37*(10), 780–790. http://doi.org/10.1080/02786820300914

Koh, J. (2007). Dyeing with disperse dyes. In P. Hauser (Ed.), *Textile Dyeing* (pp. 195-222). InTech.

Lehman-McKeeman, L. (2007). Absorption, distribution and excretion of toxicants. In C. Klaassen (Ed.), *Casarett & Doull's Toxicology: The Basic Science of Poisons* (7th ed., pp. 131-160). McGraw Hill Professional.

Leaderer, B. P., & Hammond, S. K. (1991). Evaluation of vapor-phase nicotine and respirable suspended particle mass as markers for environmental tobacco smoke. *Environmental Science & Technology*, *25*(4), 770–777. http://doi.org/10.1021/es00016a023

Martins-Green, M., Adhami, N., Frankos, M., Valdez, M., Goodwin, B., Lyubovitsky, J., … Curras-Collazo, M. (2014). Cigarette smoke toxins deposited on surfaces: implications for human health. *PloS One*, *9*(1), e86391. http://doi.org/10.1371/journal.pone.0086391

Matt, G. E., Quintana, P. J. E., Destaillats, H., Gundel, L. a, Sleiman, M., Singer, B. C., … Hovell, M. F. (2011). Thirdhand tobacco smoke: emerging evidence and arguments for a multidisciplinary research agenda. *Environmental Health Perspectives*, *119*(9), 1218–26. http://doi.org/10.1289/ehp.1103500

Nishiyama, Y., Sugiyama, J., Chanzy, H., & Langan, P. (2003). Crystal structure and hydrogen bonding system in cellulose Iα from synchrotron x-ray and neutron fiber diffraction. *Journal of the American Chemical Society*, *125*(47), 14300–14306. http://doi.org/ja0257319 [pii]

Öberg, M., Jaakkola, M. S., Woodward, A., Peruga, A., & Prüss-Ustün, A. (2011). Worldwide burden of disease from exposure to second-hand smoke: a retrospective analysis of data from 192 countries. *The Lancet*, *377*(9760), 139–146. http://doi.org/10.1016/S0140-6736(10)61388-8

Okoli, C. T. C., Kelly, T., & Hahn, E. J. (2007). Secondhand smoke and nicotine exposure: a brief review. *Addictive Behaviors*, *32*(10), 1977–88. http://doi.org/10.1016/j.addbeh.2006.12.024

Pang, X., & Lewis, A. C. (2011). Carbonyl compounds in gas and particle phases of mainstream cigarette smoke. *Science of the Total Environment*, *409*(23), 5000–5009. http://doi.org/10.1016/j.scitotenv.2011.07.065

Petrick, L., Destaillats, H., Zouev, I., Sabach, S., & Dubowski, Y. (2010). Sorption, desorption, and surface oxidative fate of nicotine. *Physical Chemistry Chemical Physics*, *12*(35), 10356–10364. http://doi.org/10.1039/c002643c

Petrick, L. M., Sleiman, M., Dubowski, Y., Gundel, L. a., & Destaillats, H. (2011). Tobacco smoke aging in the presence of ozone: A room-sized chamber study. *Atmospheric Environment*, *45*(28), 4959–4965. http://doi.org/10.1016/j.atmosenv.2011.05.076

Replace, J. (2007). Exposure to secondhand smoke. In O. Wallace & A. Steinemann (Eds.), *Exposure Analysis* (pp. 201-35). Florida: Boca Raton CRC Press.

Rehan, V. K., Sakurai, R., & Torday, J. S. (2011). Thirdhand smoke: a new dimension to the effects of cigarette smoke on the developing lung. *American Journal of Physiology. Lung Cellular and Molecular Physiology*, *301*(1), L1–8. http://doi.org/10.1152/ajplung.00393.2010

Riveles, K., Tran, V., Roza, R., Kwan, D., Talbot, P. (2007). Smoke from traditional commercial, harm reduction and research brand cigarettes impairs oviductal

functioning in hamsters (Mesocricetus auratus) in vitro. *Human Reproduction*, 22 (2), 346-355. doi: 10.1093/humrep/del380.

Sarker, A. H., Chatterjee, A., Williams, M., Lin, S., Havel, C., Jacob, P., … Hang, B. (2014). NEIL2 protects against oxidative DNA damage induced by sidestream smoke in human cells. *PloS One*, *9*(3), e90261. http://doi.org/10.1371/journal.pone.0090261

Schick, S. F., Farraro, K. F., Fang, J., Nasir, S., Kim, J., Lucas, D., … Jenkins, B. (2012). An apparatus for generating aged cigarette smoke for controlled human exposure studies. *Aerosol Science and Technology*, *46*(11), 1246–1255. http://doi.org/10.1080/02786826.2012.708947

Senthilkumar, L., Ghanty, T. K., Kolandaivel, P., & Ghosh, S. K. (2012). Hydrogen-bonded complexes of nicotine with simple alcohols. *International Journal of Quantum Chemistry*, *112*, 2787–2793. http://doi.org/10.1002/qua.23304

Sleiman, M., Gundel, L. a, Pankow, J. F., Jacob, P., Singer, B. C., & Destaillats, H. (2010). Formation of carcinogens indoors by surface-mediated reactions of nicotine with nitrous acid, leading to potential thirdhand smoke hazards. *Proceedings of the National Academy of Sciences of the United States of America*, *107*(15), 6576–81. http://doi.org/10.1073/pnas.0912820107

Talbot, P., & Lin, S. (2011). The effect of cigarette smoke on fertilization and pre-implantation development: Assessment using animal models, clinical data, and stem cells. *Biological Research*, *44*, 189–194. http://doi.org/10.4067/S0716-97602011000200011

Yolton, K., Dietrich, K., Auinger, P., Lanphear, B. P., & Hornung, R. (2004). Exposure to Environmental Tobacco Smoke and Cognitive Abilities among U.S. Children and Adolescents. *Environmental Health Perspectives*, *113*(1), 98–103. http://doi.org/10.1289/ehp.7210

Chapter 4: Cytotoxicity of Thirdhand Smoke and Identification of Acrolein as a Volatile Thirdhand Smoke Chemical That Inhibits Cell Proliferation

Introduction

Thirdhand smoke (THS) is a dynamic mixture of volatile, semi-volatile, and non-volatile chemicals, most of which are present in mainstream and secondhand tobacco smoke (Matt *et al.*, 2011). As THS ages, chemicals are continually formed and depleted in THS residue through interactions with chemicals in the ambient environment (Petrick *et al*., 2011; Sleiman *et al.*, 2010). Aging causes a build-up of nicotine derivatives, such as tobacco specific nitrosamines (TSNAs) (Thomas *et a*l., 2014;), as well as the loss of volatile organic chemicals (VOCs) (Sleiman *et al*., 2010; Sleiman *et al.*, 2014). Therefore the chemical composition of THS residue changes over time, which could impact its effects on biological systems.

While the adverse effects of mainstream and secondhand cigarette smoke are well documented (USDHHS, 2014) and can involve organs other than the respiratory system (DiCarlantonio and Talbot, 1999; Gieseke and Talbot, 2005), the health effects of THS have only recently been explored. THS can damage DNA (Hang *et al.*, 2013), alter differentiation in prenatal rat lung (Rehan *et al*., 2011), and adversely affect multiple organ systems in mice (Martins-Green *et al*., 2014). Given its potential to adversely affect health and its wide-spread distribution in indoor environments, THS has emerged as a public health concern, and further work is required to understand its effects on human health.

Human exposure to THS can occur through dermal contact (Hammer *et al*., 2011), ingestion (especially in infants and toddlers), and inhalation of the VOCs that come off surfaces containing THS residue (Bahl *et al*., 2014). Inhalation exposure is the

most difficult to avoid and could have significant health consequences across all age groups depending on the level and duration of exposure. VOCs in cigarette smoke, such as acetonitrile, dimethyl furan and 2',5'-dimethylfuran, have been reported in indoor environments where smoking occurred (Sleiman *et al*., 2014). Some chemicals, such as acrolein and acrylonitrile, were present in THS at concentrations higher than those considered safe by the State of California (OEHHA, 2014). The concentration of VOCs changed rapidly after smoking occurred, possibly due to sorption onto indoor surfaces (Sleiman *et al*., 2014). These sorbed VOCs desorb gradually into the indoor air and can be inhaled by occupants. It is important to identify those VOCs in THS that are likely to be detrimental to health (Matt *et al*., 2011)

The purpose to this study was to test the hypothesis that THS-exposed fabric contains chemicals that impair cell health, and then to identity cytotoxic chemicals in THS extracts and their mode of action. THS collected on terrycloth was extracted in cell culture medium at various times after deposition. The cytotoxicity of these extracts was determined using the MTT assay and the mode of action was evaluated using a live cell imaging assay. Authentic standards of VOCs identified in the headspace of THS extracts were further evaluated using the MTT assay. The mode of action and molecular targets were identified using a live cell imaging assay and gene expression arrays.

Materials and Methods:

Generation of THS: THS was generated in a controlled experimental chamber at the University of California San Francisco (UCSF) as described previously (Bahl *et al*., 2014; Schick *et al*., 2014).Terrycloth was exposed to cigarette smoke from Marlboro Red cigarettes for 114 hours over a span of 11 months, while polyester and paper were

exposed for 257 hours each over 6 months. We previously estimated the exposure for terrycloth to be equivalent to approximately 133 cigarettes. Using similar calculations (Bahl *et al.*, 2014), the polyester and paper were exposed to approximately 185 cigarettes. Exposed fabric was wrapped tightly in a plastic bag and stored with virtually no headspace.

Preparation of THS extracts in culture medium: Upon receipt at UCR, THS exposed terrycloth, polyester fleece and paper were stored at room temperature in amber bottles with headspace. Aqueous extracts of THS were prepared in Dulbecco's Modified Eagle Medium (DMEM). For all extractions, terrycloth, polyester fleece, and paper were weighed and cut into small pieces. A known weight of the fabric (0.125 g of fabric/ml of medium) was soaked in culture medium in 15 ml conical tubes. The tubes were subjected to constant agitation using a rotating shaker for 1 or 2 hours at either room temperature or 4^{o}C. For Figure 1, the tubes were directly centrifuged at 4,000g for 5 minutes; however, for all other data, the contents were transferred to a 3 ml plastic syringe (Sigma-Aldrich, St. Louis, MO) inside a fresh 15 ml conical tube, which was centrifuged at 4,000g for 5 minutes to recover the culture medium absorbed in the fabric. The recovered THS extract was filtered through 0.22µm sterile filters (Pall Corporation, Port Washington, NY), aliquoted into 1.5 ml vials, and stored at -80ºC. Some THS extracts of terrycloth were made immediately after receipt at UCR, and these are referred to as "fresh" in this article. Although the terrycloth had been stored at UCSF for 11 months before extraction, it was wrapped tightly in 0.06 mm thick polypropylene film and minimal loss of VOCs was expected during this time. Extracts of terrycloth were also made after 2 and 5 month of aging in amber bottles with head space at UCR. During this aging period, there was an opportunity for VOCs to escape into the headspace. THS

extracts from polyester fleece and paper were made after 1 month of storage in amber bottles at UCR.

Identification of VOCs in THS extract headspace: The volatile chemicals in THS headspace were identified at the Lawrence Berkeley National Laboratory using proton transfer reaction mass spectrometry (PTR-MS, IONICON). 1 mL of the THS extract was placed in a 20 mL glass impinger, with the inlet connected to a clean air flow of 100 mL/min and the outlet connected online to the PTR-MS and to a Tenax sorbent tube. PTR-MS mass spectrometry scan was performed in the range of m/z 18 - 150. The sampling flow for the Tenax sorbent tube was 20 mL/min, for duration of 1 hour. After sampling, the sorbent tube was analyzed using a Gerstel thermal desorption system coupled with a GC-MS (Agilent 6890, MSD5973) under operational parameters reported previously (Destaillats *et a*l., 2006).

Preparation of solutions of authentic standards of VOC: Twenty-five authentic standards of VOC (Table 1) were purchased (Fisher Scientific, Tustin, CA) then prepared in phosphate buffered saline (PBS) at stock concentrations of 0.01M. These chemicals were chosen for testing for three reasons: (1) some were identified in THS (Ueta *et al*., 2010), (2) some were identified in the air of American homes with THS, and (3) some were identified in the headspace of our THS extracts made after 2 months of aging in amber bottles. Working concentrations of each standard were prepared in the appropriate culture medium through serial dilutions and tested in the MTT or a live cell imaging assay.

In-vitro models for evaluating toxicity: In vitro models, which are rapid, predictive, and cost effective, are valuable for toxicity testing (Talbot, 2008). Whole THS

and individual chemicals were screened using mNSC, a model for neonatal brain, which is adversely affected in humans by cigarette smoke (Bruin *et al*., 2010; Dwyer *et al*., 2009). Follow-up assays were performed using human pulmonary fibroblasts (hPF) and lung epithelial cells (A549), which model the adult lung, a major target of inhaled VOC from THS. This choice of cells allowed comparison of the sensitivity of neonatal and adult cells to THS.

Culturing mouse neural stem cells (mNSC): mNSC were cultured in Dulbecco's Modified Eagle's Medium (DMEM) (Lonza, Walkersville, MD) containing 10% fetal bovine serum (Sigma-Aldrich, St. Louis, MO), 5% horse serum (Invitrogen, Grand Island, NY), 1% sodium pyruvate (Lonza, Walkersville, MD) and 1% penicillin–streptomycin (GIBCO, Invitrogen, Carlsbad, CA) (Behar *et al*., 2012). The cells were cultured in Nunc T-25 tissue culture flasks (Fisher Scientific, Tustin, CA) at 37ºC in 5% CO_2 and 95% relative humidity with medium changes on alternate days. When cells reached 80% confluency, they were used in an experiment. For detachment, cells were washed with Dulbecco's phosphate buffered saline (DPBS) then treated with 0.05% trypsin EDTA/DPBS (GIBCO, Invitrogen, Carlsbad, CA) for 1 min at 37ºC. For experiments, cells were plated using the protocol described previously (Bahl *et al*., 2012) at 2500 cell/ well (7,812 cells/cm^2) in 96 well plates for the MTT assay and at 5000 cell/ well (2,631 cell/cm^2) in 24 well plates for live imaging.

Culturing hPFs. hPF (ScienCell, Carlsbad, CA) were cultured using the suppliers' protocol (Bahl *et al*., 2012) in complete fibroblast medium containing 2% fetal bovine serum, 1% fibroblast growth serum, and 1% penicillin-streptomycin. hPFs were

grown on poly-L-lysine (ScienceCell, Carlsbad, CA) (15 µl/10 ml) coated T-25 flasks, which were prepared and incubated overnight prior to use. hPF were examined microscopically daily, and medium was changed every other day. hPF were cultured in 5% CO_2 at 37^{o}C and 95% relative humidity until 85% confluent, at which time they were used for MTT testing. For sub-culturing and experimental set up, cells were washed with DPBS and detached with 0.01% trypsin diluted in DPBS for 1 min at 37^{o}C after which FBS (Sigma-Aldrich, St. Louis, MO) was added to neutralize trypsin. Cells were plated at 5,000 cells/well (15,625 cell/cm^2), in 96 well plates, for the MTT assay and at 10,000 cells per well (5,263 cells/cm^2), in 24 well plates, for live cell imaging.

Culturing A549 lung epithelial cells: A549 cells (ATCC, Manassas, VA), which are widely used for toxicity testing (Bakand et al., 2009), were grown on non-coated T-25 flasks and cultured in F-12K medium (with L-Glutamine) with 10% A549 Specific FBS in 5% CO_2 at 37^{o}C and 95% relative humidity. A549 cells were examined microscopically daily until 85% confluent, at which time they were removed from the flask using 0.025% trypsin diluted in DPBS for 2 minutes at 37^{o}C. After 2 minutes of incubation with trypsin, cells were checked using a microscope, and the flask was tapped to loosen cells if necessary. When cells were detached, 3 ml of FBS (Sigma-Aldrich, St. Louis, MO) were added to neutralize trypsin. For the MTT assay, cells were plated at 15,000 cells/well (46,875 cells/ cm^2) in 96 well plates.

Testing THS extracts and VOCs for cytotoxicity using mNSC, hPF, and A549 cells in the MTT assay: Cells were plated in 96-well plates for 24 hours, then various concentrations of THS extract or authentic VOCs were added to wells, and plates were incubated for another 48 hours at 37ºC and 95% relative humidity. Untreated wells

adjacent to the cells with the lowest concentration of treatment served as the negative control. A vapor control column of untreated cells was also plated adjacent to the wells with the highest concentration treatments (Bahl et al., 2012). At the end of incubation, MTT (Sigma–Aldrich, St. Louis, MO) prepared at 5 mg/ml in DPBS with calcium and magnesium (Fisher Scientific, Tustin, CA) was added to each well, and plates were incubated for 2 hours at 37ºC. Plates were drained of solution, and 100 µL of dimethyl sulfoxide (DMSO) (Fisher, Tustin, CA) were added and mixed by pipetting to form a uniformly colored solution. Absorbance was read at 570 nm using the Epoch Microplate Spectrophotometer (Biotek, Winooski, VT). Each experiment was performed three times and duplicate wells were run for each group in each experiment. Similar experiments were done using hPF and A549 cells in the MTT assay with chemicals that were cytotoxic to mNSC and chemicals in the DALYs list (Sleimen *et al.,* 2014). VOCs identified in our THS headspace samples and those reported by Ueta *et al.* (2010) were also tested on mNSC by replacing the dose every 4 hours for up to 48 hours to determine if replenishing VOCs frequently would shift the dose response curves. Combinations of VOCs were also tested on mNSC to determine if their toxicity is additive or synergistic.

Live cell imaging: mNSC or hPF were plated in 24-well plates and incubated at 37ºC for 24 hours. Varying concentrations of THS or acrolein were prepared in culture medium and added to plated cells, which were transferred to a Nikon BioStation CT incubator (Nikon, Melville, NY) and imaged every 1 hour (THS) or 2 hours (acrolein) for 48 hours. For each well, data were collected from five different fields. Cell proliferation was analyzed in time-lapse images using video bioinformatics protocols created in CL-Quant software (DRVision, Seattle, WA). Each protocol was verified by comparing

ground truth obtained using ImageJ to data analyzed with CL-Quant. For proliferation, the results of ground truth and CL-Quant analyses were 95-98% similar (Fig. A.1).

Fluorescent staining for actin and tubulin: mNSC were plated on chamber slides (Ibidi, Planegg, Germany) at 2500 cells/well and incubated for 24 hours at 37ºC. Cells were treated with THS extracts for 2 hours, and then fixed using freshly prepared 4% paraformaldehyde. Cells were stained for tubulin using an anti-tubulin antibody (Cell Signaling Technologies, Danvers, MA) and for actin using phalloidin conjugated to Alexa fluor 488, (VWR, Radnor, PA) for 1 hour at room temperature. After washing with PBS to remove unbound phalloidin-Alexa fluor 488 and anti-tubulin antibody, mounting medium containing DAPI (Vector Laboratories Burlingame, CA) was added, and cells were imaged using a Nikon Ti Eclipse fluorescent microscope (Nikon, Tokyo, Japan).

RT^2 PCR Profiler Array: hPF were plated in 6 well plates at 50,000 cells/well (5,263 cells/cm^2) and allowed to attach overnight at 37ºC for 24 hours. After 24 hours, cells were treated with 1μM acrolein for 4, 24, 48 and 72 hours after which RNA was isolated using the Qiagen RNAeasy plus mini kit (Qiagen, Valencia, CA). RNA was checked for degradation using the Agilent 2100 Bioanalyzer, and only those samples having an RIN (RNA integrity number) of 7 or above were used for further processing. 400ng of RNA from each sample was used to prepare cDNA using the Qiagen RT^2 First Strand Kit (Qiagen, Valencia, CA). cDNA was amplified through a PCR reaction using primers for GAPDH to make sure that cDNA synthesis reaction has worked. Primer sequences used were as follows: 5'-GGAGccAAAAGGGTCATCATC-3' (forward) and 5'-AGTGATGGCATGGACTGTGGT-3' (reverse).

The effect of THS on the expression of 84 genes associated with the cell cycle was evaluated using the Qiagen Human Cell Cycle RT^2 Profiler Array. The reaction mixture was prepared by mixing cDNA with Qiagen RT^2 SYBR Green FAST Mastermix according to the manufacturer's protocol and then loaded on to the array plate. qPCR was performed using the BIO-RAD CFX384 Real Time PCR detection system (Bio-Rad, Hercules, CA). Ct values were entered into the online Qiagen data analysis center to obtain fold change values for gene expression.

Follow up PCR: Primers were designed for those genes whose levels were significantly altered across the three RT^2 PCR profiler array plates to confirm their changes in expression levels. Qiagen HotStarTaq Master Mix (Qiagen, Velencia, CA) was used to run PCR reactions using the BioRad Thermal Cycler (BioRad, Hercules, CA). Primers used were as follows: CASP3: 5'-TGAAACAGTATGCCGACAAG-3' (forward) and 5'-TAGAGTTCTTTTGTGAGCATG-3' (reverse); TFDP1: 5'-TTACCAAACGAGTCAGCTTAT-3' (forward) and 5'-CCTCTGTCTTTCCACCTCTAAG-3' (reverse); ANAPC2: 5'-AAAGGTTCTTCTACCGCATCTA-3' (forward) and 5'-TGGCAGAGATATAGAGGGTGAT-3' (reverse); WEE1: 5'-TATGAAAGTCCCGGTATACAACA-3' (forward) and 5'-ATCGAACTACATGAGAATGCTG-3' (reverse). Lonza DNA FlashGels were run to separate PCR products which were imaged using a Lonza FlashGel imaging system (Lonza, Walkersville, MD).

Statistical Analysis: For the MTT assay, statistical analyses were done on the raw data using GraphPad Prism software. Group means were compared using a one-way ANOVA. When $p<0.05$ in the ANOVA, Dunnett's post hoc test was used to compare

each dose to the control. For graphing, MTT absorbance data were normalized to 100% and treatment groups were expressed as a percentage of the negative control. IC_{50}s were determined from dose response curves using non-linear regression analysis in GraphPad Prism (Bahl *et al*., 2012). In cases where GraphPad could not derive an IC_{50}, the value was read off the dose response curve. The lowest observed adverse effect levels (LOAEL) (lowest dose that was significantly different than the control) and the no observed adverse effect levels (NOAEL) (the lowest dose that was not significantly different than the control) were determined.

For live cell imaging analysis, the percent area (confluency) was normalized to the area of the first frame (2 hours). 4 or 5 videos were analyzed for each treatment within every experiment, and three experiments were used for statistical analysis. Two-way ANOVA was performed by comparing area (confluency) at each time to the 4 hour data.to determine if there was a significant effect of concentration and time of treatment on area (confluency). The percentage of dead cells were analyzed using a one way ANOVA as described above with each group being compared to the untreated control using Dunnett's posthoc test.

For RT-PCR data, raw Ct values were put in the Qiagen data analysis center to identify those genes with expression levels that were significantly different than the control.

Results:

Extraction conditions affect the cytotoxicity of THS in the MTT assay: The cytotoxicity of THS extracted from terrycloth soon after receipt from USCF depended on the time and temperature of extraction (Fig. 4.1A). At an extraction ratio of 0.125g of

fabric/ml of medium, maximum cytotoxicity was observed at 30% and 100% concentrations after 1 hour of extraction at room temperature. Cytotoxicity was lost at the 30% concentration in samples extracted for 2 hours at room temperature. The extracts prepared at 4ºC for 1 hour were not cytotoxic at any concentration tested and were weakly cytotoxic at the 100% concentration when extracted for 2 hours at 4^{o}C (Fig. 4.1 A). Headspace volume of the extraction vessel was inversely correlated with cytotoxicity of the extracts (Fig. 4.1B). Extracts made for 1 hour at room temperature in tubes with 15 ml of headspace were cytotoxic at both the 30% and 100% concentrations. In contrast, extracts made for 1 hour at room temperature in T-25 flasks with 70 ml of headspace were cytotoxic only at the 100% concentration. The 2 hour extract was less cytotoxic than the 1 hour extract, and the smaller the headspace, the more potent the 2 hour extract (Fig. 4.1 B).

Aging of THS decreased the cytotoxicity of the extracts: THS-exposed terrycloth was aged in amber bottle with 250 ml of headspace for 5 months after receipt from UCSF, and then THS was extracted at room temperature for 1 and 2 hours using an extraction ratio 0.125g of fabric/ml of medium. Neither of the extracts from terrycloth aged in amber bottles for 5 months was cytotoxic to mNSC in MTT assay, in contrast to the extracts made soon after receipt from USCF, which were both cytotoxic (Fig. 4.1 C).

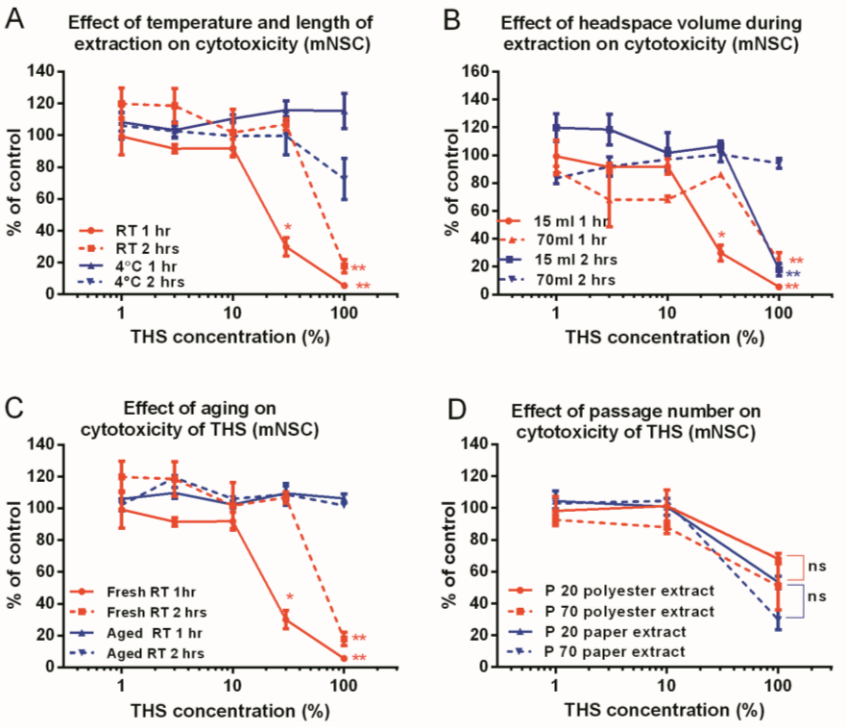

Figure 4.1. Factors affecting THS cytotoxicity in the MTT assay. MTT dose-response curves for mNSC showing absorbance (percent of control) plotted as a function of the THS extract concentration. **(A)** Effect of temperature and length of extraction on THS cytotoxicity. **(B)** Effect of headspace volume on THS cytotoxicity. **(C)** Effect of aging 5 months in amber bottles with headspace on THS cytotoxicity. **(D)** Effect of passage number on THS cytotoxicity. Samples designated "fresh" were extracted from terrycloth immediately upon receipt from UCSF without aging in amber bottles. Each point is the mean ± SEM of three or four experiments. In A, B, and C, doses were compared by ANOVA to the untreated fabric extract control. In D, the passage 20 and passage 70 data for each fabric were compared using a t-test at the 100% dose. * = $p < 0.05$; ** = $0.001 < p < 0.01$; **** $p < 0.0001$; ns = not

Passage number does not affect sensitivity to THS: To determine if cell passage number affects response to THS, extracts made from polyester fleece and paper, were tested for cytotoxicity using early and late passages of mNSC. Extracts were made at room temperature for 2 hours with extraction ratio of 0.25g of sample/ml of medium. Cells passaged 70-78 times were slightly more sensitive than those passaged 20-25 times (Fig. 4.1 D). However, the differences between the young and old passages were not significantly different at the 100% concentration when compared using an unpaired t-test ($p = 0.9632$ for polyester and $p = 0.9591$ for paper).

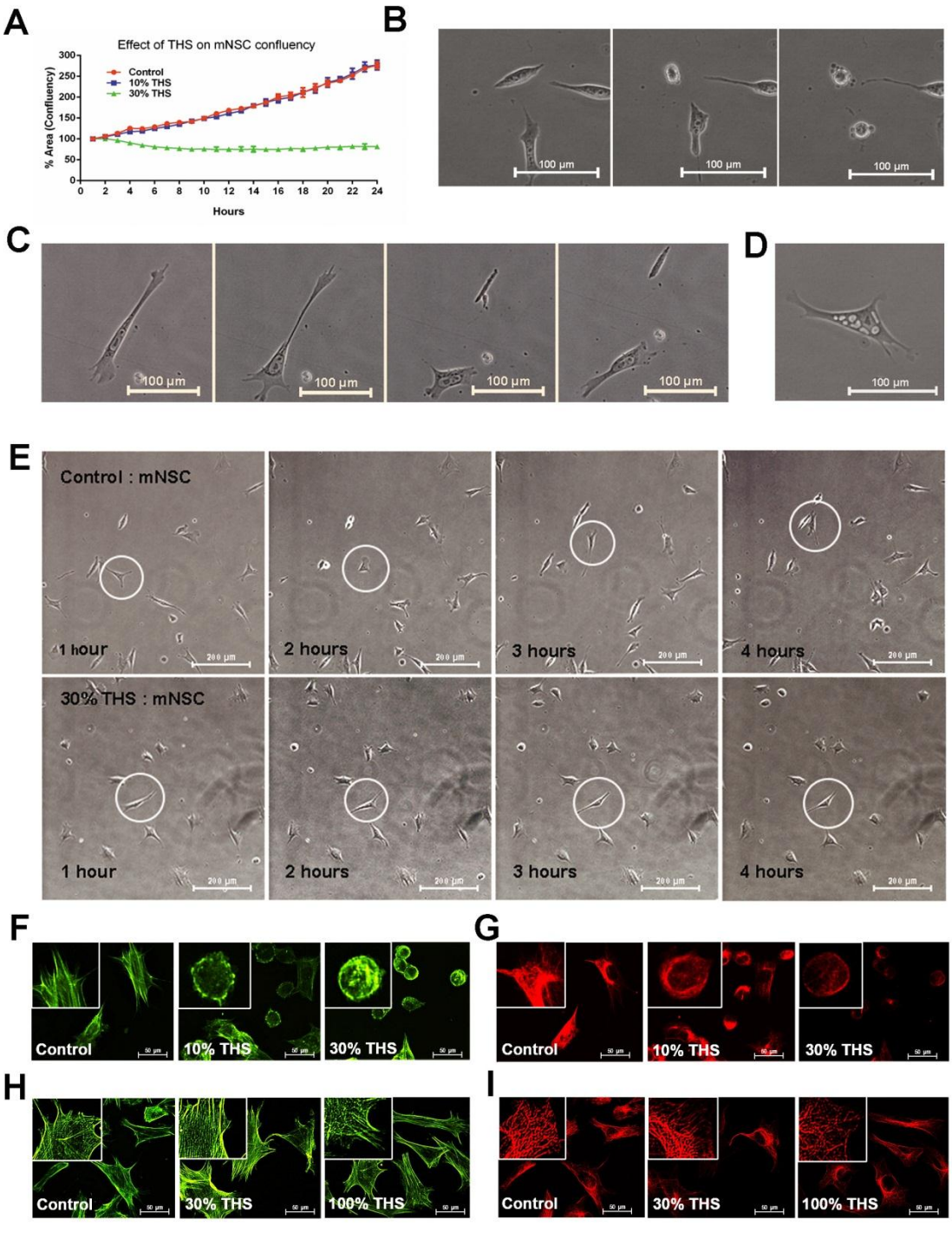
A
Effect of THS on mNSC confluency
Control
10% THS
30% THS
% Area (Confluency)
Hours
B
100 µm
C
100 µm
D
100 µm
E
Control : mNSC
1 hour
2 hours
3 hours
4 hours
30% THS : mNSC
1 hour
2 hours
3 hours
4 hours
F
Control
10% THS
30% THS
G
Control
10% THS
30% THS
H
Control
30% THS
100% THS
I
Control
30% THS
100% THS

Figure 4.2. **Effects of THS on confluency, morphology, and motility of mNSC**. mNSC were treated with THS extracted from terrycloth upon receipt of samples from UCSF, and cells were imaged live for 48 hours. **(A)** Dose-response curves showing area (confluency) vs. time. Data are plotted as means ± SEM are for three experiments. **(B)** Micrographs showing rounding and bleb formation characteristic of cells treated with 30 % THS. **(C)** Sequence of micrographs of a mNSC treated with 30% THS extract showing fragmentation during treatment. **(D)** Example of a mNSC treated with 30% THS that had vacuoles in its cytoplasm. **(E)** Sequence of images showing motility of control and treated (30% THS) mNSC; the control cells were motile over the 4 hour interval, while treated cells moved very little. Circles show the same cell at different times. **(F)** Images showing the effect of fresh THS extracts on actin microfilaments (green) and **(G)** microtubules (red) in mNSC. **(H)** Images showing that THS extracts aged in amber bottles with headspace for 5 months lost their ability to affect actin microfilaments and microtubules.

THS affected multiple cell processes: The effects of THS extract on dynamic cell processes were evaluated using live cell imaging coupled with video bioinformatics analysis (Fig. 4.2). mNSC were treated with 10% and 30% concentrations of THS extracted from terrycloth that was cytotoxic in the MTT assay. Cells treated with 10% THS extract grew at the same rate as control cells, reaching about 90% confluency by 45 hours, whereas cells treated with 30% THS did not grow (Fig. 4.2 A). In the 30% THS treatment group, confluency decreased at 3 hours and remained below the starting value throughout incubation (Fig. 4.2 A). Cells in the 30% group rounded up and appeared dead by 30 hours (Fig. 4.2 B). However, video analysis showed that the round cells could go through cycles of attaching, spreading and rounding up and sometimes rounded up and blebbed (Fig. 4.2 B) (Guan et al., 2014). Cells treated with 30% THS often fragmented and lost a portion of their cytoplasm. This occurred when the cell adhered tightly to the culture dish, and as the main body of the cell moved, the cell was torn into two fragments with the larger fragment usually containing the nucleus (Fig. 4.2 C). Some cells treated with 30% THS had vacuoles in their cytoplasm, consistent with stress (Fig. 4.2 D). The motility of mNSC treated with 30% THS extract was significantly decreased when compared to untreated controls (Fig. 4.2 E). Impaired motility was caused by disruption of the actin microfilaments and depolymerization of the microtubules and was sometimes accompanied by a change in morphology or rounding up of cells (Fig. 4.2 F-G). None of the above effects occurred when mNSC were treated with THS extracts that had aged in amber bottles and lost their cytotoxicity in the MTT assay (shown for cytoskeletal effects in Figs 4.2 H-I).

VOCs identified in THS headspace in this and in other studies: The above data are consistent with the idea that cytotoxicity was caused by VOCs in the THS

extracts. Data on VOCs in the headspace of THS extracts and homes were compiled (Table 4.1). Eleven VOCs were identified in the headspace of vials containing THS extracts from terrycloth that had aged 3 months at UCR in amber bottles, by which time extracts may not have been cytotoxic. The concentrations of these VOCs ranged from 1.05 to 14.41 μg/m^3. Some VOCs found in terrycloth extracts overlapped with VOCs found in the THS from the homes of cigarette smokers (Table 4.1, Sleiman *et al*., 2014). Table 4.1 also shows the concentrations of VOCs identified in THS from a Japanese study (Ueta *et al*., 2010), and the DALYS (disability adjusted life years) for VOCs in THS based on data in Sleiman *et al* (2014).

Table 4.1 VOCs present in THS

Chemical Name	Concentration in headspace sample[1]	Concentration in American homes with THS	Concentration reported by Ueta et al[3]	DALY's lost per year per 100,000 Sleiman[2]
Acrolein		0.1 – 1 μg/m^3		10-100
Furan		0.002 – 1 μg/m^3 0.014 nM		**1 - 10**
Acrylonitrile		1 μg/m^3 0.014 nM		0.1 1
1',3'-butadiene				0.1
Acetaldehyde				0.1
Isoprene		10 μg/m^3 0.14 nM		0.01 - 0.1
Benzene		1 – 10 μg/m^3 0.012 – 0.12	0 – 4 μg/m^3	0.01 – 0.1
Styrene		0.1 – 1 μg/m^3 0.096 – 0.96 pM		0.01 – 0.1
Toluene	4.14 μg/m^3 0.044 nM	10 μg/m^3 0.108 nM	0-10 μg/m^3	0.01 – 0.1
Acetonitrile	3.79 μg/m^3 0.092 nM	1 - 10 μg/m^3 0.024 – 0.24 nM		0.01 – 0.1
3-ethylenepyridine	14.41 μg/m^3 0.139 nM			
Phenol	8.83 μg/m^3 0.093 nM			
1H-Pyrrolo[2,3-b]pyridine,	7.26 μg/m^3 0.054 nM			
Benzaldehyde	7.64 μg/m^3 0.071 nM	0.1 – 1 μg/m^3 9 – 90 pM		

Acetophenone	5.43 µg/m^3 0.045 nM		
Quinoline	4.04 µg/m^3 0.03 nM		
Benzonitrile	3.7 µg/m^3 0.03 nM		
Acetone	2.88 µg/m^3 0.04 nM	10 – 100 µg/m^3 0.17 – 1.7 nM	
2-pentanone	2.58 µg/m^3 0.03 nM		
2-butanone	1.05 µg/m^3 0.014 nM		
2',5'-Dimethylfuran		0.1 – 1 µg/m^3 0.001 – 0.01 nM	
Ammonia			8-10 mg/ m^3 0.47 – 0.58 µM
2-furaldehyde			
Xylene			

Identification of cytotoxic VOCs using three cell types: All VOCs in Table 4.1 were screened in the MTT assay using mNSC (Fig. 4.3 and Fig. A. 2). Only phenol, 2',5'-DMF, and acrolein were cytotoxic to mNSC (Fig. 4.3).

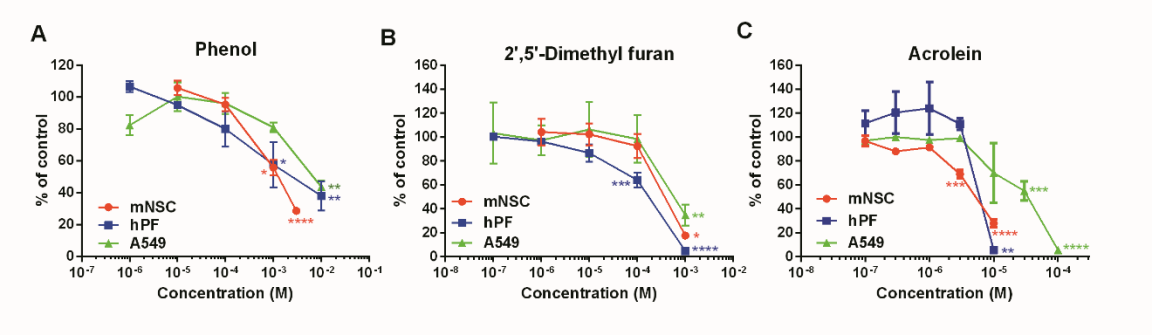

Figure 4.3. (A) Phenol, (B) 2',5'-DMF and (C) acrolein were cytotoxic to mNSC, hPF, and A549 cells in the MTT assay. Absorbance (percent of control) is plotted as a function of chemical concentration. Each curve represents means ± SEM for three experiments. Each concentration was compared by ANOVA to the untreated control. * = $p < 0.05$; ** = $0.001 < p < 0.01$; *** = $0.0001 < p < 0.001$; **** = $p < 0.0001$.

As a follow-up, phenol, 2',5'-DMF and the VOCs with highest DALYs were also tested using hPF and A549 cells (Fig. 4.3 and Fig. A.3). Only phenol, 2',5'-DMF, and acrolein were cytotoxic to all three cell types, at the concentrations tested. Acrolein was the most potent (Fig. 4.3). In general, the mNSC and hPF cells were more sensitive to the three chemicals than the A549 cells. The IC_{50}s for each chemical and each cell type are given in Table 4.2.

Table 4.2: IC_{50}, NOAEL and LOAEL values for acrolein, 2',5'-DMF and phenol

Chemical Name	mNSC	hPF	A549
Acrolein	IC_{50}: 6 x10^{-6} M LOAEL: 3 x 10^{-6} M NOAEL: 10^{-6} M	IC_{50}: 6 x10^{-6} M LOAEL: < 6 x10^{-6} M NOAEL: 3 x 10^{-6} M	IC_{50}: 4 x10^{-5} M LOAEL: 10^{-5} M NOAEL: 3 x 10^{-6} M
2',5'-dMF	IC_{50}: 4 x 10^{-4} M LOAEL: < 4 x 10^{-4} M NOAEL: 10^{-4} M	IC_{50}: 2 x 10^{-4} M LOAEL: 10^{-4} M NOAEL: 10^{-5} M	IC_{50}:6 x 10^{-4} M LOAEL: < 6 x 10^{-4} M NOAEL: 10^{-4} M
Phenol	IC_{50}: 1.1 X 10^{-3} M LOAEL: < 1.1 x 10^{-3}M NOAEL: 10^{-4} M	IC_{50}: 2 X 10^{-3} M LOAEL: 10^{-4} M NOAEL: 10^{-5} M	IC_{50}: 9 x 10^{-3} M LOAEL: 10^{-4} M NOAEL: 10^{-5} M

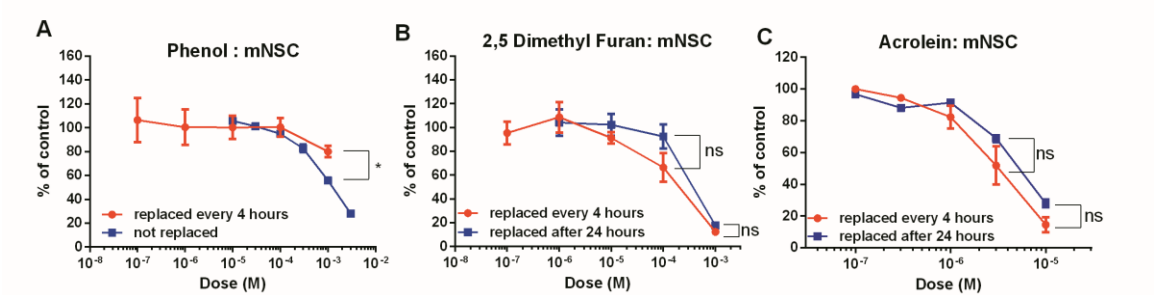

Figure 4.4. Effect of replacement of VOC on cytotoxicity to mNSC. **(A)** phenol, **(B)** 2',5'-DMF and **(C)** acrolein were replaced every 4 hours and tested on mNSC in the MTT assay. Absorbance (percent of control) is plotted as a function of chemical concentration. Each point represents the mean ± SEM for four values from two experiments. Each concentration was compared by ANOVA to the untreated control. Absorbance values for the two highest concentrations were compared in the two experiments using a t-test. * = $p < 0.05$; *** = $0.0001 < p < 0.001$: **** = $p < 0.0001$.

To determine if the evaporation of the volatile chemicals from the culture media caused underestimation of cytotoxicity, chemicals were replaced every 4 hours instead of at 24 hours (Fig. 4.4 and Fig. A.2). None of the chemicals tested were significantly more cytotoxic when replaced every 4 hours. The IC_{50} for 2',5'-DMF replaced every 4 hours = 2 X 10^{-4} M and replaced at 24 hours = 4 X 10^{-4} M. The IC_{50} for acrolein replaced every 4 hours = 3 X 10^{-6} M and replaced at 24 hours = 5 X 10^{-6} M (Fig. 4.4).

Effect of mixtures of cytotoxic chemicals on mNSC: mNSC were treated with combinations of chemicals identified by Ueta *et al*. (2010) and identified in the headspace of our THS extracts. These combinations were not cytotoxic at the doses tested (Fig. A.4). As a follow-up, acrolein, 2',5'-DMF and phenol, which were cytotoxic when tested individually, were tested in combination with mNSC and hPF (Fig. 4.5), and a significant increase in potency was observed. For mNSC, the IC_{50} of the combination (4.95 X 10^{-6} M) was very close to that of acrolein alone (3.416 x10^{-6} M); however, there was a significant effect at the 3 X 10^{-7} and 10^{-6} M concentrations, which was not seen with the individual chemicals (Fig. 4.5 A). For hPF, the IC_{50} for the combination of chemicals was 1 X 10^{-6} M, which was lower than the IC_{50} for any of the chemicals alone (Fig. 4.5 B).

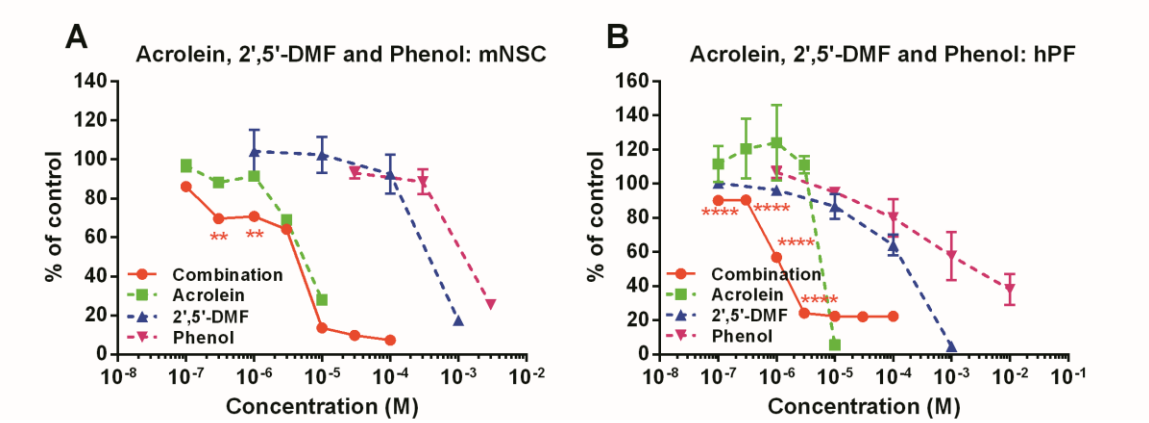

Figure 4.5. Effect of acrolein, 2',5'-DMF and phenol in combination: Dose response curves for three VOCs tested in combination on **(A)** mNSC and **(B)** hPF. Absorbance (percent of control) is plotted as a function of chemical concentration. Each point represents mean ± SEM for three experiments. * = $p < 0.05$; ** = $0.001 < p < 0.01$; *** = $0.0001 < p < 0.001$; **** = $p < 0.0001$.

Acrolein affected cell proliferation but not blebbing, fragmentation, vacuolization or motility of mNSC and hPF: Because acrolein was the most potent of the VOCs studied, follow-up experiments were done to determine its mode of action. mNSC were incubated in a BioStation CT and time-lapse images were recorded every 2

hours for 46 hours (Fig. 4.6 A). At the 10^{-5} M acrolein concentration, about 80% of the cells were dead and the growth curve was flat (Figs. 4.6 B). At the 3 x 10^{-6} M and 10^{-6} M concentrations, cell death was not significantly different from the untreated control but % area was significantly lower (Figs. 4.6 B and C). These observations are consistent with the idea that the lower confluency in these groups was due mainly to a decrease in cell proliferation.

Acrolein produced similar effects on hPF in the live cell imaging assay (Fig. 4.6 D). There were fewer cells in all concentrations of acrolein at 48 hours of treatment (Fig. 4.6 D). Acrolein at 6 X 10^{-6} M killed 100% of the cells and the growth curve was flat (Fig. 4.6 E). At the 10^{-6} M concentration, there was no cell death (Fig. 4.6 F) but growth (% area Fig. 4.6 E) was significantly lower than the untreated control, indicating acrolein inhibited cell proliferation at this concentration.

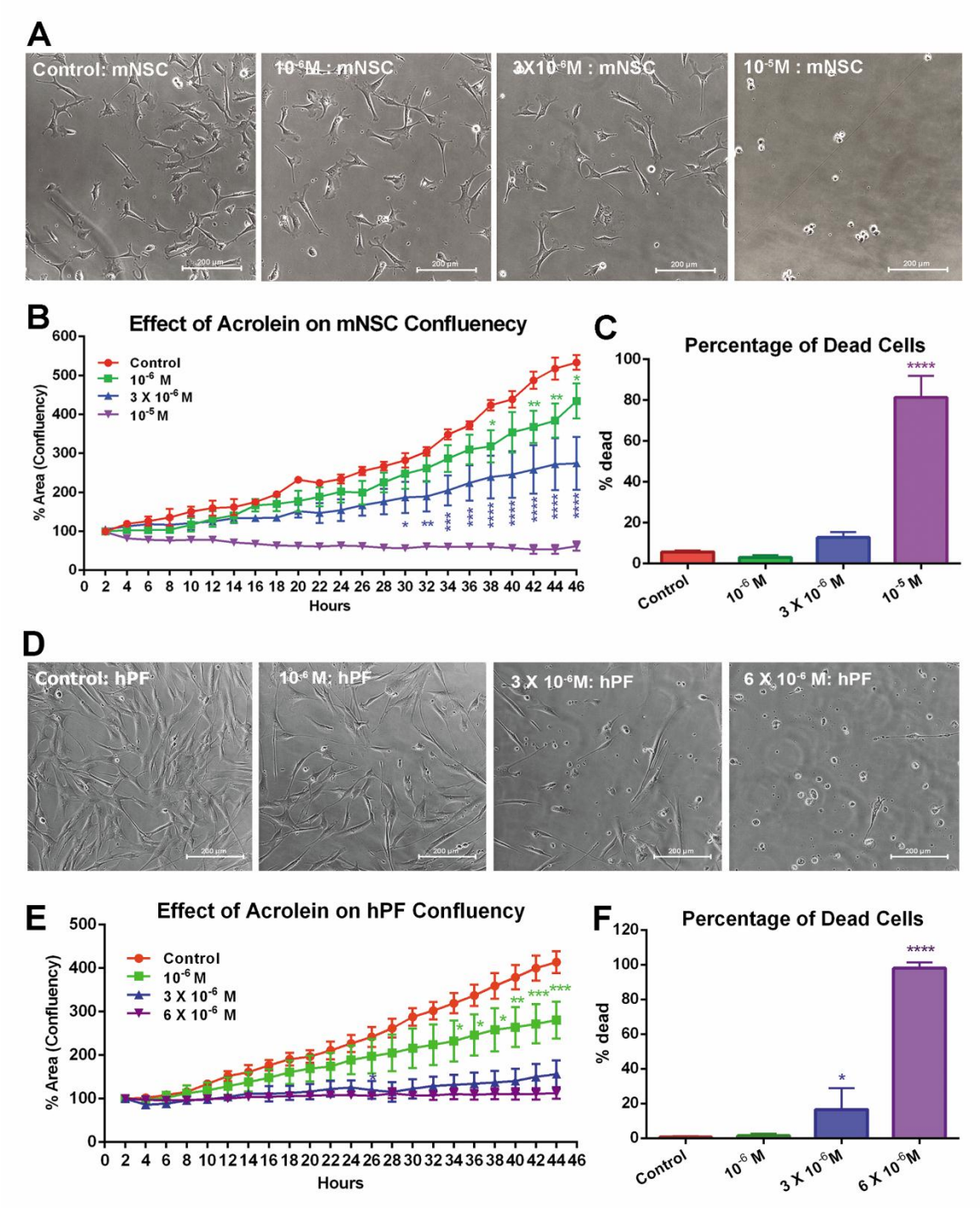
A
Control: mNSC
10-6M : mNSC
3X10-6M : mNSC
10-5M : mNSC
B
Effect of Acrolein on mNSC Confluenecy
Control
10-6 M
3 X 10-6 M
10-5 M
% Area (Confluency)
Hours
C
Percentage of Dead Cells
% dead
Control
10-6 M
3 X 10-6 M
10-5 M
D
Control: hPF
10-6 M: hPF
3 X 10-6M: hPF
6 X 10-6 M: hPF
E
Effect of Acrolein on hPF Confluency
Control
10-6 M
3 X 10-6 M
6 X 10-6 M
% Area (Confluency)
Hours
F
Percentage of Dead Cells
% dead
Control
10-6 M
3 X 10-6 M
6 X 10-6 M

Figure 4.6. Effect of acrolein on mNSC and hPF proliferation: (A) Micrographs showing mNSC confluency after treatment with acrolein for 48 hours. **(B)** Graph showing confluency of mNSC over 46 hours in control and treatment groups. **(C)** Graph showing the percentage of dead mNSC at 46 hours in each group. **(D)** Micrographs showing hPF confluency after treatment with acrolein for 48 hours. **(E)** Graph showing confluency of hPF over 46 hours. **(F)** Graph showing the percentage of dead hPF in each group at 46 hours. For B and E, area (confluency) at each time point is expressed as a percentage of confluency at 2 hours following start of treatment. Each point represents mean ± SEM for three experiments, each having 4 or 5 videos. For C and F, each bar represents mean ± SEM for three experiments, with five fields each. * = $p < 0.05$; ** = $0.001 < p < 0.01$; *** = $0.0001 < p < 0.001$; **** = $p < 0.0001$.

Acrolein altered expression of genes involved in cell cycle regulation: No changes in gene expression over 1.5 fold were observed in two pathway arrays run with samples treated 4 hour with 10^{-6} M acrolein, consistent with effect on growth not occurring at this time (Fig. 4.6 E). However, after 24 hours of exposure to acrolein,

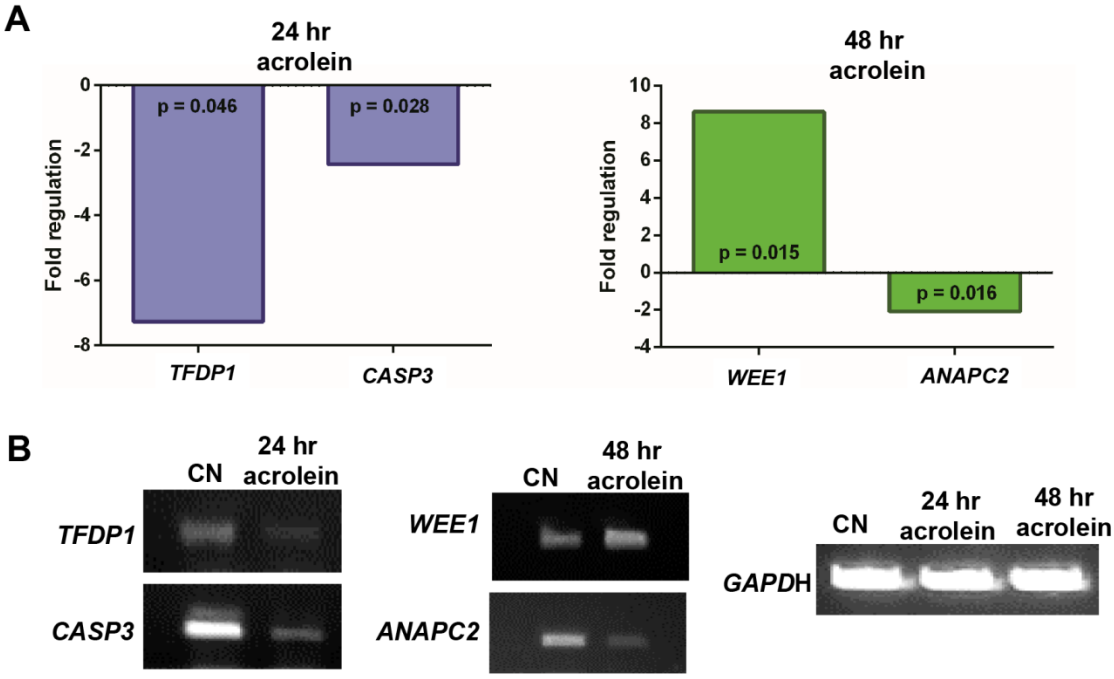

Figure 4.7. 10^{-6} M acrolein decreased expression of *TFDP1*, *CASP3* and *ANAPC2* and increased expression of *WEE1*. (A) Alteration in gene expression observed with RT^2 PCR profiler array. Each bar is an average of three experiments. **(B)** PCR products observed with gel electrophoresis. *GAPDH* was used as the housekeeping (loading) control.

expression levels of caspase 3 (*CASP3*) and transcription factor Dp-1 (*TFDP1*) were significantly decreased by 2.42 and 7.2-fold, respectively. At 48 hours, the *WEE1* G2 checkpoint kinase was significantly increased by 8.6-fold, while expression of the gene for anaphase promoting complex subunit 2 (*ANAPC2*) was significantly decreased by 2-fold (Fig. 4.7 A). Relative changes in the expression levels of these genes were confirmed by PCR (Fig. 4.7 B).

Discussion:

This study is one of the first to evaluate the cytotoxicity of THS, determine the effect of aging on THS's cytotoxicity, and identify cytotoxic VOCs in THS. Our main findings are summarized in Figure 4.8.

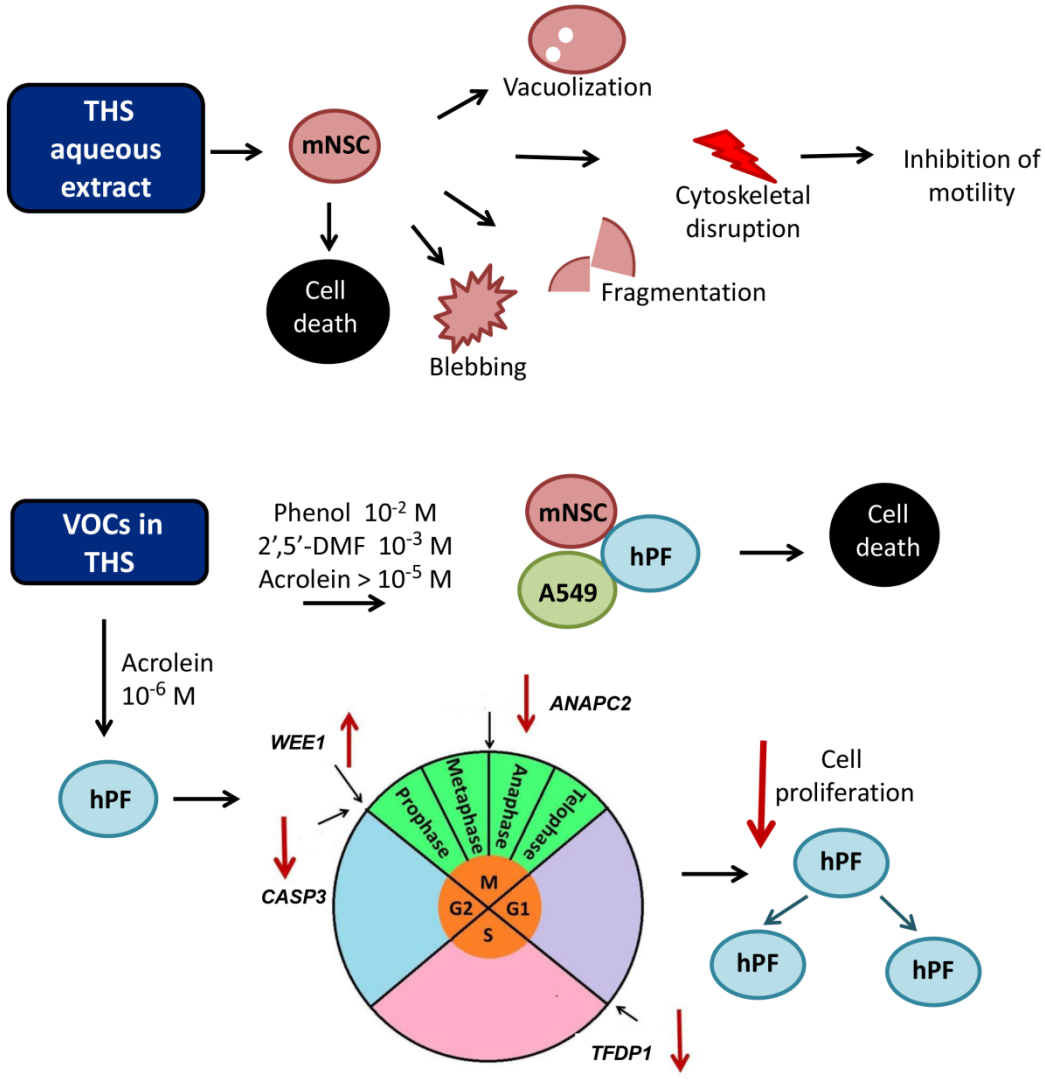

Figure 4.8. Diagram summarizing the response of cells to extracts of THS and to individual VOCs in THS: Aqueous extracts of THS caused cell death, blebbing, fragmentation, cytoskeletal disruption and vacuolization in mNSC at the 100% concentration . Phenol, 2',5'-DMF and acrolein caused cell death in mNSC, hPF and A549 cells at 10^{-2} M, 10^{-3} M and 10^{-5} M dose respectively. 10^{-6}M acrolein inhibited cell proliferation in hPF by decreasing expression of *TFDP1*, *CASP3*, *ANAPC2* and increasing expression of *WEE1.*

THS was toxic to mNSC causing cell death, blebbing, fragmentation, cytoskeletal disruption, and vacuolization. Loss of cytotoxic activity in fabric samples stored in amber jars with headspace indicated that VOCs are at least in part responsible for these effects. Of the VOCs tested, acrolein was the most cytotoxic, causing cell death at high concentrations and inhibiting cell proliferation at low concentrations. Acrolein altered expression of genes that regulate the cell cycle in a manner consistent with reduced proliferation and specifically blocked transition from G1 to S and from G2 to M. The experiments with different methods of extraction and aging in amber bottles indicated that VOCs in THS were likely responsible for the observed toxicity. This is a reason for concern since inhalation of VOCs in a THS environment is difficult to avoid. The degree of cytotoxicity of THS extracts depended on the temperature and time of extraction. The decreased cytotoxicity of extracts made at 4ºC is likely due to slower release of THS chemicals at the lower temperature. The reduced cytotoxicity of extracts prepared over 2 hours and those prepared in flasks with larger headspace are consistent with the conclusion that cytotoxicity was due to VOCs that are lost during prolonged extraction or when headspace volume is increased. The idea that VOCs contribute to cytotoxicity was also supported by the observation that THS extracts lost their cytotoxicity upon storage for 5 months in amber bottles with head space, while the concentrations of nicotine, most tobacco alkaloids, and TSNAs did not decrease significantly during storage (Bahl *et al*., 2014). While some VOCs may have been lost from terrycloth during the first 11 months of storage when they were tightly wrapped in plastic, the rate of loss was likely low as there was little headspace for desorption. From 11 months onwards, terrycloth was stored unwrapped in glass amber bottles with increased headspace which would have facilitated the loss of VOCs. The THS extracts used in this study were from fabric

that had aged without new cigarette smoke being deposited on the fabric. In a real indoor environment with smoking taking place, THS would not necessarily become less cytotoxic with time because additional cigarette smoke would be deposited periodically. This could lead to a build-up of higher levels of VOCs and novel compounds such as nitrosamines (Sleiman *et al*., 2010), which may in turn lead to a greater effect on cellular targets.

Three THS VOCs, phenol, 2',5'-DMF, and acrolein, were cytotoxic to each cell type in the MTT assay. Since a person in a THS environment would be exposed to these chemicals simultaneously, they were tested in combination and were toxic at lower concentrations. Therefore the dose response data for individual VOCs underestimates the actual cytotoxicity in THS. VOCs were screened only with the MTT assay, which evaluates the metabolism of a tetrazolium salt by mitochondrial reductases (Mosmann, 1983), and THS VOCs may have additional effects on cell health, not detected by this assay. While our study focused on 25 VOCs, there are other VOCs in THS (Sleiman *et al*., 2014), which may also be cytotoxic.

mNSC and hPF were more sensitive than A549 cells to phenol and acrolein, while hPF were more sensitive to 2',5'-DMF than mNSC and A549. This demonstrates the importance of screening multiple cell types when evaluating cytotoxicity. Because hPF were more sensitive to cytotoxic THS chemicals than A549 cells, they are an important *in vitro* model for toxicological studies dealing with adult lung.

Acrolein, a strong electrophile that reacts with proteins and DNA (Moghe *et al*., 2015), was the most cytotoxic of the VOCs tested. Acrolein adversely affects mitochondrial function, inflammation, and ciliary beating in multiple cell types (Moghe et

al., 2015; Talbot *et al*., 1998). In our study, live cell imaging showed that cell death alone could not account for decreased growth (% area) at low acrolein concentrations and that inhibition of cell proliferation was the mode-of-action of acrolein at non-lethal doses.

The cell cycle molecular targets of acrolein were identified using gene expression arrays. Acrolein is highly reactive and probably starts affecting molecular targets soon after exposure (Thompson and Burcham, 2008a), triggering a cascade of events that leads to decreased expression of caspase 3 (a protease) and *TFDP1* (a transcription factor that dimerizes with *E2F*). Inhibition of caspase 3 and down regulation of *TFDP1* arrest the cell cycle (Hashimoto *et al*., 2011; Yasui *et al*., 2003) and would block progression from G1 to S (*TFDP1*) and from G2 to M phase (caspase 3). At 48 hours, expression of *WEE1*, which blocks transition from the G2 to M phase (McGowan and Russel, 1995), was increased, while expression of *ANAPC2*, which promotes transition from metaphase to anaphase (Reddy *et al*., 2007), was decreased by acrolein. Thompson and Burchan (2008) reported genome wide transcriptional responses of A549 cells to acrolein with a greater number of genes affected than in our study. We used 1µM acrolein with primary pulmonary fibroblasts, while Thompson and Burchan (2008) used a 100µM acrolein with A549 cells. These differences likely account for the difference in the number of genes affected in the two studies. Our data clearly show effects on cell cycle regulatory genes consistent with inhibition of cell proliferation at concentrations 100 times lower than that used with A549 cells (Thompson and Burchan, 2008a).

It is important to consider how the effective concentration of acrolein *in vitro* compares to the dose a human receives in a THS environment. In our *in vitro* study, hPF proliferation was inhibited by 10^{-6} M acrolein (Fig. 4.6D, E). Because acrolein reacts

rapidly with proteins in the culture medium, only a fraction of it is available to affect cultured cells (Thompson & Burcham, 2008b). Based on values reported by Thompson & Burcham (2008b), we estimate that the concentration of acrolein actually available to cells in our studies was not 10^{-6} M but between 10^{-9} and 10^{-8} M.

The acrolein dose for nonsmokers exposed to THS will vary with factors such as the frequency of indoor smoking, ventilation, and time spent in a THS environment, and would likely be lower than in active smokers. Acrolein concentration reaching the respiratory system in a person exposed to THS can be estimated using the data of Sleiman *et al*. (2014). Acrolein concentration in a THS environment was 7μg m^{-3}, 2 hours after smoking six cigarettes (Sleiman *et al*., 2014). Considering a tidal volume of 500 ml, an adult would inhale roughly 4.2 μg of acrolein in 1 hour, assuming 20 inhalations/ minute. If all the inhaled acrolein dissolves in the extravascular lung water (EVLW), which is 3.8ml/ kg body weight (Wallin *et al*., 1994), a 50 kg person would have about 39 X 10^{-9} M of acrolein in the EVLW. While this value is an overestimation (some acrolein would be exhaled and some would turnover during 1 hour), it nevertheless supports the idea that a person in a THS environment could be exposed to enough acrolein (10^{-9} and 10^{-8} M based on our in vitro studies) to inhibit cell proliferation if not outright kill cells.

There were important differences in the responses of mNSC to 30% THS extracts and 10^{-6} M acrolein. While non-lethal concentrations of both THS and acrolein inhibited proliferation, only THS also caused blebbing, fragmentation, vacuole formation, loss of motility, disruption of microfilaments, and depolymerization of microtubules. The chemicals in THS responsible for the latter effects have not yet been identified and will be the subject of future studies.

In summary, our data support the idea that inhalation of THS VOCs has adverse effects on human health. Lung fibroblasts, which were killed by high doses of THS and acrolein and inhibited from dividing by low doses, perform important functions, such as secretion of the extracellular matrix (McAnulty, 2007) and alveolar regeneration (Plantier *et al*., 2007). A loss of lung fibroblasts due to cell death or decreased proliferation could disrupt lung homeostasis and lead to conditions such as pulmonary emphysema (Togo *et al*., 2008). While the concentrations of THS and acrolein in the brains of smokers and humans exposed to THS are not known and are likely less than that in the lung, neural stem cells were similarly affected by both THS and acrolein. An infant or small child in a THS environment is likely to take up higher levels of acrolein per unit of body mass than an adult, and toxicants can accumulate at a higher concentration in the brain of infants due to less efficient metabolism and clearance from the body (Ginsberg *et al*., 2004). These factors could have serious implications on the postnatal brain, which continues to develop throughout adolescence (Stiles and Jernigan, 2010).

.

References:

Bahl V., Jacob P., Havel C., Schick S. F., Talbot P. (2014). Thirdhand cigarette smoke: factors affecting exposure and remediation. PLoS One. 9(10), e108258. doi.org/10.1371/journal.pone.0108258

Bahl V., Lin S., Xu N., Davis B., Wang Y., Talbot P. (2012). Comparison of electronic cigarette refill fluid cytotoxicity using embryonic and adult models. Reprod. Toxicol. 34(4), 529-537. doi.org/10.1016/j.reprotox.2012.08.001

Bakand S., Hayes A., Winder C. (2009). Development of in vitro methods for toxicity testing of workplace air contaminants. IJOH 1(1), 26-33.

Behar R. Z., Bahl V., Wang Y., Weng J.-H., Lin S. C., Talbot P. (2012). Adaptation of stem cells to 96-well plate assays: use of human embryonic and mouse neural stem cells in the MTT assay. Curr. Protoc. Stem Cell Biol. Chapter 1:Unit 1C.13 doi.org/10.1002/9780470151808.sc01c13s23

Bruin J. E., Gerstein H. C., Holloway A. C. (2010). Long-term consequences of fetal and neonatal nicotine exposure: a critical review. Toxicol. Sci. 116(2), 364-374. doi.org/10.1093/toxsci/kfq103

Destaillats H., Singer B. C., Lee S. K., Gundel L. A. (2006). Effect of ozone on nicotine desorption from model surfaces : evidence for heterogeneous chemistry. Environ. Science. Technol. 40(6), 1799-1805.

Dwyer J. B., McQuown S. C., Leslie F. M. (2009). The dynamic effects of nicotine on the developing brain. Pharmacol. Ther. 122(2), 125-139. doi.org/10.1016/j.pharmthera.2009.02.003

DiCarlantonio G. and Talbot P. (1999) Inhalation of mainstream or sidestream cigarette smoke retards preimplantation embryo transport and muscle contraction in vivo. Biol. Reprod. 61(3), 651-656.

Gieseke C, and Talbot P. (2005). Cigarette smoke inhibits hamster oocyte pickup by increasing adhesion between the oocyte cumulus complex and oviductal cilia. Biol. Reprod. 73(3): 443-451.

Ginsberg G., Hattis D., Sonawane B. (2004). Incorporating pharmacokinetic differences between children and adults in assessing children's risks to environmental toxicants. Toxicol. Appl. Pharmacol. 198(2), 164-183. doi.org/10.1016/j.taap.2003.10.010

Guan B., Bhanu B., Talbot P., Lin S. (2014). Bio-driven cell region detection in human embryonic stem cell assay. IEEE/ACM Trans. Comput. Biol. Bioinforma. 11(3), 604-611.. doi.org/10.1109/TCBB.2014.2306836

Hammer T. R., Fischer K., Mueller M., Hoefer D. (2011). Effects of cigarette smoke residues from textiles on fibroblasts, neurocytes and zebrafish embryos and nicotine permeation through human skin. Int. J. Hyg. Environ. Health. 214(5), 384-391. doi.org/10.1016/j.ijheh.2011.04.007

Hang B., Sarker A. H., Havel C., Saha S., Hazra T. K., Schick S., Jacob P. 3rd, Rehan V.K., Chenna A., Sharan D., Sleiman M., Destaillats H., Gundel L.A. (2013). Thirdhand smoke causes DNA damage in human cells. Mutagenesis. 28(4), 381-391. doi.org/10.1093/mutage/get013

Hashimoto T., Kikkawa U., Kamada S. (2011). Contribution of caspase(s) to the cell Cycle regulation at mitotic phase. PLoS One. 6(3): e18449. doi:10.1371/journal.pone.0018449

Martins-Green M., Adhami N., Frankos M., Valdez M., Goodwin B., Lyubovitsky J., Dhall S., Garcia M., Egiebor I., Martinez B., et al. (2014). Cigarette smoke toxins deposited on surfaces: implications for human health. PLoS One. 9(1), e86391. doi.org/10.1371/journal.pone.0086391

Matt G. E., Quintana P. J. E., Destaillats H., Gundel L. A, Sleiman M., Singer B. C., Jacob P., Benowitz N., Winickoff J.P., Rehan V., et al. (2011). Thirdhand tobacco smoke: emerging evidence and arguments for a multidisciplinary research agenda. Environ. Health Perspect. 119(9), 1218-1226. doi.org/10.1289/ehp.1103500

McAnulty R. J. (2007). Fibroblasts and myofibroblasts: Their source, function and role in disease. Int. J. Biochem. Cell Biol. 39(4), 666-671. doi.org/10.1016/j.biocel.2006.11.005

McGowan C.H., and Russel P. (1995). Cell cycle regulation of human WEE1. The EMBO Journal. 14(10), 2166–2175.

Moghe A., Ghare S., Lamoreau B., Mohammad M., Barve S., McClain C., Joshi-Barve S. (2015). Molecular mechanisms of acrolein toxicity: relevance to human disease. Toxicol Sci. 143(2) 242-255. doi: 10.1093/toxsci/kfu233

Mosmann T. (1983). Rapid colorimetric assay for cellular growth and survival: application to proliferation and cytotoxicity assays. J. Immunol. Methods. 65(1-2), 155-161. doi.org/10.1016/0022-1759(83)90303-4

OEHHA (Office of Envirenmental Health Hazard Assessment). (2014). Ait toxicology and epidemiology. http://oehha.ca.gov/air/allrels.html

Petrick L. M., Sleiman M., Dubowski Y., Gundel L. A., Destaillats H. (2011). Tobacco smoke aging in the presence of ozone: a room-sized chamber study. Atmos. Environ. 45(28), 4959-4965. doi.org/10.1016/j.atmosenv.2011.05.076

Plantier L., Boczkowski J., Crestani B. (2007). Defect of alveolar regeneration in pulmonary emphysema: Role of lung fibroblasts. Int. J. COPD. 2(4), 463–469.

Reddy S.K., Rape M., Margansky W.A., Kirschner, M.W. (2007). Ubiquitination by the anaphase-promoting complex drives spindle checkpoint inactivation. Nature. 446, 921-925. doi:10.1038/nature05734

Rehan V. K., Sakurai R., Torday J. S. (2011). Thirdhand smoke: a new dimension to the effects of cigarette smoke on the developing lung. Am. J. Physiol. Lung Cell. Mol. Physiol. 301(1), L1-8.. doi.org/10.1152/ajplung.00393.2010

Schick S. F., Farraro K. F., Perrino C., Sleiman M., van de Vossenberg G., Trinh M. P., Hammond S.K., Jenkins B.M., Balmes J. (2014). Thirdhand cigarette smoke in an experimental chamber: evidence of surface deposition of nicotine, nitrosamines and polycyclic aromatic hydrocarbons and de novo formation of NNK. Tob. Control. 23(2), 152-159. doi.org/10.1136/tobaccocontrol-2012-050915

Sleiman M., Gundel L. A, Pankow J. F., Jacob P., Singer B. C., Destaillats H. (2010). Formation of carcinogens indoors by surface-mediated reactions of nicotine with nitrous acid, leading to potential thirdhand smoke hazards. Proc. Natl. Acad. Sci. U. S. A., 107(15), 6576-6581. doi.org/10.1073/pnas.0912820107

Sleiman M., Logue J. M., Luo W., Pankow J. F., Gundel L., Destaillats H. (2014). Inhalable constituents of thirdhand tobacco smoke: chemical characterization and health impact considerations. Environ. Sci. Technol. 48(22), 13093-13101. doi.org/10.1021/es5036333

Stiles J., and Jernigan T. L. (2010). The basics of brain development. Neuropsychol. Rev. 20(4), 327-348.doi.org/10.1007/s11065-010-9148-4

Talbot P., DiCarlantonio G., Knoll M., Gomez C. (1998) Identification of cigarette smoke components that alter functioning of hamster (Mesocricetus auratus) oviducts in vitro. Biol Reprod. 58, 1047-1053.

Talbot P. (2008). In vitro assessment of reproductive toxicity of tobacco smoke and its constituents. Birth Defects Res. C. Embryo Today. 84(1), 61-72. doi.org/10.1002/bdrc.20120

Thomas J. L., Hecht S. S., Luo X., Ming X., Ahluwalia J. S., Carmella S. G. (2014). Thirdhand tobacco smoke: a tobacco-specific lung carcinogen on surfaces in smokers' homes. Nicotine Tob. Res. 16(1), 26-32. doi.org/10.1093/ntr/ntt110

Thompson C. A., and Burcham P. C. (2008a). Genome-wide transcriptional responses to acrolein. Chem. Res. Toxicol. 21(12), 2245-2256. doi.org/10.1021/tx8001934

Thompson C. A., and Burcham P. C. (2008b). Protein alkylation, transcriptional responses and cytochrome c release during acrolein toxicity in A549 cells: Influence

of nucleophilic culture media constituents. Toxicol. Vitr. 22(4), 844-853. doi.org/10.1016/j.tiv.2007.12.018

Togo S., Holz O., Liu X., Sugiura H., Kamio K., Wang X., Kawasaki S., Ahn Y., Fredriksson K., Skold C.M. (2008). Lung fibroblast repair functions in patients with chronic obstructive pulmonary disease are altered by multiple mechanisms. Am. J. Respir. Crit. Care Med. 178(3), 248-260. doi.org/10.1164/rccm.200706-929OC

Ueta I., Saito Y., Teraoka K., Miura T., Jinno K. (2010). Determination of volatile organic compounds for a systematic evaluation of third-hand smoking. Anal. Sci. 26(5):569-574.

USDHHS (U.S. Department of Health and Human Services). the health consequences of smoking: 50 years of progress. A report of the Surgeon General. Atlanta, GA: U.S. Department of Health and Human Services, Centers for Disease Control and Prevention, National Center for Chronic Disease Prevention and Health Promotion, Office on Smoking and Health, 2014. Printed with corrections, January 2014

Wallin C.J. and Leksell L.G. (1994). Estimation of extravascular lung water in humans with use of 2H2O: effect of blood flow and central blood volume. J Appl Physiol. 76(5), 1868-75.

Yasui K., Okamoto H., Arii S., Inazawa J. (2003). Association of over-expressed TFDP1 with progression of hepatocellular carcinomas. J. Hum. Genet. 48(12), 609-613. doi.org/10.1007/s10038-003-0086-3

Chapter 5: Thirdhand Smoke: Chemical Dynamics, Cytotoxicity, and Genotoxicity in Outdoor and Indoor Environments

Introduction

While the adverse health effects of smoking and secondhand cigarette smoke exposure are well known (CDC, 2015; USDHHS, 2014), THS has only recently emerged as a public health concern (Matt et al., 2011). Experiments in cell-based systems and animal models are beginning to show that THS can be toxic. THS caused DNA damage in liver cells (Hang et al., 2013) and reduced neurite length and heart rate in zebra fish embryos (Hammer et al, 2011). In developing rat lung, 1-(N-methyl-N-nitrosamino)-1-(3-pyridinyl)-4-butanal) (NNA), a constituent of THS, disrupted signaling mechanisms by decreasing the levels of peroxisome proliferator-activated receptor and up-regulating fibronectin (Rehan et al., 2011). THS also produced detrimental effects on multiple organ systems in a mouse model (Martins-Green et al., 2014).

THS exposure can occur through inhalation, dermal contact, or ingestion. Toddlers and infants may have higher exposure to THS than adults because they are more likely to touch and mouth THS chemicals on toys, clothing, upholstery, and other indoor surfaces. Our recent work showed that THS remained on fabrics for many months after smoking had ceased (Bahl et al., 2014) In these experiments, we found significant levels of nicotine and tobacco specific nitrosamines (TSNAs), two of which (4-(methylnitrosamino)-1-(3-pyridyl)-1-butanone (NNK), and N'-nitrosonornicotine (NNN)) are known carcinogens and the third, NNA, has been reported to cause DNA damage (Hang 2010). NNA is not found in mainstream or secondhand tobacco smoke and is specific to THS (Sleiman et al., 2010). It is formed during aging of THS by reaction of nicotine with the ambient oxidant chemicals (Petrick et al., 2011; Sleiman et al., 2010).

Chemical changes that occur in THS as it ages are likely to affect its mode of action and level of toxicity.

In the present study, we investigated the cytotoxicity and genotoxicity of THS using *in vitro* cell models and controlled laboratory conditions for the generation and collection of THS. We tested THS extracted from various fabrics on mouse neural stem cells (mNSC) from the neonatal cerebellum and on adult human dermal fibroblasts (hDFs). THS extracts from terrycloth were also tested with human palatal mesenchyme cells (hPM).The use of *in vitro* models for toxicity screening is rapid, can be predictive, and serves as an excellent alternative to animal testing of environmental toxicants (Bahl et al., 2012; Behar et al., 2012a,b; Eisenbrand et al., 2002; Talbot, 2008; Yu et al., 2006).

This study was carried out to test the hypotheses that low levels of THS adversely impact cell health and survival and that the chemicals in THS change as THS ages. We generated THS in two separate experiments. In one experiment, we exposed automotive seat cover fabric and automotive carpet samples to realistic concentrations of cigarette smoke in an acrylic chamber outdoors. The automobile experiment was designed to determine how THS behaves in an automobile parked outdoors for 1 month. This experiment was scaled to mimic a scenario in which 20 cigarettes are smoked per day for 30 days. In the second experiment, we exposed 100% cotton terrycloth to cigarette smoke in a controlled indoor exposure chamber with no sunlight. The smoke was generated at irregular intervals over 16 months. THS was extracted from fabrics in both experiments and analyzed using LC-MS/MS to determine the concentrations of nicotine, related alkaloids, and tobacco specific nitrosamines (TSNAs). The MTT assay, which relies on conversion of a tetrazolium salt to a colored product through the

enzymatic activity of metabolically active cells, was used to assay cell viability/survival and cytotoxicity. Rates of proliferation were measured using live cell imaging, and genotoxicity of THS extracts was examined using single cell gel electrophoresis (comet assay), which detects single strand breaks in DNA.

Materials and Methods

Car Simulation (Outdoor) Experiment: Synthetic car seat cover fabric (Auto Expressions part 5078760) and synthetic car carpet were purchased from O'Reilly Auto Parts (Riverside, CA.) was exposed to puffs of sidestream cigarette smoke or puffs of indoor air (control) in an acrylic chamber measuring 32cm x 32cm x 60cm and having a volume of 61,440 cm^3 (about 0.06m^3), which is about 50 times smaller than the interior of an average car (3 m^3). An overview of the experimental design for the car experiment is shown in Figure 5.1 A. The car exposure chamber was closed but the lid and the three ports were not sealed to allow some ventilation. Marlboro Red cigarettes were puffed using ISO standards (2 second puffs x 35 ml puff volumes for 1 minute) on a smoking machine as described previously (Knoll and Talbot, 1998; Knoll et al., 1995) using a MasterFlex peristaltic pump (Barnart Company, Barrington, IL, Model #7520-00) to generate sidestream smoke which entered the chamber through polyvinylchloride tubing (Cole Parmer MasterFlex Tygon) for 4 minutes/day (1 minute every 2 hours for 8 hours) over a total of 30 days (Figure 5.1 B). This is equivalent to about 20 cigarettes being smoked in a car/day, assuming it takes about 10 minutes for a person to smoke one cigarette. Control chambers were similar to experimental chambers but fabric was exposed to puffs of indoor air instead of cigarette smoke. The acrylic chambers were placed outdoors in an enclosed locked area (Fig. 5.1 C), except when exposures were being done in the laboratory. During this phase of the experiment, the average highest

daily temperature was 33.6°C and average lowest daily temperature was 18.5°C. After 30 days of exposure, the seat cover and carpet fabrics were removed from the chambers and culture medium extracts of THS were made in DMEM medium and human dermal fibroblast basal medium. After smoking had stopped, a subset of each fabric was aged for 60 days in the acrylic chambers which were kept outdoors to mimic a parked car. The chambers were not sealed to allow VOCs to escape as they would from a parked car. The average highest and lowest daily temperatures were 32.4°C and

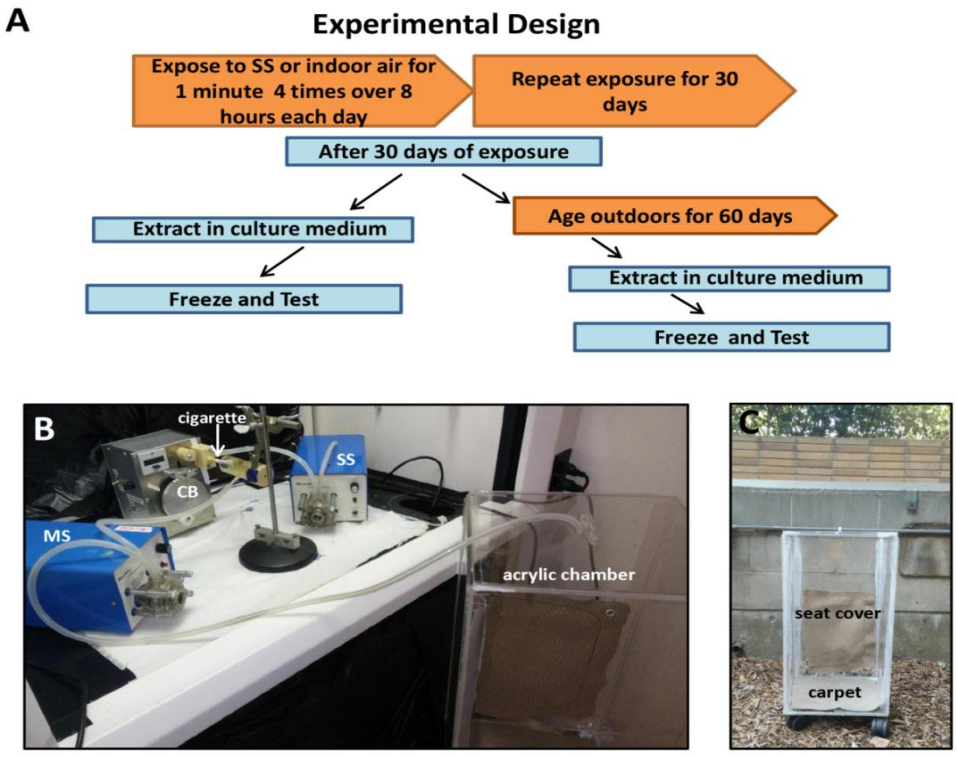

Figure 5.1. Design and THS generation for the car experiment. (A). Over view of the design used for the car experiment. **(B)** THS generation set-up showing a Marlboro Red cigarette (arrow), two peristaltic pumps that were used for the generation of mainstream (MS) and sidestream smoke (SS), and the controller box (CB). SS or indoor air was introduced in to an acrylic chamber through tygon tubing and allowed to settle on car seat cover and car carpet fabric in the chamber. SS smoke was generated for 1 minute every 2 hours, 4 times a day for 30 days. **(C)**. Acrylic chamber with car seat cover and carpet in outdoor location to mimic a car.

18.3°C during the first month and 26.6°C and 12.5°C during the second month of aging. After 60 days, THS was extracted from the aged fabrics in culture medium as described above.

Indoor Experiment: The second experiment was designed to study THS accumulation over time in a controlled indoor environment, such as a home or office. Twelve inch square pieces of terrycloth, pre-washed 2 times with Country Save Laundry detergent and line dried, were kept in a laboratory exposure chamber at the University of California San Francisco for up to 16 months as described previously (Bahl et al., 2014; Schick et al., 2014). Terrycloth was removed from the exposure chamber approximately every month and shipped overnight at ambient temperature to UCR for extraction and analysis. The number of cigarettes smoked each month varied, and in some months no smoking was done to allow aging. THS extracts were made from small pieces of each exposed sample and of un-exposed terrycloth samples. Extracts were performed as described below within 5 days after they were received at UCR. The remaining pieces of each sample were wrapped in plastic bags, stored at room temperature, and some were later extracted for further study.

Preparation of THS Extracts in Culture Medium: THS was extracted from control (unexposed) and THS exposed car seat cover, car carpeting, and terrycloth in Dulbecco's Modified Eagle Medium (DMEM) (mNSC) and in Fibroblast Basal Medium (hDF). For all extractions, the smoke-exposed fabrics and indoor air exposed controls were weighed and cut into small pieces using scissors. A known weight of the fabric (0.05g /ml of medium) was agitated in culture medium in 50 ml conical tubes, using a shaker, for 1 hour at room temperature (Bahl et al., 2014). The contents of the tube were

transferred to a 30 ml plastic syringe (Sigma-Aldrich, St. Louis, MO) to recover the medium from the fabric. This THS extract was filtered using 0.22 µm sterile filters (Pall Corporation, Port Washington, NY). After extraction, 10% fetal bovine serum (Sigma-Aldrich, St. Louis, MO), 5% horse serum (Invitrogen, Carlsbad, CA) and 1% sodium pyruvate (Lonza, Walkersville, MD) were added to the DMEM-based extracts to make complete mNSC medium, and human dermal fibroblast supplement was added to the fibroblast basal medium extracts to make complete fibroblast medium. The THS extracts were aliquoted into 1.5 ml vials and stored at -80ºC. For some experiments, extraction was done using complete mNSC culture medium containing fetal bovine serum and horse serum and complete hDF medium. Extracts from terrycloth exposed to cigarette smoke for 8 months and unexposed terrycloth were also made in human palatal mesenchyme (hPM) growth medium containing 10% serum.

Dilutions of extracts were prepared by mixing full strength (100%) extracts with complete culture medium. For example, 30% extract was made by mixing 30% full strength extract + 70% complete culture medium.

Chemical Analysis of THS Extracts: The chemical content of the THS extracts and extracts from control fabrics was analyzed by liquid chromatography coupled with tandem mass spectrometry (LC-MS/MS) as described in detail previously (Bahl et al., 2014). Briefly, the samples were analyzed at University of California San Francisco on a Thermo Scientific Vantage LC-MS/MS with an Accela UPLC system using a 3X150 mm 2.6 micron Phenomenex Kinetex PFP column (Whitehead et al., 2015).

Culturing Mouse Neural Stem Cells (mNSC): mNSC were cultured in Dulbecco's modified Eagle's medium (DMEM) (Lonza, Walkersville, MD) containing

10% fetal bovine serum, 5% horse serum, 1% sodium pyruvate (Lonza, Walkersville, MD) and 1% penicillin–streptomycin (GIBCO, Invitrogen, Carlsbad, CA) (Behar et al., 2012). The cells were cultured in Nunc T-25 tissue culture flasks (Fisher Scientific, Tustin, CA) at 37ºC in 5% CO_2 and 95% relative humidity. Medium was replaced on alternate days, and when confluency reached ~80%, cells were used in an experiment. To detach cells, plates were washed with DPBS and then treated with 0.05% trypsin EDTA/DPBS (GIBCO, Invitrogen, Carlsbad, CA) for 1 min at 37ºC. Cells were plated at 2,500 cells/well in 96 well plates for the MTT assay (7,812 cells/ cm^2) and at 5,000 cells/well in 24 well plates (2,631 cells/ cm^2) for live cell imaging using a BioStation CT. For comet assays, cells were plated at 10,000 cells/well in 24 well plates (5,263 cells/ cm^2).

Culturing Human Dermal Fibroblasts (hDF): hDF from a 56 year old Caucasian female were purchased from Promo Cell (Heidelberg, Germany) and cultured according to the supplier's protocol using complete fibroblast medium with 2% supplement at 37 °C with 5% CO_2 and 95% relative humidity. Medium was replaced on alternate days. Cells were used for an experiment when the flask was ~80-85% confluent. For detachment, cells were washed with HBSS solution (Promo Cell, Heidelberg, Germany) and then treated with trypsin-EDTA (Promo Cell, Heidelberg, Germany) for 1 minute at room temperature (RT). Trypsin was inactivated using trypsin inhibitor (Promo Cell, Heidelberg, Germany), and cells were centrifuged for 3 minutes. Cells were counted using a hemocytometer and plated in 96-well plates at 2,500 cells/well (7,812 cells/ cm^2) for the MTT assay, in 24 well plates at 7,500 cells/well (3,947 cells/cm^2) for live imaging in the BioStation CT, and in 24 well plates at 10,000 cells/well (5,263 cells/cm^2) for the comet assay. Different plating densities were used for live cell

imaging and the comet assay to get appropriate confluency at the end of the experiment which was 72 hours for live cell imaging and about 24 hours for comet assay.

Culturing Human Palatal Mesenchyme Cells (hPM): hPM cells from a female fetus were purchased from ATCC (Manassas, VA) and cultured in Eagle's Minimal Essential Medium (EMEM) (ATCC, Manassas, VA) supplemented with 10% FBS (ATCC, Manassas, VA), at 37 °C with 5% CO_2 and 95% relative humidity. Medium was replaced on alternate days and cells were used for an experiment when the flask was ~80-85% confluent. Cells were detached using 0.25% trypsin/EDTA (GIBCO, Invitrogen, Carlsbad, CA) for 1 minute and were centrifuged for 3 minutes. Cell counting was done using a hemocytometer and 4,000 cells/well (12,500 cells/ cm^2) were plated in a 96 well plate for the MTT assay.

Testing THS Extracts for Cytotoxicity Using the MTT Assay: mNSC, hDF and hPM were plated in 96-well plates. After incubation for 24 hours, test concentrations of THS were added to the wells, and the plates were incubated for another 48 hours as above. At the end of the incubation period, MTT (Sigma–Aldrich, St. Louis, MO) at 5 mg/ml in PBS containing calcium and magnesium (Fisher Scientific, Chino, CA) was added to each well, and plates were incubated for 2 h at 37ºC. The plates were drained, and 100 µl of dimethyl sulfoxide (DMSO) (Fisher, Chino, CA) was added to each well and mixed to form a uniformly colored solution. Absorbance was read at 570 nm using an Epoch Microplate Spectrophotometer (Biotek, Winooski, VT).

Live Cell Imaging: mNSC and hDF were plated in 24 well plates and incubated at 37ºC for 24 hours, after which control and THS extracts were added to wells, and plates were transferred to a Nikon BioStation CT (Nikon, Melville, NY). Images were

obtained every 2 hours for 48 hours, then analyzed using CL Quant software (DR Vision, Seattle, WA) to track dynamic cell processes, such as proliferation and death (Lin et al., 2010 a,b; Guan et al., 2014; Talbot et al., 2014).

Single Cell Gel Electrophoresis (Comet Assay): mNSC and hDF cells were treated with THS and control fabric extracts at 30% and 100% concentrations for 3 hours at 37°C. Cells treated with 100μM hydrogen peroxide for 10 minutes at 4ºC served as positive control. The Trevigen Comet Assay Kit (Trevigen, Gaithersburg, MD) was used according to the manufacturer's protocol. Cells were mixed with low melting agarose at a ratio of 1:10 for encapsulation and were subjected to electrophoresis at 21V for 30 minutes. Slides were stained with SYBR green dye (Trevigen, Gaithersburg, MD) and dried overnight at room temperature before capturing images using the Nikon Ti Eclipse microscope. CometScore software was used to score tail length, % DNA in tail, and Olive moments. The percent of cells with comet tails was calculated by counting total number of cells and number of cells with tails in every field across all treatment groups. The comet assay detects single stranded breaks in DNA even when there are low levels of damage (Tice et al., 2000).

Statistical Analysis: Statistical analyses were done using GraphPad Prism software. For the MTT assay, raw data were analyzed by comparing treatment groups to the control group using a one way ANOVA. Dunnett's post hoc test was done for comparison of treated groups to the control group. For graphing data, MTT absorbance for the negative controls were normalized to 100% in each experiment, and treatment groups were expressed as a percentage of the negative control. In the experiment done

with hPM, groups treated with 100% unexposed terrycloth extracts and 100% THS extracts for hPM were compared through t-test

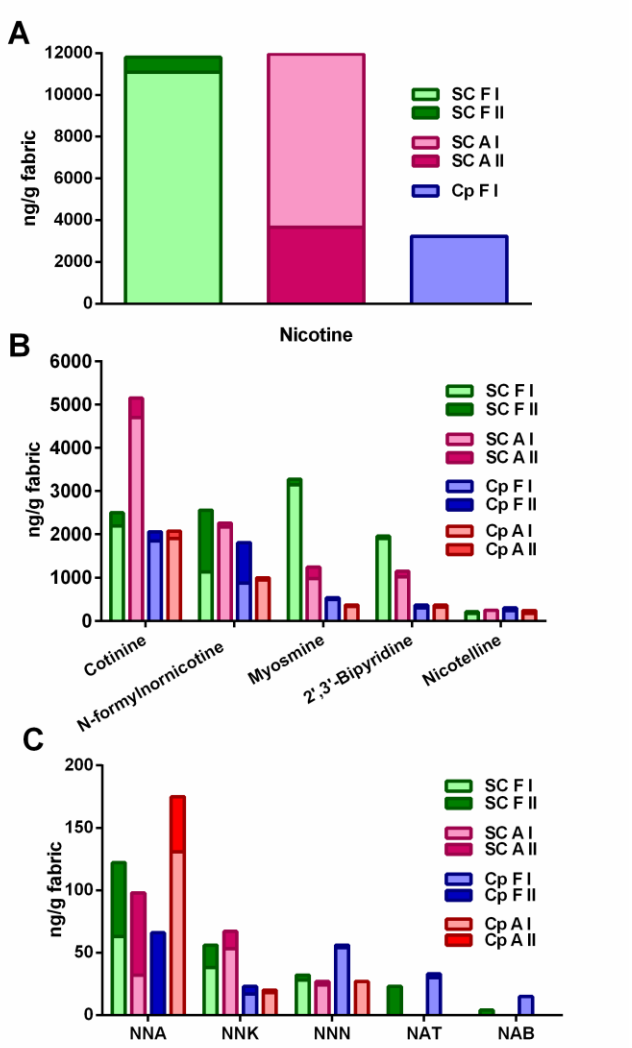

Figure 5.2. LC-MS/MS analysis of THS extracts from car seat cover and car carpet exposed to SS cigarette smoke. (A) Concentrations for nicotine. **(B)** Concentrations for tobacco alkaloids. **(C)** Concentrations for TSNAs. Each bar represents two independent LC-MS/MS analyses taken at different times from the same extract (shown in different colors). I = 1st analysis; II = 2nd analysis; SC = car seat cover; Cp = car carpet; F = fresh; A = aged.

For analysis of confluency data obtained with live cell imaging, two way ANOVA was performed. The area (confluency) at two hours was normalized to 100% and subsequent time points were expressed as percent of confluency at two hours. For two way ANOVA, area (confluency) from 4 hours onwards were compared to determine which treatment groups and time points were different from the 4 hour treatment group. Comet assay results were analyzed statistically by t-testing each treatment group to its corresponding control.

Results

Outdoor Exposure in a Simulated Car Chemical Composition of Culture Medium Extracts of Car

Fabrics Exposed to Cigarette Smoke: The concentrations of nicotine, other tobacco alkaloids, and TSNAs were measured in THS extracts using LC-MS/MS, and duplicate analyses were obtained for most extracts (Figure 5.2). THS extracts from seat cover fabric had higher concentrations of most chemicals than carpet. Nicotine concentrations in both fresh (collected immediately after 30 days of exposure) and aged (collected 60 days after exposure stopped) seat cover extracts were higher than in carpet extracts (Figure. 5.2 A). Nicotine was only detected in one of the two fresh carpet extract samples and was not detected in the THS extract from aged carpet, perhaps because its concentration was less than the limit of quantification (100ng/ml or 2000 ng/g fabric) (Fig. 5.2 A). Cotinine was higher in aged than in fresh seat cover extracts, while the concentrations of myosmine and 2',3'-bipyridine were higher in fresh seat cover extracts (Fig. 5.2 B). Nicotelline and N-formylnornicotine (N-FNNC) concentrations did not change during aging. For carpet extracts, cotinine, myosmine, 2',3'-bipyridine and nicotelline did not change during aging and were generally lower than in seat cover extracts. N-FNNC decreased during aging, although the change may not be significant as there was variation between measurements of N-FNNC in the fresh sample (Fig. 5.2 B). These variations may be due to instability of the N-FNNC group, which is easily hydrolyzed.

NNA, NNK and NNN were the most abundant of the TSNAs studied in the THS extracts. NNA was present at similar concentrations in both fresh and aged seat cover extracts, but increased significantly in aged carpet extracts (Fig. 5.2 C). NNK was higher in fresh and aged seat cover extracts than in carpet. Fresh carpet THS extract had the highest NNN concentration, which decreased upon aging. *N*'-nitrosoanatabine (NAT) and *N'*-nitrosoanabasine (NAB) were detected only in fresh THS extracts from seat cover

and carpet (Fig. 5.2 C). Extracts from SC fabric exposed to room air contained nicotine (540ng/g fabric), myosmine (5.12ng/ml), and 2',3'-bipyridine (8.24 ng/g fabric). Nicotine and other tobacco smoke-derived substances are ubiquitous in the environment, and all of the substances we have measured in this study can be measured in non-smokers' homes (Whitehead et al., 2015). Therefore, finding low levels in unexposed fabric (i.e. not exposed in our study) is to be expected. These control values were subtracted from the concentration of these chemicals found in THS extracts before plotting the data.

Culture Medium Extracts of Car Fabrics Inhibit mNSC Proliferation:

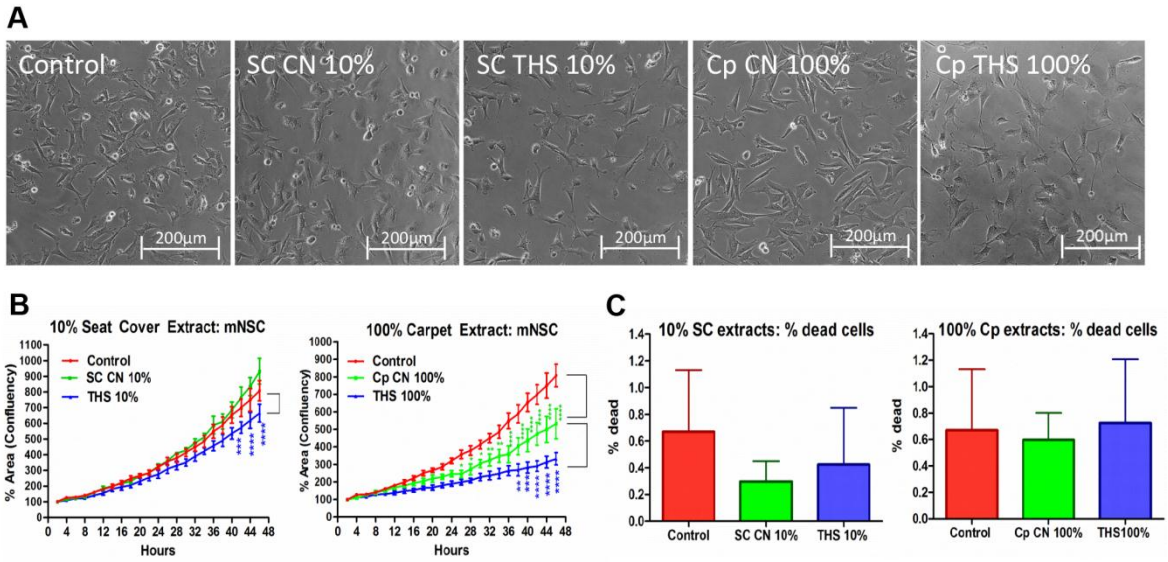

Figure 5.3. Effect of THS extracts from car seat cover (SC) and car carpet (Cp) on mNSC proliferation. (A) Micrographs of mNSC after 48 hours of treatment with extracts of seat cover (SC CN) and carpet (Cp CN) exposed to indoor air only (controls) or with extracts from seat cover (SC THS) and carpet (THS Cp) exposed to THS. Control = culture medium only. **(B)** Effect of extracts from THS exposed seat cover (THS SC) and THS exposed carpet (THS Cp) on area (confluency). Control extracts from fabrics exposed to air only are designated SC CN (seat cover) and Cp CN (carpet). Each % Area (confluency) curve is the mean ± SEM of three experiments. Fabric controls (green line) were compared to the medium only control (red line), and THS treatment groups (blue line) were compared to the fabric controls using a two-way ANOVA. Asterisks represent p values of THS with respect to SC CN or Cp CN. ** = $p < 0.01$; *** = $p < 0.001$; **** = $p < 0.0001$. **(C).** Graph showing the percentage of dead cells for 10% seat cover extracts and 100% carpet extracts. There was no significant difference between means in Figure C. SC Cn = seat cover exposed to indoor air; Cp CN = carpet exposed to indoor air. SC THS = seat cover exposed to THS. Cp THS = carpet exposed to THS.

Experiments for determining effect on proliferation included: (1) cells incubated in culture medium only (control), (2) cells incubated in extracts from seat cover fabric and carpet exposed to indoor air (SC CN and Cp CN), and (3) cells incubated in THS extract from car seat cover fabric or carpet exposed to cigarette smoke for 30 days. The effect of THS extracts on proliferation of mNSC was tested using a live cell imaging assay (Fig. 5.3 A and B). 10% extracts of THS from seat cover fabric and 100% extract form car carpet caused a significant decrease in cell proliferation (total cell area) when compared to the 10% seat cover control or 100% carpet control exposed to indoor air only (Fig. 5.3 A and B).

For seat cover extract, growth rate was significantly decreased at 42 hours of incubation and continued until 46 hours. For carpet extract, the 100% concentration decreased cell proliferation significantly, compared to indoor air exposed carpet extract starting at 38 hours (Fig. 5.3 B). This was the only group in which the unexposed control fabric was significantly different than the control incubated in culture medium only. This effect by unexposed carpet was small and indicates that the carpet had some cytotoxicity, but the THS exposed carpet had a greater effect that was significantly different than the unexposed control carpet. Percentage of dead cells in both treatment groups were not significantly different between the control and the treated groups, indicating that decreased confluency was due to decreased proliferation and not cell death (Fig. 5.3 C).

THS Extracts Caused DNA Damage: When evaluated with the comet assay, THS extracts from car seat cover and carpet induced more DNA damage in mNSC and hDF cells than extracts of air exposed control fabrics. Percentage of cells with tails,

comet tail length, % of DNA in the tails, and Olive moment were evaluated. For mNSC, extracts from the THS-exposed seat cover induced more DNA damage than the extracts from air exposed seat cover (SC CN), (Fig. 5.4 A and B). The percentage of cells with tails was significantly higher in 30% and 100% THS extracts than in the corresponding The percentage of cells with tails was significantly higher in 30% and 100% THS extracts than in the corresponding extracts from control fabric. Cells treated with THS extracted from car seat cover fabric had significantly longer tail lengths than controls. The percent DNA in the tail was higher only in cells treated with 100% THS extract. Olive moment was higher for cells treated with THS at both 30% and 100% concentrations (Fig. 5.4 C). For extracts from carpet, the percentage of cells with tails was the only parameter that was significantly higher for cells treated with THS as compared to cells treated with extracts from air exposed carpet (Cp CN) (Fig. 5.4 D). Tail length, although not significantly different, had p values close to 0.05 (aged 30%: 0.069; fresh 100%: 0.0698; and aged 100%: 0.0545). For carpet, the percentage of cells with tails was the only parameter that was significantly higher for cells treated with THS as compared to cells treated with extracts from air exposed carpet (Cp CN) (Fig. 5.4 D). Tail length, although not significantly different, had p values close to 0.05 (aged 30%: 0.069; fresh 100%: 0.0698; and aged 100%: 0.0545).

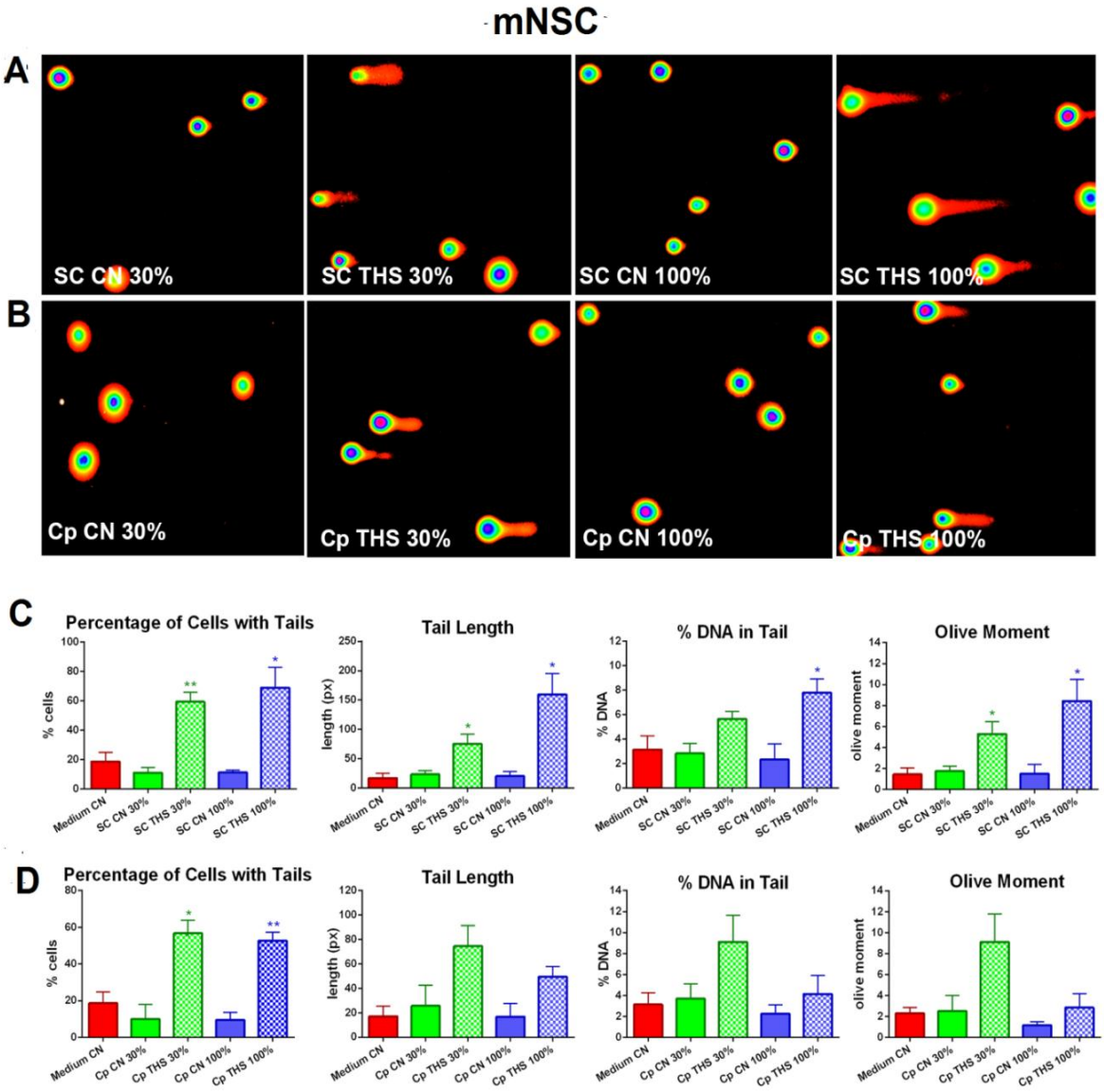

Figure 5.4. **DNA damage induced by THS in mNSC. (A)** Images showing comets from cells treated with extracts form indoor air exposed and THS exposed seat cover (SC). **(B)** Images showing comets from cells treated with extracts form indoor air exposed and THS exposed carpet (Cp). **(C)** Graphs showing the % of cells with tails, tail length, % DNA in tail, and Olive moment for cells treated with extracts seat cover. **(D)** Graphs showing the % of cells with tails, tail length, % DNA in tail, and Olive moment with extracts form. Each bar is mean ± SEM of three experiments. Groups treated with THS from SC or Cp were compared to Sc CN or Cp Cn respectively. * = $p < 0.05$; ** = $0.001 < p < 0.01$. SC Cn = seat cover exposed to indoor air; Cp CN = carpet exposed to indoor air.

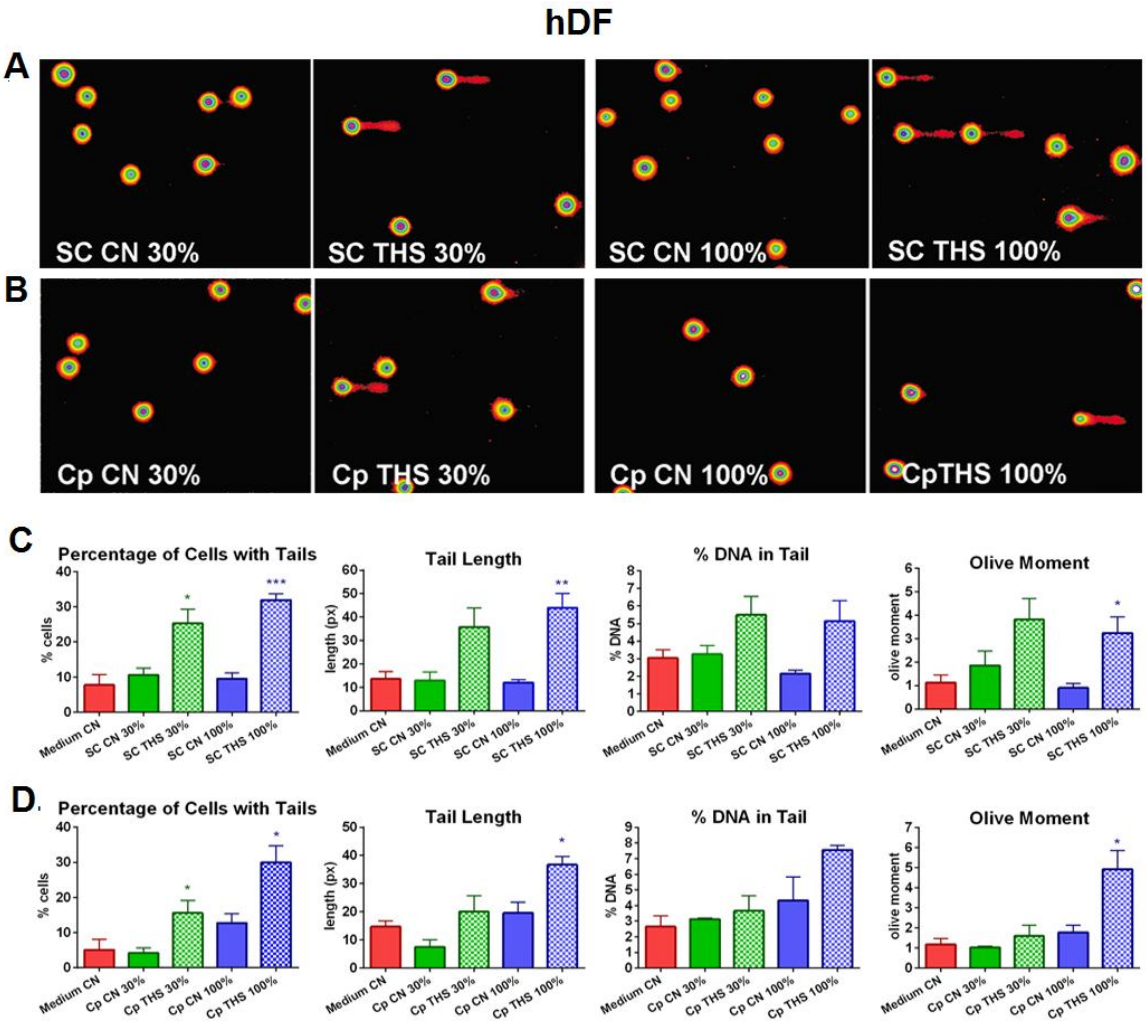

Figure 5.5. DNA damage induced by THS in hDF. (A) Images showing comets from cells treated with extracts from indoor exposed and THS exposed seat cover (SC) **(B)** Images showing comets from cells treated with extracts from indoor air exposed and THS exposed carpet (Cp). **(C)** Graphs showing the % of cells with tails, tail length, % DNA in tail, and Olive moment for cells treated with extracts from indoor air exposed and THS exposed seat cover. **(D)** Graphs showing the % of cell with tails, tail length, % DNA in tail, and Olive moment with indoor air exposed and THS exposed carpet. Each bar is the mean ± SEM of three experiments. Groups treated with THS from SC or Cp were compared to Sc CN or Cp Cn respectively. * = $p < 0.05$; ** = $0.001 < p < 0.01$. SC Cn = seat cover exposed to indoor air; Cp CN = carpet exposed to indoor air.

In hDF cells, THS extracts from both seat cover and carpet fabric had effects similar to mNSC (Fig. 5.5 A and B). For car seat cover, the percentage of cells with tails was significantly higher for the 30% and 100% THS extracts than for the 30% and 100% indoor air exposed control extracts. Tail length and Olive moment for cells treated with 100% THS was significantly higher than cells treated with SC CN extracts. The % DNA in the tail for cells treated with seat cover THS extracts was not significantly different for cells treated with SC CN extract, but the p value was close to significance ($p = 0.0612$) at the 100% concentration (Fig. 5.5 C). For carpet, the percentage of cells with tails was significantly higher at both 30% and 100% THS concentrations than the corresponding air exposed controls (Cp CN). Tail length and Olive moment for cells treated with 100% THS was significantly higher than for cells treated with control carpet extracts. The % DNA in tail for cells treated with THS extracts was not significantly different from cells treated with control extract (Fig. 5.5 D).

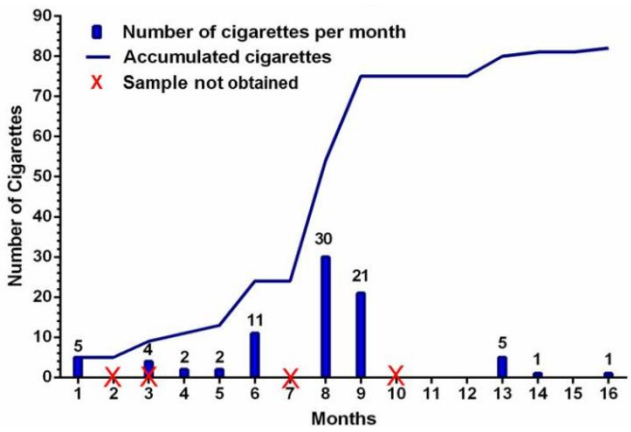

Figure 5.6. Graph showing the number of cigarettes smoked each month (bars) and the accumulated cigarettes (line) over 16 months in the THS exposure chamber experiment. Red Xs indicate months for which there was no terrycloth sample.

Indoor Exposure in Experimental Chamber

Overview of Experimental Design: Twelve pieces of terrycloth were incubated in a sidestream smoke exposure chamber for different time periods ranging from 1 to 16 months. After 1, 4, 5, 6, 8, 9, 11, 12, 13, 14, 15 and 16, months of exposure,

single pieces of terrycloth were removed from the chamber, shipped to UCR, and immediately extracted in cell culture medium. The extracts were frozen at -80°C until assayed. The number of cigarettes smoked every month varied, with the most cigarettes smoked in months 8 and 9, and none smoked during months 2, 7, 10-12 and 15. The number of cigarettes to which fabric was exposed each month and the total number of cigarettes over time are shown in Fig. 5.6.

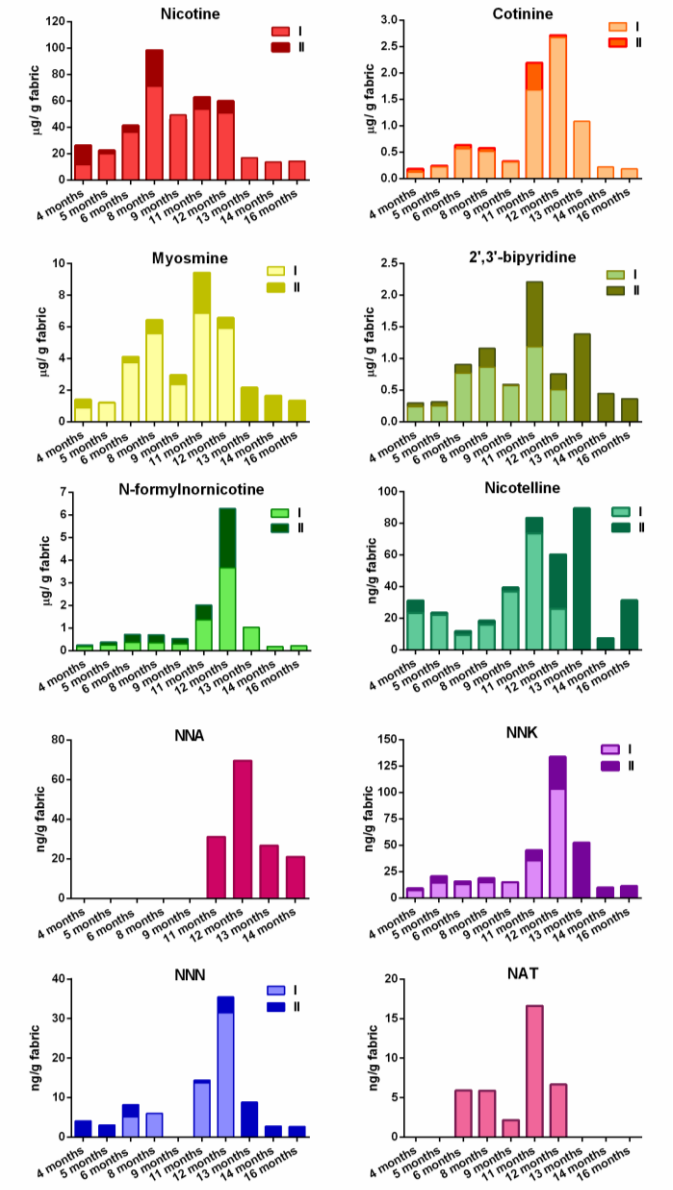

Figure 5.7. LC-MS/MS analysis of the chemicals in THS extracts from terrycloth exposed to cigarette smoke. Concentrations of nicotine, tobacco alkaloids, and TSNAs are shown for different months. Each bar represents two independent LC-MS/MS analyses made at different times for the same extract. I = 1st analysis; II = 2nd analysis.

Chemical Composition of Culture Medium Extracts of THS: THS extracts in DMEM were analyzed using LC-MS/MS for nicotine, other tobacco alkaloids, and tobacco specific nitrosamines (TSNAs) (Fig. 5.7). Nicotine, cotinine, myosmine and 2',3'-bipyridine concentration increased until 8 months and decreased during the 9th month.

Nicotine remained constant over the 11th and 12th months and then decreased at month 13.

Cotinine, myosmine, and N-formylnornicotine increased during the 11th month and 12th months and started decreasing from 13th month onwards. The increase of these nicotine derivatives at the 11th month is likely due to conversion from nicotine and/or nornicotine, another alkaloid present in tobacco smoke. 2',3'-bipyridine decreased during month 12th onwards. Nicotelline increased during the 9th and 11th months and then stayed constant over month 12 and 13 before decreasing at 14 months.

In general, the concentrations of TSNAs were highest during months 11-13 when smoking was not occurring. NNA was present at detectable levels at the 11th, 12th, 13th and 14th months. Nitrosamines NNN and NNK were more or less constant or not detected up to the 9th month and increased during the 11th and 12th months before starting to decrease by the 13th month. NAT was detectable at the 6th month, increased at 11th month and was undetectable by the 13th month.

THS Extracted in Medium Lacking Serum Proteins had Low Cytotoxicity to mNSC: Fresh culture medium (DMEM) extracts from terrycloth that was exposed to cigarette smoke for varying lengths of time as shown in Fig 6 were not cytotoxic to mNSC except the extract from terrycloth exposed for 8 months to 54 cigarettes, which significantly decreased the percentage relative to the control by about 20-25% (Fig. 5.8 A-D).

Extraction in complete medium containing serum proteins enhanced the cytotoxicity of THS extracts: Extracts prepared from terrycloth exposed to 54

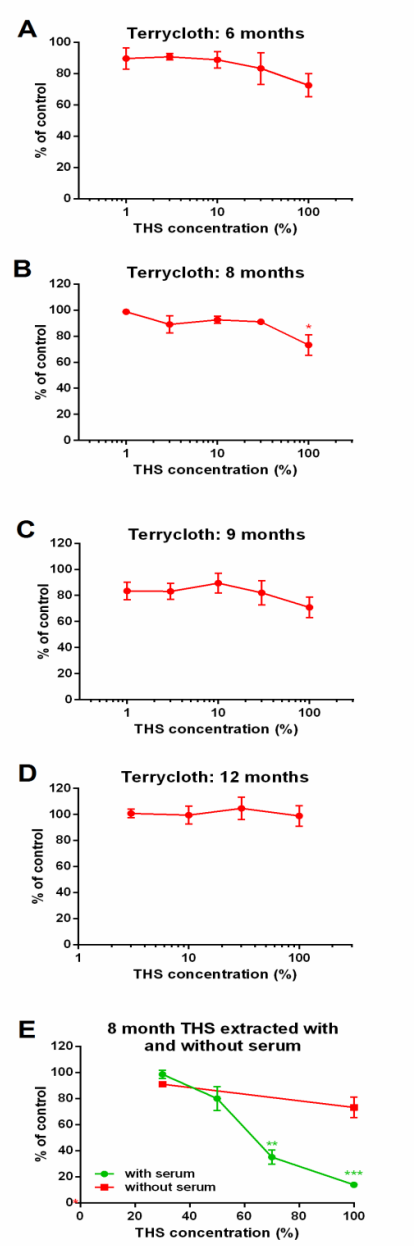

Figure 5.8. THS extracts in DMEM without serum proteins showed little cytotoxicity to mNSC. **(A-D)** Extracts were prepared from terrycloth exposed to cigarette smoke for different times and tested in the MTT assay. **(E)** The cytotoxicity of THS extracts prepared from terrycloth exposed to 54 cigarettes over 8 months with and without serum proteins. Each curve is the mean ± SEM of three experiments. * = $p < 0.05$; ** = $0.001 < p < 0.01$; *** = $0.0001 < p < 0.001$.

cigarettes over 8 months using complete medium containing fetal bovine serum and horse serum were more cytotoxic to mNSC when compared to the extracts made without serum.

Extracts made with serum caused complete cell death at the 100% concentration and more than 60% cell death at the 70% concentration (Fig. 5.8 E).

Extracts made in medium containing serum proteins were cytotoxic to mNSC but not to hDF or hPM: Extracts were made from terrycloth that was in the exposure chamber for 4, 6, 8, 9, 11 and 12 months using complete mNSC medium containing FBS and horse serum (Figure 9). Cells were treated with these extracts and with extracts from unexposed terrycloth also made in complete growth medium. Terrycloth

exposed to 4, 6, 8, 9 and 11 months were cytotoxic to mNSC at 70% and 100% concentrations whereas extract from the 12 month terrycloth was cytotoxic only at the 100% concentration (Fig. 5.9 A). None of these extracts were cytotoxic to hDF (Fig. 5.9 A). The 8 month extract was also tested for cytotoxicity to hPM cells and although it was cytotoxic at the 100% concentration, these cells were also affected by extracts from unexposed terrycloth which was almost as cytotoxic as the THS extract (Fig. 5.9 B). Groups treated with 100% extract from unexposed terrycloth was compared to group treated with 100% THS through a t-test and the p value was 0.0612.

Cytotoxicity of THS extracts was not due to VOC in THS: To determine if loss of VOC would reduce the cytotoxicity of THS, extracts made with serum proteins were pre-incubated at 37°C for up to 3 days then tested in the MTT assay. There was no effect on the cytotoxicity of pre-incubated extracts (Fig. 5.9 C).

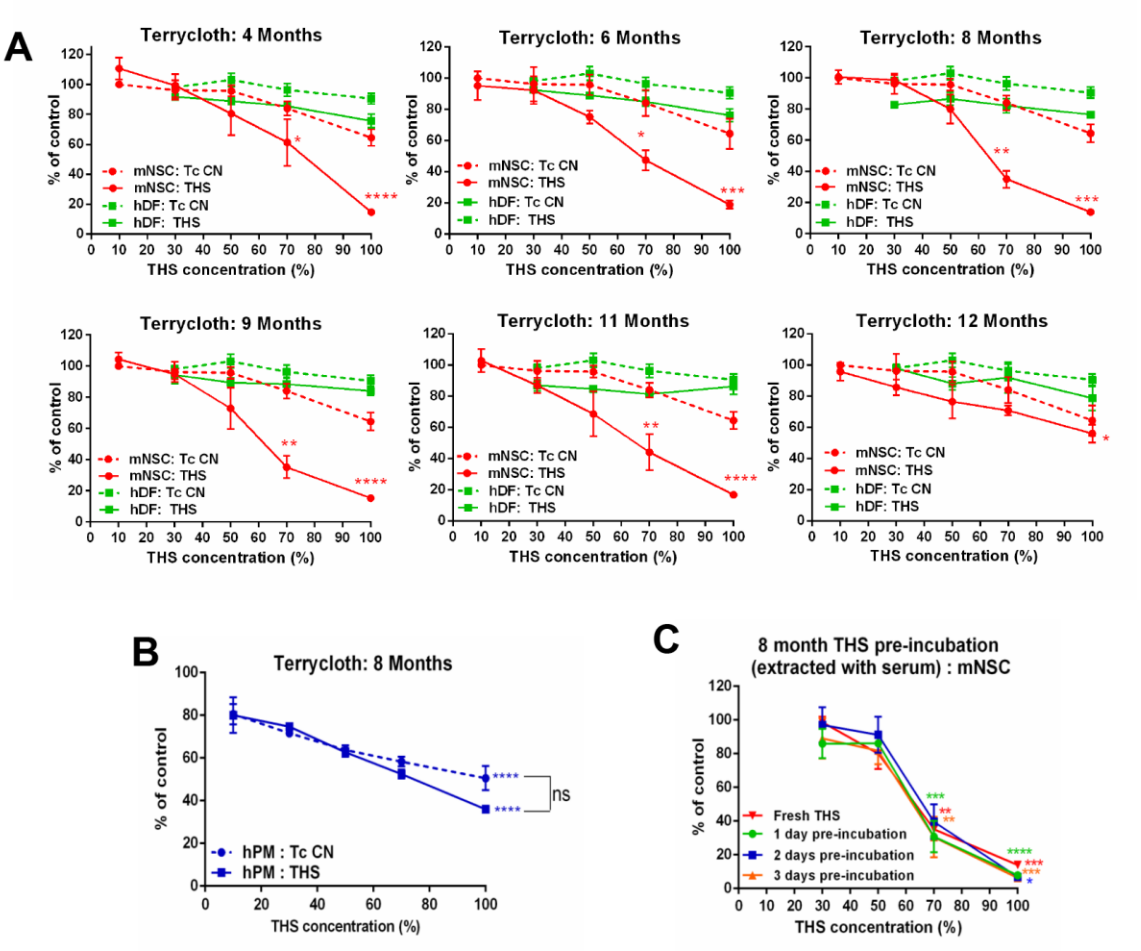

Figure 5.9. Effect of THS extracts made with serum proteins on mNSC, hDF and hPM cells. (A) Dose response curves showing the cytotoxicity of THS extracts at six different months for mNSC and hDF. In each graph, THS extract is compared to unexposed terrycloth. Each dose response curve represents the mean ± SEM of three experiments. **(B)** Dose response curve showing cytotoxicity of THS extracts from terrycloth exposed to cigarette smoke for 8 months to hPM cells. Treatment groups were compared to the untreated control using one way ANOVA before normalization of the data. Groups treated with 100% unexposed terrycloth extracts and 100% THS extracts for hPM were compared through t-test (p value = 0.0612). Tc CN = terrycloth fabric not exposed to cigarette smoke. **(C)** Effect of fresh and pre-incubated extracts prepared in complete growth medium containing serum**.** Each dose-response curve represents mean ± SEM of three experiments. Pre-incubation of the THS extract was done in a $37^{o}C/CO_2$ incubator for the time indicated. . * = $p < 0.05$; ** = $0.001< p < 0.01$; *** = $0.0001 < p < 0.001$; **** = $p < 0.0001$.

Discussion:

This study evaluated the chemical content and the cytotoxicity of extracts of fabrics containing THS. We determined the concentrations of nicotine, nicotine-related alkaloids, and TSNAs in the extracts and tested the effects of different exposure scenarios, aging and fabric extraction on cytotoxicity. One exposure scenario modeled a smoker's car in which smoke was introduced four times daily into an acrylic chamber that was incubated outdoors between smoke exposures. The other exposure scenario modeled a room with no windows and low air exchange. We found that THS chemicals change over time, that these changes are influenced by the exposure environment and fabric type, and that even low levels of THS can cause adverse effects on cells. MTT, comet, and live cell imaging assays were used to evaluate the toxicity of THS extracts on cultured mNSC and hDF. In general, mNSC were more sensitive than hDF to THS extracts, in agreement with our earlier study showing stem cells were more sensitive to electronic cigarette products than differentiated cells from the lung (Bahl et al., 2012).

Chemical dynamics in THS exposed fabrics were complex and differed in the car (outdoor) and chamber (indoor) experiment. As reported previously by Bahl et al. (2014), while terrycloth yielded higher concentrations of cigarette smoke chemicals than polyester, in this study, car seat cover and carpet gave different yields of nicotine and other tobacco alkaloids. When we tested the effects of an additional 60 days of aging outdoors in the car experiment, we saw few differences in the concentrations of the chemicals tested except for cotinine and NNA, both of which increased over 100% in concentration after 60 days. While cotinine is likely benign (Hatsukami et al., 1997), the increase in NNA, a probable carcinogen (Hang et al., 2013), is a concern. In the indoor exposure scenario, with 100% cotton terrycloth as the substrate, the concentrations of all

the chemicals we tested, except nicotine and 2',3'-bipyridine, increased after aging (months 11 and 12). Cotinine, myosmine, 2',3'-bipyridine and N-FNNC are oxidation products of nicotine and/or other tobacco alkaloids (Benowitz et al., 2009) and were likely formed by reactions of nicotine with other chemicals. Of particular interest are the TSNAs, which all increased over twofold during aging. Since additional smoke was not deposited during aging in either experiment, increases in TSNAs must have occurred through reaction of existing chemicals, such as nicotine with nitrous acid (Sleiman et al., 2010). The data further suggest that such conversion can vary depending on the location of the fabric and the presence of light, with conversion to TSNAs being more robust indoors than outdoors. The composition and weave of the fabrics may also influence chemical conversions in THS, as shown for cotinine and NNA in the car experiment. Cotinine doubled in concentration on the car seat cover but did not change on the car carpet. Conversely, NNA did not change significantly on car seat cover but more than doubled on car carpet.

THS extracted in culture medium from the car seat cover and carpet, which were exposed to realistic cigarette smoke concentrations for only 1 month, caused DNA damage to both mNSC and hDF and inhibited proliferation of mNSC. The amount of cigarette smoke deposited in the car model was scaled to give a realistic exposure of about 20 cigarettes over an 8 hour interval in a car with an interior volume of 3 m^3. The chemical analyses of THS extracts from these fabrics demonstrated a significant build-up of nicotine, TSNAs, and other alkaloids. These THS extracts were not cytotoxic in the MTT cell proliferation assay (data not shown), which measures mitochondrial reductase (Mossman, 1983); however, cytotoxicity may have been greater if extraction had been done in medium containing serum, as suggested by later experiments. The more

sensitve live cell imaging assay clearly demonstrated that THS inhibited cell proliferation. The chemical(s) inhibiting proliferation in the current study has not been identified. If similar inhibition of cell proliferation occurs *in vivo*, homeostasis and the ability to repair/replenish tissues may be impaired, particularly if stem cell populations are affected.

The car experiment also demonstrated that accumulation of THS chemicals for only 30 days was sufficient to damage DNA and fresh extracts were generally more toxic than those that had aged. Similar genotoxic effects were shown by Hang et al (2013) when THS extracts from terrycloth were tested in the comet assay. While the aforementioned study used hepatic cells in the comet assay, our study demonstrated genotoxicity in dermal fibroblasts and neural stem cells. Cigarette smoke contains genotoxic chemicals, such as polyaromantic hydrocarbons (PAHs), NNK, NNN and NNA (Brown et al., 2003; Engstrom et al, 2003), which damage DNA and cause cancer in humans and animals (Hang, 2010; Hecht & Hoffmann, 1988; Ramírez et al., 2014). We identified NNK, NNN and NNA in the extracts form cloth seat cover and carpet and this may explain the genotoxicity of THS extracts.

The indoor exposure chamber experiment was designed to evaluate how THS chemicals and their toxicity changed over a continuous exposure to varying amounts of cigarette smoke. The most important observations from this experiment were that cytotoxicity of THS extracts correlated with smoke exposure and that addition of protein to the extraction medium significantly increased the cytotoxicity of the THS extract. The increase in cytotoxicity of extracts made with serum can be attributed to the presence of serum proteins such as albumins that may have aided in the extraction of water

insoluble or semi-soluble cytotoxic THS constituents (Doppalapudi et al., 2015; Skipper and Tannenbaum, 1990) may have facilitated entry of THS toxicants into cells. The possibility of increased toxicity due to THS chemicals binding to serum proteins and rendering them non-functional or unavailable to cells is unlikely since extracts made in DMEM without serum had both FBS and horse serum added before treating cells. This finding is important when considering oral exposure of toddlers and infants to THS contaminated materials since saliva contains proteins, including albumin (de Almeida, 2008; Gleeson et al, 1991), which could enhance extraction of toxicants during mouthing.

The indoor exposure experiment demonstrated that as few as 11 cigarettes smoked over 4 months left a residue of THS that was cytotoxic to mNSC. As expected, cytotoxicity increased with increasing THS deposition. Aging (without deposition of fresh smoke) decreased the cytotoxicity of THS as seen with the extracts made after 11 and 12 months. This loss in cytotoxicity could be due to loss of VOCs, as shown in our prior study (Bahl et al., 2015). However, in the current study, the experiment in which extracts were pre-incubated for 3 days and did not lose cytotoxicity suggests that that the cytotoxic chemicals in this experiment were not volatile. The 12-month experiment (Figure 9) further suggests that degradation of cytotoxic chemicals can occur during aging. This latter idea is supported by our observations that THS chemicals are very dynamic and can be interconverted or degrade during aging. In the MTT assay, hPM were sensitive to the both unexposed terrycloth and THS extract from terrycloth exposed for 8 months. the hDF were not affected by any of the THS extracts, possibly because differentiated cells are not as sensitive to toxicants as stem cells (Grandjean et al., 2008; Bahl et al., 2012).

All the experiments in this study are acute in vitro experiments. In vitro experiments are often done with acute short-term exposures and serve as a first step for the determination of toxicity of environmental chemicals. Future long-term chronic in vitro experiments as well as in vivo studies to evaluate effects of THS on organ systems and DNA may be modeled on the results discussed here.

In summary, low levels of cigarette smoke can lead to a build-up of toxic chemicals on cloth and carpeting in cars and homes. The THS chemicals we studied are dynamic and their concentrations change over time. TSNAs in the indoor environment are particularly important as their concentrations increased even in the absence of smoking. In the car experiment, 1 month of daily cigarette smoke exposure produced a THS residue that inhibited cell proliferation and caused DNA damage, which by extension could increase morbidity and impair human health. In the indoor exposure experiment, as few as 11 cigarettes produced a residue that was cytotoxic. Media containing protein was more efficient at extracting cytotoxicity from THS exposure samples indicating that remediation of THS contamination may require multiple strategies to remove all toxicants. Finally, the efficient extraction of cytotoxic chemicals by culture medium containing protein supports the idea that toddlers who mouth THS exposed objects are at risk since saliva containing protein would be more efficient at extracting THS toxicants than simple culture media.

.

References

Bahl, V., Jacob, P., Havel, C., Schick, S. F., & Talbot, P. (2014). Thirdhand cigarette smoke: factors affecting exposure and remediation. *PloS One*, *9*(10), e108258. doi:10.1371/journal.pone.0108258

Bahl, V. Weng, N., Schick, S.F., Slieman, M., Whitehead, J., Ibarra, A., & Talbot.P (2015) Cytotoxicity of thirdhand smoke and identification of acrolein as a volatile thirdhand smoke chemcial that inhibits cell proliferation. In review.

Bahl, V., Lin, S., Xu, N., Davis, B., Wang, Y., & Talbot, P. (2012). Comparison of electronic cigarette refill fluid cytotoxicity using embryonic and adult models. *Reproductive Toxicology (Elmsford, N.Y.)*, *34*(4), 529–37. doi:10.1016/j.reprotox.2012.08.001

Behar, R. Z., Bahl, V., Wang, Y., Lin, S., Xu, N., Davis, B., & Talbot, P. (2012a). A method for rapid dose-response screening of environmental chemicals using human embryonic stem cells. *Journal of Pharmacological and Toxicological Methods*, *66*(3), 238–45. doi:10.1016/j.vascn.2012.07.003

Behar, R., Bahl, V., Wang, Y., Lin, S., & Talbot, P. (2012b) Adaptation of stem cells to 96-well plate assays: use of human embryonic and mouse neurals tem cells in the MTT assays. Current Portocols in Stem Cell Biology 23:C:1C.13:1C.13.1–1C.13.21. doi:10.1002/9780470151808.sc01c13s23

Benowitz, N. L. (2009). Pharmacology of nicotine: addiction, smoking-induced disease, and therapeutics. *Annual Review of Pharmacology and Toxicology*, *49*, 57–71. doi:10.1146/annurev.pharmtox.48.113006.094742

Brown, B. G., Borschke, A. J., & Doolittle, D. J. (2003). An analysis of the role of tobacco-specific nitrosamines in the carcinogenicity of tobacco smoke. *Nonlinearity in Biology, Toxicology, Medicine*, *1*(2), 179–98. doi:10.1080/15401420391434324

CDC (Centers for Disease Control and Prevention) (2015). Smoking and Tobacco Use. http://www.cdc.gov/tobacco/data_statistics/fact_sheets/health_effects/effects_cig_smoking/index.html

de Almeida, P.D.V., Grégio, A.M.T., Machado, M.Â.N., de Lima, A.A.S., & Azevedo, L.R. (2008). Saliva composition and functions : *The Journal of Comtemporary Dental Practice*, *9*(3), 72–80

Doppalapudi, S., Katiyar, S., Domb, A.J., & Khan, W. (2015). Biodegradable natural polymers, In: Puoci, F. (Eds.), Advanced polymers in medicine. Springer International Publishing, Switzerland, pp.33-66

Eisenbrand, G., Pool-Zobel, B., Baker, V., Balls, M., Blaauboer, B. ., Boobis, A, … Kleiner, J. (2002). Methods of in vitro toxicology. *Food and Chemical Toxicology*, *40*(2-3), 193–236. doi:10.1016/S0278-6915(01)00118-1

Engstrom, P.F., Clapper, M.L., & Schnoll, R.A. (2003). Carcinogenic and genotoxic effects of tobacco constituents, In: Kufe, D.W., Pollock, R.E., Weichselbaum, R.R. et al. (Eds.), Holland-Frei Cancer Medicine. 6th edition. Hamilton (ON): BC Decker; 2003. Available from: http://www.ncbi.nlm.nih.gov/books/NBK12437/

Gleeson, M., Dobson, A.J., Firman, D.W., Cripps, A.W., Clancy, R.L., Wlodarczyk, J.H., & Hensley, M.J. (1991).The variability of immunoglobulins and albumin in salivary secretions of children. *Scandinavian Journal of Immunology*. 33(5):533-41. doi: 10.1111/j.1365-3083.1991.tb02523.x

Grandjean, P., Bellinger, D., Bergman, A., Cordier, S., Davey-Smith, G., Eskenazi, B., … Weihe, P. (2008). The faroes statement: human health effects of developmental exposure to chemicals in our environment. *Basic & Clinical Pharmacology & Toxicology*, *102*(2), 73–5. doi:10.1111/j.1742-7843.2007.00114.x

Guan, B., Bhanu, B., Talbot, P., & Lin, S. (2014). Bio-driven cell region detection in human embryonic stem cell assay. *IEEE/ACM Transactions on Computational Biology and Bioinformatics*, *11*(3), 1–1. doi:10.1109/TCBB.2014.2306836

Hammer, T. R., Fischer, K., Mueller, M., & Hoefer, D. (2011). Effects of cigarette smoke residues from textiles on fibroblasts, neurocytes and zebrafish embryos and nicotine permeation through human skin. *International Journal of Hygiene and Environmental Health*, *214*(5), 384–91. doi:10.1016/j.ijheh.2011.04.007

Hang, B. (2010). Formation and repair of tobacco carcinogen-derived bulky DNA adducts. *Journal of Nucleic Acids*, *2010*, 709521. doi:10.4061/2010/709521

Hang, B., Sarker, A. H., Havel, C., Saha, S., Hazra, T. K., Schick, S., … Gundel, L. A. (2013). Thirdhand smoke causes DNA damage in human cells. *Mutagenesis*, *28*(4), 381–91. doi:10.1093/mutage/get013

Hatsukami, D., K., Grillo, M., Pentel, P.R., Oncken, C., & Bliss, R. (1997). Safety of cotinine in humans: physiologic, subjective, and cognitive effects. *Pharmacology Biochemistry and Behavior*, 57(4):643-50. doi:10.1016/S0091-3057(97)80001-9

Hecht, S. S., & Hoffmann, D. (1988). Tobacco-specific nitrosamines, an important group of carcinogens in tobacco and tobacco smoke. *Carcinogenesis*, *9*(6), 875–884

Knoll, M., Shaoulian, R., Magers, T., & Talbot, P. (1995). Ciliary beat frequency of hamster oviducts is decreased in vitro by exposure to solutions of mainstream and sidestream cigarette smoke. *Biology of Reproduction*, *53*(1), 29–37. doi:10.1095/biolreprod53.1.29

Knoll, M., & Talbot, P. (1998). Cigarette smoke inhibits oocyte cumulus complex pick-up by the oviduct in vitro independent of ciliary beat frequency. *Reproductive Toxicology*, *12*(I), 57–68. doi:10.1016/S0890-6238(97)00100-7

Lin, S., Fonteno, S., Weng, J-H., & Talbot, P. (2010a) Comparison of toxicity of smoke from conventional and harm reduction cigarettes using human embryonic stem cells. *Toxicological Sciences* 118:202-212. doi: 10.1093/toxsci/kfq241

Lin, S., Fonteno, S., Satish, S., Bhanu, B., & Talbot, P. (2010b). Video Bioinformatics Analysis of Human Embryonic Stem Cell Colony Growth. *Journal of Visualized Experiments : JoVE*, (39), 1933. doi:10.3791/1933

Martins-Green, M., Adhami, N., Frankos, M., Valdez, M., Goodwin, B., Lyubovitsky, J., … Curras-Collazo, M. (2014). Cigarette smoke toxins deposited on surfaces: implications for human health. *PloS One*, *9*(1), e86391. doi:10.1371/journal.pone.0086391

Matt, G. E., Quintana, P. J. E., Destaillats, H., Gundel, L. a, Sleiman, M., Singer, B. C., … Hovell, M. F. et al (2011). Thirdhand tobacco smoke: emerging evidence and arguments for a multidisciplinary research agenda. *Environmental Health Perspectives*, *119*(9), 1218–26. doi:10.1289/ehp.1103500

Mossman, B. T. (1983). In vitro approaches for determining mechanisms of toxicity and carcinogenicity by asbestos in the gastrointestinal and respiratory tracts. *Environmental Health Perspectives*, *VOL. 53*, 155–161. doi:10.1289/ehp.8353155

Pagani, L. S. (2013). Environmental tobacco smoke exposure and brain development: The case of attention deficit/hyperactivity disorder. *Neuroscience and Biobehavioral Reviews*, *44*, 195–205. doi:10.1016/j.neubiorev.2013.03.008

Petrick, L. M., Sleiman, M., Dubowski, Y., Gundel, L. A., & Destaillats, H. (2011). Tobacco smoke aging in the presence of ozone: A room-sized chamber study. *Atmospheric Environment*, *45*(28), 4959–4965. doi:10.1016/j.atmosenv.2011.05.076

Ramírez, N., Özel, M. Z., Lewis, A. C., Marcé, R. M., Borrull, F., & Hamilton, J. F. (2014). Exposure to nitrosamines in thirdhand tobacco smoke increases cancer risk in non-smokers. *Environment International*, *71*, 139–147. doi:10.1016/j.envint.2014.06.012

Rehan, V. K., Sakurai, R., & Torday, J. S. (2011). Thirdhand smoke: a new dimension to the effects of cigarette smoke on the developing lung. *American Journal of Physiology. Lung Cellular and Molecular Physiology*, *301*(1), L1–8. doi:10.1152/ajplung.00393.2010

Schick, S. F., Farraro, K. F., Perrino, C., Sleiman, M., van de Vossenberg, G., Trinh, M. P., … Balmes, J. (2014). Thirdhand cigarette smoke in an experimental chamber: evidence of surface deposition of nicotine, nitrosamines and polycyclic aromatic hydrocarbons and de novo formation of NNK. *Tobacco Control*, *23*(2), 152–9. doi:10.1136/tobaccocontrol-2012-050915

Skipper, P.L., & Tannenbaum, S.R. (1990). Protein adducts in the molecular dosimetry of chemical carcinogens. *Carcinogenesis*, 11(4), 507-518. doi: 10.1093/carcin/11.4.507

Sleiman, M., Gundel, L. A., Pankow, J. F., Jacob, P., Singer, B. C., & Destaillats, H. (2010). Formation of carcinogens indoors by surface-mediated reactions of nicotine with nitrous acid, leading to potential thirdhand smoke hazards. *Proceedings of the National Academy of Sciences of the United States of America*, *107*(15), 6576–81. doi:10.1073/pnas.0912820107

Talbot, P. (2008). In vitro assessment of reproductive toxicity of tobacco smoke and its constituents. *Birth Defects Research. Part C, Embryo Today : Reviews*, *84*(1), 61–72. doi:10.1002/bdrc.20120

Talbot, P., zur Nieden, N., Lin, S., Martinez, I., Guan, B., & Bhanu, B. (2014) Use of video bioinformatics tools in stem cell biology. In: Handbook of Nanotoxicology, Nanomedicine and Stem Cell Use in Toxicology, Eds: S. Sahu and D. Casciano, John Wiley, West Sussex, United Kingdom. pp 379-402.

Tice, R. R., Agurell, E., Anderson, D., Burlinson, B., Hartmann, A., Kobayashi, H., … Sasaki, Y. F. (2000). Single cell gel / comet assay : guidelines for In vitro and in vivo genetic toxicology testing. *Environmental and Molecular Mutagenesis*, *35*(3), 206–21. doi:10.1002/(SICI)1098-2280(2000)35:3<206::AID-EM8>3.0.CO;2-J

USDHHS (U.S. Department of Health and Human Services). *The health consequences of smoking: 50 years of progress. A report of the Surgeon General.* Atlanta, GA: U.S. Department of Health and Human Services, Centers for Disease Control and Prevention, National Center for Chronic Disease Prevention and Health Promotion, Office on Smoking and Health, 2014. Printed with corrections, January 2014.

Whitehead, T.P., Havel, C., Metayer, C., Benowitz, N.L., & Jacob, P. 3rd. (2015). Tobacco alkaloids and tobacco-specific nitrosamines in dust from homes of smokeless tobacco users, active smokers, and nontobacco users. *Chemical Research in Toxicology*, 28(5), 1007-14. doi: 10.1021/acs.chemrestox.5b00040

Yu, R., Wu, M., Lin,S., & Talbot, P. (2006). Cigarette smoke toxicants alter growth and survival of cultured ammalain cells. *Toxicological Sciences* , 93(1), 82-95. doi: 10.1093/toxsci/kfl047

Chapter 6: Thirdhand Smoke Causes Stress Induced Mitochondrial Hyperfusion and Alters the Transcriptional Profile of Neural Stem Cells

Introduction

Mitochondria are vital organelles that function in ATP production, redox signaling, cell cycle regulation, differentiation, exchange of DNA between cells to restore function, and apoptosis (Collins et al., 2012)(Rolland & Conradt, 2006)(Tan et al., 2008). They continually undergo fission and fusion. There is a fine balance between fission for the disposal of defective mitochondria (Shen et al., 2014) and fusion for exchange of mitochondrial DNA and rescue of damaged mitochondria (Hsiuchen Chen et al., 2010), and disruption of this balance can lead to compromised function (Otera, Ishihara, & Mihara, 2013). The shape and size of mitochondria can change through fission and fusion, and the internal structure can be altered in response to physiological conditions (Detmer & Chan, 2007).

Mutations in mitochondrial DNA are responsible for numerous diseases such as optic atrophy (Zanna et al., 2008), mitochondrial myopathy (Sweeney et al., 1993), and diabetes mellitus (Gerbitz, Gempel, & Brdiczka, 1996). OPA1 and MFN2 mutations have been linked to neurodegenerative diseases such as optic atrophy and Charcot-Marie Tooth type 2A, respectively (Olichon et al., 2006). Increased levels of the protein DRP1, which mediates outer mitochondrial membrane fission, are found in brains of Alzheimer's disease patients and increased mitochondrial fragmentation is also linked to Huntington's disease (Chen & Chan, 2009). An imbalance in mitochondrial dynamics is implicated in type 2 diabetes, in which the β cells in the pancreas exhibit reduced

mitochondrial membrane potential (MMP), reduced ATP production, swollen mitochondria, and impaired insulin production (Yoon, Galloway, Jhun, & Yu, 2011).

Mitochondria may be damaged by exposure to toxicants, and therefore serve as an excellent model for investigations of environmental chemicals (Meyer et al., 2013). Effects produced by toxicants include inhibition of ATP synthesis due to uncoupling of oxidative phosphorylation (Mustonen & Kinnunen, 1993), increased oxidative stress, and mitochondria-initiated apoptosis (O. Lee & O'Brien, 2010). Sometimes in the presence of environmental stress, such as UV irradiation or actinomycin, mitochondria fuse to form a highly connected network through a process called stress-induced mitochondrial hyperfusion (SIMH) (Tondera et al., 2009). This mechanism, which inactivates the fission machinery, protects cells against stress and prevents cell death (Shutt & McBride, 2013).

Cigarette smoke is an environmental toxicant that affects mitochondrial function. Some documented effects caused by cigarette smoke extracts include mitochondrial fragmentation in bronchial epithelial cells (Hara et al., 2013) and alteration of mitochondrial structure and function in airway epithelial cells (Hoffmann et al., 2013). Mitochondrial DNA mutations, including point mutations as well as insertions/deletions in the DNA sequence, have been reported in buccal cells of smokers that used at least 10 cigarettes for at least 6 months (Tan et al., 2008). Low doses of cigarette smoke also cause a change in the morphology of mitochondria, giving rise to hyperfused networks which are thought to be an adaptive response to low levels of stress (Ballweg, Mutze, Konigshoff, Eickelberg, & Meiners, 2014).

Thirdhand cigarette smoke (THS), which consists of cigarette smoke residue that settles in indoor environments after smoking has occurred, has emerged as potential health hazard (Matt et al., 2011) (Bahl, Jacob, Havel, Schick, & Talbot, 2014). THS causes detrimental effects on cell health, such as DNA strand breaks (Hang et al., 2013), impairment of pre-natal lung development in rats (Rehan, Sakurai, & Torday, 2011), and adverse effects on the multiple organ systems of mice, including non-alcoholic fatty liver disease, excessive collagen production and increased inflammatory cytokines in the lungs, and delayed wound healing in the skin (Martins-Green et al., 2014). Our studies on THS have shown that volatile organic chemicals in THS are cytotoxic to stem cells and adult cells causing inhibition of proliferation by affecting expression of genes that regulate the cell cycle. THS also caused DNA stand breaks in stem and adult cells.

Based on the above data, we have hypothesized that THS may damage mitochondria leading to cell morbidity and/or cell death. We have tested this hypothesis in post-natal and adult *in vitro* models using aqueous extracts of THS. We used mouse neural stem cells (mNSC), an *in vitro* model for postnatal brain development, human embryonic stem cells (hESC), and human dermal fibroblast (hDF), an in-vitro model for the adult skin. THS was generated in a ventilated chamber by exposing terrycloth to cigarette smoke from Marlboro Lights/Gold cigarettes as described previously (Bahl et al., 2014). THS was extracted in cell culture medium, and cells were treated with the varying concentrations of the extracts. We assessed effects on mitochondrial morphology, fusion, mitochondrial membrane potential (MMP), ATP production, reactive oxygen species (ROS) generation, oxidation of mitochondrial proteins, and the transcription of genes associated with mitochondrial function and stress. This is the first

study that describes the effect of THS on mitochondrial dynamics, structure and function and will provide valuable insights on how THS can adversely impact mitochondrial mediated processes in the cell and overall cell health.

Materials and Methods

Generation of THS: THS was generated in an experimental chamber at the University of California San Francisco (UCSF) as described previously (Bahl et al., 2014)' (Schick et al., 2014). Terrycloth, washed as described previously (Bahl et al., 2014) was exposed to cigarette smoke from approximately 133 Marlboro Red cigarettes over a span of 11 months. After exposure, terrycloth was wrapped in plastic bags and stored another 11 months. Fabric was then shipped to UCR where it was stored in amber bottles for another 15 months before extraction into culture medium. Two other batches of terrycloth were also exposed to cigarette smoke in the same experimental chamber. One batch was exposed to 11 cigarettes for 4 months and extraction was carried out within 1 week of removal from the chamber. The other batch was exposed to 75 cigarettes for 9 months and kept in the chamber for another 2 months to age, after which it was extracted. All the experiments except those labeled in Figure 3 as 11 cigarettes and 75 cigarettes, were done with THS extracts from terrycloth exposed to 133 cigarettes.

Preparation of THS extracts in culture medium: Aqueous extracts of THS were prepared in Dulbecco's Modified Eagle Medium (DMEM). A known weight of unexposed or THS exposed terrycloth (0.125 g of fabric/ml of medium) was soaked in culture medium in 15 ml conical tubes. The tubes were subjected to constant agitation using a rotating shaker for 1 hour at room temperature, after which the contents were

transferred to a 3 ml plastic syringe (Sigma-Aldrich, St. Louis, MO) inside a fresh 15 ml conical tube which was centrifuged at 4,000 x g for 5 minutes to recover the culture medium absorbed in the fabric. The recovered THS extract was filtered through 0.22 µm sterile filters (Pall Corporation, Port Washington, NY), supplemented with fetal bovine serum, horse serum, sodium pyruvate and penicillin-streptomycin, and aliquoted into 1.5 ml vials before storing at -80ºC.

Culturing mouse neural stem cells (mNSC): mNSC were cultured in Dulbecco's modified Eagle's medium (DMEM) (Lonza, Walkersville, MD) containing 10% fetal bovine serum, 5% horse serum, 1% sodium pyruvate (Lonza, Walkersville, MD) and 1% penicillin–streptomycin (GIBCO, Invitrogen, Carlsbad, CA) (Behar et al., 2012). The cells were cultured in Nunc T-25 tissue culture flasks (Fisher Scientific, Tustin, CA) at 37ºC, in 5% CO_2 and 95% relative humidity. Medium was replaced on alternate days, and when confluency reached about 80%, cells were used in an experiment. To detach cells, plates were washed with DPBS then treated with 0.05% trypsin EDTA/DPBS (GIBCO, Invitrogen, Carlsbad, CA) for 1 min at 37ºC.

Culturing Human Embryonic Stem Cells (hESC): H9 hESC obtained from WiCell (Madison, WI) were maintained on Matrigel (Fisher Scientific, Bedford, MA) coated 6-well plates (Falcon, Fisher Scientific, Chino, CA) containing complete mTeSR®1 Medium (Stem Cell Technologies, Vancouver, BC, Canada) (Lin & Talbot, 2011)). Cells were incubated in a 5% CO_2 incubator at 37ºC and 95% relative humidity. Each day cultures were observed for normal morphology, and medium was changed and cells were used for experiments when they were about 60-80% confluent. To detach the

cells, wells were washed with Dulbecco's phosphate buffered saline (DPBS) (GIBCO, Invitrogen, Carlsbad, CA), and colonies were enzymatically detached using Accutase (eBioscience, San Diego, CA). Large cell clumps were mechanically broken down using sterile glass beads, and cells were then plated on Matrigel coated Ibidi chamber slides.

Examination of mitochondrial morphology in MitoTracker Red CMXRos labeled cells: Cells were plated at 2,500 cells/well for mNSC and hDF and 20,000 cells/well for hESC on 8-well chamber slides (Ibidi, Planegg, Germany) and incubated for 24 hours. They were treated with different doses of THS for 24 hours after which MitoTracker Red CMXRos (Life Technologies, Grand Island, NY.) at a final concentration of 300 nM was added to each well and incubation continued for 30 minutes at 37ºC. Cells were then washed with PBS and fixed with 4% paraformaldehyde at room temperature. Slides were covered with Vectashield mounting medium containing DAPI (Vector Laboratories Burlingame, CA) and imaged using the Nikon Eclipse TI microscope (Nikon, Melville, NY). For all imaging experiments, fluorescence intensity was adjusted so that the group having strongest fluorescence was imaged first at non-saturating levels, and the other groups were imaged using the same exposure parameters so that fluorescence could be compared across groups.

Quantification of the number of cells with different mitochondrial morphologies: MitoTracker Red labeled cells were evaluated for different mitochondrial morphologies (dots, tubes, networks, loops and blobs). The number of cells having different types of mitochondria in the control and treatment groups was evaluated through visual inspection. For this, each cell was classified according to the predominant mitochondrial morphology. In some cells, there was more than one predominant

morphology, so that cell fell into two categories. 155 to 180 cells were analyzed in the different treatment groups. Interactomes demonstrating the distribution of different mitochondrial morphologies among cells in control and treated groups were prepared using the Cytoscape software (http://www.cytoscape.org/).

Live cell imaging of mitochondrial fusion: mNSC transfected with MitoTimer were plated on chamber slides at 2,500 cells/well and allowed to attach for 24 hours after which they were treated with THS extract at 30% and 100% concentrations. After 24 hours of treatment, the chamber slide was transferred to an incubation unit attached to Nikon Eclipse Ti inverted microscope. Real time videos, which were obtained over 2 minutes of recording, were visually inspected for mitochondrial morphology transitions and fusion.

Evaluation of MMP: Cells treated with 30% and 100% concentrations of THS for 24 hours and labeled with MitoTracker Red CMXRos were used to determine if THS affected mitochondrial membrane potential (MMP). Mitotracker Red CMXRos accumulation in live mitochondria is dependent on the mitochondrial membrane potential, and the probe is well retained after fixation. After treatment and labeling with Mitotracker Red, cells were fixed and imaged as described in the section on evaluation of mitochondrial morphology.

ATP assay: Cells were plated at 10,000 cells/well in 12 well plates and were incubated for 24 hours, after which various concentrations of THS were added. After 1, 4 and 24 hours of incubation, cells were lysed at room temperature for 30 mins using lysis buffer containing 10 mM Tris at pH 7.5, 100 mM NaCl, 1 mM EDTA and 0.01% Triton X 100. Cells were centrifuged at 4ºC for 5 minutes at 12,000g and supernatant was used

to determine ATP concentrations. An ATP Determination Kit (Life Technologies, Grand Island, NY) was used according to manufacturer's instructions to obtain luminescence readings using a Lucetta luminometer (Lonza, Portsmouth, NH). 20 mM sodium azide treatment for 1 hour was used as a positive control.

MitoSOX Red labeling for evaluation of superoxide production: Cells were plated at 2,500 cells/well on chamber slides (Ibidi, Planegg, Germany) and incubated for 24 hours at 37°C. Cells were then incubated in 5μM MitoSOX Red Mitochondrial Superoxide Indicator solution (Life Technologies, Grand Island, NY) prepared in PBS for 15 minutes at 37°C, after which medium was removed and cells were washed two times with PBS warmed to 37°C. THS extracts were then added to the cells and images of live cells were acquired after 4 hours of treatment using the Nikon Ti Eclipse microscope (Nikon, Melville, NY).

Evaluation of mitochondrial protein oxidation using MitoTimer transfected cells: MitoTimer is a mutant of the red fluorescent protein dsRed that becomes localized in the mitochondria through a mitochondrial targeting sequence. The fluorescence of this protein changes from green to red with increased oxidation of the Mitotimer protein (Hernandez et al., 2013). Mitotimer transfected cells (mNSC) were plated at 2,500 cells/well on chamber slides (Ibidi, Planegg, Germany) and incubated for 24 hours at 37°C. They were then treated with THS for 24 hours and imaged using a Nikon Ti Eclipse microscope (Nikon, Melville, NY). Images were analyzed using a protocol developed with CL-Quant software (DR Vision, Seattle, WA) to obtain ratios of red/green fluorescence.

Long-term exposure to THS: For long-term experiments spanning 15 and 30 days, cells were plated in 12-well plates at 10,000 cell/well and allowed to attach for 24 hours, after which THS was added. THS was replaced on alternate days. Cells were passaged on reaching 80% confluency and re-plated onto fresh 12 well plates at 10,000cells/well in THS extract. On the second to last day of the treatment, cells were trypsinized and plated on chamber slides (Ibidi, Planegg, Germany) at 2,500 cells/well for MitoTracker Red CMXRos staining. On the second to last day of each experiment, cells were also plated onto 24 well plates at 5,000 cell/well for cell growth evaluation with a live cell imaging assay using Nikon BioStation CT (Nikon, Melville, NY). THS was added at 10% and 30% concentrations, and cells were allowed to attach at 37ºC for 24 hours. After 24 hours, plates were transferred to a Nikon BioStation CT incubator (Nikon, Melville, NY) and imaged every 2 hours for 46 hours. For each well, data were collected from five different fields. Cell proliferation was analyzed in time-lapse images using video bioinformatics protocols created in CL Quant software (DR Vision, Seattle, WA) (Talbot et al., 2014).

RT^2 PCR Profiler Array: mNSC were plated in 6 well plates at 30,000 cells/well and allowed to attach overnight at 37ºC for 24 hours. After 24 hours, cells were treated with THS extracts at 100% concentration for 1, 4 or 24 hours. RNA was isolated using the Qiagen RNAeasy plus mini kit (Qiagen, Velencia, CA). RNA was checked for degradation using the Agilent 2100 Bioanalyzer, and only those samples having a RIN (RNA integrity number) of 7 or above were used for further processing. 400ng of RNA from each sample were used to prepare cDNA using the Qiagen RT^2 First Strand Kit (Qiagen, Velencia, CA). cDNA was amplified through a PCR reaction using primers for

beta-actin to make sure that the cDNA synthesis reaction has worked. Primer sequences used were as follows: 5'-TGGC ATTGTTACCAAGTGGGACGAC-3' (forward) and 5'-GGAACCGCTCGTTGCCAATAGTGAT-3' (reverse).

The effect of THS on expression of 84 genes associated with mitochondrial function was evaluated using the Qiagen Mitochondria RT^2 Profiler Array. Reaction mixtures were prepared by mixing cDNA with Qiagen RT^2 SYBR Green FAST Mastermix according to manufacturer's protocol. Mixtures were loaded on to the array plate. RT PCR was performed using the BIO-RAD CFX384 Real Time pCR detection system. Data were uploaded to the Qiagen Data Analysis Center for analysis and obtaining fold changes in gene expression.

Follow up PCR: The accuracy of the RT^2 Profiler Array was checked through RT-PCR for two genes that were down–regulated on the array. Qiagen HotStarTaq Master Mix (Qiagen, Velencia, CA) was used to run PCR reactions with the BioRad Thermal Cycler (BioRad, Hercules, CA). Primers used were as follows:

Fis1: 5' – AAAGTATGTGCGAGGGCTGT - 3' (forward) and 5' - ACAGCCAGTCCAATGAGTCC - 3' (reverse); and *Aifm2*: 5'-GGTGAGCAACCTGGAGGAAC-3' (forward) and 5'- GGTATCGGCACAGTCACCAA-3' (reverse). Lonza DNA FlashGels were run to separate PCR products which were imaged using a Lonza FlashGel imaging system (Lonza, Walkersville, MD).

Statistical analysis: GraphPad Prism software was used to perform statistical analyses. For fluorescent intensity data, the 30% THS and 100% THS groups were individually compared to the control group using a t-test. For ATP generation data, which

did not satisfy the assumptions of ANOVA, the non-parametric Kruskal-Wallis test was performed. ATP values for treatment and control groups were normalized to the total protein in each group and were transformed using the arcsine function before comparing treated and control groups. When significance was found, Dunn's post hoc test was used to isolate the significance of the specific treatment groups. For MitoTimer experiments, the raw data from 30% and 100% THS treated groups were compared to control groups using a t-test. RT-PCR data was uploaded to the Qiagen data analysis center to obtain fold changes that were statistically significant.

Results:

THS treatment altered mitochondrial morphology: The morphology of mitochondria in control mNSC and cells treated 24 hours with THS extract was examined after labeling with Mitotracker Red CMXRos (Fig. 6.1 A and B). Control mNSC had numerous mitochondria clustered around the nucleus (Fig. 6.1 B). Most mitochondria in control cells were categorized as small "dots" (Fig. 6.1 A and B). In THS treated mNSC, four morphologies of mitochondria were observed: dots, tubes, networks, and loops/blobs (Fig. 6.1 A and B). While a few cells in the control group had multiple mitochondrial morphologies, most control cells had mainly dot mitochondria. In contrast, in the THS treatment groups, most cells had tubular, networked, looped and blob mitochondria with fewer cells having dot mitochondria (Fig. 6.1 B). To demonstrate this difference, interactomes were constructed for the control and THS treated groups (Fig. 6.1 C). Colored circles in the interactomes represent different mitochondrial morphologies, while the small white circles are individual cells. Lines connecting the cells to different circles represent the presence of those mitochondrial morphologies in the cells. It is clear from the increased complexity of the treatment group interactomes

that treated cells had fewer dot mitochondria and more of the other types of mitochondrial morphologies relative to the control (Fig. 6.1 C).

Changes in mitochondrial morphology occurred through mitochondrial fusion: To test the hypothesis that the changes in mitochondrial morphology observed in THS treated cells were due to fusion of mitochondria, control and treated cells were labeled with Mitotracker Red CMXRos, and videos were made of cells to observe their behavior over time. In both control and treated groups, mitochondria were constantly moving within cells. During movement, mitochondria in treated cells underwent fusion either with adjacent mitochondria or with themselves as shown in Figures 6.1 D and 6.1 E. Dot mitochondria fused to each other to form blobs (Fig. 6.1 D) or tubes (not shown). Tubular mitochondria either fused with each other to form networks (not shown) or curled so that their ends could fuse to form loops (Fig. 6.1 E). Loops eventually filled into become blobs (not shown). These transitions occurred within seconds to minutes. While some mitochondrial fission occurred, mitochondrial fusion was dominate in THS treated cells. These data support the hypothesis that THS treatment produced stress-induced mitochondrial hyperfusion (SIMH), as described by Tondera et al (2009).

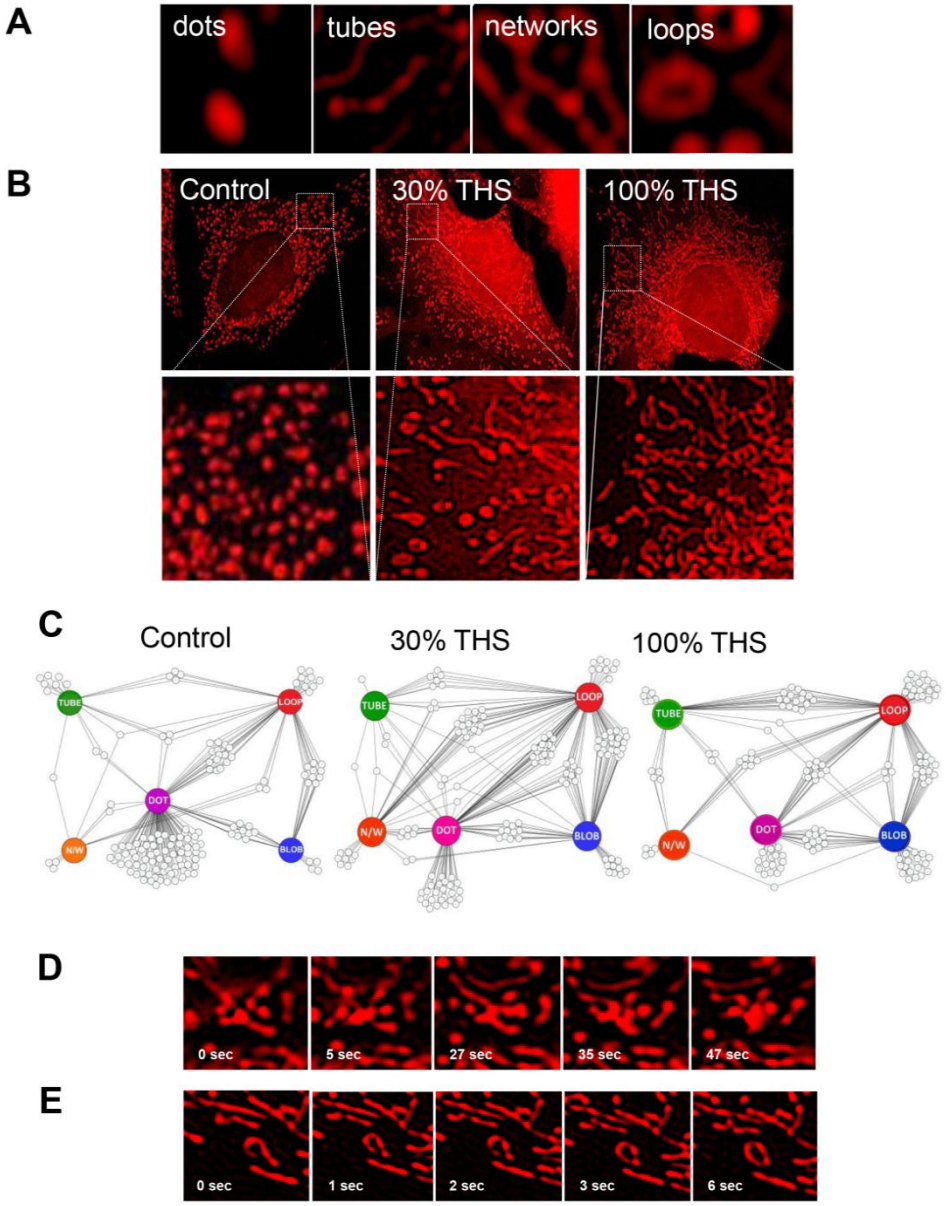

Figure 6.1. Micrographs showing different mitochondrial morphologies in THS- treated mNSC. (A) Examples of four mitochondrial morphologies present in mNSC. **(B)** Mitochondrial morphologies in control and THS treated groups. **(C)** Interactomes representing distribution of different mitochondrial morphologies in cells from control and treatment groups. Each interactome represents 150 cells that were inspected visually. Hollow circles represent individual cells and colored circles represent morphology types. Connecting lines between hollow and colored circles represent the presence of a particular morphology in a cell. (**D**) Filmstrips showing aggregation of dotted mitochondria to form blob-like mitochondria through fusion. (**E**) Filmstrips showing the transition of a tubular mitochondrion into a loop though circularization of the tube and fusion of its ends.

THS treatment increased mitochondrial membrane potential (MMP) and ATP production in mNSC: SIMH was shown by Tondera et al (2009) to increase ATP production. We hypothesized that THS would increase ATP levels and mitochondrial membrane potential (MPP) of treated cells. To test this, mNSC were treated with extracts from terrycloth that had been exposed to THS from 11, 75, or 133 cigarettes. After 24 hours of treatment, cells were labeled with MitoTracker Red CMXRos, which accumulates in mitochondria in direct proportion to the MMP and is retained after fixation. All THS extracts increased the mitochondrial membrane potential (MMP) of mNSC (Fig. 6.2 A-C) as demonstrated by increased fluorescence in the treated groups. The increased fluorescence was greatest for cells treated with extracts from terrycloth exposed to 133 cigarettes, indicating a dose dependency. Cells treated with extracts from unexposed terrycloth had fluorescence intensity similar to that of cell incubated in culture medium (control cells). hESC showed a similar increase in fluorescence in the THS treated groups; however, these cells were not studied further as their mitochondria were difficult to resolve due to the compact nature of the hESC cytoplasm (Fig. B.1). The number of mitochondria/cell that had a fluorescent intensity above 160 was quantified, and the 100% THS treated group was significantly higher than the control (Fig. 6.2 D). Since an increase in MMP and SIMH are likely accompanied by increased ATP production, we incubated cells in 30% and 100% THS extracts for 24 hours, then tested cell lysates for levels of ATP using a luminescence based assay. ATP production increased in groups treated with both 30% and 100% THS;, significance when compared to the untreated control was found in the higher dose, which had about 1.5 times as much ATP as the control (Fig. 6.2 E).

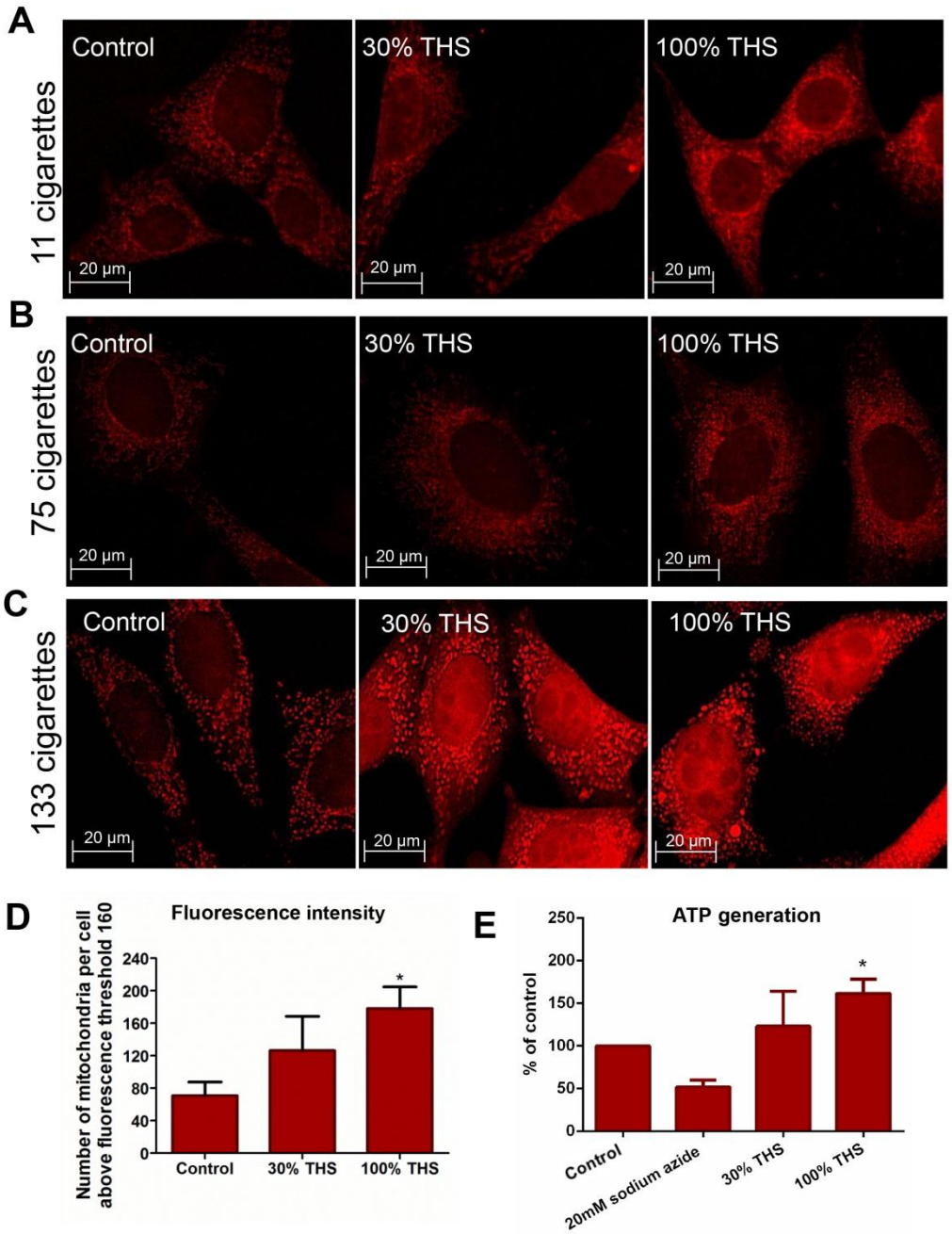

Figure 6.2. THS treatment increased MMP in mNSC as seen with MitoTracker Red CMX Ros labeling. (A) mNSC cells treated with THS extract from terrycloth exposed to 11 cigarettes over 4 months. **(B)** mNSC treated with THS extract from terrycloth exposed to cigarette smoke from 75 cigarettes over 9 months. **(C)** mNSC treated with THS from terrycloth exposed to 133 cigarettes over 11 months and aged for 15 months. (**D**) Graph showing number of mitochondria/per cell with fluorescent intensity above 160 in control cells and cells treated with 30% and 100% THS from fabric exposed to 133 cigarettes. Each bar is a mean ± SEM of three experiments. **(E)** Graph showing ATP generation in control and treated cells. Each bar shows mean ± SEM of three experiments. * = $p < 0.05$; ** = $p < 0.01$.

THS increased ROS production and oxidation of mitochondrial proteins: To test the hypothesis that increased MMP and ATP production would be accompanied by an increase in ROS, cells were treated for 6 hours with THS extract then incubated in MitoSOX Red, which fluoresces in the presence of superoxide anions (Fig. 6.3 A). 30% and 100% THS extracts increased superoxide anion production demonstrated by MitoSox Red labeling. MitoSOX Red fluorescence was concentrated in the mitochondria of most THS treated cells, while mitochondria in the control group did not show MitoSOX Red fluorescence (Fig. 6.3 A). Oxidative stress was further evaluated using MitoTimer transfected mNSC. MitoTimer is a mutant of red fluorescent protein dsRed which is inserted into mitochondria through a targeting sequence derived from cytochrome c oxidase subunit VIII, that is used to deliver proteins to the mitochondria (Hernandez et al., 2013). Newly synthesized MitoTimer protein emits green fluorescence, which changes to red upon protein aging and oxidative damage. An increase in the red/green fluorescence ratio is an indicator of accumulated oxidation in mitochondrial proteins (Hernandez et al., 2013). mNSC exposed to THS for 24 were imaged using a fluorescence microscope, and both the 30% and 100% THS extracts caused an increase in the red/green fluorescence ratio when compared to the control cells (Fig. 6.3 B). Quantification of the red/green fluorescence ratio using CL-Quant software confirmed that oxidation of the Mitotimer protein increased during exposure to THS extract (Fig. 6.3 C).

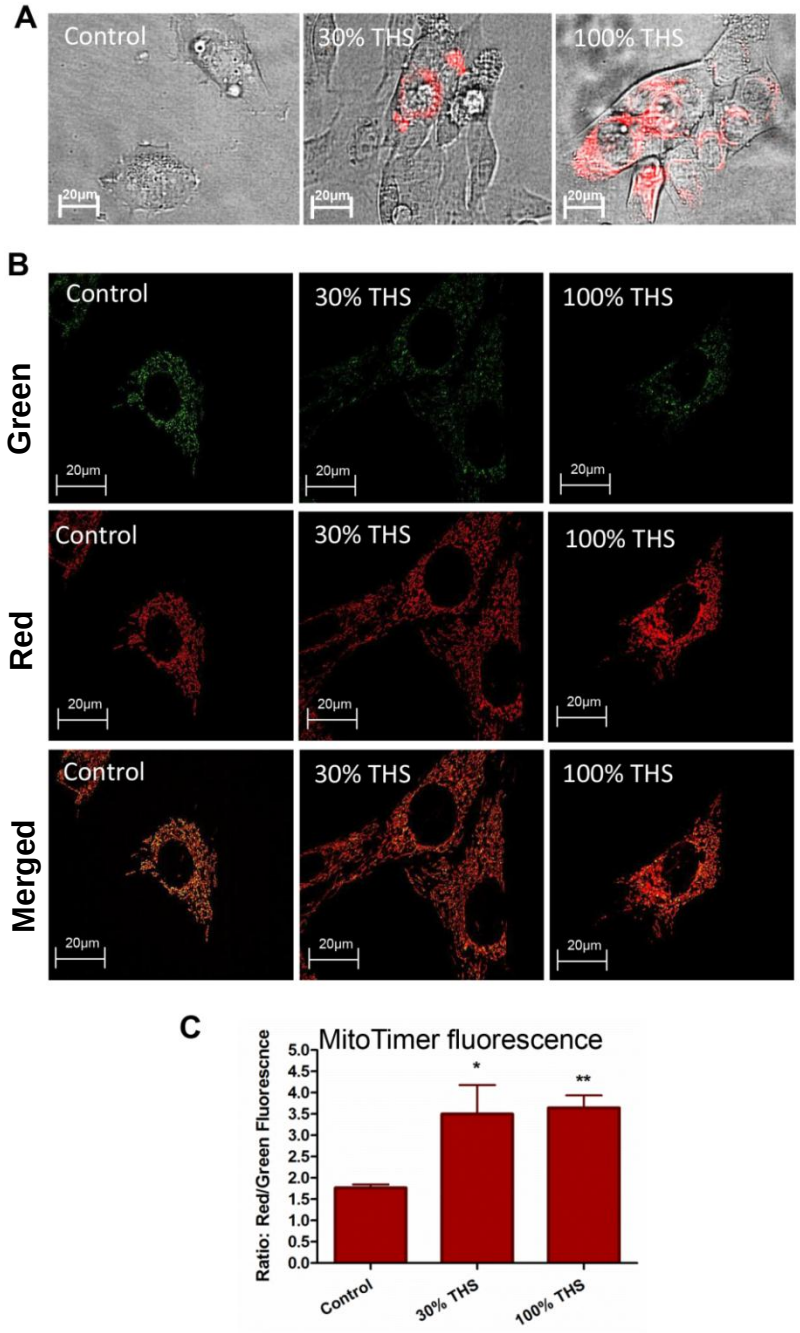

Figure 6.3. THS increased oxidative stress. (A) Micrographs showing control and THS treated mNSC labeled with MitoSOX Red. Fluorescent images are superimposed on phase images to demonstrate the localization of MitoSOX labeling in mitochondria clustered around the nuclei in treated cells. **(B)** Micrographs showing mNSC transfected with MitoTimer. Red and green fluorescent images are shown individually as well as superimposed. **(C)** Ratio of MitoTimer red/green fluorescence in control and THS-treated cells. Each bar shows mean ± SEM of three experiments. 30% THS and 100% THS grouped were compared to the control by a t test. * = $p < 0.05$; ** = $0.001 < p < 0.01$.

Long term treatment of mNSC with THS caused a reduction in MMP: To test the hypothesis that prolonged exposure to THS leads to deceased mitochondrial function and cell growth, mNSC were treated with 30% and 100% THS extracts for 15 or 30 days, then labeled with MitoTracker Red and imaged. After 15 days, MitoTracker Red fluorescence was higher in the THS treated groups (Fig. 6.4 A), indicating that MMP can remain elevated for over 2 weeks in THS treated cells. By 30 days of exposure, fluorescence in the treated groups was less than the control (Fig. 6.4 B). The number of mitochondria/cell with a fluorescent intensity above 160 was reduced in at the 30% concentration (Fig. 6.4 E), indicating that MMP can be compromised by prolonged exposure (30 days) to THS. There is variation in fluorescence at the 10% concentration among the experiments because it is a medium dose.

THS treatment altered cell proliferation rate in the long term experiment: To determine if cell growth rate was affected by prolonged exposure to THS, cells were trypsinized and replated at 5000 cells/well in 24 well plates on day 14 of treatment in the 15 day experiment and on day 29 of treatment in the 30 day experiment. Cells were then imaged live for 46 hours starting on day 15 and day 30 of the treatment, respectively. In the 15 day experiment, cell confluency was higher in the THS treated groups when compared to the control group, indicating increased proliferation (Fig. 6.4 C). In the 30 day experiment, THS treated groups had fewer cells than control groups indicating decreased proliferation (Fig. 6.4 D). Consecutive frames were checked visually for presence of dead cells, but no dead cells were found. Area confluency was quantified using CL-quant. After 15 days of treatment, the proliferation rate was higher for 10% and 30% THS treated groups (Fig. 6.4 E), and after 30 days the proliferation rate was lower in the 10% and 30% THS treatment groups (Fig. 6.4 F).

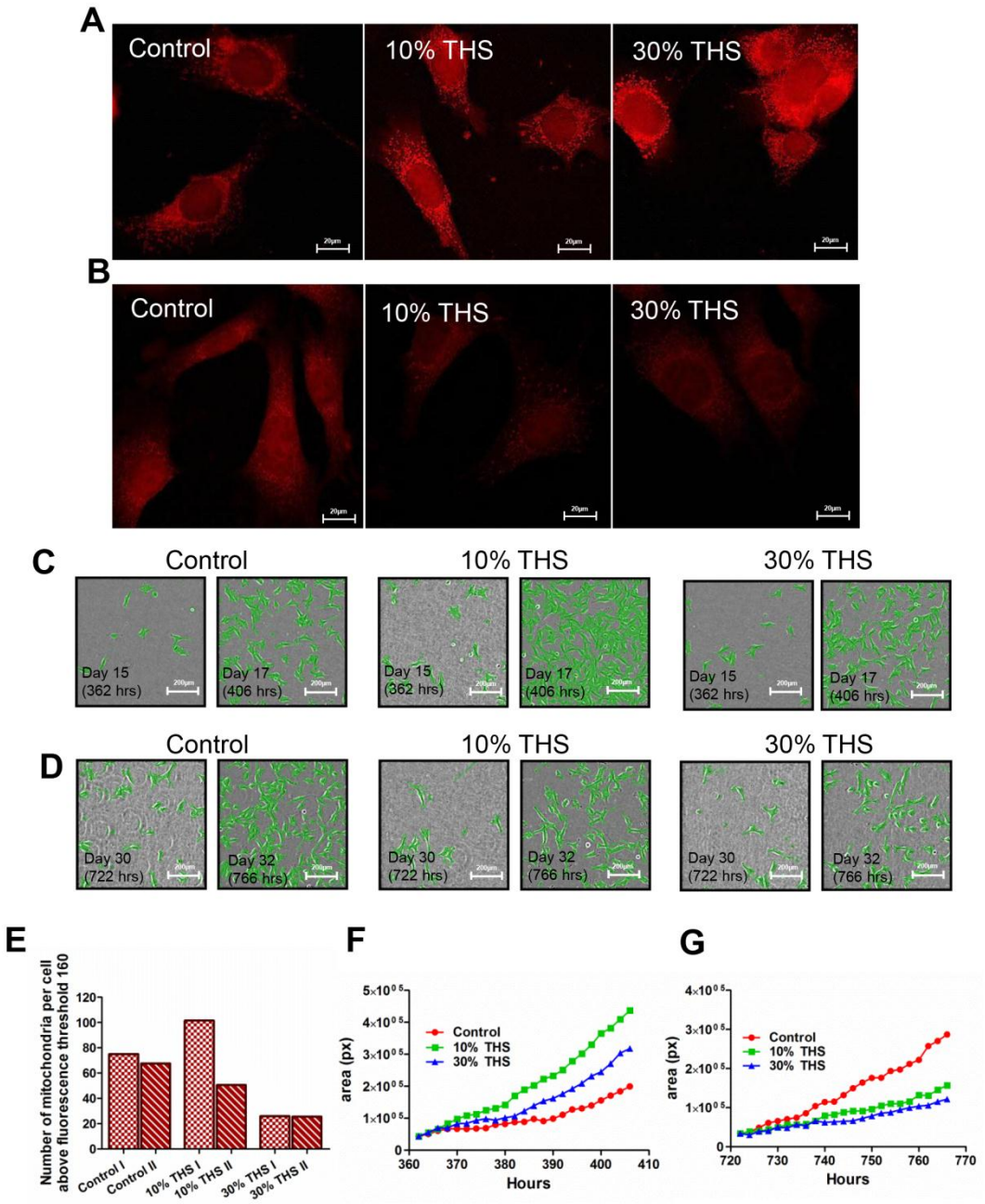

Figure 6.4. MMP and cell growth rate decreased after long-term THS exposure. (A) Micrographs showing control and treated cells labeled with MitoTracker Red CMXRos after 15 days of treatment. **(B)** Micrographs showing control and treated cell labeled with MitoTracker Red CMXRos after 30 days of treatment. **(C)**. Masked micrographs showing cell density of mNSC after 15-17 days of treatment. **(D)** Masked micrographs showing cell density of mNSC after 30-32 days of treatment. **(E)** Graphs showing number of mitochondria/cell with a fluorescent intensity above 160 in two individual 30 day experiments. **(F)** Graphs showing cell proliferation data from one representative experiment in which cells treated with THS for 17 days. **(G)** Graphs showing cell proliferation data from one representative experiment in which cells were treated with THS for 32 days.

THS altered the transcriptional profile of genes associated with mitochondrial function: Gene expression was evaluated using Qiagen RT^2 Profiler Arrays after 1, 4 and 24 hours of exposure to THS. After 1 hour of treatment, expression of the mitochondrial membrane transporter *Slc25a25* was decreased by 2.14 fold, while expression of *Ucp4* and *Taz* increased by over 2 fold (Fig. 6.5 A). At 4 hours of treatment, 25 genes associated with mitochondrial health showed a twofold or greater reduction in expression. These include *Fis1, Aifm2, Bbc3, Bid, Tspo, Ucp2, Ucp4* and *Ucp5* (Fig. 6.5 B), and transporters from the SLC25A and TIMM families. A complete list of the affected genes and their function is given in Table 1. PCR was used to confirm the array results for 2 of the genes that were affected by treatment (Fig. 6.5 C). No significant gene expression alterations were observed at 24 hours of treatment.

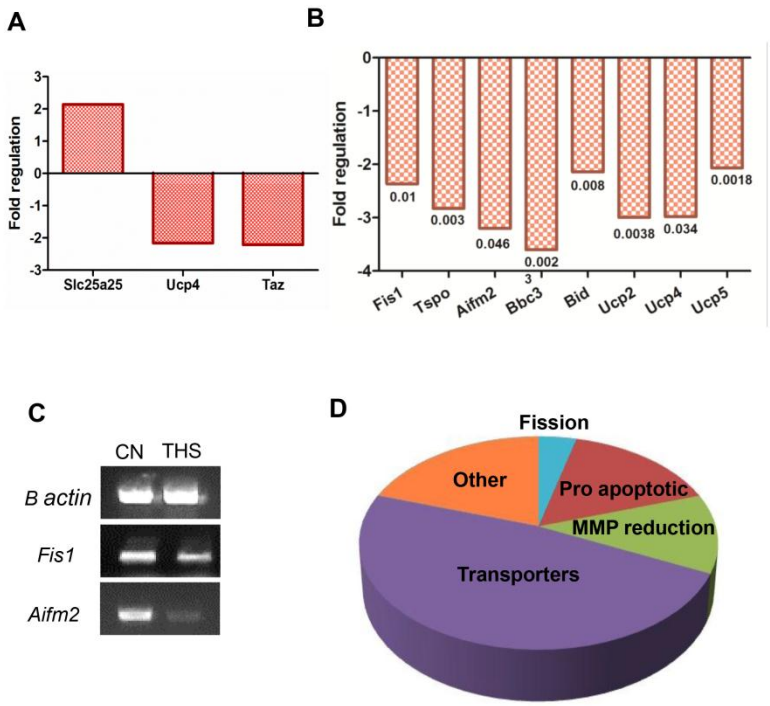

Figure 6.5. THS caused significant changes in expression of genes associated with mitochondrial function. (A) Gene expression changes after 1 hour of treatment with THS. Each bar is an average of two experiments. **(B)** Gene expression changes after 4 hours of treatment with THS. Each column represents the average of three experiments. The numbers below each column represent p value. **(C)** PCR products observed with gel electrophoresis. β-actin was used as the housekeeping (loading) control. **(D)** Pie chart showing relative abundance of genes related to different functions that were down regulated at 4 hours of THS treatment. .

Table 6.1. List of genes that had deceased expression in response to THS exposure

Gene	Fold regulation	P – value	Function
Fis1	-2.36	0.011	Mitochondrial fission
Tspo (18kD translocator protein)	-2.8	0.004	Increases mitochondrial membrane permeability
Aifm2 (apoptosis inducing factor – mitochondrial 2)	-3.2	0.046	Pro apoptotic
Bbc3 (Bcl binding component 3)	-3.6	0.002	Pro apoptotic
Bid (BH3 interacting domain death agonist)	-2.14	0.008	Mediates apoptosis and mitochondrial damage
Msto1	-2.5	0.001	Mitochondrial restructuring
Sls25a8/ Ucp2 (uncoupling protein 2)	-2.99	0.004	Prevents OXPHIOs and promoted glycolysis
Taz (Tafazzin)	-4.8	0.0013	Acylation of cardiolipin
Dnajc19/ Hsp40	-2.11	0.004	Associated with prohibitins that play a role in cardiolipin acylation
Cp2 (carnitine acyltransferase)	-3.2	0.006	Involved in fatty acid metabolism
Aip (aryl hydrocarbon receptor interacting protein)	-2.13	0.0014	Aryl hydrocarbon activated transcription factor regulating xenobiotic metabolizing enzymes
Mipep (mitochondrial intermediate peptidase)	-2.09	0.005	Maturation of proteins entering the mitochondria

Timm10b (Mitochondrial Import Inner Membrane Translocase Subunit Tim9 B)	-2	0.01	Import and insertion of membrane protein into mitochondrial membrane
Timm17b (Mitochondrial Import Inner Membrane Translocase Subunit Tim17-B)	-2.89	0.0014	Transport of mitochondrial proteins from cytosol in to mitochondria
Timm22	-2.32	0.0008	
Immp21	-2.71	0.02	
Slc25a1 (Solute Carrier Family 25)	-2.29	0.018	Citrate transport across mitochondrial inner membrane
Slc25a14 / *Ucp5*	-2.06	0.0018	Reduction of mitochondrial membrane potential
Slc25a15	-2.29	0.0009	Ornithine transport from cytosol to mitochondria
Slc25a16	-2.38	0.0009	Molecular exchange between cytosol and mitochondria
Slc25a17	-2.53	0.0016	Molecular exchange between cytosol and mitochondria
Slc25a19	-2.82	0.0009	Transport of thiamine pyrophosphate into mitochondria
Slc25a20	-2.46	0.008	Transport of acylcarnitine into mitochondrial matrix for oxidation by the fatty acid oxidation pathway
Slc25a23	-3.07	0.01	Calcium dependent mitochondrial solute carrier

Slc25a27/ Ucp4	-2.98	0.034	Lowering of mitochondrial membrane potential

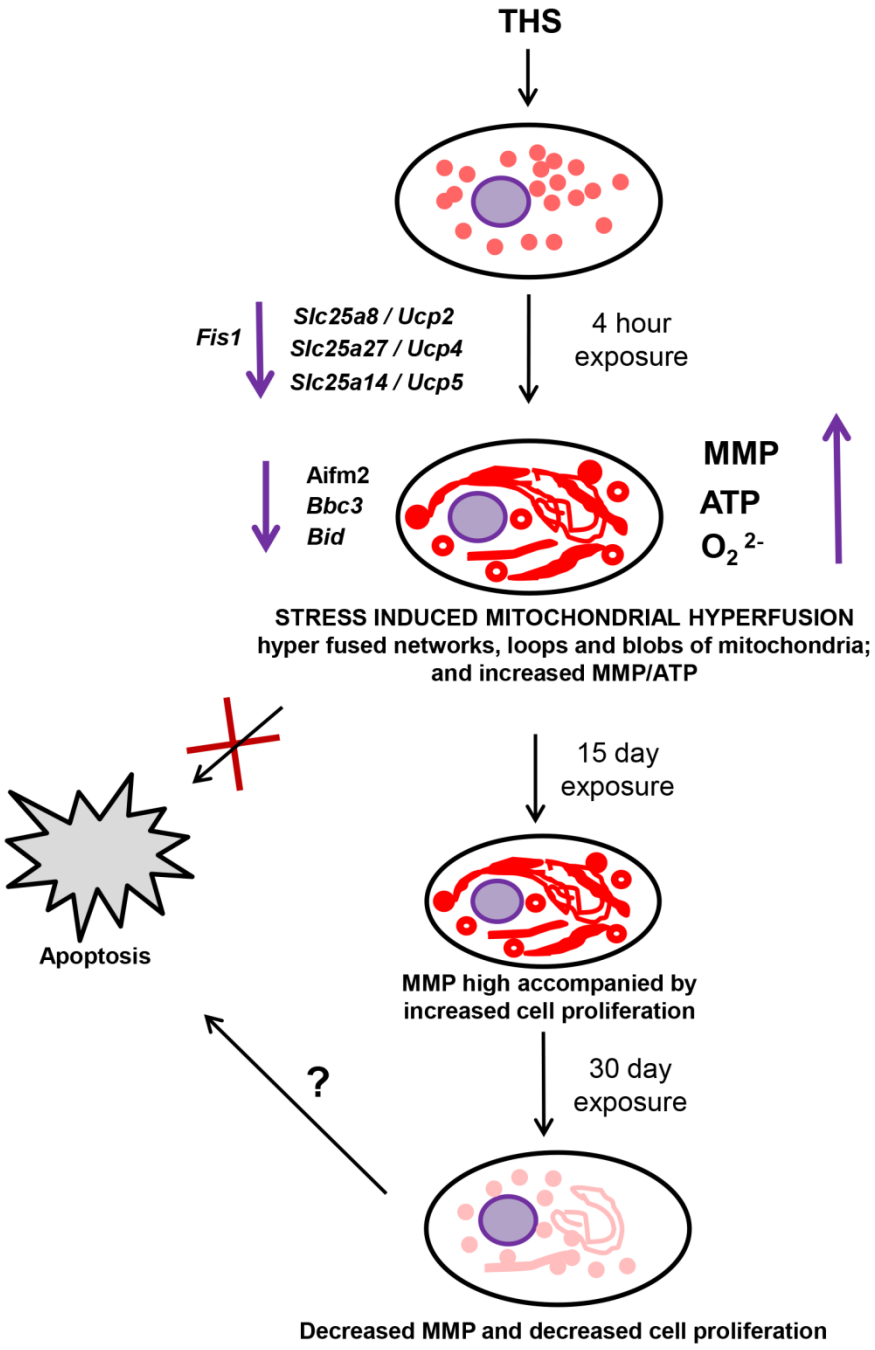

Figure 6.6: Summary of effects on mitochondrial and cell health induced by THS: Short term exposure of mNSC to THS cause SIMH accompanied by increased MMP and ATP production and increased oxidative stress. This is likely a pro survival mechanism mediated by decreased expression of *Fis1* and pro apoptotic genes. After long term exposure up to 15 days, the cell still had a high MMP, but 30 day exposure eventually lead to decreased MMP and decreased cell proliferation.

Discussion:

Mitochondria are excellent organelles for monitoring cell health and can report on multiple responses to environmental stress (Meyer et al., 2013). In this study, batches of THS that were not effective in the MTT assay had profound morphological and physiological effects on mitochondria leading to the results summarized in Figure 6.6.

These effects included SIMH or the formation of elongated networked mitochondria and blob mitochondria from dot-shaped mitochondria. SIMH in mNSC was accompanied by increased MMP (also observed in hESC) with increased ATP production, increased levels of superoxide, and increased oxidation of mitochondrial proteins. Alterations in gene expression in treated cells were consistent with reduced mitochondrial fission and protection of cells from apoptosis. Extended exposure to THS for 15 days led to an increase in both MMP and cell proliferation, while treatment for 30 days resulted in a decrease in both MMP and cell proliferation , suggesting that long-term exposure to THS can reduce the rate of cell division. Our study is, to the best of our knowledge, the first report to show that sub-lethal doses of THS can cause SIMH and alter mitochondrial function in a manner that could protect cells in the short term, but lead to cell loss/death with chronic exposure.

While mitochondria often fragment in response to external stress (Leboucher et al., 2012), Tondera et al (2009) reported that mitochondria in mouse embryonic fibroblasts (mEF) undergo SIMH following exposure to certain types of environmental stress including treatment with actinomycin D and UV radiation (Tondera et al., 2009). It was previously reported that 10% and 12.5% solutions of cigarette smoke extract (smoke from 4 cigarettes bubbled through a 50 ml solution was considered 100%) caused

fragmentation of mitochondria in BEAS-2B cells, but at the 1% concentration there was branching and hyperfusion of mitochondria (Hoffmann et al., 2013). Alveolar epithelial cells have also been shown to undergo mitochondrial hyperfusion when treated with nontoxic doses of 25% cigarette smoke extracts. (where smoke from six cigarettes was bubbled through 100 ml of medium and served as the 100%) (Ballweg et al., 2014). Our results match these studies as the batch of THS that we used was not cytotoxic in the MTT assay and did not affect the normal morphology and motility of mNSC but did induce hyperfused mitochondrial networks like those reported with cigarette smoke in the above mentioned studies.

SIMH is likely a protective response to stress that allows healthy mitochondria to rescue those that are damaged (van der Bliek, 2009) and enables treated cells to produce sufficient ATP to combat stress (Tondera et al., 2009). In addition, it is likely to protect mitochondria from autphagosomic degradation due to the large size of hyperfused mitochondria (Gomes, Di Benedetto, & Scorrano, 2011). SIMH occurs when the balance between fusion and fission tipped in favor of fusion by either an increase in level of pro fusion genes like Mitofusin (Tondera et al., 2009) or a decrease in pro fission proteins like *Fis1* (current study). Although we did not observe an increase in mitofusin 1 expression, which is involved in SIMH (Tondera et al., 2009), we did find that expression of *Fis1*, was reduced. This could create an imbalance between *Fis1* and mitofusin 1 and tip the balance toward fusion, as was suggested by hyperfused mitochondrial networks in our study. This is similar to a decrease in DRP1, another gene responsible for fission that was observed by Gomes et al (2011)(Gomes et al., 2011) during mitochondria hyperfusion. The data in our study when compared to the study by Tondera et al (2009)

suggest that different mechanisms may exist for regulating SIMH and these mechanisms could vary with cell type and/or source of the stress.

Highly networked and tubular mitochondria, as were observed in response to THS, have also been reported to play a protective role against cell death in conditions of nutrient starvation (Rambold, Kostelecky, Elia, & Lippincott-Schwartz, 2011). The networked mitochondria observed in our study may protect against THS induced stress, which is further supported by the decreased expression of genes associated with apoptosis. Apoptosis inducing factor-mitochondrial 2 (*Aifm2*), Bcl binding component 3 (*Bbc3*), and BH3 interacting domain death agonist (Bid), which are all involved in apoptosis (Joza et al., 2001)' (Han et al., 2001)' (Li, Zhu, Xu, & Yuan, 1998), were down regulated in cells treated with THS. Translocator protein (*Tspo*, which was also down regulated) may be involved preventing apoptosis, as its down regulation leads to reduced mitochondrial outer membrane permeablization, thus restricting the release of pro-apoptotic factors such as apoptosis inducing factor (Gatliff & Campanella, 2012). In addition, decreased expression of *Fis1* protects cells from apoptosis (Lee, Jeong, Karbowski, Smith, & Youle, 2004), perhaps by favoring hyperfusion, which occurred in our study.

SIMH was accompanied by increases in MMP, ATP, and mitochondrial ROS levels (Mitosox Red). Our RNA profiling data showed that three genes associated with decreasing MMP (*Slc25a8 / Ucp2, Slc25a27 / Ucp4* and *Slc25a14 / Ucp5*) were down regulated in THS treated cells, which may have contributed to the MMP increase that we observed. *UCP* 2, 3 and 4 are members of the solute carrier family *SLC25A* and cause uncoupling of mitochondrial oxidative phosphorylation, thus diminishing oxidative stress

in cells (Brand & Esteves, 2005), (Ramsden et al., 2012) . *UCP2* in human pluripotent stem cells regulates energy metabolism by preventing oxidative phosphorylation and promoting glycolysis, which is the primary energy production pathway in stem cells (Zhang et al., 2011). Since neural stem cells also rely mainly on glycolysis (Candelario, Shuttleworth, & Cunningham, 2013), *Ucp2* could possibly be playing a similar role and it's down regulation during SIMH could be facilitating increased oxidative phosphorylation which is supported by increased MMP and ATP production and could lead to the increased ROS that we observed. Increased oxidative stress is believed drive stem cell differentiation (Rafalski & Brunet, 2011), but mNSCs treated with THS did not seem to be differentiated as is indicated by their stem cell-like morphology even after 15 or 30 days of exposure to THS. MMP stayed high through 15 days of exposure to THS and was accompanied by an increase in cell proliferation. At 15 days of exposure, the cells seemed healthy as indicated by normal morphology and motility. It is likely that the ATP being generated during SIMH is used to support increased proliferation and that oxidative stress during SIMH drives proliferation instead of differentiation. After 30 days of exposure, cells had a decreased MMP accompanied by a decrease in proliferation, indicating that at some point, cells succumb to the stressor and eventually stop dividing and die.

Increased MMP and ATP production were likely consequences of SIMH, which increased ATP in mouse embryonic fibroblast exposed to UV light or actinomycin (Tondera et al., 2009). Networked mitochondria, similar to those found in SIMH, have also been associated with increased oxidative phosphorylation in cancer cells (Rossignol et al., 2004). Certain mitochondrial morphologies, like blobs, are associated with increased ROS production in BEAS 2B cells, a cell line from normal human bronchial

epithelium (Ahmad et al., 2013). The high number of blobs in mNSC treated with 100% THS in our experiments would be consistent with the report of Ahmed et al (Ahmad et al., 2013). Our hypothesis that the increase in mitochondrial ROS would lead to oxidation of mitochondrial proteins was confirmed by the color shift in the Mitotimer protein to predominantly red fluorescence, which is indicative of protein oxidation in the THS treated group. Although not evaluated in this study, increased ROS generation can cause DNA and membrane damage in cells (Waris & Ahsan, 2006), (Stark, 2005), (Squier, 2001) and eventually in conjunction with protein damage lead to adverse health outcomes including carcinogenesis and neurodegenerative diseases (Ziech, Franco, Pappa, & Panayiotidis, 2011) (Uttara, Singh, Zamboni, & Mahajan, 2009).

The THS exposed terrycloth used in this study was aged at room temperature for 15 months prior to extraction. During aging, the THS VOCs present in the fabric were lost, and the extracts were most likely devoid of any volatile compounds, indicating that the mitochondrial effects were likely caused by non-volatile or semi-volatile chemicals. The main routes of exposure for the chemicals in extracts would dermal for people in all age groups and ingestion for toddlers and infants. Exposure to THS through ingestion could be risky as THS chemicals can readily dissolve in saliva and intake through ingestion would likely be much higher than through the skin. Even though the THS chemicals may get diluted in saliva, a toddler mouthing a THS contaminated fabric for a long time could ingest enough THS to affect mitochondrial health in exposed cells. It is important to emphasize that when cells were exposed to THS for 30 days, the 10% dose caused a reduction of MMP and decreased cell proliferation indicating that low doses when available chronically can adversely impact mitochondrial health. Moreover, infants and children exposed to THS environments are likely to receive a higher dose/kg of body

weight than adults. THS induced mitochondrial stress and decreased proliferation of neural stem cells over time may adversely affect brain development in infants and children. Also noteworthy, a very low number of cigarettes was used to generate THS, but in a real scenario, THS deposition could occur for years and lead to a significant buildup of toxic chemicals.

Conclusions

Our data demonstrate that THS from relatively few cigarettes can produce a stress response in mitochondria and alter the transcriptional profile of genes involved in mitochondrial function, which may in turn affect mitochondrial and cellular health. Our findings further indicate that SIMH induced by THS at levels that do not rapidly kill cells is a pro survival mechanism that protects cells from undergoing apoptosis, although longer exposure to THS adversely affects mitochondrial MMP as well as cell proliferation, and likely leads to cell death. The most important conclusion from this study is that even though low dose of THS may not directly kill cells, it induces a stressed state that may potentially compromise cellular function, survival and replication and in turn adversely affect the health of an exposed individual. Our data could be useful to agencies that regulate indoor smoking and may help parents make informed decisions regarding exposure of their children to THS.

References:

Ahmad, T., Aggarwal, K., Pattnaik, B., Mukherjee, S., Sethi, T., Tiwari, B. K., … Agrawal, a. (2013). Computational classification of mitochondrial shapes reflects stress and redox state. *Cell Death & Disease*, *4*(1), e461. http://doi.org/10.1038/cddis.2012.213

Bahl, V., Jacob, P., Havel, C., Schick, S. F., & Talbot, P. (2014). Thirdhand cigarette smoke: factors affecting exposure and remediation. *PloS One*, *9*(10), e108258. http://doi.org/10.1371/journal.pone.0108258

Ballweg, K., Mutze, K., Konigshoff, M., Eickelberg, O., & Meiners, S. (2014). Cigarette smoke extract affects mitochondrial function in alveolar epithelial cells. *AJP: Lung Cellular and Molecular Physiology*, *307*(11), L895–L907. http://doi.org/10.1152/ajplung.00180.2014

Behar, R. Z., Bahl, V., Wang, Y., Weng, J.-H., Lin, S. C., & Talbot, P. (2012). Adaptation of stem cells to 96-well plate assays: use of human embryonic and mouse neural stem cells in the MTT assay. *Current Protocols in Stem Cell Biology*, *Chapter 1*(November), Unit 1C.13. http://doi.org/10.1002/9780470151808.sc01c13s23

Brand, M. D., & Esteves, T. C. (2005). Physiological functions of the mitochondrial uncoupling proteins UCP2 and UCP3. *Cell Metabolism*, *2*(2), 85–93. http://doi.org/10.1016/j.cmet.2005.06.002

Candelario, K. M., Shuttleworth, C. W., & Cunningham, L. A. (2013). Neural stem/progenitor cells display a low requirement for oxidative metabolism independent of hypoxia inducible factor-1alpha expression. *Journal of Neurochemistry*, *125*(3), 420–429. http://doi.org/10.1111/jnc.12204

Chen, H., & Chan, D. C. (2009). Mitochondrial dynamics-fusion, fission, movement, and mitophagy-in neurodegenerative diseases. *Human Molecular Genetics*, *18*(R2), R169–R176. http://doi.org/10.1093/hmg/ddp326

Chen, H., Vermulst, M., Wang, Y. E., Chomyn, A., Prolla, T. A., McCaffery, J. M., & Chan, D. C. (2010). Mitochondrial fusion is required for mtDNA stability in skeletal muscle and tolerance of mtDNA mutations. *Cell*, *141*(2), 280–289. http://doi.org/10.1016/j.cell.2010.02.026

Collins, Y., Chouchani, E., James, A., Menger, K., Cochemé, H., & Murphy, M. (2012). Mitochondrial redox signalling at a glance., 801–806. http://doi.org/10.1242/jcs.110486

Detmer, S. a, & Chan, D. C. (2007). Functions and dysfunctions of mitochondrial dynamics. *Nature Reviews. Molecular Cell Biology*, *8*(11), 870–879. http://doi.org/10.1038/nrm2275

Gatliff, J., & Campanella, M. (2012). The 18 kDa translocator protein (TSPO): a new perspective in mitochondrial biology. *Current Molecular Medicine*, *12*(4), 356–68. http://doi.org/10.2174/1566524011207040356

Gerbitz, K.-D., Gempel, K., & Brdiczka, D. (1996). Mitochondria and diabetes: genetic, biochemical, and clinical implications of the cellular energy circuit. *Diabetes*, *45*(2), 113–126.

Gomes, L. C., Di Benedetto, G., & Scorrano, L. (2011). During autophagy mitochondria elongate, are spared from degradation and sustain cell viability. *Nature Cell Biology*, *13*(5), 589–598. http://doi.org/10.1038/ncb2220

Han, J., Flemington, C., Houghton, a B., Gu, Z., Zambetti, G. P., Lutz, R. J., … Chittenden, T. (2001). Expression of bbc3, a pro-apoptotic BH3-only gene, is regulated by diverse cell death and survival signals. *Proceedings of the National Academy of Sciences of the United States of America*, *98*(20), 11318–23. http://doi.org/10.1073/pnas.201208798

Hang, B., Sarker, A. H., Havel, C., Saha, S., Hazra, T. K., Schick, S., … Gundel, L. a. (2013). Thirdhand smoke causes DNA damage in human cells. *Mutagenesis*, *28*(4), 381–91. http://doi.org/10.1093/mutage/get013

Hara, H., Araya, J., Ito, S., Kobayashi, K., Takasaka, N., Yoshii, Y., … Kuwano, K. (2013). Mitochondrial fragmentation in cigarette smoke-induced bronchial epithelial cell senescence. *American Journal of Physiology. Lung Cellular and Molecular Physiology*, *305*(10), L737–46. http://doi.org/10.1152/ajplung.00146.2013

Hernandez, G., Thornton, C., Stotland, A., Lui, D., Sin, J., Ramil, J., … Gottlieb, R. a. (2013). A novel tool for monitoring mitochondrial turnover MitoTimer, *9*(11), 1852–1861. http://doi.org/10.4161/auto.26501

Hoffmann, R. F., Zarrintan, S., Brandenburg, S. M., Kol, A., de Bruin, H. G., Jafari, S., … Heijink, I. H. (2013). Prolonged cigarette smoke exposure alters mitochondrial structure and function in airway epithelial cells. *Respiratory Research*, *14*(1), 97. http://doi.org/10.1186/1465-9921-14-97

Joza, N., Susin, S. a, Daugas, E., Stanford, W. L., Cho, S. K., Li, C. Y. J., … Zu, J. C. (2001). Essential role of the mitochondrial apoptosis-inducing factor in programmed cell death. *Nature*, *410*, 549–54. http://doi.org/10.1038/35069004

Leboucher, G. P., Tsai, Y. C., Yang, M., Shaw, K. C., Zhou, M., Veenstra, T. D., … Weissman, A. M. (2012). Stress-Induced Phosphorylation and Proteasomal Degradation of Mitofusin 2 Facilitates Mitochondrial Fragmentation and Apoptosis. *Molecular Cell*, *47*(4), 547–557. http://doi.org/10.1016/j.molcel.2012.05.041

Lee, O., & O'Brien, P. J. (2010). 1.19 - Modifications of Mitochondrial Function by Toxicants. In C. A. B. T.-C. T. (Second E. McQueen (Ed.), (pp. 411–445). Oxford: Elsevier. http://doi.org/http://dx.doi.org/10.1016/B978-0-08-046884-6.00119-6

Lee, Y., Jeong, S.-Y., Karbowski, M., Smith, C. L., & Youle, R. J. (2004). Roles of the Mammalian Mitochondrial Fission and Fusion Mediators Fis1, Drp1, and Opa1 in Apoptosis. *Molecular Biology of the Cell*, *15*(11), 5001–5011. http://doi.org/10.1091/mbc.E04-04-0294

Li, H., Zhu, H., Xu, C. J., & Yuan, J. (1998). Cleavage of BID by caspase 8 mediates the mitochondrial damage in the Fas pathway of apoptosis. *Cell*, *94*(4), 491–501. http://doi.org/10.1016/S0092-8674(00)81590-1

Lin, S., & Talbot, P. (2011). Embryonic Stem Cell Therapy for Osteo-Degenerative Diseases, *690*(2), 31–56. http://doi.org/10.1007/978-1-60761-962-8

Martins-Green, M., Adhami, N., Frankos, M., Valdez, M., Goodwin, B., Lyubovitsky, J., … Curras-Collazo, M. (2014). Cigarette smoke toxins deposited on surfaces: implications for human health. *PloS One*, *9*(1), e86391. http://doi.org/10.1371/journal.pone.0086391

Matt, G. E., Quintana, P. J. E., Destaillats, H., Gundel, L. a, Sleiman, M., Singer, B. C., … Hovell, M. F. (2011). Thirdhand tobacco smoke: emerging evidence and arguments for a multidisciplinary research agenda. *Environmental Health Perspectives*, *119*(9), 1218–26. http://doi.org/10.1289/ehp.1103500

Meyer, J. N., Leung, M. C. K., Rooney, J. P., Sendoel, A., Hengartner, M. O., Kisby, G. E., & Bess, A. S. (2013). Mitochondria as a target of environmental toxicants. *Toxicological Sciences*, *134*(1), 1–17. http://doi.org/10.1093/toxsci/kft102

Mustonen, P., & Kinnunen, P. K. (1993). On the reversal by deoxyribonucleic acid of the binding of adriamycin to cardiolipin-containing liposomes. *The Journal of Biological Chemistry*, *268*(2), 1074–80. Retrieved from http://www.ncbi.nlm.nih.gov/pubmed/7678246

Olichon, A., Guillou, E., Delettre, Cè., Landes, T., ArnaunÈ-Pelloquin, L., Emorine, L. J., … Belenguer, P. (2006). Mitochondrial dynamics and disease, OPA1. *Biochimica et Biophysica Acta (BBA) - Molecular Cell Research*, *1763*(5-6), 500–509. http://doi.org/10.1016/j.bbamcr.2006.04.003

Otera, H., Ishihara, N., & Mihara, K. (2013). New insights into the function and regulation of mitochondrial fission. *Biochimica et Biophysica Acta*, *1833*(5), 1256–68. http://doi.org/10.1016/j.bbamcr.2013.02.002

Qu, Q., & Shi, Y. (2009). Neural Stem Cells in the Developing and Adult Brains. *Journal of Cellular Physiology, 22*(1), 5-9. doi:10.1002/jcp.21862

Rafalski, V. a., & Brunet, A. (2011). Energy metabolism in adult neural stem cell fate. *Progress in Neurobiology*, *93*(2), 182–203. http://doi.org/10.1016/j.pneurobio.2010.10.007

Rambold, A. S., Kostelecky, B., Elia, N., & Lippincott-Schwartz, J. (2011). Tubular network formation protects mitochondria from autophagosomal degradation during nutrient starvation. *Proceedings of the National Academy of Sciences of the United States of America*, *108*(25), 10190–5. http://doi.org/10.1073/pnas.1107402108

Ramsden, D. B., Ho, P. W.-L., Ho, J. W.-M., Liu, H.-F., So, D. H.-F., Tse, H.-M., … Ho, S.-L. (2012). Human neuronal uncoupling proteins 4 and 5 (UCP4 and UCP5): structural properties, regulation, and physiological role in protection against oxidative stress and mitochondrial dysfunction. *Brain and Behavior*, *2*(4), 468–78. http://doi.org/10.1002/brb3.55

Rehan, V. K., Sakurai, R., & Torday, J. S. (2011). Thirdhand smoke: a new dimension to the effects of cigarette smoke on the developing lung. *American Journal of Physiology. Lung Cellular and Molecular Physiology*, *301*(1), L1–8. http://doi.org/10.1152/ajplung.00393.2010

Rolland, S., & Conradt, B. (2006). The role of mitochondria in apoptosis induction in Caenorhabditis elegans: more than just innocent bystanders? *Cell Death and Differentiation*, *13*(8), 1281–1286. http://doi.org/10.1038/sj.cdd.4401980

Rossignol, R., Gilkerson, R., Aggeler, R., Yamagata, K., Remington, S. J., & Capaldi, R. a. (2004). Energy Substrate Modulates Mitochondrial Structure and Oxidative Capacity in Cancer Cells. *Cancer Research*, *64*(3), 985–993. http://doi.org/10.1158/0008-5472.CAN-03-1101

Schumacher, J., Green, C., Best, F., & Newell, M. (1977). Smoke composition. An extensive investigation of the water-soluble portion of cigarette smoke. *Journal of Agricultural and Food Chemistry, 25*(2), 310-320. doi:10.1021/jf60210a003

Schick, S. F., Farraro, K. F., Perrino, C., Sleiman, M., van de Vossenberg, G., Trinh, M. P., … Balmes, J. (2014). Thirdhand cigarette smoke in an experimental chamber: evidence of surface deposition of nicotine, nitrosamines and polycyclic aromatic hydrocarbons and de novo formation of NNK. *Tobacco Control*, *23*(2), 152–9. http://doi.org/10.1136/tobaccocontrol-2012-050915

Shen, Q., Yamano, K., Head, B. P., Kawajiri, S., Cheung, J. T. M., Wang, C., … van der Bliek, A. M. (2014). Mutations in Fis1 disrupt orderly disposal of defective mitochondria. *Molecular Biology of the Cell*, *25*(1), 145–59. http://doi.org/10.1091/mbc.E13-09-0525

Shutt, T. E., & McBride, H. M. (2013). Staying cool in difficult times: Mitochondrial dynamics, quality control and the stress response. *Biochimica et Biophysica Acta (BBA) - Molecular Cell Research*, *1833*(2), 417–424. http://doi.org/10.1016/j.bbamcr.2012.05.024

Squier, T. C. (2001). Oxidative stress and protein aggregation during biological aging. *Experimental Gerontology*, *36*(9), 1539–1550. http://doi.org/10.1016/S0531-5565(01)00139-5

Stark, G. (2005). Functional consequences of oxidative membrane damage. *Journal of Membrane Biology*, *205*(1), 1–16. http://doi.org/10.1007/s00232-005-0753-8

Sweeney, M. G., Bundey, S., Brockington, M., Poulton, K. R., Winer, J. B., & Harding, a E. (1993). Mitochondrial myopathy associated with sudden death in young adults and a novel mutation in the mitochondrial DNA leucine transfer RNA(UUR) gene. *The Quarterly Journal of Medicine*, *86*(11), 709–713.

Talbot, P., Nieden, N. I., Lin, S., Martinez, I., Guan, B., & Bhanu, B. (2014). Use of Video Bioinformatics Tools in Stem Cell Toxicology. *Stem Cell Toxicology*, (August 2015). http://doi.org/10.1002/9781118856017.ch21

Tan, D., Goerlitz, D. S., Dumitrescu, R. G., Han, D., Seillier-Moiseiwitsch, F., Spernak, S. M., … Shields, P. G. (2008). Associations between cigarette smoking and mitochondrial DNA abnormalities in buccal cells. *Carcinogenesis*, *29*(6), 1170–1177. http://doi.org/10.1093/carcin/bgn034

Tondera, D., Grandemange, S., Jourdain, A., Karbowski, M., Mattenberger, Y., Herzig, S., … Martinou, J.-C. (2009). SLP-2 is required for stress-induced mitochondrial hyperfusion. *The EMBO Journal*, *28*(11), 1589–1600. http://doi.org/10.1038/emboj.2009.89

Uttara, B., Singh, A. V, Zamboni, P., & Mahajan, R. T. (2009). Oxidative stress and neurodegenerative diseases: a review of upstream and downstream antioxidant therapeutic options. *Current Neuropharmacology*, *7*(1), 65–74. http://doi.org/10.2174/157015909787602823

Van der Bliek, A. M. (2009). Fussy mitochondria fuse in response to stress. *The EMBO Journal*, *28*(11), 1533–4. http://doi.org/10.1038/emboj.2009.130

Wohlrab, H. (2009). Transport proteins (carriers) of mitochondria. *IUBMB Life, 61*(1), 40–46-40–46. doi:10.1002/iub.139

Waris, G., & Ahsan, H. (2006). Reactive oxygen species: role in the development of cancer and various chronic conditions. *Journal of Carcinogenesis*, *5*, 14. http://doi.org/10.1186/1477-3163-5-14

Yoon, Y., Galloway, C. a, Jhun, B. S., & Yu, T. (2011). Mitochondrial dynamics in diabetes. *Antioxidants & Redox Signaling*, *14*(3), 439–457. http://doi.org/10.1089/ars.2010.3286

Zanna, C., Ghelli, A., Porcelli, A. M., Karbowski, M., Youle, R. J., Schimpf, S., … Carelli, V. (2008). OPA1 mutations associated with dominant optic atrophy impair oxidative phosphorylation and mitochondrial fusion. *Brain*, *131*(2), 352–367. http://doi.org/10.1093/brain/awm335

Zhang, J., Khvorostov, I., Hong, J. S., Oktay, Y., Vergnes, L., Nuebel, E., … Teitell, M. a. (2011). UCP2 regulates energy metabolism and differentiation potential of human pluripotent stem cells. *The EMBO Journal*, *30*(24), 4860–4873. http://doi.org/10.1038/emboj.2011.401

Ziech, D., Franco, R., Pappa, A., & Panayiotidis, M. I. (2011). Reactive oxygen species (ROS)--induced genetic and epigenetic alterations in human carcinogenesis. *Mutation Research*, *711*(1-2), 167–173. http://doi.org/10.1016/j.mrfmmm.2011.02.015

Chapter 7: Conclusion

Overview

Experiments were conducted to evaluate the toxicity of THS using *in vitro* models and to quantify nicotine, nicotine alkaloids and TSNAs in extracts of THS and aged THS. Experiments were set up to simulate different scenarios such as rooms and automobiles, and various fabrics that are widely used in houses, offices, and automobiles (such as cotton and polyester) were used to collect THS. The relative sensitivity of embryonic, neonatal, and adult cells to cytotoxic batches of THS extracts was determined, thereby providing by extrapolation insight into the organs that may be affected by THS exposure. Different assays were employed for evaluating endpoints such as cell viability, proliferation rate, genotoxicity, mitochondrial toxicity and gene targets for THS and acrolein (an important volatile organic chemical in THS).

Key Findings

Chapter 2: A cell counting method based on spectrophotometric readings of a cell suspension was developed to replace the traditional hemocytometer method. This method allows faster counting and greater accuracy and has been extremely valuable for medium throughput screening of THS and its constituents in the experiments described throughout this dissertation.

Chapter 3: Nicotine, nicotine-related alkaloids and TSNAs are extractable in aqueous medium and remain in fabrics when fresh smoke is not deposited: The key result regarding the composition of THS that emerged from this study was that relatively low exposure to cigarette smoke deposits significant amounts of nicotine, its derivatives (e.g. cotinine, myosmine, 2',3'-bipyridine), and TSNAs on fabrics. These

chemicals, which are easily washed out of fabrics in aqueous medium, stay on the fabrics even after smoking has stopped. These findings as discussed in Chapter 3 are important as THS contaminated materials can be sources of exposure to nicotine and TSNAs, both known to cause adverse health effects. In addition, natural fabrics, such as cotton, absorb/release more nicotine and its derivatives than synthetic fabrics. These results demonstrate important differences between fabrics in terms of their ability to act as reservoirs of THS. Calculations were done based on the amounts of nicotine and TSNAs recovered from THS exposed fabrics, and these were related to exposure that an adult or an infant would receive in a particular scenario. An adult wearing a 500 g cotton fabric would be exposed to 7,894 µg of nicotine/day and 32.7 µg of TSNAs/day, if the outfit contained THS from 20 cigarettes. In this scenario, only a fraction of these chemicals would be available for intake. The exposure scenario would be different for infants or toddlers who are exposed to THS through mouthing of contaminated toys and other objects that do not get washed regularly. A 12 kg toddler mouthing a 5 gram terrycloth object with THS from about 133 cigarettes, (as was used in Chapter 3), for 1 hour, would receive 44 µg/kg body weight of nicotine and 0.183µg/kg body weight of TSNAs/day. These levels are lower than those received by an active smoker but higher than respiratory exposure in passive smokers. Since cigarette smoke exposure during infancy can adversely affect development, these data indicate that there is need for policies to limit or eliminate their exposure to THS.

Chapter 4: THS adversely affects cell survival and causes cytoskeletal disruption in mouse neural stem cells. THS extracts in culture medium obtained from terrycloth exposed to smoke from 133 cigarettes over 11 months adversely affected

survival of mouse neural stem cells in the MTT assay at the 30% and 100% concentrations. The cells that survived at these concentrations lost their motility, had disrupted or depolymerized of cytoskeletal proteins, underwent fragmentation, and had a large number of vacuoles in their cytoplasm. These changes are associated with cell stress.

Chapter 4: Volatile organic chemicals in THS affect cell viability:

Experiments described in Chapter 4 indicate that VOCs present in THS are responsible for the cytotoxicity of THS observed in the MTT and live cell imaging assays. This is suggested by several observations: **1**. extracts made using conditions that allow the VOCs to escape, such as longer extraction time and higher headspace volume, resulted in the extracts being less cytotoxic to mNSC, **2**. aging of THS exposed fabrics at room temperature for 5 months rendered the THS non-cytotoxic in the MTT assay. Out 25 THS VOCs that were tested using the MTT assay, only phenol, 2',5'-dimethyl furan, and acrolein caused death of mNSC, hPF and A549 (bronchial epithelial) cells. Acrolein was the most potent VOC, causing cell death at 10^{-5}M and inhibiting proliferation at 10^{-6}M in mNSC and hPF. Mixtures of the three chemicals were about 10 times more potent than acrolein by itself.

Chapter 4: Acrolein inhibited cell proliferation at low concentrations:

Acrolein inhibited cell proliferation at concentrations that did not cause cell death in the MTT and live cell imaging assays. Acrolein treatment altered the expression of four genes that are involved in cell cycle regulation, as demonstrated by RT PCR experiment described in Chapter 4. After 24 hours of treatment, acrolein caused a down regulation in *TFDP1* and *CASP*3, which would inhibit the progression of cells from G1 to

the S phase of the cell cycle. At 48 hours of treatment, acrolein caused an increase in the expression of *WEE1*, which would prevent progression from G2 to the mitotic phase and a decrease in expression of *ANAPC2*, which would prevent progression from metaphase to anaphase. It is important to note here that the effective concentration of acrolein that the cells take up is about 100- 1000 fold lower that what is added to the medium. This is because acrolein rapidly reacts and binds to proteins in the culture medium, as is discussed in detail in Chapter 4. Therefore the effective concentration of acrolein is not 10^{-6} M but between 10^{-9} to 10^{-8} M. These concentrations may be close to the acrolein concentration present in the extravascular lung water of a person breathing in a THS environment, although the level of acrolein intake will depend on several factors like extent of smoking, ventilation rate and length of time spent in a THS environment. These data are valuable as they show that exposure to THS VOCs, especially acrolein, can have adverse effects on cells. Since exposure to VOCs occurs through inhalation, exposure to acrolein from THS is difficult to avoid.

Chapter 5: THS deposited from short term exposure to cigarette smoke can induce DNA damage: As seen in the car experiment presented in Chapter 5, very low levels of THS are sufficient to produce DNA damage in mouse neural stem cells (mNSC) and adult human dermal fibroblasts (hDF). The THS generation experiment simulated a car with 20 cigarettes being smoked in it per day for 1 month. The aqueous extracts from deposited THS, which contained about 100-200 ng of total tobacco specific nitrosamines/gram of fabric, induced DNA damage in both mNSC and hDF as evaluated by comet assay. This finding is important since chronic exposure of skin, oral or respiratory cells to TSNAs in THS residue may damage the DNA potentially leading to carcinogenesis.

Chapter 5: Proteins aid in extraction of cytotoxic THS chemicals: The presence of proteins in aqueous medium aided in the extraction of cytotoxic THS chemicals, making these extracts more cytotoxic than those extracted without serum proteins. A likely explanation for this is that serum proteins bind to water insoluble or semi-soluble components of THS and act as carriers of these molecules. This finding had important implications for oral exposure to THS in toddlers and infants, who may efficiently extract cytotoxic chemicals from THS contaminated objects due to proteins in their saliva. These data also show that mere washing of THS contaminated surfaces with water during remediation may not remove all the cytotoxic residue. Therefore, in addition to indicating the potential impact of oral exposure, these findings underline the importance of efficient remediation protocols.

Chapter 5: Aging decreased the cytotoxicity of THS in the MTT assay, possibly due to degradation of cytotoxic chemicals that are extracted in presence of serum proteins. Chapter 5 discusses an indoor exposure chamber experiment in which terrycloth was exposed to varying levels of cigarette smoke for up to 16 months. There was no smoke deposition during months 10, 11, and 12 to give the THS on these fabrics an opportunity to age before evaluation. The extracts that were obtained from fabric removed from the THS generation chamber after 11 and 12 months were less cytotoxic in the MTT assay than those removed from the chamber after 9 months. These observations are similar to those reported in Chapter 4 showing that aging decreases the toxicity of THS extracts. However, in the chamber experiment, the decrease in cytotoxicity may have been due to both a loss of VOCs and more efficient extraction of cytotoxic chemicals by medium containing serum proteins. There were

clearly some toxicants in this experiment that were not very volatile as toxicity was retained even after extracts were pre-incubated at 37^{o}C for 30 days.

Chapter 5: **Different cell types have varying degree of sensitivity to THS:** Various cell types from fetal, neonatal and adult origin were exposed to THS in the MTT assay, and they differed in their sensitivities to THS. Neural stem cells were the most sensitive, followed by embryonic palatal mesenchyme cells, and finally dermal fibroblasts, which were not affected in the MTT assay. This provides evidence that not all cell types are similar and respond differently to toxicants. By extrapolation, this suggests that different organs will be impacted by THS to different degrees. For example, the neonatal brain, represented by neural stem cells could be far more sensitive than dermal fibroblasts of the skin if exposed to THS.. It must be emphasized however that different cells types may have different sensitivity depending on the endpoint being tested. For instance, both neural stem cells and dermal fibroblasts sustained DNA damage at concentrations that did not kill either cell type. These findings also emphasize the need for testing different cell types and different endpoints for *in vitro* toxicological evaluation of environmental toxicants that may have more than one route of exposure.

Chapter 6: THS causes stress-induced mitochondrial hyper fusion (SIMH) at sub-lethal concentrations: Sub lethal concentrations of THS caused stress induced mitochondrial hyperfusion (SIMH) in mNSC, which was correlated with decreased expression Fis1, the gene responsible for mitochondrial fission. This was accompanied by increased ATP production and increased oxidative stress. During SIMH, mitochondria form hyperfused networks to rescue the damaged mitochondria through

fusion with healthy ones. This response is similar to a stress response reported in literature that is induced by prolonged exposure to very low levels of cigarette smoke as is discussed in Chapter 6. This phenomenon is also protective against apoptosis and our gene expression data confirms this, since four pro apoptotic genes were down regulated by THS. These include *Tspo1, Aifm2, Bbc3* and *Bid*. The down regulation observed in some other genes that are related to mitochondrial membrane transport may adversely affect the normal functioning of mitochondria thus impacting cell health. These findings are highly significant since such effects in brain stem cells of infants and children could adversely affect brain development, and may eventually lead to unwanted cell death. It is noteworthy that prolonged exposure to sub lethal concentrations of THS caused decreased mitochondrial membrane potential and decreased cell proliferation. These data are a cause for concern as exposure in a real scenario would be prolonged and is likely to adversely impact mitochondrial functioning and cell survival..

Significance

The results obtained from this study will be valuable to agencies involved in framing policies and laws to regulate indoor smoking in multiuser buildings and work places where most THS exposure takes place. Such policies can protect public health and help ameliorate long-term health problems due to THS exposure. The results of this study can change the perception of policy makers as well as the general public about areas chronically polluted with THS such as homes, restaurants, hotel rooms, houses occupied previously by smokers, and vehicles owned by smokers. This study could also help in framing laws pertaining to remediation of public places having THS residue and cleaning and removal of THS residue before property or vehicles owned by smokers are

sold. Dissemination of these findings through peer reviewed publications as well as other print and electronic media will enable physicians and allied health professionals to better educate the public about potential health hazards of THS and increase awareness about the risks of THS exposure. Such findings could empower and benefit expectant mothers and reduce harm to their children by minimizing or avoiding exposure to THS throughout pregnancy and after birth throughout childhood. These data will make parents aware of the hazards their children face in a THS polluted environment, and can help them to make better informed decisions.

This study is important from both public health and policy perspectives, as it is one of the first attempts to assess the impact of THS on human health. The data presented in this dissertation provide new information on how cellular processes are altered by THS exposure and the maximum dose that produces no effects. It will help establish which VOCs in THS are the most cytotoxic and the doses that produce harm. The effects produced by THS on cells will give important clues about its effect on human physiology and health. The results will help establish maximum acceptable exposure levels when policies for THS exposure and remediation are developed. Further research to investigate the health hazards of THS involving *in vitro* as well as *in vivo* methods can be based on the results obtained from this project. Moreover, the standardized extraction protocol can also be applied to remediation procedures to remove THS residues in homes and work places.

Future Directions

This work will form a strong foundation for future studies that can focus on particular endpoints such as genotoxicity or organelle and organ specific toxicity. Future

studies may be designed to re confirm and extent the findings presented here using more cell types and/or *in vivo* models. Further work needs to be done to identify those chemicals in THS that cause specific cellular responses or adverse health effects. Long term studies with *in vitro* and *in vivo* models, when designed realistically, will help determine the effects of THS on organ systems and in turn the entire organism.

.

Appendix A: Supporting Information for Chapter 4

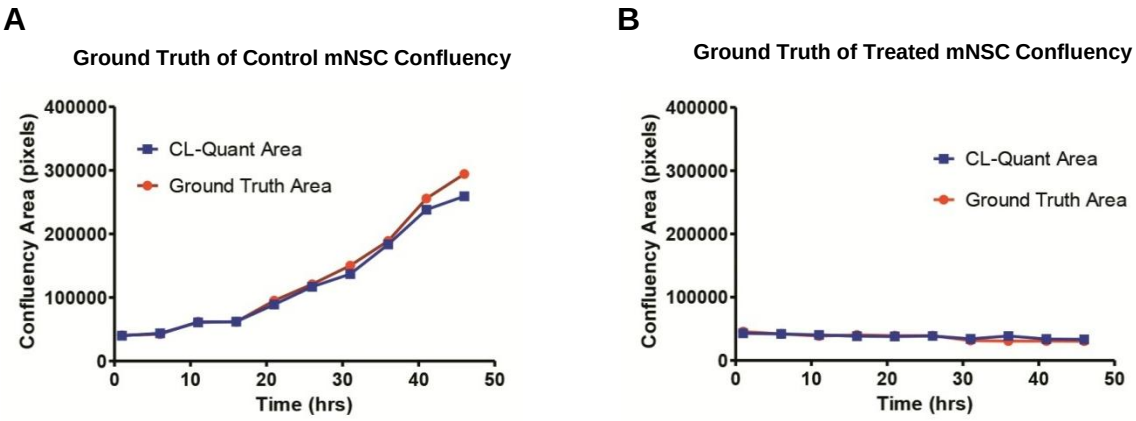

Figure A.2. A comparison of area (confluency) evaluated using either CL- Quant software or ground truth analysis (obtained by hand-tracing the area of the cells using ImageJ software). **(A)** Ground truth for control cells. **(B)** Ground truth for cells treated with 30% THS. Ground truth results validate the CL-Quant protocol. Each point is the mean of two experiments.

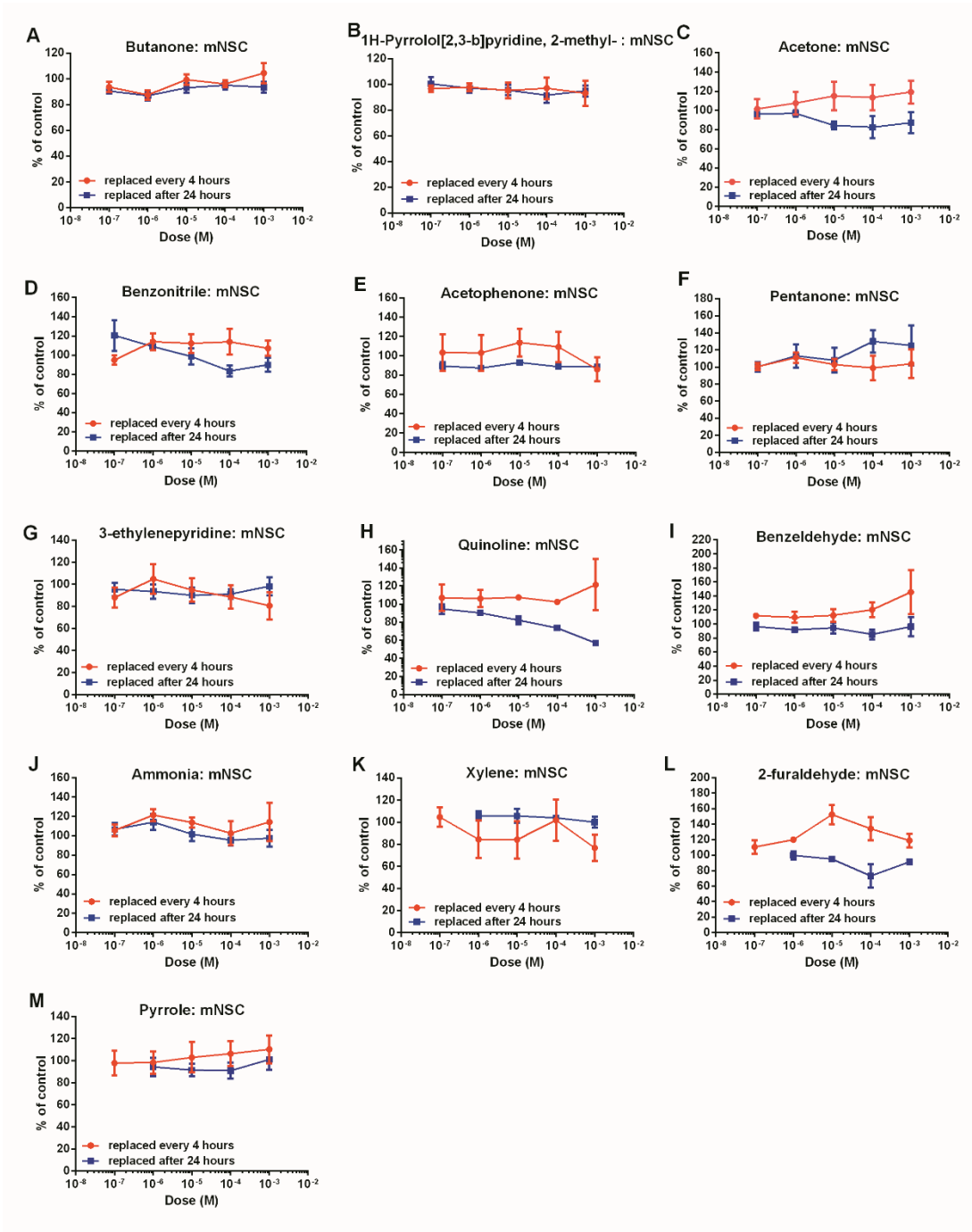

Figure A.2. MTT assay data for 13 VOCs identified in the headspace of THS extracts tested on mNSC. Each chemical was tested in two separate experiments which were then averaged. Chemicals were replaced every 24 hours and every 4 hours in two separate sets of experiments. Absorbance data for each dose are plotted as a percent of the untreated control. Each graph represents mean ± SEM of two experiments.

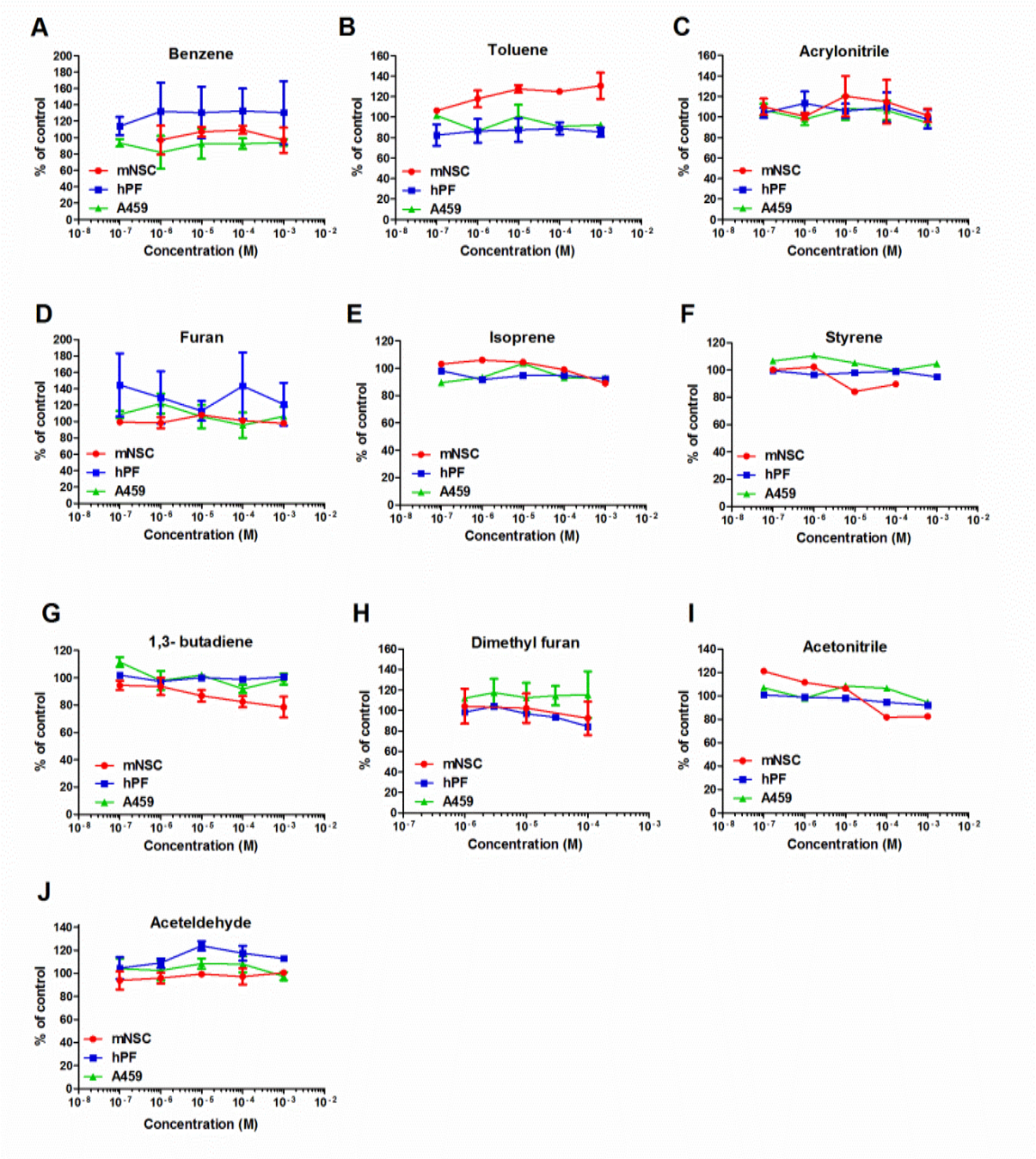

Figure A.3. MTT assay data showing the effects of chemicals with the highest number of DALYs on mNSC, hPF and A549 cells. Each graph represents mean ± SEM of two experiments.

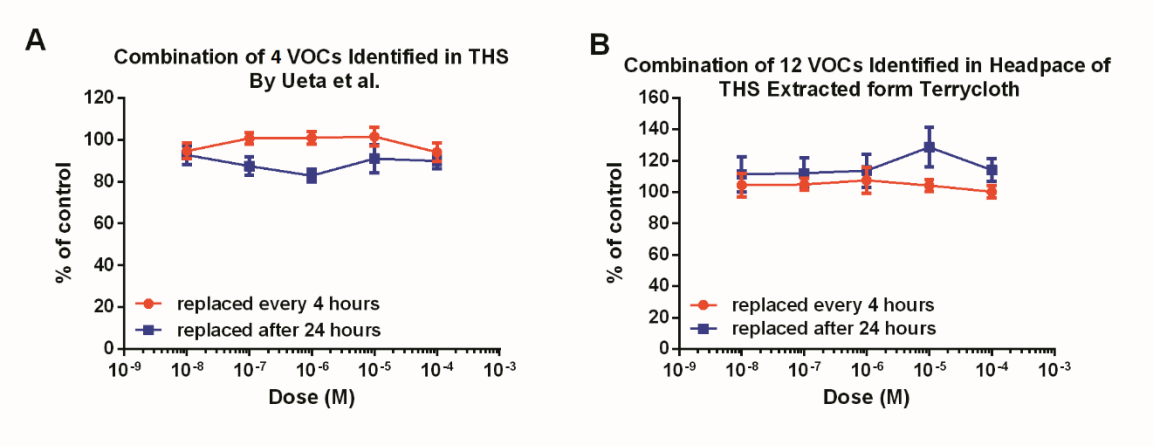

Figure A.4. MTT assay data showing the effect of combinations of VOCs on mNSC. (A) Benzene, toluene, ammonia and pyrrole were tested in combination. **(B)** Acetonitrile, 3-ethylenepyridine, toluene, phenol, benzaldehyde, acetophenone. quiniline, benzonitrile, acetone, 2-pentanone, 2-butanone and 1H-Pyrrolo[2,3-b]pyridine 2-methyl- were tested in combination. Each graph represents mean ± SEM of two experiments

Appendix B: Supporting Information for Chapter 6

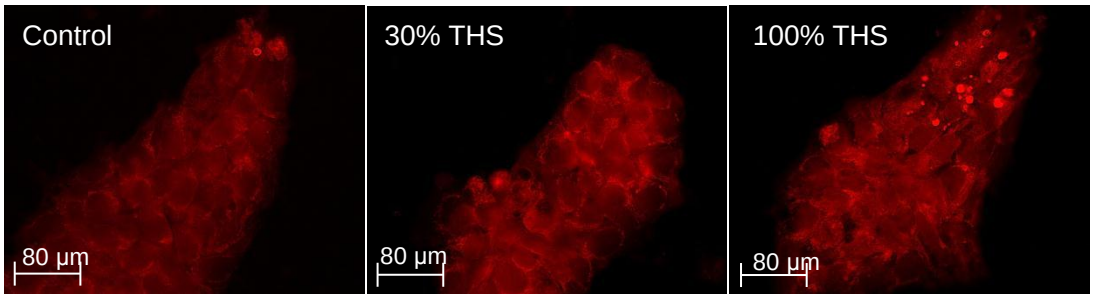

Figure B.1. Control hESC and THS treated hESC labeled with MitoTrackerRed CMX Ros. Treated cell have brighter mitochondria indicating that THS increased the MMP.